NCKRI SYMPOSIUM 6
Proceedings of DeepKarst 2016: Origins, Resources, and Management of Hypogene Karst

Edited by: Todd Chavez and Pete Reehling

National Cave and Karst Research Institute

www.nckri.org

NCKRI SYMPOSIUM 6   Proceedings of DeepKarst 2016: Origins, Resources, and Management of Hypogene Karst

2016

PROCEEDINGS OF DEEPKARST 2016: ORIGINS, RESOURCES, AND MANAGEMENT OF HYPOGENE KARST

April 11-14, 2016
Carlsbad, New Mexico, USA

EDITORS:

Todd Chavez
University of South Florida
Tampa, Florida, USA

Pete Reehling
University of South Florida
Tampa, Florida, USA

National Cave and Karst Research Institute

Cover Photo:
Spongework in the Capitan Reef limestone near the Big Room of Carlsbad Cavern, New Mexico. This feature is commonly called "Boneyard" because of its appearance. This is commonly interpreted as a classic example of dissolution by slow-moving phreatic water. However, a more feasible process is condensation of moisture from moving air masses above the water table. Solutional aggressiveness can be produced by absorption of gases from the cave air—e.g., carbon dioxide to form carbonic acid, and/or a mixture of hydrogen sulfide and oxygen to produce sulfuric acid. This type of spongework is common where air has moved slowly through the porous limestone that separates large rooms. Photo by Art Palmer.

CONTENTS

Regional Case Studies in Hypogenic Speleogenesis

Hypogenic Speleogenesis and Petroleum

Hydrothermal Karst

Hypogenic Drivers for Ecosystems

Local Case Studies in Speleogenesis

Banquet Lecture

ORGANIZING COMMITTEE

Chairman
- George Veni, Ph.D., P.G., National Cave and Karst Research Institute, Carlsbad, New Mexico

Proceedings Editors
- Todd Chavez, University of South Florida, Tampa, Florida
- Pete Reehling, University of South Florida, Tampa, Florida

Proceedings Associate Editors
- Chelsea Johnston, University of South Florida, Tampa, Florida
- Alexander Klimchouk, Ph.D., Dr.Sci., National Academy of Sciences of Ukraine, Kiev, Ukraine
- Amos Frumkin, Ph.D., The Hebrew University, Jerusalem, Israel

Program
- Cory Blackeagle, University of Kentucky, Lexington, Kentucky

Program w/ Abstracts Editor
- Anita Eröss, Eötvös Loránd University, Budapest, Hungary

Meals, Hotels, and Registration
- Debbie Herr, National Cave and Karst Research Institute, Carlsbad, New Mexico

Logo and Website
- Jill Orr, San Antonio, Texas

Field Trips
- Lewis Land, New Mexico Bureau of Geology and Mineral Resources and National Cave and Karst Research Institute, Carlsbad, New Mexico

Optional Field Trips
- Art Palmer, Ph.D. and Peggy Palmer, Oneonta, New York

Educational Accreditation
- Dianne Joop, National Cave and Karst Research Institute, Carlsbad, New Mexico

EDITORS' PREFACE

Today is Good Friday—and the end of a very busy week. Many of our colleagues—and not a few students—elected to take a day away from the university to celebrate the beginning of spring or to prepare for an active weekend.

We did not.

We just returned from the University of South Florida School of Geosciences' 2016 "Best of Karst" event poster session. Now 10 years old, this event is an opportunity for students, faculty, and other interested individuals, including librarians, to share information concerning developments in research in karst environments. This year's guest scholar was Dr. Jay L. Banner, Jackson School of Geosciences at the University of Texas.

We were invited because we have the privilege of being one of the four founding organizations and the hosts for the Karst Information Portal project. The poster session was an opportunity to get a broad snapshot of the work of the next generation of geoscientists with an interest in this critical area of research.

And we returned inspired.

One source of the inspiration lay in the event's attendees. In addition to Dr. Banner, Drs. Bogdan Onac and Philip van Beynen were present with a host of their students. It is always a pleasure to witness firsthand the excellence of our students; it is a testament to Bogdan and Phil's commitment.

Another source of inspiration from this year's gathering came from the presence of Maggie, Grace, Emily, Sarah, and Katherine. Who are they? They are a group of young scientists from grades 5 to 7 who are interested in karst environments. They created and narrated posters describing surface karst, the bolide that formed the Chesapeake Bay, the evolution and morphology of speleothems, and the south China karst. They were very knowledgeable about and confident in their descriptions of the topics they elected to present. And while none of their areas of focus touched upon deep karst, their contributions suggest that we may have met the next generation to join the community of karst researchers.

In this volume, we are pleased to present to you—and to the next generation of karst researchers—papers and abstracts describing the range of research presented at the DeepKarst 2016 conference held in Carlsbad, New Mexico in April 2016. Following the keynote address by Professor Carol A. Hill of the Department of Earth and Planetary Sciences at the University of New Mexico, the technical sessions covered hypogenic speleogenesis models, regional and local case studies, petroleum environments, hydrothermal karst, and hypogenic drivers for ecosystems. In the lecture accompanying the banquet closing out the conference's formal sessions, Professor Barbara Tewksbury (Hamilton College) employed a scientific version of Sherlock Holmes' technique for deducing the solution to the mystery, "Is Hypogenic Karst a Plausible Model for Formation of Extensively Developed Non-Tectonic Synclines in Eocene Limestone of the Western Desert, Egypt?"

We sincerely hope that this volume makes a useful addition to the growing body of published karst research.

Todd Chavez
University of South Florida
Tampa, Florida, USA

Pete Reehling
University of South Florida
Tampa, Florida, USA

KEYNOTE LECTURE

BRIEF HISTORY OF THE HYPOGENE SPELEOGENESIS MODEL, GUADALUPE CAVES, NEW MEXICO, USA

Carol A. Hill
Department of Earth and Planetary Sciences
University of New Mexico, Albuquerque, New Mexico, USA

Abstract

Internationally renowned cave mineralogist and geologist Carol Hill will trace her early involvement with the caves of the Guadalupe Mountains since 1967, specifically with respect to their hypogene speleogenetic origin. The Guadalupe Mountains form the physical backdrop of this DeepKarst conference and will be the focus of most conference field trips. Their study started with the Guadalupe Cave Survey—a group of cavers who were given permission to survey in Carlsbad Cavern in the late 1960s. This group provided the organization and interfacing with the National Park Service that was needed before scientific studies could begin in Carlsbad Cavern and then branch out to other Guadalupe-area caves under federal land management.

Carol's lecture will highlight the ongoing (in time) contributions of scientists/cavers such as Steven Egemeier, Donald Davis, Michael Queen, Carol Hill, Harvey DuChene, Dave Jagnow, Victor Polyak, Diana Northup, Penny Boston, Doug Kirkland, and Art and Peg Palmer, all of whose work has been based on, and has contributed to, the ever-developing model of hypogene speleogenesis. This model has now been applied to many other parts of the world, including the caves of Grand Canyon—possibly the deepest hypogene karst system in the world.

HYPOGENIC SPELEOGENESIS MODELS

SULFURIC ACID VS. EPIGENIC CARBONIC ACID IN CAVE ORIGIN AND MORPHOLOGY

Arthur N. Palmer

Department of Earth and Atmospheric Sciences
State University of New York
Oneonta, NY 13820-4015, USA, arthur.palmer@oneonta.edu

Abstract

Sulfuric acid speleogenesis (SAS) is one of the most effective and best-known processes of hypogenic cave origin. By recognizing the various steps involved, and their chemical effects on the surrounding rock, it is possible to explain and predict the patterns of the resulting caves and to make comparisons with other cave types. Sulfuric acid can have various sources, but only H_2S oxidation is considered here. Epigenic cave origin depends mainly on soil-generated CO_2. Carbonic acid and sulfuric acid have similar potential for cave origin but they differ in chemical dynamics and cave patterns. Epigenic caves maintain great continuity in dissolution along groundwater flow paths, whereas sulfuric acid caves show much variation in enlargement rates with distance and time. SAS tends to produce zones of intense cave enlargement that diminish rapidly in the down-flow direction. Most cave enlargement by SAS takes place subaerially but produces morphologies that superficially resemble those of phreatic origin. Features such as cupolas and spongework, which are often attributed to phreatic dissolution, are more likely to be of vadose origin. The rate and effectiveness of sulfuric acid processes depends on two contradictory aspects of cave aeration: an influx of oxygen from the surface fuels the production of acid, whereas loss of CO_2 to the surface diminishes the amount of carbonate rock that can be dissolved. Recognizing the difference in chemical processes and byproducts in these two contrasting modes of origin makes it possible to interpret relict caves of both types, even in scattered remnants.

Introduction

In this paper, hypogenic sulfuric acid and epigenic carbonic acid are compared in terms of process and rate of cave development, resulting morphologies, and production of secondary minerals. Many contrasts are already well known, so the goal here is to discuss a few points that clarify the style of cave origin and help to distinguish the nature of cave origin where only fragmented relics are present. This paper is concerned only with primary dissolution processes and features, and not with secondary aspects such as weathering and speleothems.

Chemical Systems

In a typical epigenic cave fed by infiltration or runoff from the land surface, dissolved CO_2 is the nearly ubiquitous source of aggressiveness toward carbonate rock. Dissolution rates slowly decrease in the downstream direction, except where the solutional capacity is enhanced by convergence and mixing of water sources of varied chemistry, or by oxidation of organic material. The typical result is a fairly uniform cave enlargement along the entire flow path. Interpretation of epigenic caves is aided by recognizing the strong continuity of their flow and chemistry. Where abrupt changes in cross section or size are present, the causes are easily recognized, e.g., by processes such as diversion to lower routes or floodwater invasion. Sulfuric acid speleogenesis (SAS) involves several rate-limiting steps: (1) production of H_2S, e.g., by reduction of sulfates in the presence of organic compounds, or by volcanic processes; (2) delivery of H_2S to sites favorable to cave origin; (3) conversion of H_2S to H_2SO_4, typically in several steps, by subaqueous contact with dissolved oxygen; (4) reaction between the acid and bedrock; (5) retention or release of CO_2; and (6) environmental effects on reaction rates. Oxidation of pyrite can also produce sulfuric acid, but its effects are more local and predictable, so they are not described here.

Production of H_2S is most common where sulfate rocks are exposed to hydrocarbons. Sulfates are reduced to sulfides, and carbon compounds are converted to carbonates. Calcite supersaturation is a common result. Below ~80ºC the reduction process must be microbially mediated, but above about 100ºC it can be spontaneous (Machel, 2001).

H_2S is one of the most soluble gases. Free-energy calculations show that at 25ºC H_2S is 3 times more soluble than CO_2 and 77 times more soluble than oxygen (Palmer and Palmer, 2000). Dissolved H_2S tends to disperse into the surrounding water toward areas of lower H_2S concentration, but where it is drawn into major paths of converging groundwater flow it can form concentrated plumes. At typical concentrations, H_2S

is too soluble to form bubbles unless the water rises to within a few meters of the water table. As the H_2S-rich water migrates toward outlets such as potential caves or springs, it concentrates along major fractures or zones of high permeability, which determine the location of sulfuric acid caves. These patterns of groundwater flow and gas dispersion are based on field observation, as well as analysis of the probable potential fields. Sulfuric acid speleogenesis requires oxidation of H_2S to H_2SO_4 within a carbonate aquifer. A supply of oxygen-rich water is required, and this is a major limiting factor. Deep-phreatic convergence of H_2S plumes with oxygen-rich groundwater seems possible, but most deep groundwater is poor in oxygen because so much is lost during infiltration through soil. More oxygen is retained by groundwater in arid climates (Winograd and Robertson, 1982), which may help to explain certain SAS examples. Slightly enlarged fissures rising to the water table in known sulfuric acid caves seem to pro-vide evidence for deep mixing of this kind. But most of the vertical extent of these caves is produced subaerially, as shown below.

Production of sulfuric acid is greatly accelerated by microbial mediation. The reactions are $H_2S + 2O_2 \rightarrow$ H_2SO_4 (usually in several steps) $\rightarrow$ $2H+ + SO_4= \leftarrow\rightarrow$ $H+ + HSO_4-$, all in aqueous solution. An additional equilibrium ($2H+ + SO_4= \leftarrow\rightarrow$ $H+ + HSO_4-$) is significant only at very low pH, e.g., where the acid forms on non-carbonate substrates such as chert, gypsum, or organic filaments (Hose et al, 2000; Northup et al., 2000). Element-al sulfur (So) is a common by-product at those low pH values.

Aqueous H_2S by itself is a potent solvent (hydrosulfuric acid), but where it is formed by sulfate reduction, the groundwater usually becomes supersaturated with calcite. Mixing of waters of differing H_2S concentration can produce mild undersaturation with respect to carbonate rocks (Palmer, 1991), but a strong capacity for SAS depends mainly on oxidation to sulfuric acid.

Sulfuric acid systems tend to be far more complex than those fed by shallow meteoric water. For example, sulfide-rich karst springs in the Sierra de Chiapas, Mexico, give isotopic evidence for meteoric recharge, but with chemical components that indicate a deep brackish-water component (Rosales Lagarde et al., 2014). These authors give chemical and thermal evidence for three subsurface environments, with mixing taking place among them. Relatively freshwater springs demonstrate epigene speleogenesis, whereas brackish sulfide-rich springs show evidence for hypogene speleogenesis.

Comparison of Solutional Potential

Sulfuric acid is capable of producing low, or even negative, pH in natural settings. Carbonic acid is a weak acid in which the pH rarely drops below 4 except in deep high-pressure zones. There seems to be no contest as to which is the more formidable agent in speleogenesis.

Most production of carbonic acid in groundwater is governed by the partial pressure of CO_2 in the atmosphere or soil in contact with the water. Sulfuric acid is generated by oxidation of H_2S, generally within the carbonate rock at the site of cave origin. Its concentration depends on the rates of the complex process shown in the opposite column, as well as by how quickly the acids react with the local bedrock. In SAS, much of the sulfuric acid is consumed at or near the site of H_2S oxidation, so it has a more local effect than carbonic acid.

But exactly how do the two acids compare in their potential to form caves? To explore this topic, equilibrium constants and software supplied by the U.S. Geological Survey are used (e.g., http://www/brr. cr.usgs.gov/projects/GWCcoupled/phreeqc.v1/).

In the carbonic acid system, PCO_2 is the standard beginning point for estimating solutional potential. But here the equivalent molar CO_2 concentration is used, to allow a more direct comparison with H_2SO_4. Total calcite solubility is calculated in each example. Water temperature = 25ºC for all.

1. Open system, $CO_2 = 0.001M$ (= 0.0294 atm PCO_2), $H_2SO_4 = 0$: Calcite solubility = 244 mg/L.
2. Open system, CO_2 held at 0; $H_2SO_4 = 0.001M$: Calcite solubility = 105 mg/L. CO_2 generated by the reaction is lost. Carbonic acid is clearly more potent in this comparison (#1 vs. #2).
3. Open system, $CO_2 = 0.001M$; $H_2SO_4 = 0.001M$: calcite solubility = 326 mg/L. CO_2 lost by the carbonic acid reaction is replaced from the atmosphere of the open system. CO_2 generated by the sulfuric acid reaction has no effect on the local PCO_2. Total dissolution is less than the sum of #1 + #2, because the increased dissolved load builds up a back-reaction that prevents the solubility from increasing linearly with an increase in the amount of solvent.
4. Closed system: initial $CO_2 = 0.001M$; $H_2SO_4 = 0$: calcite solubility = 152 mg/L; CO_2 decreases to 0.00027M (0.0079 atm) by reaction with calcite.
5. Closed system: initial $CO_2 = 0$; $H_2SO_4 = 0.001M$: calcite solubility = 186 mg/L; CO_2 rises to

0.000093M ($PCO_2 = 0.0027$ atm), because it is generated by the H_2SO_4 reaction. Increase in calcite solubility vs. #4 is caused by retention of CO_2. Sulfuric acid is more potent in this example. However, a closed system is not likely to occur naturally, because generation of H_2SO_4 requires exposure to oxygen.

6. Closed system, all byproducts retained: initial $CO_2 = 0.001M$; $H_2SO_4 = 0.001M$: calcite solubility = 286 mg/L. CO_2 drops to 0.00027M ($PCO_2 =$ 0.00794 atm). Total dissolved calcite is less than the sum of #4 + #5 because the calcite saturation concentration is not linearly dependent on the concentration of reactants (as in #3).

In summary, it appears that the two acids have roughly equal potential to dissolve calcite, given equal concentrations. That makes sense because similar molarities of acid might be expected to provide the same amount of dissolution. That is not quite true because of differences in concentration of ion pairs (e.g., $CaHCO_3^+$), and by the complex interplay between CO_2 consumed by the carbonic acid reaction and the liberation of CO_2 by the sulfuric acid reaction. Carbonic acid is widely available from surface sources, whereas sulfuric acid is generated in local areas, and often in irregular pulses. The sulfuric acid reaction reaches its full potential only if the generated CO_2 remains in solution. This requires an open system in which the PCO_2 is high enough to prevent the release of CO_2 produced by the sulfuric acid.

Field Measurements of Solution Rate

Another way to contrast the effects of carbonic acid with those of sulfuric acid is to make direct measurements of solutional retreat of bedrock in active caves. Dissolution rates are small and difficult to measure, but the results are more convincing than equilibrium calculations.

In carbonic acid systems, limestone dissolution rates decrease slowly as the concentration of dissolved rock increases. Measurements in cave streams show maximum dissolution rates of approximately 1 mm/yr (e.g., Covington et al., 2015), with long-term averages of roughly 0.05–0.1 mm/yr (High and Hanna, 1970; Coward, 1975). These rates are validated by laboratory measurements (e.g., Rauch and White, 1977; Plummer and Wigley, 1976; Plummer et al., 1978). During low flow, many cave streams are supersaturated. Bedrock retreat is greater where mechanical erosion is present, and during floods it is possible for erosion by bed load and suspended particles to exceed the dissolution rate (Newson, 1971), but only the chemical effects are of concern in comparing rates of carbonic acid systems vs. SAS.

Chemical measurements have been made by Engel et al. (2004) in the H_2S-rich stream in Lower Kane Cave, Wyoming, which is colonized by thick microbial mats (Figure 1). They found that most of the H_2S is consumed in the stream by microbial oxidation, and that only a small percentage volatilizes into the cave air (contrary to the hypothesis of Egemeier, 1973, 1981).

Figure 1.
Main passage of Lower Kane Cave, Wyoming, showing oxide-rich stream bed with microbial filaments. Note white piles of secondary gypsum that have fallen from the walls and ceiling. Photo by Kevin Downey, with permission.

This system is very close to equilibrium, with calcite dissolution rates dependent on dissolved sulfide concentration and degree of calcite undersaturation. Acidity is focused at the sites where bacterial filaments are in contact with carbonate rock. Dissolved Ca^{2+} increases downstream where microbial growth is greatest, while SO_4^{2-} increases only slightly. Secondary gypsum on the cave walls and floors show that sub-aerial dissolution takes place from H_2S escaping into the air, but its long-term rate is unknown.

The small subaerial H_2S flux could not explain present SAS processes. Instead, almost all of the H_2S is consumed by subaqueous sulfur-oxidizing bacteria. The bacteria drive SAS by attachment to carbonate surfaces and by generation of sulfuric acid, which focuses local carbonate undersaturation and dissolution. Sulfur-

oxidizing bacteria can catalyze autoxidation below the water table and extend the depth to which porosity and conduit enlargement can take place (Engel et al., 2004). This process can explain the development of narrow solutionally enlarged infeeders to caves, and although they are generally too small to explore, they are important in focusing H_2S-rich recharge to sulfuric acid caves.

Long-term measurements of SAS have been conducted in the Frasassi Cave System in Italy (Galdenzi et al., 1997, 2008). Limestone tablets were placed for as long as five years directly in the main H_2S-rich stream, while others were suspended above stream level. Subaqueous tablets dissolved at 0.028–0.088 mm/cm^2/yr while the subaerial tablets dissolved at 0.56–0.64 mm/cm^2/yr (mean rock density measured at 2.5 g/cm^3). A later study under similar conditions (Galdenzi 2012) showed higher rates in the stream (0.06–0.11 mm/cm^2/yr), which demonstrate large temporal variations in H_2S-H_2SO_4 level. Large short-term H_2S variations have also been observed in the air of Cueva de Villa Luz, Mexico, which is strongly ventilated to the surface (Hose et al., 2000; see Figure 2).
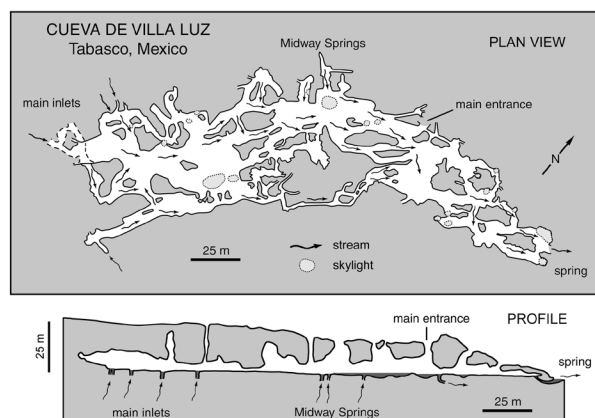
Figure 2.
Map and profile of Cueva de Villa Luz, Tabasco, Mexico. The cave stream is fed by a variety of water inlets, some H2S-rich and others oxygen-rich. The cave contains a complex system of chemoautotrophic biota ranging from filamentous microbes to fish. Figure is simplified from a more detailed version by Bob Richards in Hose et al. (2000).

Although the Frasassi data might suggest that the rate of subaerial corrosion is only marginally higher than in the stream, the tablets exposed to air represent only a tiny fraction of the area of subaerial cave walls. The total volumetric rate of dissolution above the stream is far greater than that in the stream channel.

Further support for the dominance of subaerial SAS in Frasassi is given by Jones et al. (2015), who show that the major destination for sulfide is H_2S degassing into the cave air, with rates of 0.9 to 80 μmol/m^2/sec, compared to microbial oxidation rates of 0.15 to 2.0 μmol/m^2/sec in the stream.

Subaerial H_2S must be absorbed by moisture before it can be converted to sulfuric acid. In the experiments by Galdenzi et al. (1997, 2008) described above, the limestone tablets hanging by strings were not only exposed to rising H_2S, but also must have accumulated condensate from water vapor. The initial condensate contains no dissolved solids, so its entire solutional potential is exerted on the tablet surfaces. In a fresh aqueous solution, H_2S alone can dissolve a large amount of carbonate, about 90% as much as equal molarities of CO_2 (Palmer, 1991). Sulfuric acid is produced when oxygen is also absorbed by the moisture and reacts with the H_2S. This process lowers the concentrations of both O_2 and H_2S, so the two gases continue to be absorbed by the moisture to sustain carbonate dissolution. On non-carbonate surfaces (e.g., gypsum, chert or microbial filaments) the pH can continue to drop, even to below zero. In the sulfide-rich atmosphere of Cueva de Villa Luz, pH values as low as 0.07 were measured in water droplets after calibration with a pH 1.6 buffer, and many attempts simply gave error messages (Palmer and Palmer, 1998). Accuracy at pH near zero requires special calibration, which was not performed. But the feasibility of even negative pH values has been reported by Nordstrom et al. (2000), who measured pH as low as -3.6 in mines where pyrite is oxidizing. The solubility of oxygen in water is only about 1.3% as great as H_2S (at 25 ºC), but the partial pressure of O_2 in the atmosphere of an active sulfuric acid cave is typically more than 100 times greater than that of H_2S. Even in the toxic sulfide-rich atmosphere of Cueva de Villa Luz, the ratio of PO_2 to PH_2S is rarely less than 500 (Hose et al., 2000). The chemistry and microbial systems of the cave walls are undoubtedly more complex than those of freshly cut tablets. A well-adapted microbial culture on the walls probably gives the surfaces an additional potential for dissolution. H_2S-rich feeders to cave streams are already at or near calcite saturation. Oxidation of H_2S in a low-velocity stream with small surface area is relatively slow, although it can increase greatly with turbulence, surface area, and microbial activity.

Although sulfuric acid and carbonic acid are roughly equivalent in solutional potential, they have greatly different effects on cave morphology. Much carbonic acid is "wasted" at the soil-rock interface where water

first infiltrates into limestone, and much residual aggressiveness remains at springs, especially during high flow. The rate of subaqueous dissolution in sulfuric acid streams can be roughly equivalent to that in subaqueous carbonic acid systems, but subaerial dissolution can be far greater than subaqueous dissolution.

Effects of Cave Aeration

Caves formed by carbonic acid tend to enlarge rather uniformly along their length. However, in a cave that is fed mainly by seepage through overlying soil, an open entrance along an active stream passage can allow significant loss of CO_2 to the surface. Ordinarily the effect goes unnoticed; but in rare situations there can be enough degassing from the cave stream to cause calcite to precipitate on the stream floor. This condition is temporary and only noticeable during extremely dry periods (Palmer, 2007). The calcite is usually removed during the next episode of high flow. The effect of CO_2 escape through entrances can usually be detected only by measured variations in calcite saturation in the cave streams. Such examples have little significance in carbonic acid caves, but gas flux through entrances has a much greater effect on sulfuric acid caves.

SAS depends strongly on exchange of gases between cave and surface. Most important is the input of oxygen necessary to oxidize H_2S in cave streams and vadose moisture. An open entrance is ideal, but apparently seepage of air through narrow fissures is sufficient. Changes in atmospheric pressure can be significant in driving the gas flux into and out of the caves. SAS increases preferentially in areas of high oxygen supply, so these inputs are most likely to enlarge into cave entrances. Many such entrances are located high above the stream level, which gives evidence for long-term upward diffusion and convection of H_2S, despite the fact that much of the aggressiveness is consumed near the H_2S inputs. The contours of cave rooms and passages provide information on the distribution of vadose dissolution, and therefore on subaerial gas circulation. Open entrances in sulfuric acid caves are usually unavailable until late in the history of cave development.

Dissolution rate in sulfuric acid caves diminishes rapidly away from air inputs, as is typically shown by abrupt lateral variations in passage size (see Figure 2). H_2S may be distributed irregularly within the cave by the pattern of air currents, which complicates the interpretation of water flow and distribution of gas sources. In such caves it is usually the spring exit that enlarges least. Many spring outlets have low ceilings or no air space. The spring outlets at Frasassi and Villa Luz are water-filled, and the exit of Lower Kane Cave is one of the most

constricted parts of the cave. Many inactive SAS caves show similar relationships.

The Concept of Breakthrough Time

The origin of an epigenic cave passage involves a lengthy "breakthrough time" during which it enlarges slowly at very small levels of undersaturation. This time is a function of initial fissure width, passage length, hydraulic gradient, and $P\text{CO}_2$ (Palmer, 1991; Dreybrodt, 1996). Beyond breakthrough, the passage enlarges rather uniformly at a comparatively rapid pace. In long passages the breakthrough time can be tens or even hundreds of thousands of years (validated by dating of well-documented passage levels). Passages in maze caves develop more rapidly, and simultaneously, because of short flow distances, great initial width, and/or steep gradients, so the breakthrough times are negligible.

Breakthrough time applies to some hypogenic caves, but not to those formed by SAS (at least not in an easily quantified way). Rates of initial cave enlargement depend on simultaneous supplies of H_2S and oxygen. Sulfuric acid caves convey the impression of being dependent only on deep-seated processes because of their irregular patterns; but in fact their evolution is closely tied to aeration through surface connections, although not necessarily through cave-size openings.

Bedrock Alteration by Sulfuric Acid

Sulfuric acid dissolution of carbonate rock can result in precipitation of gypsum: $2CaCO_3 + H_2SO_4 + 2H_2O \rightarrow CaSO_4 \cdot 2H_2O + Ca^{2+} + 2HCO_3^-$. The molar volume of gypsum is almost exactly twice that of calcite (within 1%), so if this reaction remains balanced, the replacive gypsum will have the same volume as the original calcite, and all the grain shapes and textures in the original limestone will be preserved as gypsum. For this replacement to be optimized, loss of CO_2 to the cave air must be minimized by the confining action of the gypsum mantle. In this case, even the shapes of fossils in the limestone may be preserved in the gypsum (Queen, 1973; Queen et al., 1977; Buck et al., 1994). Dolomite bedrock can be replaced in a similar manner, but the volumetric balance with gypsum is less exact. If enough CO_2 is lost through entrances to diminish the solutional capacity of the local cave moisture, the speleogenetic gypsum will occupy more volume than the original bedrock and the original textures are disrupted.

The acid-bedrock interface can be observed in many active sulfuric acid caves. In cross section, lobes of gypsum and anhydrite are visible in the limestone walls (Figure 3). Anhydrite ($CaSO_4$) is not a stable end-member of this reaction, but it forms where the

reaction is rapid and/or the supply of water is limited. Anhydrite gradually alters to gypsum as the sulfate rind thickens.
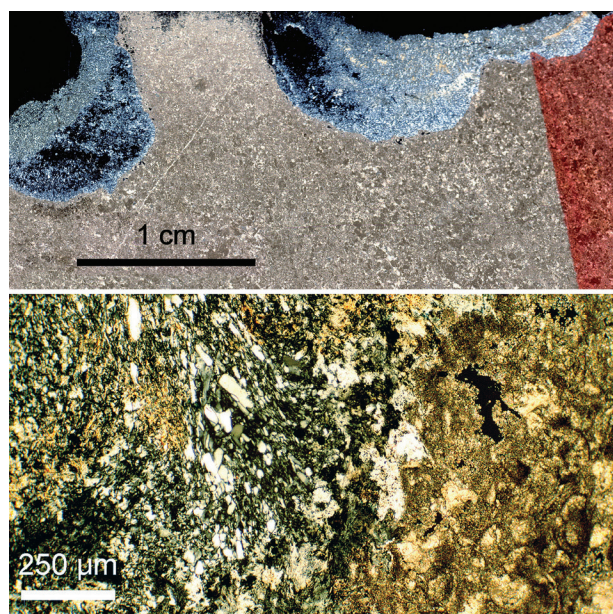
Figure 3.
Thin-section photomicrographs of limestone dissolution embayments in Cueva de Villa Luz. Top: Lobate sulfuric acid replacement fronts of gypsum (light gray) encroaching on limestone bedrock (brown). Light yellow inclusions in the gypsum are anhydrite needles (CaSO4). Red stain on right is alizarine red, a test for CaCO3. Cross-polarized light.
Bottom: Enlarged view, with limestone on right and replacive gypsum on left containing aragonite needles. Cross-polarized light.

The reaction to form H_2SO_4 tends to continue in moisture that clings to the outer surface of the replacement gypsum. For SAS to take place in the limestone beneath the gypsum rind, it is necessary for ionic diffusion to take place through the moisture held in the gypsum. A two-way ionic diffusion takes place, even if there is no significant water movement; but the moisture can also move in response to capillary potential gradients. These conclusions are based on the mineral processes observed in cross sections such as those in Figure 3.

Gypsum crusts on the cave walls thicken where sulfuric acid is dissolving the underlying carbonate rock. Eventually blocks of gypsum fall to the floor. Large bodies of fallen gypsum may fuse together into extensive glacier-like masses. Gypsum masses can

absorb moisture like a sponge, and the reaction between H_2S and O_2 in the water tends to build up sulfuric acid. Water that drips off the bottoms of gypsum bodies can form drill-holes and rills in exposed carbonate rock below.

Blocks of fallen secondary gypsum may accumulate on a sloping bedrock wall, and if low-pH water seeps or flows along the underlying carbonate rock, prominent rills may form that can be puzzling to observers after the gypsum has been removed by later dissolution (Figure 4).

Figure 4.
Rills in Carlsbad Cavern, N.M., formed by drainage of sulfuric acid from gypsum bodies that once covered the ledges. The gypsum has been removed by later dissolution, leaving no clue to the original water source.

Many caves of clearly epigenic origin also contain gypsum crusts on limestone walls. Some involve sulfuric acid generated by pyrite oxdidation (White and White, 2003), but this is yet another example of the sulfuric acid process.

Sulfuric acid can leave a variety of other diagnostic byproducts, which can linger in caves that are no longer active. Alteration of clay by strong H_2SO_4 can result in distinctive byproducts such as alunite, hydrated halloysite, gibbsite, Fe-Mn oxides and hydroxides, and opal (Polyak & Güven, 2000). All can occur as inclusions in replacive gypsum or as residuum on weathered bed-rock. Fe and Mn are most soluble at low pH and/or Eh and tend to precipitate with an increase in either or both of these variables. Fe oxides/

hydroxides can be scattered within replacive gypsum, whereas Mn oxides/hydroxides tend to concentrate on carbonate surfaces where acidity is less intense. Spilde et al. (2005) demonstrate microbial enhancement of Fe-Mn corrosion in the Guadalupe caves. These minerals and associations are rarely present in caves formed by carbonic acid.

Contrasting Cave Patterns

The origin of inactive caves, and even isolated cave fragments, can usually be determined by applying the relationships described here. Those formed by carbonic acid can usually be distinguished from sulfuric acid caves with little difficulty. The geologic setting alone is usually enough to determine the origin. Remnants of features such as bedrock alteration products are helpful but may have long disappeared by weathering.

Epigenic stream caves preserve a great continuity of cross-sectional area with distance. Changes in cross-sectional area are easily explained, for example by local collapse, convergence of flow, and headward stream entrenchment. An epigenic origin for maze caves is easily recognized if they have formed by floodwater or stream diversion around collapse zones. Large mazes with rather uniform passage spacing are usually the product of uniform recharge, e.g., where seepage takes place through insoluble strata (see Palmer, 1991, 2007), although the prospect of rising groundwater should also be investigated. The geomorphic and hydrologic setting should provide clues.

Sulfuric acid caves and their origin are not so predict-able. The presence of a suitable H_2S source is not sufficient. Rapid SAS also requires preexisting aerated openings—for example a system of paleokarst or wide fractures that allow exchange of air with the land surface. As the cave grows, aeration tends to increase, so there is a positive feedback.

Major inputs of sulfide-rich groundwater can form large and complex caves in which much of the dissolution takes place in the vicinity of the stream at or near floor level. Note the complexity of Cueva de Villa Luz, with its multiple high-discharge inlets (Figure 2) compared to Lower Kane Cave (Figure 1) composed of essentially a single passage along a fracture zone.

In sulfuric acid caves, much of the solutional capacity is exhausted over relatively short distances. Acidic water in direct contact with carbonate rock is quickly buffered by release of bicarbonate ions, so the water approaches a pH of about 6.3–7.2 (Hose et al., 2000). Meanwhile, rapid cave growth depends on a continued influx of H_2S

and O_2, either of which may be the limiting factor in the process.

Air rising toward the surface can follow sinuous routes that are clearly not the product of vadose streams. Smooth curving paths are typical. Abrupt changes in passage size and morphology are typical, and they are best interpreted in terms of patterns of H_2S migration, aided by air currents. SAS in aerated parts of a cave tends to diminish with elevation above the aqueous H_2S source. The largest rooms tend to be above and somewhat downstream from H_2S inputs, and passage size diminishes rapidly in the down-flow direction. Other H_2S inputs farther downstream also tend to produce abrupt enlargements.

Zones of major enlargement in certain sulfuric acid caves are tightly clustered, with passages tapering downward around the periphery. Explorers are often frustrated by the abrupt size reduction that forces one to crawl, squeeze, or turn back. These zones often contain spongework mazes that form connections between the more spacious areas (Figure 5).

Figure 5.
The Boneyard in Carlsbad Cavern, N.M. is a fine example of spongework. Such features are almost universally considered phreatic in origin, but their locations in the cave suggest that they may instead be pores enlarged in the vadose zone by acidic moisture films.

Sulfuric acid caves contain many places where large, apparently independent portions of a cave are connected by spongework. This is especially true in caves of the Guadalupe Mountains (e.g., Carlsbad Cavern and Lechuguilla Cave). These tight mazes appear to be remnants of early porosity that have been enlarged by dissolution. Phreatic dissolution is normally given as the mechanism, because there is no gravitational

orientation. But the dense arrays of pockets are also paths of air movement, and subaerial dissolution by $H_2S + O_2$ absorbed by moisture films may be equally credible. They would also enlarge the pockets with no gravitational effect.

Thus the spongework mazes may seem to contradict the concept that maze caves require large discharge and/or width, short flow lengths. Although that concept was not designed for subaerial SAS, the flow distances are in fact short and the initial openings are relatively wide.

The best clues to long-term patterns of air flow are ear-shaped hollows in cave walls and speleothems, as well as speleothems that grow preferentially into the wind by evaporation (Queen, 1994). Much of the dissolution today in dry caves like Carlsbad Cavern is limited to condensation moisture. But while the cave was actively enlarging by sulfuric acid, these (or similar) air-flow patterns must have played a significant role in determining the patterns of dissolution.

Many of the most diagnostic features of SAS caves are secondary—e.g., speleothems, biological evidence, wall weathering, alteration products, sediments, minor dissolution features. For further information, see the cited references.

Conclusions

Caves formed by sulfuric acid have no inherent advantage in potential cave size compared to caves formed by epigenic processes. Epigenic CO_2 and hypogenic H_2S-H_2SO_4 have essentially equal capacity to dissolve carbonate rock. However, cave development by sulfuric acid must overcome several hurdles, which include a reliable supply of H_2S, its transport to a favorable location, and exposure to oxidizing conditions before the gas escapes to the land surface. In view of these limitations, it is no wonder that sulfuric acid caves are relatively uncommon. The wonder is that there are so many large and magnificent examples throughout the world. Their true value is not only their size or beauty, but the enormous amount of information they provide about past geologic history, deep-seated geochemical processes, and microbial systems.

References

Buck MJ, Ford DC, Schwarcz H. 1994. Classification of cave gypsum deposits derived from oxidation of H_2S. Proceedings of Karst Waters Institute conference, Breakthroughs in karst geomicrobiology and redox geochemistry: Special Publication 1, Charles Town, W.Va.: 5-9.

Covington MD, Gulley JD, Gabrovšek F. 2015. Natural variations in calcite dissolution rates in streams: controls, implications, and open questions. Geophysical Research Letters 42: 2836-2843. http://dx.doi.org/10.1002/2015GL063044

Dreybrodt W. 1996. Principles of early development of karst conduits under natural and man-made conditions revealed by mathematical analysis of numerical models. Water Resources Research 32: 2923-2935. http://dx.doi.org/10.1029/96WR01332

Egemeier, SJ. 1973. Cavern development by thermal waters with a possible bearing on ore deposition [PhD dissertation]. Stanford (CA): Stanford University, 88 p.

Egemeier, SJ. 1981. Cavern development by thermal waters. National Speleological Society Bulletin 43 (2): 31-51.

Engel AS, Stern LA, Bennett PC. 2004. Microbial contributions to cave formation: New insights into sulfuric acid speleogenesis. Geology 32: 369-372. http://dx.doi.org/10.1130/G20288.1

Galdenzi S. 2012. Corrosion of limestone tablets in sulfidic ground-water: measurements and speleogenetic implications. International Journal of Speleology: 41 (3): 149-159. http://dx.doi.org/10.5038/1827-806X.41.2.3

Galdenzi S, Menichetti M, Forti P. 1997. La corrosione di placchette calcaree ad opera di acque sulfuree: dait sperimentali in ambiente ipogeo. Proceedings of 12th International Congress of Speleology, La Chaux-de-Fonds, Switzerland, 1: 187-190.

Galdenzi S, Cocchioni M, Morichetti L, Amici V, Scuri S. 2008. Sulfidic ground-water chemistry in the Frasassi Caves, Italy. Journal of Cave and Karst Studies 70: 94-107.

High CJ, Hanna GK. 1970. A method for the direct measurement of erosion of rock surfaces. British Geomorphological Research Group, Technical Publication 5, 24 p.

Hose LD, Palmer AN, Palmer MV, Northup DE, Boston PJ, DuChene HR. 2000. Microbiology and geochemistry in a hydrogen-sulphide-rich karst environment. Chemical Geology 169: 399-423. http://dx.doi.org/10.1016/S0009-2541(00)00217-5

Jones DS, Polerecky L, Galdenzi S, Dempsey BA, Macalady JL. 2015. Fate of sulfide in the Frasassi cave system and implications for sulfuric acid speleogenesis. Chemical Geology 410: 21-27. http://dx.doi.org/10.1016/j.chemgeo.2015.06.002

Machel HG. 2001. Bacterial and thermochemical sulfate reduction in diagenetic settings ─ old and new insights. Sedimentary Geology 140: 143-175. http://dx.doi.org/10.1016/S0037-0738(00)00176-7

Newson MD. 1971. The role of abrasion in cavern development. Cave Research Group of Great Britain, Transactions 13: 101-107.

Nordstrom DK, Alpers CN, Ptacek CJ, Blowes DW. 2000. Negative pH and extremely acidic mine waters from Iron Mountain, California. Environmental Science and Technology 34 (2): 254-258.
http://dx.doi.org/10.1021/es990646v

Northup DE, Dahm C, Melim L, Spilde M, Crossey L, Lavoie K, Mallory L, Boston P, Cunningham K and Barns S. 2000. Evidence for geomicrobiological interactions in Guadalupe caves. Journal of Cave and Karst Studies 62: 149-160.

Palmer AN. 1991. Origin and morphology of limestone caves. Geological Society of America Bulletin 103 (1): 1-21.
http://dx.doi.org/10.1130/0016-7606(1991)103<0001:OAMOLC>2.3.CO;2

Palmer AN. 2007. Cave geology. Dayton (OH): Cave Books.

Palmer AN, Palmer MV. 1998. Geochemistry of Cueva de Villa Luz, Mexico [abs.]: an active H2S cave. Journal of Cave and Karst Studies 60 (3): 188.

Palmer AN, Palmer MV. 2000. Hydrochemical interpretation of cave patterns in the Guadalupe Mountains, New Mexico. Journal of Cave and Karst Studies 62 (2): 91-108.

Palmer MV, Palmer AN. 2012. Petrographic and isotopic evidence for late-stage processes in sulfuric acid caves of the Guadalupe Mountains, New Mexico. International Journal of Speleology 41 (2): 231-250.
http://dx.doi.org/10.5038/1827-806X.41.2.10

Plummer LN, Wigley TML. 1976. The dissolution of calcite in CO_2-saturated solutions at 25°C and 1 atmosphere total pressure. Geochimica et Cosmochimica Acta 40: 191-202.
http://dx.doi.org/10.1016/0016-7037(76)90176-9

Plummer LN, Wigley TML, Parkhurst DL. 1978. The kinetics of calcite dissolution in CO_2-water systems at 5° to 60°C and 0.0 to 1.0 atm CO_2. American Journal of Science 278: 179-216.
http://dx.doi.org/10.2475/ajs.278.2.179

Polyak VJ, Güven N. 2000. Clays in caves of the Guadalupe Mountains, New Mexico. Journal of Cave and Karst Studies 62 (2): 120-126.

Polyak VJ, Provencio P. 2001. By-product materials related to H_2S-H_2SO_4 influenced speleogenesis of Carlsbad, Lechuguilla, and other caves of the Guadalupe Mountains, New Mexico. Journal of Cave and Karst Studies 63 (1): 23-32.

Queen JM. 1973. Large-scale replacement of carbonate by gypsum in some New Mexico caves [abs.]. National Speleological Society, abstracts of national convention, Bloomington, Indiana: 12.

Queen JM, Palmer AN, Palmer MV. 1977. Speleogenesis in the Guadalupe Mountains, New Mexico: gypsum replacement of carbonate by brine mixing. Proceedings of 7th International Congress of Speleology, Sheffield, UK: 333-336.

Queen JM. 1994. Speleogenesis in the Guadalupes: The unsettled question of the role of mixing, phreatic or vadose sulfide oxidation. Proceedings of Karst Waters Institute, Breakthroughs in karst geomicrobiology and redox geochemistry: Special Publication 1; Charles Town, W.Va., 64-65.

Rauch HW, White WB. 1977. Dissolution kinetics of carbonate rocks. 1. Effects of lithology on dissolution rate. Water Resources Research 13: 381-394.
http://dx.doi.org/10.1029/WR013i002p00381

Rosales Lagarde L, Boston PJ, Campbell A, Axen G, Stafford KW. 2014. Hydrogeology of northern Sierra de Chiapas, Mexico: a conceptual model based on a geochemical characterization of sulfide-rich karst brackish springs. Hydrogeology Journal 22 (6): 1447-1467.
http://dx.doi.org/10.1007/s10040-014-1135-z

Spilde M, Northup D, Boston P, Scholble R, Dano K, Crossey L, Dahm C. 2005. Geomicrobiology of cave ferromanganese deposits: A field and laboratory investigation. Geomicrobiology Journal 22 (3-4): 99-116.
http://dx.doi.org/10.1080/01490450590945889

White WB, White EL. 2003. Gypsum wedging and cavern breakdown: Studies in the Mammoth Cave System, Kentucky: Journal of Cave and Karst Studies 65 (1): 43-52.

Winograd IJ, Robertson FN. 1982. Deep oxygenated ground water: Anomaly or common occurrence? Science 216: 1227-1230.
http://dx.doi.org/10.1126/science.216.4551.1227

A RE-EVALUATION OF HYPOGENE SPELEOGENESIS: DEFINITION AND CHARACTERISTICS

George Veni

National Cave and Karst Research Institute
400-1 Cascades Avenue
Carlsbad, New Mexico 88220, USA, gveni@nckri.org

Extended Abstract

Alexander Klimchouk's (2007) seminal work on hypogenic karst consolidated and synthesized the body of research on the topic. For a definition, he proposed:

> *Hypogenic speleogenesis is defined here, following the recent suggestion of Ford (2006), as "the formation of caves by water that recharges the soluble formation from below, driven by hydrostatic pressure or other sources of energy, independent of recharge from the overlying or immediately adjacent surface."*

Klimchouk's work spurred broad additional research internationally, much of which is included in Klimchouk and Ford (2009), Stafford et al. (2009), and Klimchouk et al. (2014). Consequently, questions have arisen, some of which are summarized below, that challenge Klimchouk's definition for possible expansion and/or refinement, as well as a closer consideration of what features unequivocally qualify as hypogenic.

By definition, all hypogene speleogenetic water is phreatic, but not all phreatic water is hypogenic. Klimchouk (2007) identifies many caves as hypogenic based on morphologic evidence, yet some morphologies can develop in non-hypogenic regimes. A most notable example, although some discussion remains, comes from Mylroie and Mylroie (2009), who identified several of these morphologies in unconfined flank margin caves developed in eogenetic limestones along sea coasts at freshwater-saltwater mixing zones.

Audra et al. (2009a) observed a great variety of cave pattern morphologies attributed to hypogene processes: isolated geodes, 2-D and 3-D multistory systems following joints and bedding planes, giant phreatic shafts, water table mazes, isolated chambers, upwardly dendritic spheres, water table caves, and "smoking" shafts. The morphologies differed according to the specific conditions of the caves' structural and stratigraphic settings. They concluded that

"each hypogenic cave seems to be unique, with few characteristics in common with the other hypogenic caves in terms of their patterns."

Dublyansky (2014) found ambiguity in recognizing hypogene caves when "the demonstrable lack of the deep-seated sources of aggressiveness in waters which enter the soluble formation from below, places speleogenesis in the 'grey area,' where its attribution to hypogene category becomes equivocal." Additionally, the concept of the hypogene water not originating in the "immediately adjacent" area (Klimchouk, 2007) may be intuitively understood but remains technically vague.

Meanwhile, Kempe (2014) asks "How deep is hypogene?" Hypogenic origin results from water rising "from below" (Klimchouk, 2007) but from how deep? Does the amount of rise define hypogene conditions? Klimchouk (2014) indicates that upwelling of water along fractures into soluble rocks is responsible for some hypogenic karst, but is not a prerequisite. In some areas, hypogene speleogenetic conditions occur where groundwater only occurs in the soluble rock and is taken to a confining depth by the dip and/or faulting of the strata.

While the authors above raise questions that may be answered by a refined definition for hypogene speleogenesis, basic misunderstandings of the terminology may be reduced by a revised definition. For example, during much of my professional career, I've seen geologists drill into unconfined karst aquifers, intersect a phreatic conduit, watch the water level rise in the borehole above the elevation of the conduit, and claim the presence of artesian conditions. More recently, I've seen "hypogene" conditions claimed in similar situations.

The rise in water level in these situations is simply a matter of drilling through a section of unfractured low-permeability limestone and intersecting a highly permeable conduit. If the well bore stopped above the conduit, given time, water would have risen to the

same level through the low permeability rock, only slowly. Similarly, water in a phreatic, non-hypogenic conduit will rise into fractures in the ceiling of the conduit, dissolving them to create cupolas. Caution is clearly needed when interpreting certain speleogens as hypogenic. Klimchouk (2007, 2009) and Audra et al. (2009b) describe many hypogenic speleogens and illustrate that the most reliable as hypogenic indicators show focused and often channelized upward flow. It is clearly important that the full hydrogeologic context of any speleogens and cave patterns must be considered before a particular hydrogeologic origin can be concluded, yet these speleogens and patterns remain useful tools as guidance toward understanding their origins.

In 2009, Klimchouk made an important addition to clarify his definition of hypogene speleogenesis by specifying the need for a leaky upper confining unit that allows upward discharge of water. This creates focused flow through the soluble rock below and sufficient circulation to prevent chemical saturation of the groundwater to allow dissolution of the soluble rock. This leaky unit was discussed in his earlier work, but not made part of the definition. Implicit in this is the presence of a spring or zone of diffuse discharge above the confining unit, of which there is seldom direct evidence in relict hypogene settings. This discharge would not need to occur directly above the hypogene cave; permeable rock above the confining unit could carry the groundwater laterally for considerable distances before discharging it from a spring.

Klimchouk (2014) follows his earlier work with a compelling case that hypogene speleogenesis is a hydrogeologic process that can occur in any soluble rock independent of any specific chemistry of the groundwater. He offers a general definition for hypogene speleogenesis. I propose the following specific definition as a refinement of previous efforts, and in an attempt to address previous limitations and encompass the broad array of speleogens and cave patterns by emphasis on the essence of hypogenic processes:

Hypogene speleogenesis is the origin of caves through the predominantly upward flow of chemically aggressive groundwater, relative to a soluble rock, that leaks to the surface through a confining unit, with its groundwater originating beyond the limits of the confining unit.

In applying this or other hydrogeologic definitions, it is crucial to recall that similar features occur in different contexts. Correct interpretation of any form of speleogenesis—and the morphologies, patterns, and other characteristics of its caves, conduits, and aquifer—depends on the proper interpretation of their local hydrogeologic conditions and histories.

References

Audra P, Mocochain L, Bigot J-Y, Nobécourt J-C. 2009a. Hypogene cave patterns. In: Klimchouk AB, Ford DC, editors. Hypogene speleogenesis and karst hydrogeology of artesian basins. Special Paper 1. Simferopol (UA): Ukrainian Institute of Speleology and Karstology. p. 17-22.

Audra P, Mocochain L, Bigot J-Y, Nobécourt J-C. 2009b. Morphological indicators of speleogenesis: hypogenic speleogens. In: Klimchouk AB, Ford DC, editors. Hypogene speleogenesis and karst hydrogeology of artesian basins. Special Paper 1. Simferopol (UA): Ukrainian Institute of Speleology and Karstology. p. 23-32.

Dublyansky YV. 2014. Hypogene speleogenesis – discussion of definitions. In: Klimchouk A, Sasowsky I, Mylroie J, Engel SA, Engel AS, editors. Hypogene cave morphologies. Selected papers and abstracts of the symposium held February 2-7, 2014, San Salvador Island, Bahamas. Special Publication 18. Leesburg (VA): Karst Waters Institute. p. 1-3.

Kempe S. 2014. How deep is hypogene? Gypsum cave in the south Harz. In: Klimchouk A, Sasowsky I, Mylroie J, Engel SA, Engel AS, editors. Hypogene cave morphologies. Selected papers and abstracts of the symposium held February 2-7, 2014, San Salvador Island, Bahamas. Special Publication 18. Leesburg (VA): Karst Waters Institute. p. 57-64.

Klimchouk A. 2007. Hypogene speleogenesis: hydrogeological and morphogenetic perspective. Special Paper No. 1. Carlsbad (NM): National Cave and Karst Research Institute.

Klimchouk A. 2009. Principle features of hypogene speleogenesis. In: Klimchouk AB, Ford DC, editors. Hypogene speleogenesis and karst hydrogeology of artesian basins. Special Paper 1. Simferopol (UA): Ukrainian Institute of Speleology and Karstology. p. 7-15.

Klimchouk A. 2014. The methodological strength of the hydrogeological approach to distinguishing hypogene speleogenesis. In: Klimchouk A, Sasowsky I, Mylroie J, Engel SA, Engel AS, editors. Hypogene cave morphologies. Selected papers and abstracts of the symposium held February 2-7, 2014, San Salvador Island, Bahamas. Special Publication 18. Leesburg (VA): Karst Waters Institute. p. 4-12.

Klimchouk A, Sasowsky I, Mylroie J, Engel SA, Engel AS, editors. 2014. Hypogene cave morphologies. Selected papers and abstracts of the symposium held February 2-7, 2014, San Salvador Island, Bahamas. Special Publication 18, Karst Waters Institute.

Klimchouk AB, Ford DC, editors. 2009. Hypogene speleogenesis and karst hydrogeology of artesian basins. Special Paper 1. Simferopol (UA): Ukrainian Institute of Speleology and Karstology.

Mylroie JE, Mylroie JR. 2009. Diagnostic features of hypogenic karst: is confined flow necessary? In: Stafford KW, Land L, Veni G, editors. NCKRI Symposium 1, Advances in Hypogene Karst Studies. Carlsbad (NM): National Cave and Karst Research Institute. p. 12-26.

Stafford KW, Land L, Veni G, editors. 2009. Advances in Hypogene Karst Studies. NCKRI Symposium 1. Carlsbad (NM): National Cave and Karst Research Institute.

A SUPERCRITICAL CO$_2$ HYPOGENE SPELEOGENESIS MODEL: THE ORIGIN OF SPAR CAVES AND CAVE SPAR IN THE GUADALUPE MOUNTAINS, USA

David D. Decker
University of New Mexico, Radiogenic Isotopes Lab, Department of Earth & Planetary Sciences, MSC003-2040, Albuquerque, NM 87131-0001

Victor J. Polyak
University of New Mexico, Radiogenic Isotopes Lab, Department of Earth & Planetary Sciences, MSC003-2040, Albuquerque, NM 87131-0001

Yemane Asmerom
University of New Mexico, Radiogenic Isotopes Lab, Department of Earth & Planetary Sciences, MSC003-2040, Albuquerque, NM 87131-0001

Abstract
We introduce a new model of speleogenesis that incorporates supercritical CO$_2$, and represents an improvement on the basic CO$_2$ hypogene speleogenesis model. The supercritical CO$_2$ hypogene speleogenesis model explains both the origin of the spar caves and spar from the same geologic event and considers both the beginning (limestone dissolution) and end (spar precipitation) of these speleogenesis events that are coeval with regional magmatic events.

Introduction
Spar caves can be found throughout the Guadalupe Mountains of southeastern New Mexico and west Texas (Hill, 1987). These spar caves are essentially large dogtooth spar-lined geodes truncated by sulfuric acid speleogenesis in many cases, and exposed at the surface by erosion and stream down-cutting along entrenched meanders in other cases.

These caves are less than one to several tens of meters in diameter and are partially to entirely encrusted with scalenohedral (dogtooth) calcite spar (Figure 1). When did these spar caves form? What process or processes caused them to be found where they are? Why are they filled with giant crystals of calcite? There is little in the literature on how or when these spar caves formed and what exists is inadequate to explain the repeated cycles of spar cave speleogenesis and spar deposition that we now know to exist (Decker et al., 2015). Lundberg et al. (2000) published the first U-Pb age of a spar crystal from Big Canyon (90 Ma). They attribute the origin of the spar to tectonic activity and uplift during the Laramide. In this study we used U-Th-Pb and Sr isotope geochemistry to tease out the age and origin of these enigmatic voids.
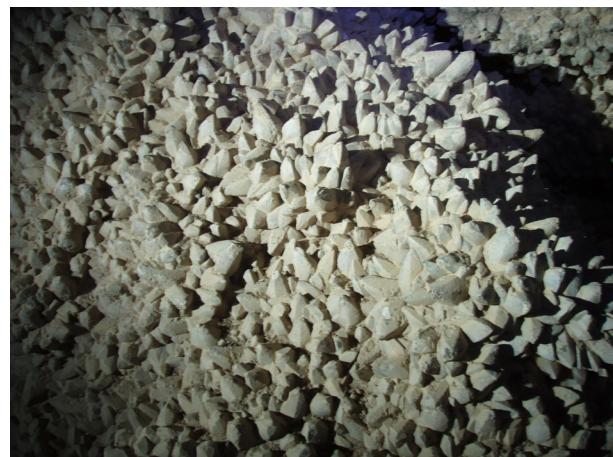
Figure 1.
Example of spar lining the walls of a Guadalupe Mountains cave. Spar crystals are approximately 4 cm in length.

Methods and Results
For this study, 18 different spar caves in the Guadalupe Mountains were visited in a variety of locations throughout the region (Figure 2). Twenty-seven spar samples were collected for U/Pb geochronology and Sr isotope geochemistry. All samples were previously broken, so no new damage was done to any of the sample sites. Elevation and location data for each spar sample was also collected. Of those, 22 samples had the appropriate U to Pb ratio, based on Thermo X-series mass spectrometer elemental analysis, to proceed with
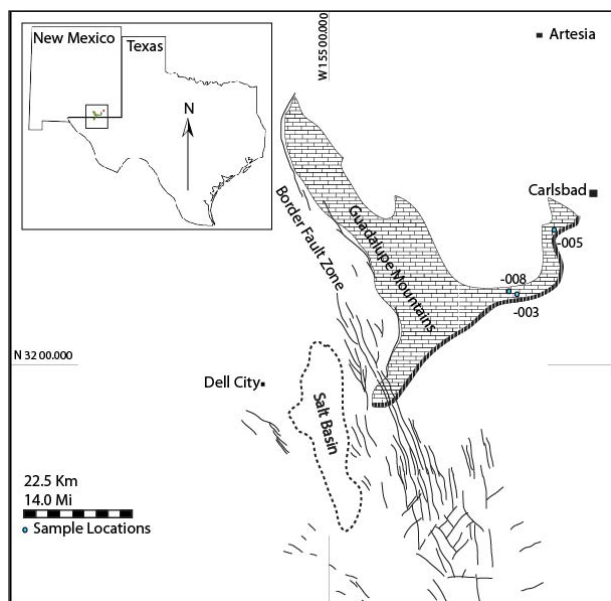
Figure 2.
Field area—Guadalupe Mountains, southeastern New Mexico and west Texas, USA. Sample locations are by sample number and approximate only.

U-Th-Pb chemistry and isotope analyses. Approximately 50 mg of each sample was taken from near the center of each crystal to avoid any surface contamination. These were cleaned in 3% HNO_3, weighed, then dissolved in 15 N HNO_3 and spiked with ^{205}Pb-^{229}Th-^{233}U-^{236}U mixed spike for U-Pb work, and spiked with ^{84}Sr spike for the Sr isotope analyses. The U-Th-Pb and Sr were separated from the calcite matrix using standard anion resin chromatography and Sr-spec resin. These samples were then introduced into the Thermo Neptune multi-collector inductively coupled plasma mass spectrometer (MC-ICPMS) at the University of New Mexico Radiogenic Isotope Laboratory to determine isotope ratios and abundances. U-Pb isochrons were calculated using Pb-Dat (Ludwig, 1993) to reduce the data from the MC-ICPMS and Isoplot (Ludwig, 2000) was used to produce the isochron ages.

U-Pb ages of these spar samples match the timing of the ignimbrite flare-up (32 to 28 Ma); (Chamberlin et al., 2002). For example, sample BLMC-20122-005 from BLM-NM-060-030 cave yielded a U-Pb spar age of 29.28 ± 0.45 Ma and two other samples from Carlsbad Cavern used to determine depth of spar formation dated to 9.45 ± 0.14 Ma and 13.5 ± 0.52 Ma (Decker et al., 2015). Sr-isotope values of our cave spar in the range of 0.709 to 0.716 are consistent with fluid that shows evidence of mixing with brines that were in equilibrium

with basement rock rather than the Permian limestone (0.707) (Burke et al., 1982) and indicate a deeper origin for the spar.

When the elevation and location data were plotted against the distance from Carlsbad Springs (an artesian spring where the Capitan aquifer intersects the surface) in the town of Carlsbad, NM, and then rotated 1.3° southwest to restore the Guadalupe Mountains tectonic block to a level elevation, all of the sample locations were within 250 m in elevation of each other (Figure 3), which is half the thickness of the cave-forming strata that includes the Capitan reef and the immediately adjacent backreef and forereef limestones and dolostones (approximately 500-750 m) (Harris and Grover, 1989; Hill, 1996; Zimmerman, 1962).

Discussion and Conclusion

The current CO_2 hypogene speleogenesis model explains dissolution and precipitation of deeply formed, usually single-chambered caves using standard knowledge about the amount of CO_2 that can be held in solution, which is determined by the temperature and pressure of the water (Andre and Rajaram, 2005; Dublyansky, 2000). Cooler water can hold more CO_2, so as water cools towards shallower depths, its increased CO_2 partial pressure results in more acidic conditions and can dissolve more limestone. At shallower depths (i.e., 500 m), the pressure is reduced to the point where CO_2 begins to degas so that the water becomes alkaline and precipitates the calcite. This model cannot adequately explain the deposition of cave spar in the voids left behind by dissolution without invoking a reduction in the head of the water column. It also does not explain what happens to the CO_2 in the warmer, deeper brines (beyond that, it is less corrosive), or even necessarily where the CO_2 originates (magmatic origin, hydrocarbons, or de-carbonation of limestone). A model that accounts for both the dissolution of the spar caves and the spar itself, and that does not require a lowered water table, is needed to explain cave spar speleogenesis. This model must also explain the origin and route travelled of the CO_2 to the spar cave/spar crystal forming depths.

We have been able to directly measure the depth of spar formation from three samples, one from the Grand Canyon and two from the Guadalupe Mountains.

In the Grand Canyon, we dated a spar crystal from a small cave in the Redwall Limestone at 232 Ma. Assuming no unknown unconformities in the Grand Canyon strata, we can say that at 232 Ma the Chinle Formation was being deposited in a fluvial estuarine environment at or near sea level (inter-bedding of
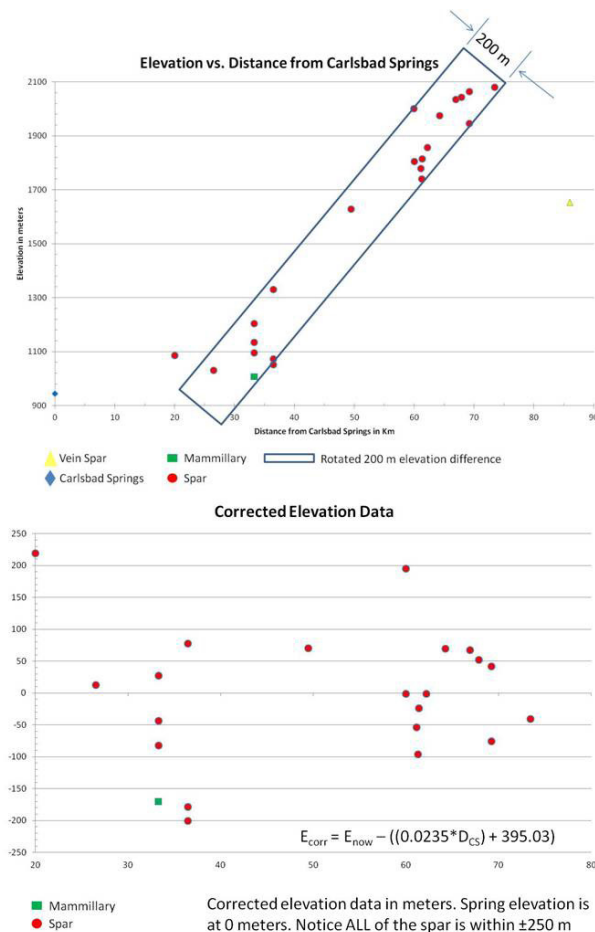
Figure 3.
Elevation and location data plotted from Carlsbad Spring in Carlsbad, NM. When the elevation data is restored to horizontal, all data points are within 250 m of each other.

shallow marine and near-sea-level fluvial deposits). The Chinle is approximately 750 m stratigraphically above the Redwall Limestone spar cave. Since the spar was forming at the same time the Chinle was being deposited, we can infer that it was precipitating from solution at approximately 750 m below the water table (Decker et al., 2015).

The depth of origin of two spar crystals (samples CAVE-02399-003 and CAVE-02399-008 from the Bell Room and New Mexico Room respectively) in different areas of Carlsbad Cavern have been determined using alunite dates from Carlsbad Cavern (Polyak et al., 1998). Alunite is a hydrous K-sulfate mineral formed by the sulfuric acid speleogenesis process at or near the water table. Interpolating the depth of the water table based on the ages of alunite samples from Carlsbad Cavern and then comparing that to the age and depth of the

spar samples from nearby locations shows that these spar crystals grew at depths of 360 m (New Mexico Room spar) and 700 m (Left Hand Tunnel spar) below a preexisting water table (Figure 4).

These three depths (750, 700, and 360 m) are all depths within the range of the transition from supercritical CO_2 (scCO_2) to subcritical CO_2 (subCO_2). This occurs at 500 ± 250 m below the water table depending on both geothermal gradient and hydrostatic pressure (or overpressure, as the case may be) (Decker et al., 2015). This transition occurs at $31.1°C$ and 7.4 MPa (André et al., 2007; Domingo et al., 2004; Kharaka et al., 2006), and this transition region can move up or down as local or regional temperature and pressure changes occur with new or waning magmatism and/or basin filling or denudation. In areas like the Basin and Range, where tensional forces are dominant, decompression melting occurs quite easily. When melting occurs at these depths, the magma degasses releasing CO_2 interpreted here to be in the supercritical state (Lowenstern, 2001). ScCO_2 is much less dense and less viscous than water, and moves rapidly through the pore spaces of the rock until it encounters the basinal brines where it is dissolved into the pore fluids (Heinrich et al., 2003). If enough scCO_2 is generated, it can displace the brine. At the brine/scCO_2 interface, dissolution of carbonate rock is intense enough to form caves (Andre et al., 2010). A model has been proposed, based on our depths of origin of spar crystals that corresponds to the depth of scCO_2-subCO_2 transformation, that uses this CO_2 process to explain the origin of the spar caves (Decker et al., 2015). With many samples having spar ages that are coeval with the ignimbrite flare-up, the model also suggests that scCO_2 speleogenesis is related to magmatic activity and is therefore probably relatively short-lived (i.e., 1-2 Ma). This scCO_2 speleogenesis model has the retreating brine that carries the dissolved carbonate with it leaving void spaces which are then filled with scCO_2. As magmatic activity wanes, generation of scCO_2 declines and eventually the brines return to fill the voids of scCO_2 dissolution. These brines are still super-saturated with scCO_2, but as the temperature decreases, the scCO_2/subCO_2 transition zone moves downward. This causes an increase in subCO_2 partial pressure and a corresponding degassing of the brines, lowering the CO_2 content as well as the capacity of the brines to hold dissolved $CaCO_3$ (Moore et al., 2005; Spycher et al., 2003). At this point, calcite begins to precipitate slowly, and at these temperatures and pressures, scalenohedral spar is the most likely crystal form to occur (Domingo et al., 2004). The model explains both the origin and timing of origin of both the spar caves and the cave spar.
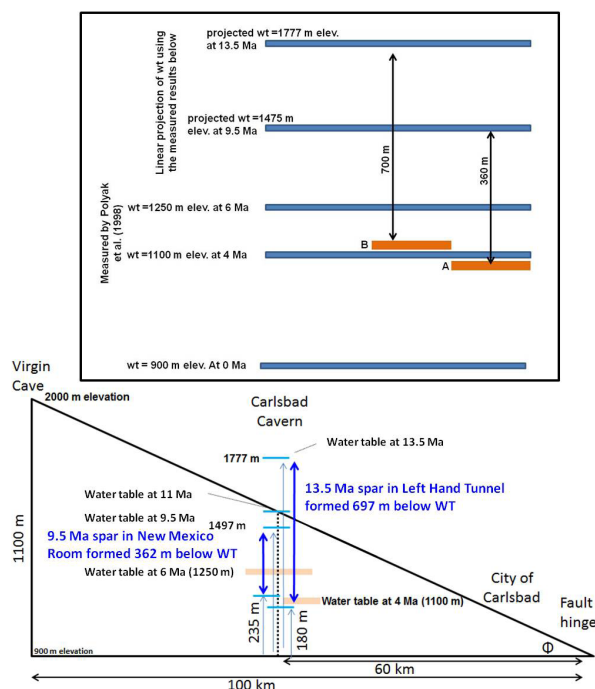
Figure 4.

Top: depths of formation for the two youngest cave spar sites are based on measured water table elevations at 6 and 4 Ma by Polyak et al. (2008) for cave sites in Carlsbad Cavern and Lechuguilla Cave, Guadalupe Mountains. Bottom: a linear projection of water table elevations at 9.5 and 13.5 Ma from those results.

In the top diagram, A = elevation of the 9.5 Ma cave spar, and B = elevation of the 13.5 Ma cave spar. wt = water table. In the bottom diagram, the same results are acquired when a fault hinge is projected and an angle of tilt (Φ) is calculated over the period of faulting.

All of this is consistent with the plotted elevation and location data for each of the samples, that, when rotated back to a horizontal position, place all of the spar samples within 250 m of each other, and by our model, 500 m beneath the Ochoan evaporite which may have comprised the paleo-land surface at approximately 30 Ma. This new CO_2 hypogene speleogenesis model describes the origin and travel of the CO_2 and the process which dissolves the voids and precipitates the spar crystals and improves the understanding of this highly complicated regime without having to invoke multiple stages of water table movement over several hundred meters and tens of millions of years.

References

Andre BJ, Rajaram H. 2005. Dissolution of limestone fractures by cooling waters: early development of hypogene karst systems. Water Resources Research 41 (1).
http://dx.doi.org/10.1029/2004WR003331

André L, Audigane P, Azaroual M, Menjoz A. 2007. Numerical modeling of fluid–rock chemical interactions at the supercritical CO_2–liquid interface during CO_2 injection into a carbonate reservoir, the Dogger aquifer (Paris Basin, France). Energy Conversion and Management 48 (6): 1782-1797.
http://dx.doi.org/10.1016/j.enconman.2007.01.006

Andre L, Azaroual M, Menjoz A. 2010. Numerical simulations of the thermal impact of supercritical CO_2 injection on chemical reactivity in a carbonate saline reservoir: Transport in Porous Media 82 (1): 247-274.
http://dx.doi.org/10.1007/s11242-009-9474-2

Burke WH, Denison RE, Hethreington EA, Koepnick RB, Nelson HF, Otto JB. 1982, Variations of seawater [87]Sr/[86]Sr throughout Phanerozoic time. Geology 10 (10): 516-519.

Chamberlin RM, Chapin CE, McIntosh WC. 2002. Westward migrating ignimbrite calderas and a large radiating mafic dike swarm of Oligocene age, central Rio Grande Rift, New Mexico: surface expression of an upper mantle diapir? Geological Society of America Annual Meeting; 2002 Oct. 27-30; Denver, CO. Paper No. 191-21

Decker DD, Polyak VJ, Asmerom Y. 2015. Depth and timing of calcite spar and 'spar cave' genesis: implications for landscape evolution studies. Geological Society of America, GSA Special Publication 516 - Caves and Karst Across Time.

Domingo C, García-Carmona J, Loste E, Fanovich A, Fraile J, Gómez-Morales J. 2004. Control of calcium carbonate morphology by precipitation in compressed and supercritical carbon dioxide media. Journal of Crystal Growth 271 (1): 268-273
http://dx.doi.org/10.1016/j.jcrysgro.2004.07.060

Dublyansky YV. 2000. Dissolution of carbonates by geothermal waters. In Klimchouk AB, Ford DC, Palmer AN, Dreybrodt W, editors. Speleogenesis - evolution of karst aquifers. Huntsville (AL): National Speleological Society. p. 158-159.

Harris PM, Grover GA. 1989. Subsurface and outcrop examination of the Capitan shelf margin, northern Delaware basin. San Antonio (TX): Society of Economic Paleontologists and Mineralogists.

Heinrich JJ, Herzog HJ, Reiner DM. 2003. Environmental assessment of geologic storage of CO_2. Second National Conference on Carbon Sequestration; 2003 May 6; Washington, D.C.

Hill CA. 1987. Geology of Carlsbad Cavern and other caves in the Guadalupe Mountains, New Mexico and Texas. Socorro (NM): New Mexico Bureau of Mines and Mineral Resources.

Hill CA. 1996. Geology of the Delaware Basin, Guadalupe, Apache and Glass Mountains, New Mexico and West Texas. Albuquerque (NM): Permian Basin Section - SEPM.

Kharaka Y, Cole D, Hovorka S, Gunter W, Knauss K, Freifeld B. 2006. Gas-water-rock interactions in Frio Formation following CO_2 injection: implications for the storage of greenhouse gases in sedimentary basins. Geology 34 (7): 577-580. http://dx.doi.org/10.1130/G22357.1

Lowenstern JB. 2001. Carbon dioxide in magmas and implications for hydrothermal systems. Mineralium Deposita 36 (6): 490-502. http://dx.doi.org/10.1007/s001260100185

Ludwig KR. 1993. PBDAT: a computer program for processing Pb-U-Th isotope data. US Geological Survey Open-File Report 88-542.

Ludwig KR. 2000, User's manual for Isoplot/Ex version 2.2: a geochronological toolkit for Microsoft Excel. Berkeley (CA): Berkeley Geochronology Center.

Lundberg JL, Ford DC, Hill CA. 2000. Preliminary U-Pb Date on cave spar, Big Canyon, Guadalupe Mountains, New Mexico, USA. Journal of Cave and Karst Studies 62 (2): 144-148.

Moore J, Adams M, Allis R, Lutz S, Rauzi S. 2005. Mineralogical and geological consequences of the long-term presence of CO_2 in natural reservoirs: an example from the Springerville-St. Johns Field, Arizona, and New Mexico, U.S.A. Chemical Geology 217 (3/4): 365-385. http://dx.doi.org/10.1016/j.chemgeo.2004.12.019

Polyak VJ, McIntosh WC, Necip G, Provencio P. 1998. Age and origin of Carlsbad Cavern and related caves from [40]Ar/[39]Ar of alunite. Science 279 (5358): 1919-1922. http://dx.doi.org/10.1126/science.279.5358.1919

Spycher N, Pruess K, Ennis-King J. 2003. CO_2-H_2O mixtures in the geological sequestration of CO_2. I. Assessment and calculation of mutual solubilities from 12 to 100°C and up to 600 bar. Geochemica et Cosmochimica Acta 67 (16): 3015-3031. http://dx.doi.org/10.1016/S0016-7037(03)00273-4

Zimmerman JB. 1962. Permian of the Central Guadalupe Mountains, Eddy County, New Mexico, West Texas. Roswell and Hobbs Geological Society Guidebook, Publication 62-48.

CLIMATE, SEA LEVEL CHANGES, AND DEEP KARST

Shouyue Zhang
Institute of Geology and Geophysics
Chinese Academy of Sciences
Beijing, 100029, China, syzhangjin822@163.com

Yuzhang Jin
Institute of Geology and Geophysics
Chinese Academy of Sciences
Beijing, 100029, China

Abstract

Karst base level changes are relative to neotectonic movement and sea level change. A chapter of *Deep karst and depth of karstification* has been discussed in the "Research of China Karst" (1979, 1987). The stages of karst base levels show neotectonic movements since the Cenozoic in Anhui Province of east China. Sea level changes related to karst processes since the Pleistocene still must be solved. Quaternary sea level history reveals that the level of the ocean has been beneath its present height for most of the past several hundred thousand years. Karst has therefore generally evolved in response to lower base levels than at present. As a result, geomorphological evidence of past sea level changes isn't preserved in coastal karst areas. Records of changing climate from carbon dioxide, temperature, and sea levels from human presence 400,000 years ago provide useful information here. According to these records, about 300,000 years ago, sea level was 40 m lower than today. Sea levels were even lower during the glacial period, by about 100-120 m. During the last interglacial period about 12,500 years ago, sea level was 4 or more meters higher than today. Karst base levels were even lower or further from the sea than today's levels.

The minimum time needed for speleogenesis is believed to be 5-20 ka up to 100 ka. Cave systems may be formed in a short duration and deepened by the cause of glaciologist-eustatic sea level changes, such as during the Late Quaternary period. Examples of deep karst phenomena include:

- Along the eastern Adriatic coast, a number of submerged karst phenomena have been found due to the recent (Q3-Q4) sea level rise of 120 m. A submarine cave is located on the southwest coast of the Dugi Otok Island, Croatia. Caves and sinkholes are common below sea level. Most of them were formed under subaerial conditions during periods of lower sea levels.

- Flooded collapse dolines or depressions and submarine cave systems in Florida, USA; Yucatan, Mexico; and southeast Australia are the products of subaerial karst processes.
- The tower karst in Ha Long Bay, Vietnam and Phuket Island in the southwest Gulf of Siam, Thailand are karst fenglin (peak forest) flooded by sea level rise.
- A blue hole located on the atoll of Jinqin Island. It is 290 sea kilometers from Hainan Province, China. A diver went into the blue hole to a depth of 40 m and found it another 40 m deep by sonar.

Karst processes are affected by numerous thresholds and agents including geological conditions (lithology, geotectonic and geological structure, and neotectonic movement), karst hydrogeological texture (aquifer and aquifuge, hydrodynamic and hydrochemical fields, and hydrological balance and regime), and climatic conditions (climatic zone and index, temperature, precipitations, and water volumes). Epigenic karst by sea level rise could be found deeper than normal in carbonate rock massifs, even far from modern sea coasts.

POSTER SESSION

MORPHOMETRIC ANALYSIS OF LIMESTONE HYPOGENE CAVES IN THE WESTERN UNITED STATES

Patricia Kambesis
Center for Human Geo-Environmental Studies
Department of Geography and Geology
Western Kentucky University
Bowling Green, KY 42101, pat.kambesis@wku.edu

Joel D. Despain
Mendocino National Forest
825 N. Humboldt Avenue
Willows, CA 96008, jddespain@fs.fed.us

Abstract
Hypogene caves are identified by hydrogeological setting, and a combination of features including characteristic mineralogies, meso-morphological features, and overall cave footprint. Research emphasis has been on identifying hydrological settings, characteristic mineral suites, and meso-morphological features. Though the morphological footprint of a cave is included in the list of hypogene identifiers, little work has been done to actually quantify the footprint of hypogene caves. Using fractal analysis of cave patterns, we quantitatively described the three-dimensional footprints of a set of limestone caves of known hypogene origin from the western United States (US). Our preliminary results show that different hypogene processes may produce distinct caves patterns that can be quantified by ranges of fractal indices. The fractal indices do not define process or predict speleogenetic outcomes but do identify cave patterns that are characteristic of specific processes and speleogenetic conditions. With the appropriate consideration of geological and hydrogeological context, the morphological footprint of caves as described by fractal indices may be used to augment the identification and differentiation of hypogene speleogenic processes.

Introduction
Hypogene caves are formed in a variety of geological and tectonic settings by different dissolutional mechanisms that operated on various rock types (Klimchouk, 2009). Despite these differences, hypogene caves display similarity in the morphology of their internal features. However, the mineralogical contents of the cave can vary depending on the hypogene process that formed the cave and the spatial and temporal relationship to a paleo-water table (Poylak et al., 2014).

In the western US, two types of hypogene speleogenesis have been identified for limestone caves: $H_2S-H_2SO_4$-dominated speleogenesis that takes place near a paleo-water table and CO_2-dominated speleogenesis that occurs tens to hundreds of meters below a paleo-water table that can be later overprinted by epigene processes (Poylak et al., 2014). Palmer (1991, 2007, 2011) showed that mode of recharge and bedrock structural properties determined overall cave patterns (morphological footprint) and passage relationships in karstic caves; hence, morphological footprints are a strong indicator of the processes that formed a given cave.

Though the morphological footprint of a cave may act as hypogene speleogenesis identifier, little work has been done to actually quantify the (three-dimensional) footprint of hypogene caves. The purpose of our research was to use fractal indices to analyze the morphological footprint of a set of known limestone hypogene caves located within the western US to determine if different hypogene processes produced distinct morphological footprints.

As with other shapes and forms in nature, cave morphologies are heterogeneous and display to some degree self-similar, irregular, and fragmented geometries which by definition make them fractals (Curl, 1986). Fractal indices have been utilized to calculate cave length, characterize individual cave morphologies, and identify spatial distributions (Curl, 1986; Laverty, 1987; Florea and Wicks, 2001; Pardo-Iguizquiza et al., 2011; Pardo-Iguizquiza et al., 2012). Kambesis et al. (in press) (Figure 1) showed that cave patterns, such as some of those described by Palmer (2011), could be differentiated based on analysis of their fractal geometry and ascertained that distinct cave morphologies displayed characteristic ranges of fractal indices.
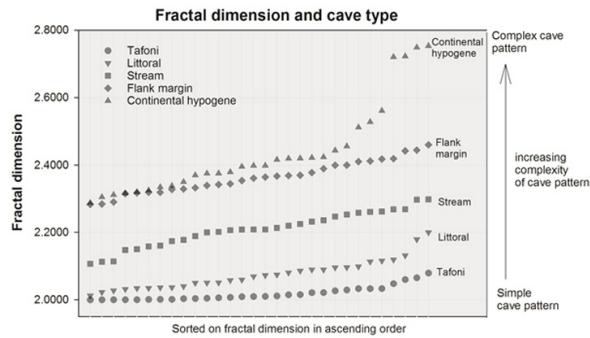
Figure 1.
Fractal dimension vs. cave type.

Methods

The data used in the fractal analyses was three-dimensional digital cave survey data. Cave data was converted either to 3-D shape files or to digital bitmap images depending on the vertical extent of the cave. Three software packages were utilized for image processing and fractal analysis. ArcScene10.2® was used to produce 3-D grayscale image files from the caves with less than 10 meters of vertical extent. Caves with vertical extent of greater than 10 meters were sliced into vertical layers or stacks of equal value, and each layer exported as a grayscale bitmap image for compilation by the image processing software. Fractal dimension was calculated using FRACTAL© version 3.4.7, which can process individual grayscale bitmap files or stack-series files

Fractal dimension was calculated through the box-counting method, which analyzes the complexity and texture of the perimeter of the digital pattern by determining pixel distribution and density over multiple iterations conducted at ever-decreasing box resolutions. Data resolution for both fractal indices was recorded to 10-4 in order to capture subtle variations between cave morphology.

Results

Table 1 lists the fractal dimensions for the caves analyzed. The mode of hypogene speleogenesis had already been determined by other researchers (Hill, 2000; Palmer and Palmer, 2009; Polyak et al., 2014). Cave morphological footprint increases in complexity as fractal dimension increases as illustrated in Table 1. The quantitative morphological distinction between caves of different hypogenic origin proved to be statistically significant, via a t-test.

Discussion

In general, caves formed by sulfuric acid speleogenesis (SAS) had a more complex morphological footprint than caves formed by CO_2-dominated speleogenesis. The quantitative morphological distinction between caves of different hypogenic origin proved to be statistically significant (via a t-test) so the implications are that different modes of hypogene development are expressed in the morphological footprint of the cave.

Though fractal indices are not direct indicators of specific processes or geologic and hydrogeological conditions, they do identify patterns and ranges of patterns that may be characteristic of processes, or geological and hydrological conditions.

The cave patterns with the greatest values for fractal dimension (Wind, Jewel, Lechuguilla, and Carlsbad Cavern) all share the characteristic of being polygenetic. Caves that are polygenetic have undergone multiple stages of development, some of which may overprint earlier morphologies. Figure 1 lists specific caves analyzed in this study with the highest fractal dimensions. These caves rank among the longest and most complex cave systems in the world. All caves are polygenetic to some degree, but the largest cave systems show this tendency to a greater extreme.

Conclusion

Fractal analyses were calculated for a set of limestone caves of known hypogene origin from the western United States (Halliday, 1954; Despain, 2004). The statistical analyses showed that the differences in cave patterns as identified by fractal indices proved to be significant between the subset of cave types analyzed for this study.

Cave pattern complexity is reflected in the fractal dimension calculated for each cave. SAS cave patterns have the most complex morphologies.

The cave patterns with the highest fractal dimension within their groups all share the characteristic of being polygenetic. Polygenetic caves are the result of multiple stages and sometimes multiple processes of cave development. All caves are polygenetic to some degree, but the largest and oldest cave systems show that tendency to the extreme and should be treated as multifractals.

Summary

This study was a proof-of-concept for the idea that fractal indices could be used to describe and differentiate cave types. The method for determining fractal indices involved converting three-dimensional cave data to digital images that were analyzed by pattern recognition software. Fractal indices were

calculated using box counting algorithms. The quantitative morphological distinctions in cave patterns as identified by fractal dimension proved to be statistically significant within the subset of cave types analyzed for this study.

Fractal indices do not define process or predict speleogenetic outcomes, but do identify cave patterns that are characteristic of specific processes and speleogenetic conditions. As long as geological and hydrogeological context are taken into consideration, cave pattern morphology as described by fractal indices could be used to augment the identification and differentiation of karstic processes and conditions that formed them.

References

Curl RL. 1986. Fractal dimensions and geometries of caves. Mathematical Geology 18 (2): 765-783. http://dx.doi.org/10.1007/BF00899743

Despain JD. 2004. Hidden beneath the mountains – caves of Sequoia and Kings Canyon National Parks. Dayton (OH): Cave Books.

Florea LJ, Wicks CM. 2001. Solute transport through laboratory-scale karstic aquifers. Journal of Cave and Karst Studies 63: 59-66.

Halliday WR. 1954. Basic geology of Goshute Cave, Nevada: Technical Note #12, Salt Lake City Grotto. National Speleological Society.

Hill CA. 2000. Overview of the geologic history of cave development in the Guadalupe Mountains, New Mexico. Journal of Cave and Karst Studies 62 (2): 60-71.

Klimchouk A. 2009. Morphogenesis of hypogenic caves. Geomorphology, May 2009. http://dx.doi.org/10.1016/j.geomorph.2008.09.013

Laverty M. 1987. Fractals in karst. Earth Surface Processes and Landforms 12: 475-480. http://dx.doi.org/10.1002/esp.3290120505

Palmer AN. 1991. Origin and morphology of limestone caves. Geological Society of America Bulletin 103: 1-25. http://dx.doi.org/10.1130/0016-7606(1991)103<0001:OAMOLC>2.3.CO;2

Palmer AN. 2007. Cave geology. Dayton (OH): Cave Books.

Palmer AN. 2011. Distinction between epigene and hypogene maze caves. Geomorphology 134: 9-22. http://dx.doi.org/10.1016/j.geomorph.2011.03.014

Pardo-Iguzquiza E, Dowd PA, Xu C, Duran-Valsero JD. 2012. Stochastic simulation of karst conduit networks. Advances in Water Resources 35: 141-150. http://dx.doi.org/10.1016/j.advwatres.2011.09.014

Pardo-Iguzquiza E, Duran-Valsero JD, Rodriguez-Galiano V. 2011. Morphometric analysis of three-dimensional networks of karst conduits. Geomorphology 132: 17-28. http://dx.doi.org/10.1016/j.geomorph.2011.04.030

Table 1.

Select Limestone Caves of Hypogene Origin - Western United States.

Cave	State	Area	Fractal Dimension	
Premonition	CO	White River Plateau	2.2877	CO2
Goshute	NV	Goschute Canyon Wilderness	2.2901	CO2
Empire Mine	CA	Sequoia Kings Canyon	2.2978	CO2
Ancient Palace	CA	Shasta Trinity National Forest	2.2738	CO2
Cave of Winds	CO	Williams Canyon	2.3162	CO2
Lewis and Clark	MT	Northern Rockies	2.3175	CO2
Groaning	CO	White River Plateau	2.3201	CO2
Lehman Cave	NV	Great Basin	2.3249	CO2
Narrows	CO	Williams Canyon	2.3382	CO2
Pedros	CO	Williams Canyon	2.3442	CO2
Fixin-to-Die	CO	White River Plateau	2.3491	C02
Hubbards	CO	Glenwood Canyon	2.3499	CO2
Huccacove	CO	Williams Canyon	2.3592	C02
McKittrick	NM	McKittrick Hill	2.3659	SAS
Breezeway	CO	Williams Canyon	2.3754	C02
Bighorn/Horsethief	WY/MT	Northern Rockies	2.3846	SAS
Porcupine	SD	Black Hills	2.3953	C02
Slaughter Canyon	NM	Guadalupe Mtns	2.3984	SAS
Sand Cave	NM	Guadalupe Mtns	2.4031	SAS
Spider	NM	Guadalupe Mtns	2.416	SAS
Bethlehem	SD	Black Hills	2.4198	C02
Three Fingers Cave	NM	Guadalupe Mtns	2.4217	SAS
Yellowjacket	NM	Guadalupe Mtns	2.4238	SAS
Endless	NM	Guadalupe Mtns	2.4557	SAS
Virgin	NM	Guadalupe Mtns	2.4886	SAS
Dry Cave	NM	Guadalupe Mtns	2.5118	SAS
Fairy	CO	Glenwood Canyon	2.5278	SAS
Carlsbad	NM	Guadalupe Mtns	2.7208	polygenetic
Jewel	SD	South Dakota	2.7227	polygenetic
Wind	SD	South Dakota	2.7488	polygenetic
Lechuguilla	NM	Guadalupe Mtns	2.7536	polygenetic

IBERGER TROPFSTEINHÖHLE, IBERG, HARZ MOUNTAINS, GERMANY: HYPOGENE MORPHOLOGY AND ORIGIN BY SIDERITE WEATHERING

Stephan Kempe

Institute for Applied Geosciences, Technische Universität Darmstadt
Schnittspahnstr. 9
D-64287 Darmstadt, Germany, kempe@geo.tu-darmstadt.de

Ingo Bauer

Institute for Applied Geosciences, Technische Universität Darmstadt
Schnittspahnstr. 9
D-64287 Darmstadt, Germany, bauer@geo.tu-darmstadt.de

Ortrud Krause

HöhlenErlebnisZentrum Iberger Tropfsteinhöhle
An der Tropfsteinhöhle 1 (B 242)
D-37539 Bad Grund (Harz), Germany, ortrud.krause@hoehlen-erlebnis-zentrum.de

Abstract

The Iberger Tropfsteinhöhle is one of the smaller show caves in Germany developed in Devonian massive limestone. It is composed of four separate cavities that are connected by artificial tunnels. We re-surveyed these with a 3D Faro 120 Scanner to document the caves' morphology. It is dominated by sloping side-walls ("facets") and stacked, upward-directed, concave cupolas, indicative of a phreatic origin by slowly convecting density currents. Three of the cavities contain or contained goethite (FeO-OH) loam, a high-grade iron ore that was mined in the Iberg for centuries. It originates from siderite ($FeCO_3$) weathering due to oxidation. Thereby, CO_2 is liberated at depths that can dissolve isolated cavities around and above the siderite deposit, a process to be included in various forms of hypogene cave genesis. The show cave is only a very small example of an extensive cave and mine system known as the Eisenstein-stollen-System, which comprises an estimated 8 km of passages. This mélange of natural caves, mined cavities, and mine tunnels is concentrated in a section (250 m wide by 250 m long) on the southeast side of the Iberg, the site of the former siderite lode. Cave formation could not have started until the top of the Iberg was exposed, so that oxygen-charged seepage water could react with the siderite. Once the valleys around the Iberg started to cut down, the water level dropped in stages. Two of these stages are documented in the cave as negative (undercutting) water level marks, about 5 m vertically apart. A newly dated stalagmite yielded an age of 400 ka equivalent to the interglacial MIS 11 (Holsteinian). At that time, the caves must have latest fallen dry.

Introduction

The Iberger Tropfsteinhöhle (Iberg Dripstone Cave) (Kempe et al., 1985) is one of about 50 show-caves of Germany (Kempe, 1982; Döppes et al., 2008). It is one of the smaller German show caves, situated on the SE side of the Iberg in the western Harz Mountains. There, an estimated 8 km of passages exist within an area of about 250 m². Many of these passages are accessible today through the Eisenstein-stollen, situated below the Iberger Tropfsteinhöhle. Due to the mining of iron ore over several centuries, these caves were discovered and connected by mine passages. Because of this, an exact length or volume of natural versus artificial cavity cannot be given. The show cave features four independent cavities, two of which had originally been accessed by miners (Figure 1). Today, the caves are connected by 200-m-long access galleries. The larger of the three caves is listed with a length of 123 m and an altitude difference of 27 m. It forms a loop due to a short artificial connection. It contains some flowstone, unlike most of the other caves in the quadrant. The morphology of these caves testify to their hypogene origin, a feature displayed by many of the German show caves (Kempe, 2014), but it is the only one generated by siderite weathering. This makes the cave unique, possibly globally (Kempe, 1975).
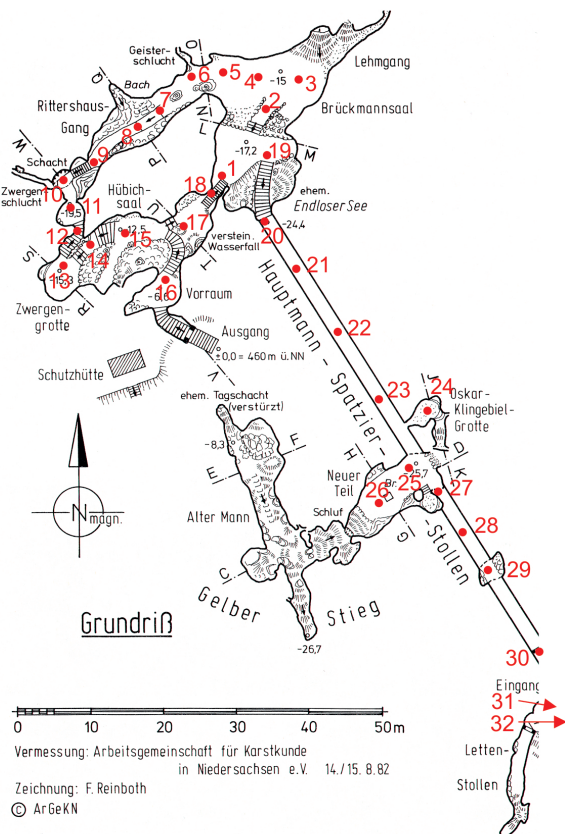
Figure 1.
*Ground plan of the Iberger Tropfsteinhöhle.
It shows the three sections "Gelber Stieg,"
"O. Klingebiel Grotte," and the "Iberger
Tropfsteinhöhle" proper (in the north)
connected by the "Hauptmann Spatzier
Stollen" from 1911, here corrected in length
to the new scan-survey (plan altered after
Kempe et al., 1985; drawing by F. Reinboth).*

The Iberger Tropfsteinhöhle (Iberg Dripstone Cave)

A Former Coral Reef

An impressive limestone massif rises above the mining town of Bad Grund, covering an area of about 1.5 km[2] and consisting of two mountains, the Iberg and the adjacent Winterberg (Figure 2). The Winterberg has been quarried for limestone since 1939, but the Iberg is protected. They are Middle to Upper Devonian reef bodies composed of "Massenkalk" (massive limestone). The reef started growing 385 million years ago south of the equator at about the latitude of present-day Madagascar, and was probably about 600 m thick. Today it is surrounded by Carboniferous shales and massive greywackes.
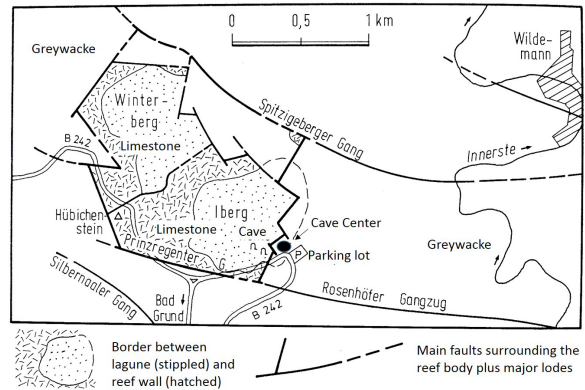
Figure 2.
*Tectonic overview map of the Iberg/
Winterberg and the situation of the Iberger
Tropfsteinhöhle ("Cave") west of the parking
lot (after Kempe et al., 1985; altered after
Franke, 1973).*

Reef organisms include stromatopores, rugose, and tabulate corals and contributions by crinoids, brachiopods, and cephalopods. Most of the limestone is micritic limestone, possibly of cyanobacterial origin.

Until recently, the Iberg was interpreted as an atoll with a reef wall enclosing a shallow lagoon and covering an area of some 5 km[2]. It was further assumed that the former top of the reef, the present Winterberg, was sheared off to the north when the Harz Mountains were thrusted up (e.g., Franke, 1973; Gischler, 1992). However, unexpected fossil finds, tectonic considerations (Heydecke, 2011), and observations in the quarry since 2012 (Knolle et al., 2008; Knappe, 2014; Meischner, 2014) have caused a reconsideration of this model. These observations not only confirm a repeated karst influence during the Lower Carboniferous and younger stages of karst leading to younger sediment fills within the Devonian limestone, but also interpret the Winterberg as an elongated structure interrelated with the Iberg reef.

During the Kellwasser Event 370 million years ago, at the Frasnium/Famennium boundary, the reef-growth stopped worldwide (e.g., Joachmisky and Buggisch, 1993), most likely by an overturn of the anaerobic ocean (e.g., Kempe and Kazmierczak, 1994). After the Iberg reef perished, it became an island with marginal splash-karst and subaerial epigene karst and repeated inundations depositing thin Lower Carboniferous carbonate layers characterized by goniatites, trilobites, or brachiopods (Knappe, 2014). Later, the island was covered with siliciclastic sediments, massive greywacke, and slate deposits that still surround the Iberg today.

Ongoing tectonic stress led to fractures in the reef body filled with sediment (sedimentary dikes).

During the Variscan orogeny about 300 million years ago, the rigid block of Iberg limestone resisted folding but was affected by faults. The resulting fissures played an important role in the later development of ore deposits and caves in the Iberg. But before these came into being, the Harz Mountains were transgressed once more by the Permian Zechstein Sea.

The Iberg limestone not only provided the possibility of cave formation, but also a locality where more than 40 different minerals occur. These minerals were deposited in the Mesozoic when mineral-containing waters rose into the fissures. Iron-containing water gave rise to the formation of large masses of iron carbonate (siderite) in connection with barite and quartz veins.

When the present Harz was uplifted during the Upper Cretaceous and the Cenozoic, the Iberg reached the zone of oxygenic ground water. This started the conversion of siderite to goethite and limonite.

Siderite Weathering

The astounding cave density on the SE side of the Iberg remained a speleogenetic riddle for a long time, until 1971, when it was first suggested that siderite wreathing may have been its cause (Kempe, 1971, 1975, 1998, 2008, 2009; Svensson and Kempe, 1989).

The basic reaction is the oxidation of the ferrous carbonate siderite to a ferric oxy-hydroxide (goethite) according to:

$$4FeCO_3 + O_2 + 6H_2O \rightarrow 4FeO(OH) + 4HCO_3^- + 4H^+ \rightarrow 4FeO(OH) + 4H_2O + 4CO_2$$
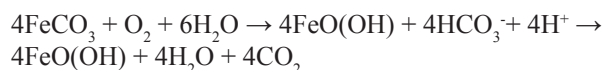
The reaction produces protons and/or free CO_2. These can in turn attack surrounding limestone, thus generating solutional power deep below the water level and around the siderite lodes. Svensson (1988) showed that this process is continues today (Svensson and Kempe, 1989). In a small pond left by mining in the Eisenstein-stollen-System, oxygen depletes downward and alkalinity increases, leaving characteristically colored deposits depending on the decreasing redox-potential. The Fe-content of siderite is 48.2% and the Goethite content is 62.85%. It is therefore a very valuable iron ore, even more so because of the ease of its removal due to its clay-like consistency.

Mining in the Iberg and its Caves

The Harz was a very important mining district until the second half of the 20th century. Mining was mostly concerned with copper, zinc, lead, and silver. Only in the Iberg was iron the focus, because goethite and limonite were easy to mine. Limonite was important because of its high manganese content, making it an excellent "steel ore." The siderite not oxidized to limonite occurs at greater depth and was mined only in the late 19th century.

The oldest iron slag found on the Iberg is more than 2,000 years old, making the Iberg one of the oldest exploited iron deposits in Central Europe. In the 13th century, the Iberg was probably the region's primary source of iron. Early miners worked near-surface cavities and fissures. Gradually, they widened them into mines, connecting natural cavities with artificial tunnels and shafts.

The Cistercian Monastery Walkenried on the southern edge of the Harz ranked among the most important medieval mine owners. It not only extracted copper and lead at the Rammelsberg, but also processed iron ore from the Iberg. Around 1500, its industrial area became the property of the Dukes of Braunschweig-Wolfenbüttel. Soon, numerous ironworks and steel forges were established at the foot of the Iberg in the town of Grund (today known as Bad Grund), the first of the seven free towns of Upper Harz mining. This led to the second golden age of mining at the Iberg, with 138 documented individual mines.

During the 18th century, the Iberg iron ores were seriously depleted. With increasing depth, mining became more strenuous, more expensive, and much more dangerous. Mining flourished for the last time in the 19th century. Even though the ore pillars that supported the cavities and the overlying rock were dug away, the development of safety structures was neglected. The cavities were finally filled in using public funds in 1855. After more than 2,000 years, mining in the Iberg was discontinued in 1885. In 1992, mining in Bad Grund ended altogether when the "Hilfe Gottes," a deep non-ferrous mine, stopped operating as Germany's last metal ore mine.

The Iberg was also the location of a large water management project, begun in 1528. A 2-km-long gallery was constructed, draining the Iberg mines. A ditch more than 3 km in length once supplied a pond with water to drive the water wheels in connection with the Upper Harz Water Management System (a UNESCO World Heritage Site since 2010).

The Show Cave

The first of the natural cavities today serves as a meeting point for a guided tour through the cave. It

was first entered by miners around 1500, when it was called "Gelber Stieg." Back then, half of the cavity was filled with earthy iron ore. The deposit was covered by flowstone, remains of which still mark the former level of the fill all around the cavity.

Around the same time, the miners probably also discovered the Iberg dripstone cave nearby. This cave is marked as "Baumann Cave" on older maps (not to be confused with the original Baumann Cave at Rübeland, Harz). It probably attracted little interest because it was largely devoid of iron ore deposits. But the flowstones glittering in the light of miners' lamps, ancient fossilized marine creatures, and the younger flowstones cascades and stalagmites may have given rise to the old legends about Hübich, the King of the Dwarfs, whose kingdom was said to be in the Iberg.

Many dripstones have been lost as "souvenirs" or "medicine" in former times. The most important flowstone figures in the cave are the petrified waterfall, the organ, the oven of the dwarfs or the wishing turtle, and the large stalagmite, among a few others. The foot of the large stalagmite was sampled in 2014 by the authors. It was U/Th dated by Dr. J. Fohlmeister at the University of Heidelberg by ICP-Q-MS (ThermoFischer, iCAP). The sample yielded an age of 399.5 +79 –50 ka. The large standard deviation is due to a very low uranium content. Nevertheless, the date coincides with the Interglacial MIS 11, the Holsteinian— a pronounced warm phase in Europe (e.g., Nitychoruk et al., 2006). Thus, the cave must have been above the groundwater table at least 400,000 years.

The physician and scientist Franz Ernst Brückmann was the first to describe the cave in 1734. To make the cave accessible for regular visitors, in 1871, stairs with 136 steps were installed and the floor was smoothed. Also, the two ends of the cave were connected by a short artificial stairwell, guiding visitors in a loop. Petrol lamps were used for lighting. In 1911, a 78-m-long access tunnel was driven into the lower end of the cave. It started at a natural abri that also served as shelter for waiting visitors. While this tunnel is not part of the present show cave, it was key in discovering the other two cavities (Gelber Stieg and O. Klingebiel Grotto). At the same time as the tunnel was first created, electric lighting was also installed. Thus, visitors could enter through the tunnel and leave the cave through the historic entrance higher up on the mountain.

In 2008, a second access tunnel was dug, so now visitors enter at the level of the parking lot behind a new museum and the HöhlenErlebnisZentrum (Cave Experience Center). The cave was also furnished with LED lighting in 2013.

The HöhlenErlebnisZentrum (Cave Experience Center)

Since 2008, the Cave Experience Center has been important for local tourism. It is a new visitor magnet in the Harz. Designed for the young and old, amateurs and specialists, it offers a vivid encounter with the history of the Earth and of humanity, highlighting fascinating aspects of European cave archaeology. The upper floor is dedicated to sensational discoveries at the Lichtenstein Cave, a gypsum cave 15 km away. Lichtenstein Cave was used as a burial cave for a late Bronze Age family clan nearly 3,000 years ago. The life and death of the clan is illustrated by diverse objects like bronze jewellery, glass beads, tools, clay pots, plant and food remains, and animal bones. The exceptionally good preservation of the human bones allowed for detailed DNA analysis to clarify family ties and full facial reconstruction. DNA comparison with living people from the village yielded the oldest and longest genetically verifiable family tree in the world. The bones and their DNA retrieved from this cave were so well-preserved that researchers from the University of Göttingen used them to develop a process for the analysis and comparison of ancient DNA.

Blasted out of the former reef itself is the *Museum in the Mountain,* where visitors learn the fascinating story of the creation of the Iberg in the Devonian, its long journey to the North due to plate tectonics, and what happened to the cave during these travels before entering the cave itself.

The museum is an excellent starting point for walks in the Iberg's karst landscape. What first appears to be idyllic natural scenery turns out to be a historic "industrial landscape" and a three-dimensional picture book of what took place inside and on the mountain: cave formation, karst development, and mining.

More information is available at *www.hoehlen-erlebnis-zentrum.de*.

3-D Scanning of the Iberger Tropfsteinhöhle

To complement the existing survey of the Arbeitsgemeinschaft für Karstkunde Niedersachsen e.V. from 1982 (Figure 1) (compare Kempe et al., 1985), we scanned the Iberger Tropfsteinhöhle on 11 June 2014 with a Focus3D-S120 laser scanner by FARO. A total of 32 stations were occupied (Figure 1). Each scan covered an area of 360° horizontally and 90° to -60° vertically.

The resolution amounted to 10,240 points/360°, which adds up to 44 million points per scan. Each point was defined by its polar coordinates and a reflexion value. The reflexion value is a measure of the intensity of the reflected laser beam and yielded a graphic representation of grey shades similar to a black and white picture. An integrated compass and inclinometer were used to give direction and horizontality to the point cloud. Reference spheres of 14-cm diameter assured the linkage of the individual scans in a precise geometric way by triangulation. Linkage of point clouds and graphic representation were carried out with the SCENE program package provided by FARO EuropeGmbH.

Scanning the Cave

Beginning in Brückmann Hall in the area of the former "endless lake" (Scan 001), the main cave was scanned counterclockwise through the Rittershaus Passage, followed by the Dwarf Grotto, Hübich Hall, and the Antechamber (Vorraum). Scan 017 connected with Scan 001, closing the loop. Next, in Scan 018, the Hauptmann-Spatzier-Passage was scanned, again connecting to Scan 001. Scan 024 tied the Oskar-Klingebiel-Grotto and Scans 025 and 026 the hall of the "Gelber Stieg" into the net. The passage beyond the crawl in the "Gelber Stieg" was not scanned because of battery, time, and space limitations. This passage is not part of the show cave. Scan 029 documented an ore-containing section that was not mined and was incidentally intersected by the Hauptmann-Spatzier-Passage. Finally, Scans 031 and 032 recorded the Pfannenberg-Abri, formerly the entrance to the show cave and the fourth section of the cave. Now the entrance follows the new 160-m-long tunnel leading to the CaveExperienceCenter, branching off at Scan 30. The entrance was not scanned.

Scan stations were chosen according to two principles. First, three to four of the reference spheres had to be visible connecting to the previous and the following station. Second, stations were placed to avoid as many shadows as possible. In a morphologically diverse cave, like the Iberger Tropfsteinhöhle, this is not possible for every niche, fissure, and cupola. Thus sections of the Lehmgang ("loam passage"), the Geisterschlucht ("Ghost Canyon"), and Zwergenschlucht ("Dwarf Ravine") were not recorded. The resolution of the scans chosen resulted in a gap of 6 mm between points at a distance of 10 m, further away from the scanner.

Comparisons Between the Surveys from 1982 and 2014

The survey of 1982 followed standard cave survey techniques using a magnetic compass, clinometer,

and measuring tape. The dimensions of passages were estimated. Therefore, differences should be expected between the older tape and the newer scan survey. Figure 3 shows these differences by aligning the two surveys along the main tunnel. It is immediately apparent that the tunnel is much longer (by about 15 m) than according to the old survey. Also, the main cave is less tilted to the south than on the original map. This may be because of the different loop-closure techniques used then by the SCENE software. Otherwise, the outer borders show a high similarity, testifying to the excellent sketching talents of the original authors.
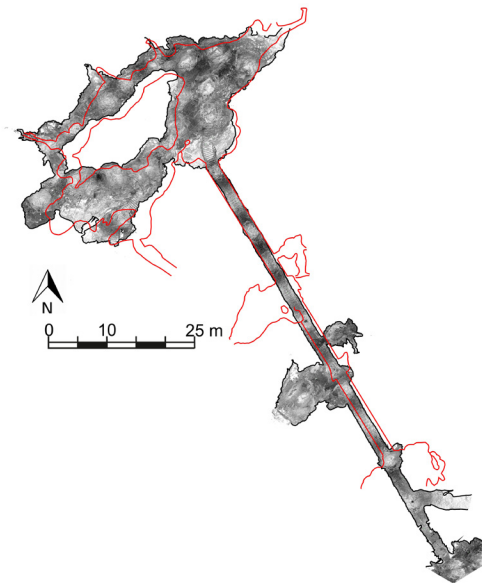
Figure 3.
Comparison of the original 1982 survey (outline in red) with the new scan of the Iberger Tropfsteinhöhle (outline in black).

The Morphology of the Iberger Tropfsteinhöhle

Ford and Williams (1989) and, later, Worthington and Ford (1995) defined hypogene caves as those formed by hydrothermal water or by waters containing hydrogen sulfide. In case of the Iberg, there is no indication for the ascent of hydrothermal waters. Palmer (2000) gives a broader interpretation: "hypogenetic caves are formed by water in which the aggressiveness has been produced at depth beneath the surface, independent of surface or soil CO_2 or other near surface acid sources." Referring to Palmer's definition, the Iberger Tropfsteinhöhle is clearly an example of hypogene speleogenesis because the acid source is autochthonous caused by siderite weathering. Palmer does not consider oxygen in his definition, but it is understood that the caves of the Guadalupe Mountains (such as Carlsbad

Cavern, Lechuguilla, and others) are made possible only by atmospheric oxygen infiltrating the deep-seated reservoirs of H_2S from the surface. Thus, the source of the oxygen, which itself is not cave-forming, does not play a role in the definition of what is considered to be a hypogene cave formation.

For Klimchouk (2012, p.750) it is important that "the cave-forming agent" rises from below. This definition is independent of the direction of water movement because the "cave-forming agent" can be anything, such as gases or acid-producing matter. Siderite obviously cannot rise from below, but it is the "cave-forming agent" situated at depth. Therefore, it is a special case of hypogene cave formation.

Klimchouk (2007) lists criteria to distinguish hypogene from epigene cave origin. A typical property of epigene caves is their branching pattern, with tributary passages converging downstream. In contrast, the Iberger Cave shows a highly irregular morphology with wide and narrow passages alternating in short intervals. It forms a series of halls reaching from the former entrance down to the Zwergen Schlucht (Dwarf Gorge), almost doubling back on itself. While Brückmann Hall has a width of approximately 10 m, the subsequent Rittershaus Passage diminishes to an extent of 1 m at its narrowest point. The former end of the cave is now connected to the Hübichsaal above by an artificial passage with stairs.

Figure 4.
Goethite containing loam in the Iberger Tropfsteinhöhle, probably part of a mud flow.

Furthermore, there is no evidence of lateral flow, like scallops in the cave, and fluvial sediments are absent. The sediment of the Loam Passage (Lehmgang) is composed of clayey goethite and material that probably represents mud flows from an uphill cavity or even the surface (Figure 4). More sediment and reddish goethite

is visible in the depression called "Endloser See." None of these deposits were investigated in detail. It is unclear if goethite has ever been commercially mined from the main cave.

Wall and Ceiling Features

On the other hand, the cave shows all morphological features of a phreatic origin shaped by slow natural (i.e., density-driven) convection. The walls show sloping side walls ("facets"; Figure 5) and sets of ceiling, blind-ending concave cupolas (Figure 6) (e.g., Kempe, 2008; Klimchouk, 2007). The Oskar-Klingebiel-Grotto (Figure 7) is an isolated small cave, not belonging to the Iberger Tropfsteinhöhle. It was not immediately noticed when the Haupmann-Spatzier-Passage was dug. The Grotto was filled halfway with goethite loam and only excavated in 1941. A NE-SW striking fracture (Figure 6, bottom left) provided for the ascent of iron-rich solution when the small siderite deposit was formed and CO_2-bearing water when the siderite decomposed to goethite, which caused stacked cupolas to form (Figure 7).

Figure 5.
"Facet" (sloping side wall) in the Rittershaus Passage, a typical feature of slow phreatic convection. Note the cupola on its lower edge.

The "Neuer Teil" (New Part) was rediscovered in 1911 during the construction of Hauptmann-Spatzier-Stollen. Fragments of a pitcher showed that this cave was part of a small mine named "Gelber Stieg." Miners had removed an about 2-m-thick goethite layer. Remains of this reddish clay are still found in pockets on the walls. The deposit was once covered with a thin flowstone layer, the remains of which form a small shelf around the cavity (see arrows in Figure 8).

Similar to the New Part and the Grotto, the morphology of the main cave is dominated by cupolas and facets (Figure 9).

Figure 6.
3-D scanned picture of sets of symmetrical cupolas aligned along fractures in the ceiling of the Oskar-Klingebiel-Grotto, an originally isolated chamber of the cave.

Figure 7.
3-D scan of the Oskar-Klingebiel-Grotto seen from the NW, revealing actual dimensions of the cupolas above the former siderite deposit in the lower part of the cavity. The transparent sections are shadows on both sides of the cave not visible for the scanner.

Figure 8.
3-D Scan 026, "Neuer Teil."Arrows indicate flowstone shelf. Below it, the cavity was filled by goethite loam, dug out as part of the mine "Gelber Stieg." Notice the ceiling, with its dense pattern of concave cupolas.
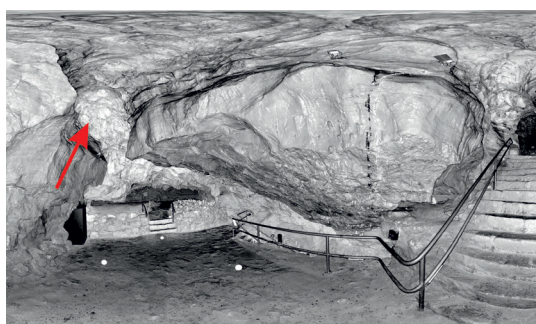
Figure 9.
3-D Scan 001 of Brückmann Hall in panorama mode. Notice walls and ceiling structured by cupolas and half cupolas. The arrow points to a ceiling channel, formed by buoyancy differences in slowly convecting water. The channel is gently inclined, connecting Brückmann Hall with Hübich Hall to the right.

Thus, all of the cavities show clear signs of a phreatic origin by slowly convecting aggressive water. Goethite deposits suggest that siderite deposits were oxidized, releasing the CO_2 needed to sustain this sort of cave formation. Thus, cave formation must predate the current valleys around the Iberg.

However, the oxidation of the siderite was still active when the valleys started to cut down. This is evident from two negative water level marks found in the main cave: the upper one in Hübich Hall (Figures 10 and 11) and the lower one in Brückmann Hall about 5 m lower (Figure 12). Until the building of the Hauptmann-

Spatzier-Tunnel, there was a small pond at the bottom of Brückmann Hall, giving evidence to the impermeability of the underlying goethite deposit. This lake, however, did not leave a water level mark, so that the oxidation of the former siderite deposit may have come to conclusion in this part of the Iberg.

There is one more piece of evidence that testifies to the model of slow convective enlargement of the caves: the irregular dissolution of fossil remains protruding from the walls. The larger the crystals are, the more they protrude. Figure 13 shows a prominent example of a cephalopod (goniatite) exposed in the wall of the Brückmann Hall. If

Figure 10.
Hübich Hall, E-wall: the most prominent of several water level undercuttings.
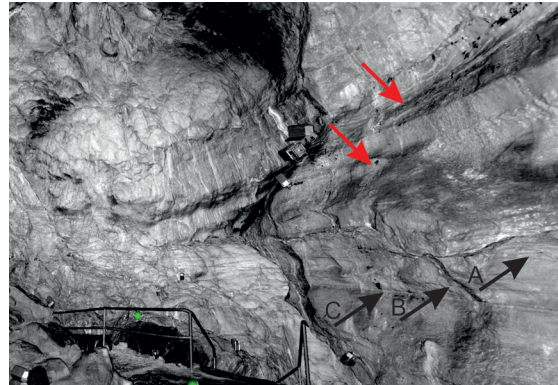
Figure 11.
3-D Scan 015, Hübich Hall, E-wall: facetted wall (red arrows) originating from density currents during phreatic stage. Three water level marks (black arrows) represent a stagnating water table.
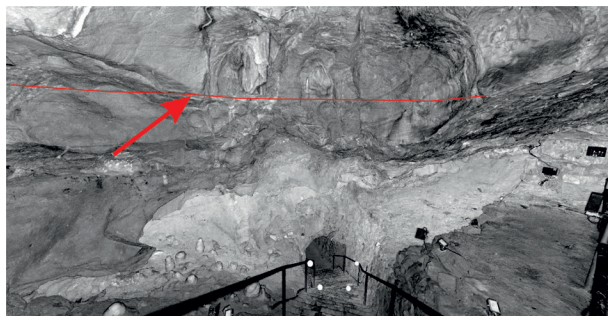
Figure 12.
3-D Scan 019, viewing SW of Brückmann Hall towards the opening of the Hauptmann-Spatzier-Tunnel. Undercut water level mark (red line) is indicative of stagnating groundwater level.

Figure 13.
Fossil cephalopod protruding from a wall of Brückmann Hall, indicating slow movement of convective phreatic water etching the micritic rock faster away than the larger crystals of the shell and the sparitic fill of the cambers.

stronger erosive motion was in action, the shells would not have been protruding from the walls.

Conclusions

The Iberger Tropfsteinhöhle is the only show cave in Germany (and probably the world) that was created by the oxidation of siderite to goethite and the subsequent release of CO_2 into a stagnant ground water body. Cave formation occurred under phreatic conditions. The three cavities comprised by the show cave are only a small portion of the entire complex of caves on the SE side of the Iberg. For many centuries, these caves were mined for their easily extractable goethite loam. The underlying siderite deposit was extracted as well, but only in the lower part of the Eisensteinstollen-System

below the Iberger Cave in the late phase of 19th century mining activity. There is evidence for ongoing siderite weathering in at least one of the ponds. The pond is probably less than 200 years old, thus showing that the oxidation rate is relatively fast (geologically speaking), provided enough oxygen is available. Therefore, the rate-limiting factor of this kind of cave formation is the availability of oxygen, supplied by seepage water from the surface. Thus, cave formation could not have started at any appreciable rate before the surface of the Iberg was exposed, allowing fractures to transmit oxygen-containing seepage water toward the siderite lodes.

In principle, the size of the resulting cavities is equal to the molar size of the siderite deposit, since the oxidation

reaction produces one mole CO_2 per mole of siderite. This CO_2 can in turn dissolve one mole of limestone. The vanishing siderite is replaced by goethite. Since the densities of both minerals relates 3.87 to 4.27, an initial volume of about 10% is created in addition to the limestone dissolved. Thus, one can roughly compare the volume of the open cave to the original volume of the siderite deposit. This approach is probably oversimplified because mudflows can transport surface sediment into the caves and processes like mixing corrosion could add to cave volume.

Cave formation proceeded as long as the groundwater table was high. As erosion of the valleys around the Iberg continued, the water table dropped, leaving two water level marks in the cave about 5 m apart vertically. Their presence suggests that the siderite weathering was not complete before the groundwater drained the cave. Dating of these stages remains open at this time, but the cave was last dry 400 ka ago, as our U/Th date from the big stalagmite shows.

References

Döppes D, Kempe S, Rosendahl W. 2008. Schauhöhlen in Deutschland, Österreich und der Schweiz. In: Kempe S, Rosendahl W, editors. Höhlen: verborgene Welten. Darmstadt (DE): Wissenschaftliche Buchgesellschaft Darmstadt. p. 151-160.

Ford DC, Willams PW. 1989. Karst geomorphology and hydrology. London (GB): Unwin Human.

Franke W. 1973. Fazies, Bau und Entwicklungsgeschichte des Iberger Riffes (Mitteldevon bis Unterkarbon III, NW-Hart, W-Deutschland). Geol. Jahrb. Reihe A, Heft 11.

Gischler E. 1992. Das devonische Atoll von Iberg und Winterberg im Harz nach Ende des Riffwachstums. Geol. Jahrb. Reihe A, Heft 129.

Heydecke S. 2011. Geologische Kartierung im Tagebau Winterberg bei Bad Grund unter Berücksichtigung der strukturgeologischen und faziesbedingten Einflüsse auf die Qualitätsverteilung der abbaurelevanten Kalksteine [diplom thesis]. Clausthal-Zellerfeld (DE): Institut für Geologie und Paläontologie, Technische Universität Clausthal-Zellerfeld. Unpublished.

Joachimski MM, Buggisch W. 1993. Anoxic events in the late Frasnian—causes of the Frasnian–Famennian faunal crisis? Geology 21: 675-678.

Kempe S. 1971. Speläogenetisch wirksames CO_2 durch Verwitterung von Siderit? Mitt. Verb. dt. Höhlen- u. Karstforsch. 17: 38.

Kempe S. 1975. Siderite weathering, a non-biogenetic source of CO_2 (illustrated by the Iberg/Harz/Fed. Rep. of Germany). Ann. de Spéléologie 30 (4): 703-704.

Kempe S. 1982. Ergebnisse einer Umfrage bei den Schauhöhlen der Bundesrepublik Deutschland. Die Höhle 33 (1): 8-13.

Kempe S. 2008. Vom Urkanal zur unterirdischen Kathedrale, Höhlenformen und ihre Entstehung. In: Kempe S, Rosendahl W, editors. Höhlen: verborgene Welten. Darmstadt (DE): Wissenschaftliche Buchgesellschaft Darmstadt. p. 54-64.

Kempe S. 2009. Siderite weathering as a reaction causing hypogene speleogenesis: the example of the Iberg/Harz/Germany. In: Klimchouk A, Ford D, editors. Hypogene speleogenesis and karst hydrogeology of artesian basins. Simferopol (UA): Ukrainian Institute of Speleology and Karstology. Special Paper 1, p. 59-60.

Kempe S, 2014. Hypogene limestone caves in Germany: geochemical background and regionality. In: Klimchouk A, Sasowsky ID, Mylroie J, Engel SA, Engel AS, editors. Hypogene Cave Morphologies, Karst Waters Inst. Spec. Publ. 18: 48-56. (Proc. San Salvador, Bahamas Feb. 2-7, 2014).

Kempe S, Kazmierczak J. 1994. The role of alkalinity in the evolution of ocean chemistry, organization of living systems and biocalcification processes. In: Doumenge F, editor. Past and Present Biomineralization Processes: Considerations about the Carbonate Cycle. Bulletin de l'Institut océanographique de Monaco, No. Spec. 13: 61-117.

Kempe S, Rosendahl W, editors. 2008. Höhlen: verborgene Welten. Darmstadt (DE): Wissenschaftliche Buchgesellschaft Darmstadt.

Kempe S, Reinboth F, Knolle F. 1985. Die Iberger Tropfsteinhöhle bei Bad Grund (Harz). Bad Grund (DE): Bad Grund.

Klimchouk AB. 2007. Hypogene speleogenesis: hydrogeological and morphogenetic perspective. Special Paper No.1. Carlsbad (NM): National Cave and Karst Research Institute.

Klimchouk AB. 2012. Speleogenesis, hypogenic. In: White W, Culver DC, editors. Encyclopedia of caves, 2nd ed. Amsterdam (NL): Academic Press. p. 748-765. http://dx.doi.org/10.1016/B978-0-12-383832-2.00110-9

Knappe H. 2014. Die Entwicklung der Karststrukturen im Riffkalkstein von Iberg und Winterberg bei Bad Grund (Westharz). Mitteilungen Verb. dt. Höhlen- u. Karstforscher 60 (3/4): 80-90.

Knolle F, Meischner D, Stedingk K. 2008. Spaltenbildung, vulkanogene Höhlen und Hydrothermalkarst im Winterberg – Anmerkungen zur Speläogenese. In: Fricke U, editor. Höhlen des Winterberg-Steinbruchs bei Bad Grund/Harz. Karst und Höhle 2006/2007, München.

Meischner D. 2014. Das Iberger Riff – Aufbau und Zerfall eines ozeanischen Atolls. Vortrag 18. Bernburger Kolloquium über das historische Berg- und Hüttenwesen des Harzes, Museum Schloss Bernburg, 9.10.1999, Transkript, 5 pp., 19 Overheadfolien, von Knolle, F, Mitteilungen der Arbeitsgemeinschaft für Karstkunde Harz 35 (1,2): 3-13.

Nitychoruk J, Bińka K, Ruppert H, Schneider J. 2006. Holsteinian interglacial = marine isotope stage 11? Quaternary Science Reviews 25 (21-22): 2678-2681. http://dx.doi.org/10.1016/j.quascirev.2006.07.004

Palmer AN. 2000. Hydrogeologic control of cave patterns. In: Klimchouk A, Ford D, Palmer A, Dreybrodt W, editors. Speleogenesis: evolution of karst aquifers. Huntsville (AL): National Speleological Society. p. 77-90.

Reimer A, Kempe S. 1989. Recent and paleokarst systems and their relation to ore mineralization in the Iberg-reef-complex, Harz Mountains. Proceedings of the 10th International Congress of Speleology, Budapest, August 13-20, 1989: 1-2.

Svensson U. 1988. Hydrochemische Untersuchungen an dolomitischen Karstwässern einer bergbaulich überprägten Großhöhle im Iberg/Harz [diplom thesis]. FB Geologie, Universität Hamburg. 130 p. Unpublished.

Svensson U, Kempe S. 1989. Hydrochemistry of karst waters in the Iberg-reef-complex, Harz Mountains. Proceedings of the 10th International Congress of Speleology, Budapest, August 13-21, 1989: 3-5.

Worthington SRH, Ford DC. 1995. High sulfate concentrations in limestone springs: an important factor in conduit initiation? Environmental Geology 25: 9-15. http://dx.doi.org/10.1007/BF01061825

NEW DEVELOPMENTS IN THE SCIENCE OF HYPOGENE CAVES IN NEW SOUTH WALES, AUSTRALIA

Robert Armstrong Osborne
Education & Social Work, A35
The University of Sydney, NSW 2006 Australia, armstrong.osborne@sydney.edu.au

Abstract
Limestone caves in eastern Australia are mostly developed in small north-south trending impounded karsts developed in Palaeozoic limestones. Of the approximately 100 bodies of cavernous Palaeozoic limestone in New South Wales, Australia, only 16 have ponors, while caves at 11 localities are known to intersect palaeokarst deposits. Hypogene morphologies and speleogens have been recognized in caves at 25 karst areas in NSW, including all but one of the 10 most cavernous karsts. Osborne (2010) reviewed the understanding of karst caves in the whole of eastern Australia and noted that "old hypogene caves often occur in close relationship to large regional faults and/or cross faults intersecting limestone bodies." One characteristic not reported by Osborne (2010) is the almost complete absence of groundwater-deposited gypsum in eastern Australian caves, with the major sources of cave gypsum being guano and the weathering of pyrite in the bedrock. Recent work shows that while there is evidence for some high-temperature crystal palaeokarst, wall coatings with indicated temperatures of 50°C or higher are uncommon. What is increasingly recognized in the hypogene caves of NSW is evidence for present and past degassing of carbon dioxide from the groundwater. This takes the form of contemporaneously deposited calcite rafts, lithified raft breccias, and mammillary deposits. Isotopic ratios of these deposits can be distinctly different from those of vadose speleothems in the same cave. As a result of these findings, a new phase of investigation has found evidence for degassing at more sites, making more isotopic determinations, and investigating the isotopic ratios of carbon dioxide itself in the caves. The indications are that hypogene speleogenesis in NSW has mostly been driven by carbon dioxide-rich water rather than by hot or sulfurous water. There is evidence that in at least one locality degassing water has been around for as much as five million years.

New technology, particularly the use of point cloud images from the Zebedee laser scanning system, has revealed previously unrecognized complex morphologies and, through image rotation, the possibility that some caves are the result of the integration of originally separate cavities.

Reference
Osborne RAL. 2010. Rethinking eastern Australian caves. In Bishop P, Pillans B, editors. Australian Landscapes. Geological Society of London Special Publication 346: 289-308.

TYPES OF HYPOGENE SPELEOGENESIS

Alexander Klimchouk
Institute of Geological Sciences of the National Academy of Sciences of Ukraine
55-bGonchara Street, Kiev, Ukraine, 01054, klim@speleogenesis.info

Abstract

Two fundamental types of speleogenesis, hypogene and epigene, differentiate due to distinct hydrodynamic characteristics of the respective groundwater flow systems: (1) stratiform confined aquifer systems or fracture-vein flow systems of varying depths and degrees of confinement, and (2) hydraulically open, near-surface unconfined systems. Hypogene speleogenesis develops where ascending flow and disequilibrium conditions causing dissolution were supported, continuously or intermittently, during a sufficiently long time—mainly in zones of discharge and/or interaction of groundwater (fluid) flow systems and regimes of different nature, depth, and scales. Further genetic subdivision of hypogene speleogenesis into three types is proposed, based on the regularities and driving forces of groundwater (fluid) circulation in different hydrodynamic zones.

Introduction

The general postulate of the supremacy of groundwater flow in speleogenesis (Worthington & Ford, 2009; Klimchouk, 2011, 2015) implies that hydrogeological criteria are decisive in distinguishing the types of speleogenesis. Two fundamental types of speleogenesis, hypogene and epigene, are determined mainly by distinct hydrodynamic characteristics of the respective groundwater flow systems: (1) stratiform confined aquifer systems or fracture-vein flow systems of varying depths and degrees of confinement, and (2) hydraulically open, near-surface unconfined systems.

As speleogenesis is the primary mechanism in karst formation, genetic types of karst are to be distinguished based on types of speleogenesis. Accordingly, two major genetic types of karst within the upper part of the Earth's crust are hypogene karst and epigene karst. They differentiate due to fundamental differences in boundary conditions and hydrodynamic regimes of fluid flow and speleogenesis and in lithological, structural, and geochemical settings, as well as due to differences in the evolutionary trajectories of corresponding karst systems. Since hypogene karst during formation is almost exclusively represented by voids and conduits, the terms "hypogene karstification" and "hypogene speleogenesis" are virtually interchangeable.

Hypogene speleogenesis is defined as the formation of solution-enlarged permeability structures (void-conduit systems) by fluids that recharge the cavernous zone from below, driven by hydrostatic pressure or other sources of energy, independent of recharge from the overlying or immediately adjacent surface karst landscapes (modified from Klimchouk, 2007). It operates in various tectonic and geological/hydrogeological conditions, at varying depths (ranging from the shallow subsurface to several kilometers) and in rocks of different compositions (all kinds of carbonate rocks, gypsum, conglomerates, sandstones, and quartzites) and ages (from Neoproterozoic to Pleistocene). The distribution of hypogene speleogenesis is not limited to continents, also occuring in the seafloor. In view of such broad variability of conditions, further subdivision into genetic subtypes within this genetic category should be elaborated.

Genetic subtypes of hypogene speleogenesis are often distinguished according to the dissolution chemistry involved: sulphuric acid speleogenesis (SAS), hydrothermal speleogenesis, "mixing corrosion" speleogenesis, evaporite-dissolution speleogenesis, etc. However, dissolution mechanisms themselves do not determine the origin of caves. Generally, patterns and morphologies of hypogene void-conduit systems do not exhibit singularities specific to the dissolutional mechanisms. To the contrary, hypogene caves formed by different dissolutional mechanisms in different lithologies often demonstrate remarkable multifaceted similarity in patterns, morphologies, and other characteristics. For some caves, different dissolutional mechanisms were shown to operate, either simultaneously or in a sequence, during their speleogenetic evolution.

In any given geological environment, the potential for dissolution, distribution of its effects, localization, patterns, and morphology of forming void-conduit systems are determined largely by the regime, pattern, and intensity of fluid flow, i.e., by hydrogeologic factors. They systematically change with depth, which is expressed in the vertical hydrodynamic zoning. The latter can be used for further genetic subdivision of hypogene speleogenesis.

Hydrodynamic Zoning of the Upper Part of the Earth's Crust

The views on hydrodynamics below the zone of unconfined groundwater flow significantly changed during the second half of the 20th century. For gravity-driven meteoric groundwater flow systems, the traditional artesian paradigm was based on the views of lateral confined through-flow along largely isolated aquifers from marginal recharge areas toward distant discharge areas. The hydrodynamic zoning commonly included three zones according to the dynamics of groundwater exchange: (1) intense, (2) restrained, and (3) inhibited (of stagnant regime). Most researchers placed the lower boundary of the zone of intense groundwater exchange at the top of the first regionally extensive aquitard below the erosional valleys, i.e., commonly at depths of about 100-300 m. Aquifers between regionally extensive aquitards were commonly thought to be in the zone of restrained groundwater exchange.

The above paradigm was gradually replaced by the paradigm of the basin-wide hydraulic continuity, which implies significant vertical groundwater exchange between aquifers in a system across separating aquitards throughout the entire area of a basin (Shestopalov, 1981, 1988, 1989; Toth, 1995, 2009). The amount and direction of cross-stratal hydraulic communication depends on the vertical pressure gradients between adjacent aquifers, which are guided by the topography of the water table in the major unconfined aquifer above the confined aquifer system, and eventually by the surface topography. For a given aquifer in the confined multi-story aquifer system, recharge and discharge across confining units can take place simultaneously and occur throughout the whole area of its lateral extent. Across the area, the alternation of areas of downward and upward hydraulic communication across aquitards, along with lateral flow components within aquifers, creates the pattern of local hydrodynamic cells that may encompass several aquifer systems. Regional hydrogeological data and modeling studies suggest that the groundwater exchange in such systems is determined mainly by vertical leakages rather than sub-regional and regional lateral flows, and that the topographic influence over the hydrodynamics may extend up to depths of 1000-1500 m or more (Shestopalov, 1989). Upwelling cross-stratal flow below topographic lows, especially river valleys, commonly is more localized and intense, and extends to greater depths than downward flow induced by topographic highs.

In the deeper parts of the sedimentary cover, below the zone of the dominant gravity-driven flow regime, the hydrodynamics are increasingly determined by the expulsion regimes, often overpressurized due to the internal drives for flow: compactional, compressional (tectonic), and thermobaric/metamorphic (dehydration, devolatilization). Over the past decades, a dramatic increase of data about this zone, related mainly to prospecting and exploration of hydrocarbon resources, has significantly changed previous views about deep hydrodynamics. One of the most characteristic features of this zone is mosaic and fragmented distribution of fluid properties in lateral directions, with the presence of high-gradient boundaries. This zone contains numerous anomalies in parameters of thermal, baric, hydrochemical, geochemical, and permeability fields, commonly related to deep-rooted tectonic disruptions. Such disruptions often allow the rise of fluids that originate from the devolatilization of still-deeper parts of the crust and the upper mantle. In many cases, the anomalies are traced vertically across the overlying aquifer/aquitard systems, pointing to cross-formational communications. The upward movement along cross-formational structures, often pulsating in the geological time-scale, dominates fluid dynamics. These characteristics rule out a possibility of regionally extensive lateral flows in this zone.

Similar considerations of leading factors that determine major regularities of water exchange led Shestopalov (2014) to propose distinguishing three main hydrodynamic zones in the upper part of the Earth crust: (1) the zone of orohydrographic/climatic influence, (2) the intermediate (transitional) zone, and (3) the zone of fluid-geodynamic (endogenous) influence. The intermediate zone is characterized by restrained influence of both external and endogenous factors.

Types of hypogene speleogenesis

Based on hydrodynamic considerations, Klimchouk (2012) distinguished three types of hypogene speleogenesis, redefined below in the view of the above discussion:

1. *Artesian hypogene speleogenesis*, related to the upward cross-stratal hydraulic communication in confined multi-story aquifer systems, in the hydrodynamic zone of orohydrographic/climatic influence. This type of speleogenesis is particularly common (although not exclusive) for cratonic sedimentary (artesian) basins and post-orogenic regions marked by massive and deep penetration of the gravity-driven meteoric regime of groundwater exchange.
2. *Endogenous hypogene speleogenesis*, related to upwelling flow in or from the zone of fluid-

geodynamic influence, commonly localized along cross-formational fluid-conducting disruptions. It may occur within the upper hydrodynamic zone when it is pierced by deep-rooted anomalies dominated by rising deep fluids. Speleogenesis of this type is common for cratonic artesian basins, especially in areas of the extensional tectonic regimes, as well as for active margins and collision fold-thrust zones.

3. *Combined artesian/endogenous hypogene speleogenesis*, where deep basinal and/or endogenous fluids rise along cross-formational disruptions and significantly interact with overlying stratiform aquifers within the hydrodynamic zone of orohydrographic/climatic influence.

Hypogene speleogenesis of all types localizes where ascending flow and disequilibrium conditions causing dissolution were supported, continuously or intermittently, during a sufficiently long time—mainly in zones of discharge and/or interaction of groundwater (fluid) flow systems and regimes of different nature, depth, and scales. The localization is controlled by the particularities of regional hydrogeological structure and geodynamic and geomorphic evolution. Peculiar features of hydrodynamics in different zones cause distinctions in cave-forming flow patterns, flow regimes, and chemical mechanisms involved in hypogene speleogenesis of different types, resulting in different characteristics of caves. The variety of patterns of void-conduit systems (Klimchouk, 2012) can be broadly grouped into three categories: (1) stratiform, (2) cross-formational, and (3) complex (combined). The first category is common for artesian hypogene speleogenesis, the second category is common for endogenous hypogene speleogenesis, but all categories may form by combined artesian/endogenous hypogene speleogenesis.

References

Klimchouk AB. 2007. Hypogene speleogenesis: hydrogeological and morphogenetic perspective. Carlsbad (NM): National Cave and Karst Research Institute.

Klimchouk AB. 2011. Self-development of the water exchange structure as a system-forming property of karst. Geologichesky Zhurnal 1: 85-110. (In Russian.)

Klimchouk AB. 2012. Speleogenesis, Hypogenic. In: White WB, Culver DC, editors. Encyclopedia of caves. 2nd ed. Chennai (IN): Elsevier, Academic Press. p. 748-765. http://dx.doi.org/10.1016/B978-0-12-383832-2.00110-9

Klimchouk AB. 2015. The karst paradigm: Changes, trends and perspectives. Acta Carsologica, submitted.

Shestopalov VM. 1981. Natural resources of underground water of platform artesian basins of the Ukraine. Kiev (UA): Naukova Dumka. (In Russian.)

Shestopalov VM. 1988. Methods of study of underground water natural resources. Moscow (RU): Nedra. (In Russian.)

Shestopalov VM, editor. 1989. Water exchange in hydrogeological structures of Ukraine. Water exchange under natural conditions. Kiev (UA): Naukova Dumka. (In Russian.)

Shestopalov VM. 2014. On hydrodynamic zoning and water exchange in hydrogeologic structures. Geologichesky Zhurnal 4 (349): 9-26. (In Russian.)

Tóth J. 1995. Hydraulic continuity in large sedimentary basins. Hydrogeology Journal 3 (4): 4-15. http://dx.doi.org/10.1007/s100400050250

Tóth J. 2009. Gravitational systems of groundwater flow: Theory, evaluation, utilization. Cambridge (UK): Cambridge University Press. http://dx.doi.org/10.1017/CBO9780511576546

Worthington S, Ford DC. 2009. Self-organized permeability in carbonate aquifers. Groundwater 47 (3): 326-336. http://dx.doi.org/10.1111/j.1745-6584.2009.00551.x

REGIONAL CASE STUDIES IN HYPOGENIC SPELEOGENESIS

HYPOGENIC MORPHOLOGIES AND SPELEOTHEMS IN CAVES IN THE MURCIA REGION, SOUTHEASTERN SPAIN

Fernando Gázquez
Department of Earth Sciences, University of Cambridge
Downing Street, Cambridge, CB2 3EQ, United Kingdom, f.gazquez@ual.es

José María Calaforra
Department of Biology and Geology, University of Almeria,
Carretera de Sacramente s.n, La Cañada de San Urbano, Almería, 04720, Spain, jmcalaforra@ual.es

Andrés Ros
Centre for Natural and Marine Environmental Studies, CENM-naturaleza
Alcántara, 5, Cartagena, Murcia, 30394, Spain, cenm@cenm.es

José L. Llamusí
Centre for Natural and Marine Environmental Studies, CENM-naturaleza
Alcántara, 5, Cartagena, Murcia, 30394, Spain, cenm@cenm.es

Juan Sánchez
Centre for Natural and Marine Environmental Studies, CENM-naturaleza
Alcántara, 5, Cartagena, Murcia, 30394, Spain, cenm@cenm.es

Abstract

Evidence for hypogenic speleogenesis has been detected in nine caves within a radius of 60 km in the Murcia Region (SE Spain), in many cases revealing active speleogenetic mechanisms that are rarely observed in hypogene cavities elsewhere in the world. Processes related to ancient and current hydrothermal activity, the discordance of permeability structures in the adjacent beds, and the spatial arrangement of the regional hydrogeology have given rise to networks of maze patterns and typical subaqueous hypogenic morphologies. These include spongework mazes, rising wall channels and shafts, feeders, bubble trails, solution pockets, scallops, zenithal ceiling tubes, and cupolas. Carbonic speleogenesis is responsible for the formation of most of these cave features; however, evidence of sulphuric acid speleogenesis (SAS) has been observed in Cueva del Puerto and Sima del Pulpo, which host massive secondary gypsum deposits. Speleothems typically linked to hydrothermal water upwelling and CO_2 degassing close to the water table are present in most of these cavities, including folia, calcite spar crystals, cave clouds, tower cones, calcite rafts and several types of cave raft cones. Other morphologies related to subaerial hypogenic speleogenesis, such as micritized bedrock crusts, ferromanganese coatings, and boxwork, have been observed in several caves, including Sima de la Higuera. The wide variety of hypogenic speleogenesis indicators and speleothems whose genesis is unconnected to meteoric water seepage reveals that the hydrothermal field of the Murcia Region hosts one of the densest active hypogenic subterranean networks in the world.

Introduction

The Murcia Region is located in southeastern Spain. Its climate is characterized by low annual mean rainfall (<500 mm/yr) and annual mean temperatures of ~18°C. Despite limited surface water resources, this region hosts extensive karstic aquifers that have been historically exploited for agricultural purposes. Groundwater overexploitation over the past 50 years has produced a dramatic lowering of the water table on a regional scale, which has allowed access to several phreatic caves that were previously flooded (Ros et al., 2011; 2014a,b). Many aquifers in this region are hydrothermal, with temperature exceeding 40°C.

Some of these caves show marked hypogenic morphologies, suggesting hypogenic/thermal mechanisms were involved during certain stages of their formation. Most hypogenic caves form as a result of circulation of thermal water, usually from depth, and are unconnected with surface water flows (Palmer, 2011). The term "hypogenic" does not refer specifically to extremely deep caves but rather to the origin of the

fluids responsible for the development of these caves (Klimchouk, 2009).This kind of system is represented in over 5–10% of the cavities worldwide (Forti, 1996; Forti et al., 2002).
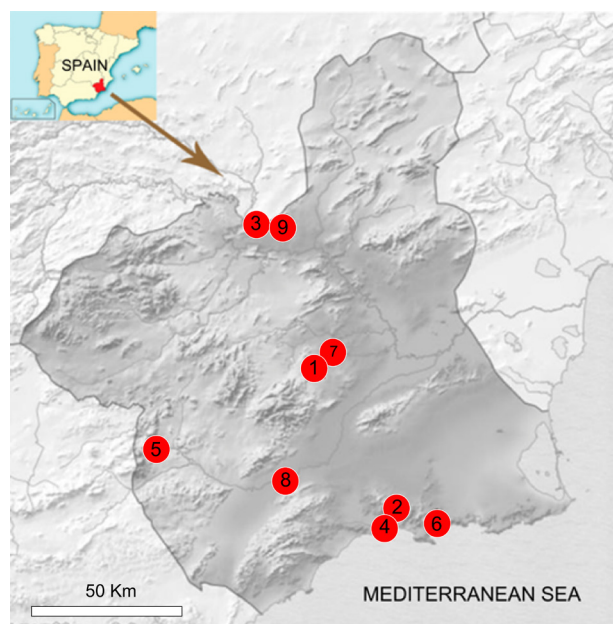

Figure 1.
Location of the main hypogenic caves in Murcia Region.
(1) Sima de la Higuera, (2) Sima Destapada, (3) Cueva del Puerto, (4) Cueva del Agua, Cartagena, (5) Cueva de Luchena, (6) Cueva del gigante, (7) Sima del Almez, (8) Cueva del Agua, Lorca, (9) Sima del Pulpo.

The lack of relationship between subterranean morphologies and seepage water from the surface can serve as a criterion for identifying hypogenic caves. However, relict or fossil hypogenic features can be easily masked by sediment accumulation or epigenic elements, especially in humid climates. These traits have motivated the search for recognizable signatures of hypogenic speleogenesis that allow clear identification of this kind of cave. Recent studies have proposed a series of indicators to flag hypogenic caves, including morphological features and characteristic speleothems (Klimchouk, 2007; Osborne, 2004; Armstrong and Osborne, 2005; Audra, 2009).

In the Murcia Region, these distinctive patterns are widespread in many caves that have recently been suggested as having a hypogenic origin (Gázquez et al., 2012; Gázquez and Calaforra, 2013). In the present study, we selected nine caves for preliminary description and morphological analysis: Sima de la Higuera,

Sima Destapada, Cueva del Puerto, Cueva del Agua-Cartagena, Cueva de Luchena, Cueva del Gigante, Sima del Almez, Cueva del Agua-Lorca, and Sima del Pulpo.

Evidence for Morphologic Suite of Rising Flow (MSRF) and Hypogenic Morphologies

The model of *morphologic suite of rising flow* (MSRF) was initially proposed by Klimchouk (2007) and has been widely applied to characterize hypogenic caves. This includes a set of so-called hypogenic patterns that result from water upwelling, usually thermal fluids. These features can be split into three categories: (1) inlet of ascending flow into the system (feeders), usually located at the bottom of chambers and master passages; (2) transition wall and ceiling features that connect the cave levels with upper passages (usually ceiling domes, channels, and solution pockets); and (3) upward leakage structures (outputs), typically located on the ceilings of upper cave levels.

Feeders are very abundant in the context of the hypogenic caves in Murcia. For example, in Sima de la Higuera, a 10-m-long diaclase along the floor of Paradise Chamber seems to have acted in the past as a feeder of deeper thermal water into this cave level (-98m).

In Sima Destapada, 50-m-deep pits connect the intermediate emergent cave levels with the hydrothermal aquifer (~30ºC) at -221m depth from the cave entrance (Figure 2). Also, blind shafts (without man-size access to the lower level) are found in the floor of upper galleries that probably acted as feeders in the past. Transitional features connect passages and chambers at different depths. For example, in Cueva del Puerto, several 100-m-deep subvertical fractures connect the Chamber of the Desert (~-80 m) with the shallower Chamber of the Blocks (~-40 m) (Figure 3). In this cave, the hydrothermal flow to the system occurred through a 100-m-long diaclase located 114 m below the current cave mouth. Likewise, in Cueva del Agua-Lorca, the recent lowering of the water table has allowed access to several vertical shafts that acted as feeders in the past.

The hydrothermal dissolution of the host rock occurred preferentially along fractures, giving rise to labyrinthine passages (three-dimensional "maze caves") that are typical of hypogenic caves and which are especially well-developed in Sima de la Higuera and Cueva del Puerto. In places, dissolution of this wall has left pillars where some of the galleries have partly disappeared and been incorporated into bigger chambers. Sima Destapada, Cueva del Almez and Cueva del Puerto display multiple examples of these morphologies (Figure 4). Features related to phreatic
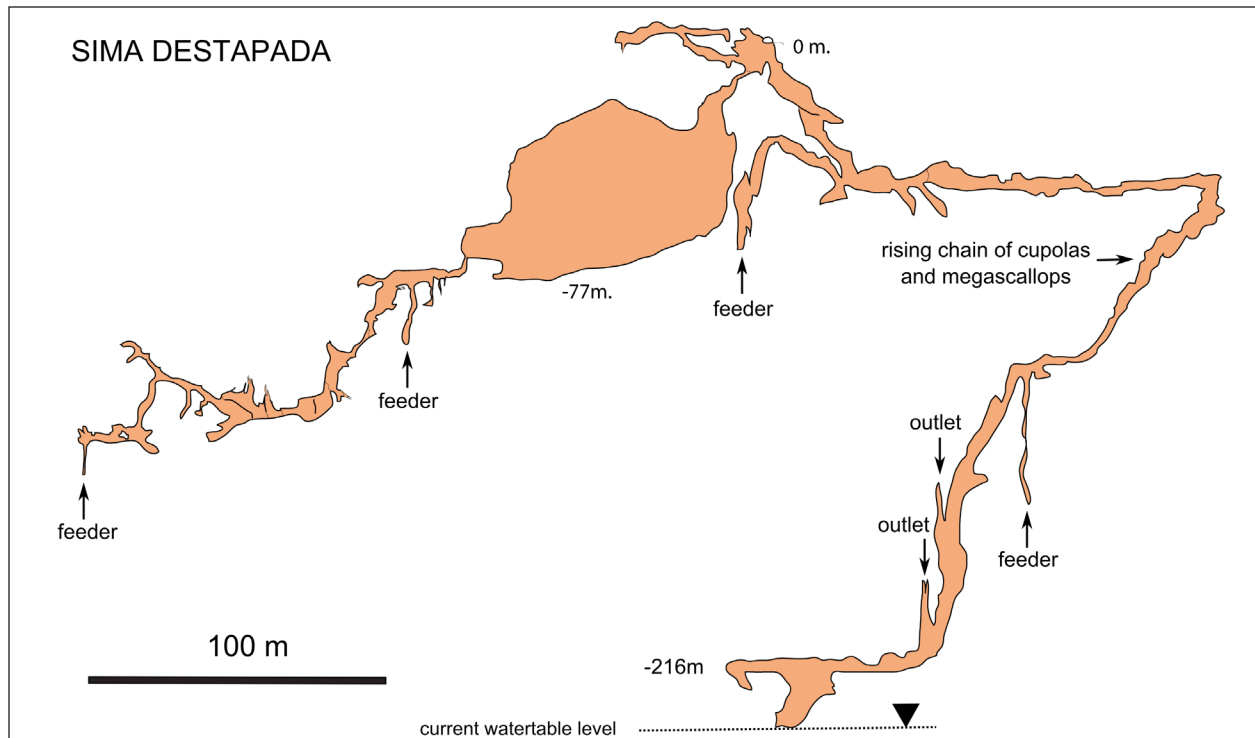
Figure 2.
Topographic profile of Sima Destapada and its main hypogenic morphologies.
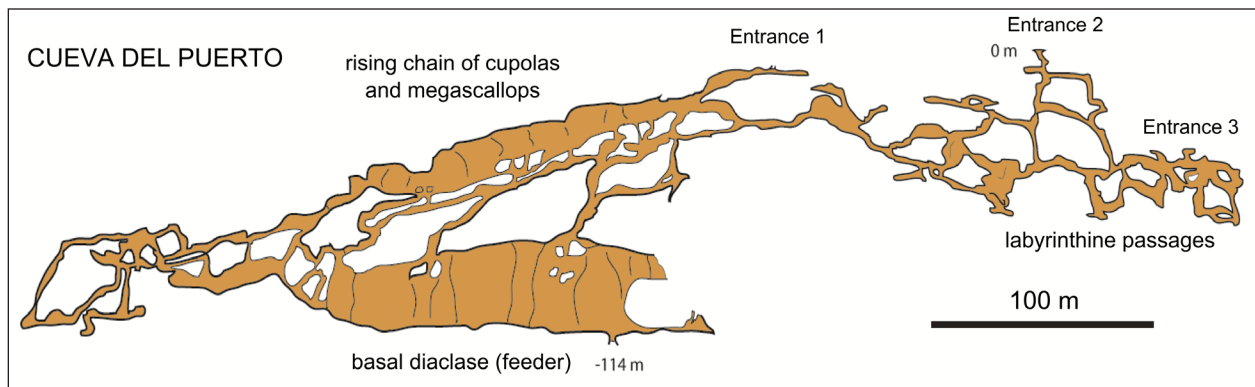
Figure 3.
Topographic profile of Cueva del Puerto and its main hypogenic morphologies.

dissolution-corrosion, like pendants, have been identified in Sima de la Higuera and Sima Destapada (Figure 4A). In Sima Destapada, Cueva del Puerto and Cueva del Almez, linear half-tube structures with smooth surfaces (ceiling half-tubes) are evidence of water flows that dissolved the carbonate host rock (Figure 4B). Sometimes, the CO_2 bubbles followed an ascending path, producing vertical dissolution channels.

These dissolution features are well exhibited in Sima de la Higuera, for example (Fig. 4C).

The ascending flow of thermal water carved the carbonate host rock, giving rise to typical dissolution patterns related to the slow movement of water, including scallops and phreatic domes that are especially well exhibited in Sima la Higuera (Figure 4D), Cueva del Gigante (Figure 4E) and Cueva del Puerto. Rising
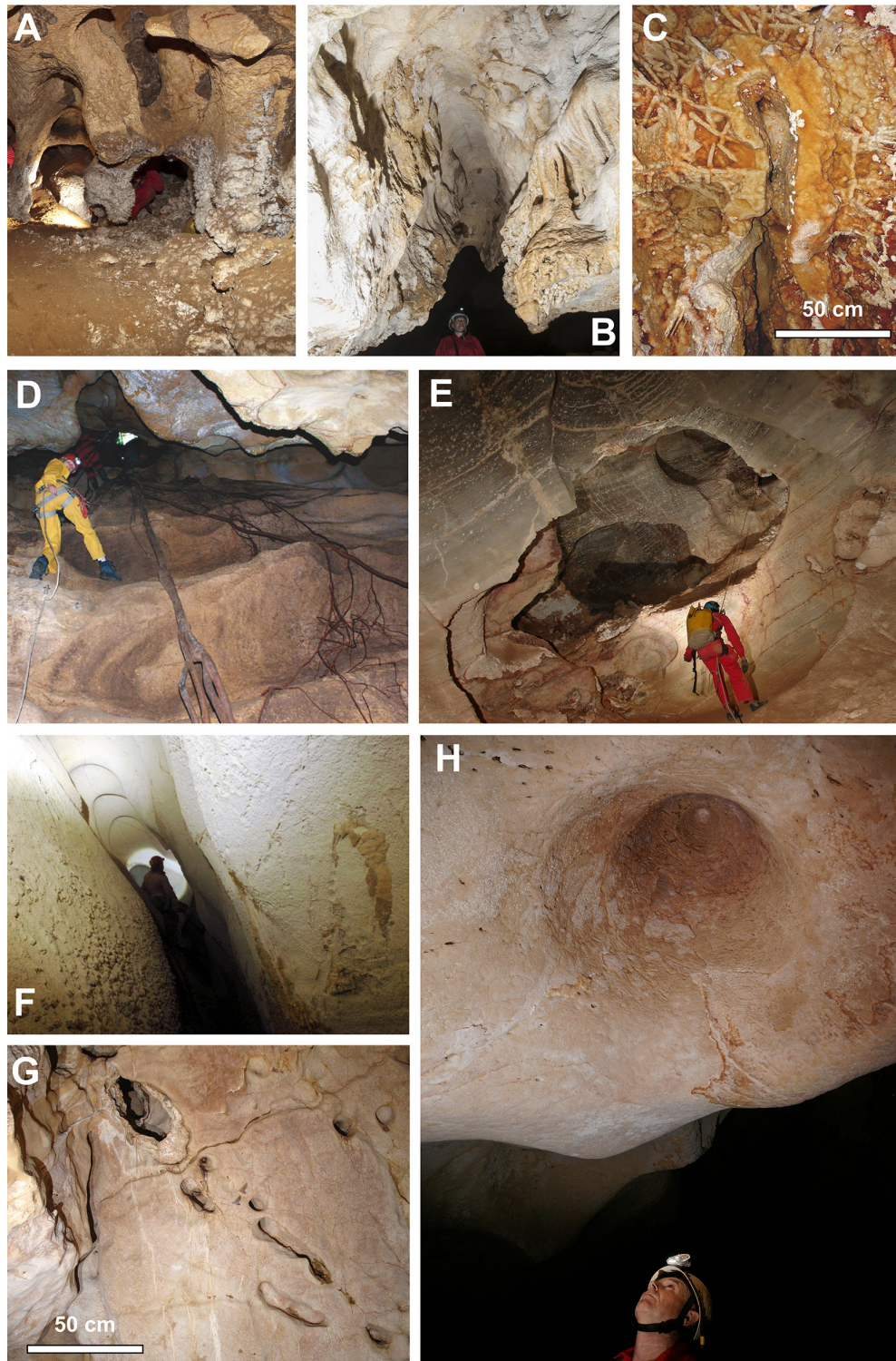
Figure 4.
Hypogenic morphologies in caves in the Murcia Region. (A) Pendants in Sima Destapada; (B) Ceiling half-tubes in Sima del Almez; (C) Bubble trails in Sima de la Higuera; (D)Mega-scallops in Sima de la Higuera; (E)Mega-scallops in Cueva del Gigante; (F) Rising chain of cupolas in Cueva de Luchena; (G) Solution pocket in Sima del Almez; (H) Cupola in Cueva del Puerto. (Photos: Andrés Ros, Llamusí, A, B, E, G, H. Victor Ferrer and C, D, Antonio Gónzalez F)

chains of ascending cupolas have been observed in Cueva de Luchena (Figure 4F). On occasions, the accumulation of air bubbles on the cave ceiling under phreatic conditions generated solution pockets and corrosion cupola, usually attributed to a condensation-corrosion mechanism resulting from the high content of CO_2 from water degassing (Cigna and Forti, 1986).

These features are splendidly displayed in Sima del Almez (Figure 4G) and Cueva del Puerto (Figure 4H). Even more interesting is that this mechanism is still active in the flooded passages of Cueva del Agua, Cartagena, where small hemispherical air chambers 20 cm in diameter can be found between the host rock and the hydrothermal water at the depth of -14 m.

Table 1.
Hypogenic features in caves in the Murcia Region.

	Higuera	Destapada	Puerto	Agua-Cartagena	Luchena	Gigante	Agua-Lorca	Almez	Pulpo
Location	Pliego	Cartagena	Calasparra	Cartagena	Lorca	Cartagena	Lorca	Pliego	Cieza
Length (m)	5,500	3,400	4,389	2,560	561	610	546	220	4,780
Air temperature (ºC)	21º	29º	20º	30º	n.m	21º	21º	n.m	n.m
Hypogenic morphologies									
Maze caves	X	X	X	X	X	X	X		
Chimneys	X	X	X		X	X	X		
Bubble trails	X			X			X	X	X
Scallops	X	X	X	X	X		X	X	X
Zenithal tubes		X	X	X	X	X	X	X	X
Ceiling pockets	X	X	X		X	X	X	X	
Cupola and domes	X	X	X		X	X			
Feeders	X	X	X	X	X		X	X	X
Pendants	X	X	X	X			X		X
Blind ascending passages	X	X	X	X	X				X
Boxwork	X	X	X			X	X		
Micritic crusts	X								
Hypogenic speleothems									
Cave cones	X						X		
Coral towers	X								
Cave clouds	X								X
Calcite spars	X	X	X				X		X
Folia	X								X
Calcite rafts	X	X	X				X		X
Ferromanganese crusts	X	X	X	X		X	X		X
Gypsum crusts			X						X
Gypsum chandeliers									
Gypsum fibres and flowers			X						X
Calcite crusts				X		X			
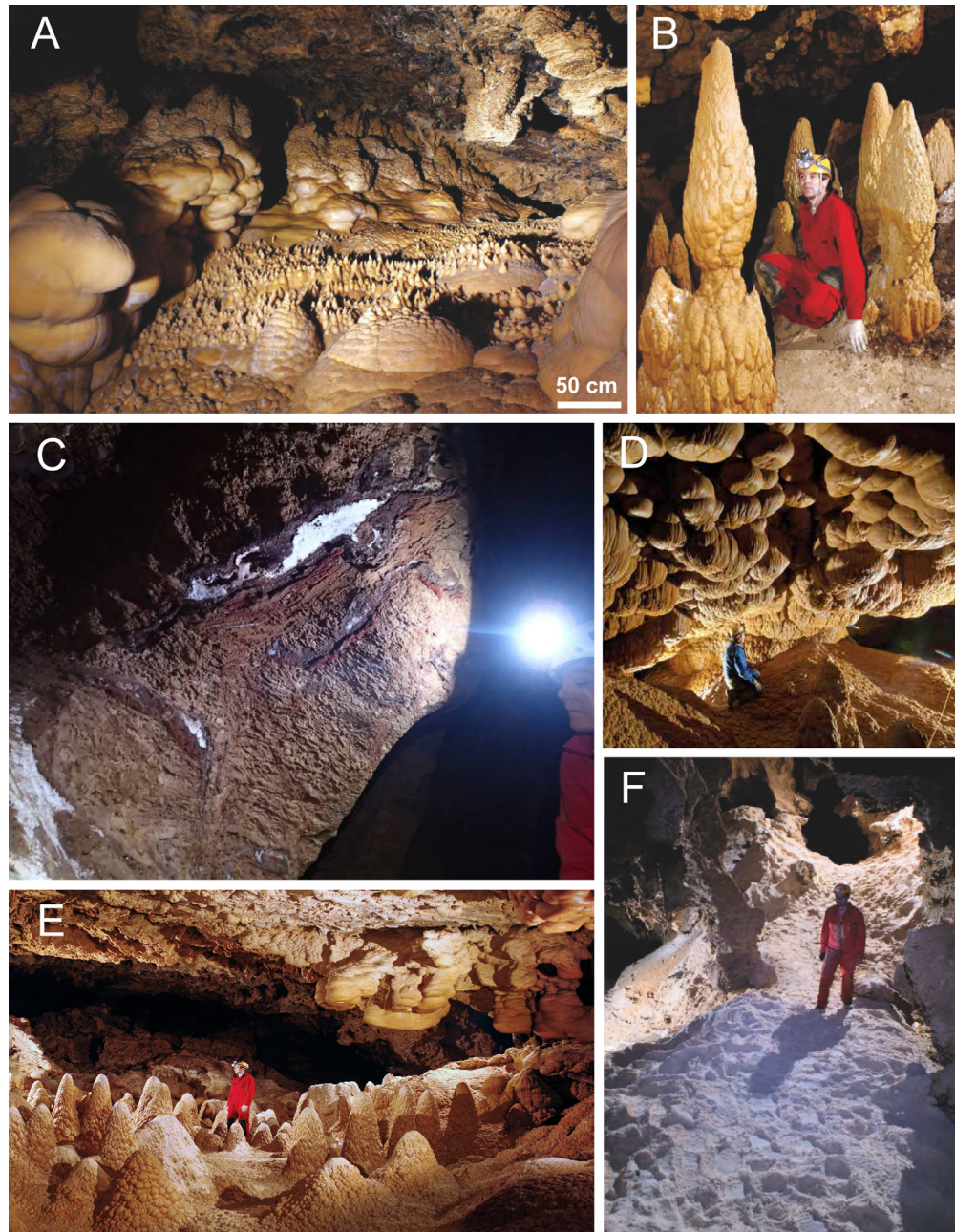
Figure 5.
Hypogenic speleothems in caves in the Murcia Region. (A) Coral towers, folia and cave clouds in Sima de la Higuera; (B) Double-tower cones in Sima de la Higuera; (C) Hydrothermal calcite infill in Cueva del Agua-Cartagena; (D) Cave clouds in Sima de la Higuera; (E) Cave cones in Sima de la Higuera; (F) Piles of calcite rafts in Sima de la Higuera (Photos: A, B, E, and F by Víctor Ferrer; D by Andrés Ros and J.L. Llamusí)

In caves where the current water table is tens of meters below the lower accessible levels, the action of subaerial hypogenic speleogenesis is especially evident. For example, in Cueva del Gigante, Cueva del Puerto, Sima de la Higuera, and Sima Destapada, many corrosion cupolas show strongly foliated micritized surfaces, whose alteration could be related to condensation-corrosion mechanisms due to the diffusion of CO_2 into condensation water under subaerial conditions (Palmer and Palmer, 2012).

Speleothems with a Hypogenic Origin

The presence of speleothems formed under subaqueous conditions from a solution that was highly saturated in calcium carbonate can provide evidence of the hypogenic origin of caves. In the caves in Murcia Region, a wide variety of speleothems usually related to hydrothermal flows has been identified. It is worth mentioning that most of these caves still show positive thermal anomalies with respect to the mean external temperature (~18ºC) (Table 1). This provides further evidence of the hypogenic/hydrothermal origin of these cavities.

Of these caves, Sima de la Higuera hosts most of the typical speleothems described for hypogenic caves, including calcite spars that fill fractures in the host rock, cave clouds, folia, tower coral, and calcite raft cones (Figure 5). All these speleothems are usually precipitated under phreatic or epiphreatic conditions, with water that is highly saturated in calcium carbonate, typical of hydrothermal environment. Nevertheless, it is worth mentioning that the presence of these types of speleothem is not restricted to hydrothermal caves but has also been described in non-thermal, epigenic caves (D'Angeli et al., 2015), where high saturation in calcite is reached due to elevated production from plants, as well as intense CO_2 degassing and evaporation in the cave.

Interestingly, in the Paradise Chamber (-85 m) of Sima de la Higuera, 92 cave cones have been inventoried. Roughly 40% can be considered as tower cones (or simple-tower cones), whilst the remaining 60% have a notch in the middle and look like two cones, one superimposed over the other (Figure 5B and E). The genetic mechanism of the double-tower cones includes the typical sinking of calcite rafts by dripwater and an intermediate stage of rapid precipitation of a calcite raft, caused by a drop in the water table and changes in cave ventilation; this leads to greater CO_2 degassing and evaporation over the surface of the thermal lake where these speleothems formed (Gázquez and Calaforra, 2013). Today, calcite raft deposits are scarce in this shallower level (above -82m) but they do appear at the depth of the Paradise Chamber of Sima de la Higuera,

and are especially abundant in deeper passages, such as the Four Paths Chamber (-117 m) (Figure 5F), where abundant calcite raft piles are found (Gázquez and Calaforra, 2013). Likewise, Cueva del Puerto, Sima Destapada, and Sima del Pulpo display vast deposits of calcite rafts that suggest intense CO_2 degassing, typical of hydrothermal water.

Other speleothems formed by the sinking of calcite rafts in shallow (~20 cm) pools have been observed in Sima la Higuera and Sima Destapada, such as coral towers (Figure 5A). The Sima de la Higuera also shows outstanding examples of folia, which usually form under subaqueous conditions near the water surface as a result of CO_2 degassing. Folia are also present in Sima del Pulpo. On most occasions, these speleothems appear at the same level as other speleothems of hydrothermal origin, including cave clouds and calcite crusts (Figure 5A). Sima de la Higuera and Sima del Pulpo host relevant examples of these types of crust speleothems. Calcite infilling of cracks in the host rock, sometimes in the form of spars, can be found in Sima de la Higuera and Cueva del Agua-Cartagena (Figure 5C). In addition to carbonate speleothems, gypsum is present in Cueva del Puerto and Sima del Pulpo. In these caves, gypsum appears as crusts and gypsum flowers. The origin of sulphates is probably linked to sulphuric acid speleogenesis (SAS) as has been described in many other caves worldwide (e.g., Palmer and Palmer, 2012; Audra et al., 2015).

Conclusions

Signs of hypogenic mechanisms have been detected in nine caves in the Murcia Region. CO_2-based hydrothermal mechanisms are proposed for the formation of Sima de la Higuera, Sima Destapada, Cueva del Agua-Cartagena, Cueva de Luchena, Cueva del Gigante, Sima del Alméz, and Cueva del Agua-Lorca. By contrast, Cueva del Puerto and Sima del Pulpo, where massive deposits of gypsum have been identified, were likely generated by SAS mechanisms. The wide range of hypogenic speleogenesis indicators and hydrothermal speleothems reveals that the hydrothermal field of the Murcia Region hosts one of the densest active hypogenic subterranean networks in the world.

José L. Carcelén, Antonio Latorre, José Soto, Andrés Marín, José David Lisón, José Florencio, Jesús López, and David Bayón. More information about these caves can be found at www.cuevashipogenicasdemurcia.es.

References

Armstrong R, Osborne L. 2005. Partitions, compartments and portals: cave development in internally impounded karst masses. International Journal of Speleology 34 (1): 71-81. http://dx.doi.org/10.5038/1827-806X.34.1.6

Audra P, Mocachain L, Bigot J-Y, Nobercourt J-C. 2009. The association between bubble trails and folia: a morphological and sedimentary indicator of hypogenic speleogenesis by degassing, example from Adaouste Cave (Provence, France). International Journal of Speleology 38 (2): 93-102. http://dx.doi.org/10.5038/1827-806X.38.2.1

Audra P, Gázquez F, Rull F, Bigot J-Y, Camus H. 2015. Hypogene sulfuric acid speleogenesis and rare sulfate minerals in Baume Galinière Cave (Alpes-de-Haute-Provence, France). Record of uplift, correlative cover retreat and valley dissection. Geomorphology 247: 25-34. http://dx.doi.org/10.1016/j.geomorph.2015.03.031

Cigna AA, Forti P. 1986. The speleogenetic role of air flow caused by convection. 1st contribution. International Journal of Speleology 15 (1): 41-52. http://dx.doi.org/10.5038/1827-806X.15.1.3

D'Angeli I, De Waele J, Ceballo Melendres O, Tisato N, Sauro F, Grau-Gonzalez E, Bernasconi SM, Torriani S, Bontognali TRR. 2015. Genesis of folia in a non-thermal epigenic cave (Matanzas, Cuba). Geomorphology 228: 526-535. http://dx.doi.org/10.1016/j.geomorph.2014.09.006

Forti P. 1996. Thermal karst systems. Acta Carsologica 25: 99-117.

Forti P, Galdenzi S, Sarbu SM. 2002. The hypogenic caves: a powerful tool for the study of seeps and their environmental effects. Continental Shelf Research 22 (16): 2373-2386. http://dx.doi.org/10.1016/S0278-4343(02)00062-6

Gázquez F, Calaforra JM, Rull F. 2012. Boxwork and ferromanganese coatings in hypogenic caves: an example from Sima de la Higuera Cave (Murcia, SE Spain). Geomorphology 117-118: 158-166. http://dx.doi.org/10.1016/j.geomorph.2012.07.022

Gázquez F, Calaforra JM. 2013. Origin of double-tower raft cones in hypogenic caves. Earth Surface and Landform Processes 38: 1655-1661. http://dx.doi.org/10.1002/esp.3399

Klimchouk AB. 2009. Morphogenesis of hypogenic caves. Geomorphology 106: 100-117. http://dx.doi.org/10.1016/j.geomorph.2008.09.013

Osborne RAL. 2004. The troubles with cupolas. Acta Carsologica 33: 9-36.

Palmer AN. 2011. Distinction between epigenic and hypogenic caves. Geomorphology 134: 9-22. http://dx.doi.org/10.1016/j.geomorph.2011.03.014

Palmer MV, Palmer AN. 2012. Petrographic and isotopic evidence for late-stage processes in sulfuric acid caves of the Guadalupe Mountains, New Mexico, USA. International Journal of Speleology 41 (2): 231-250. http://dx.doi.org/10.5038/1827-806X.41.2.10

Ros A, Llamusí JL, Sánchez J. 2011. Exploración en Sima Destapada y Cueva del Agua, dos cavidades de origen hidrotermal (Murcia), VIII Simposio Europeo de Espeleología, Marbella.

Ros A, Llamusí, JL, Sánchez J. 2014a. Cuevas hipogénicas en la Región de Murcia (España). I Congreso Iberoamericano y V Congreso Español sobre Cuevas Turísticas. Aracena-Huelva.

Ros A, Llamusí JL, Sánchez J. 2014b. Cuevas hipogénicas en la Región de Murcia (España) vol. I. Edita CENM-naturaleza, Murcia

VARIOUS SETTINGS FOR THE DEVELOPMENT OF HYPOGENIC CAVES AND PALEOKARST FEATURES IN THE ARBUCKLE MOUNTAINS, OKLAHOMA, USA

Kevin William Blackwood

Oklahoma State University
105 Noble Research Center
Stillwater, OK 74078, USA, karstgeoscience@gmail.com or blackkw@ostatemail.okstate.edu

Abstract

The Arbuckle Mountains are a complex geologic province, characterized by thick sequences of intensely folded and faulted carbonates, sandstones, and shales of the Late Cambrian through Pennsylvanian. Cave, karst, and paleokarst features occur in relatively high densities within several limestone and dolostone formations and contain morphogenic signatures of both epigenic and hypogenic karst development. Hypogenic karst signatures can be found in caves throughout the Arbuckle Mountains, but occur most commonly in the regimes where deformation is most severe, such as the north flank of the Arbuckle anticline. However, there is evidence that hypogenic speleogenesis may have occurred on the south flank of the Arbuckle anticline where the semi-confining Simpson Group overlaid the upper Arbuckle Group, producing solutionally widened joint networks, with some apertures wide enough to permit physical exploration and resemble network mazes; however, epigenetic process now dominate on the south flank at present. Hypogenic karst development appears to continue today where the soluble carbonates are overlain by confining units along the edges of the anticline where fresh and saline waters mix and microbial interactions with hydrocarbons provide the fluid geochemistry allowing carbonate dissolution.

Introduction

The Arbuckle Mountains geological province consists of a huge inlier of folded and faulted Paleozoic and Precambrian rocks, covered on its northern, eastern, and western sides by Late Pennsylvanian and Permian strata and on its southern side by Early Cretaceous sediments of the Gulf Coast Plain.

The inlier encompasses an area of roughly 2,600 km^2 in Murray, Carter, Johnston, and Pontotoc Counties (Figure 1) and contains 3,350 m of Late Cambrian through Devonian strata, almost all of which are comprised of carbonate rocks. Sandstones and thin interbedded shales comprise only a small fraction of the total stratigraphic column (Ham, 1973). The carbonates of the Cambrian

and Ordovician Arbuckle Group exposed in road cuts along Interstate 35 have been measured to be more than 2,040 m thick (Fay, 1989).

Studies in the Arbuckle Mountains show evidence for several types of structural and geochemical environments favorable for hypogene speleogenesis. Several hypogene caves are known on the north flank of the Arbuckle anticline north of the Chapman Ranch Fault (Figure 2) (Blackwood et al., 2015), but determining which geochemical process led to their development or whether multiple process occurred simultaneously remains unclear.
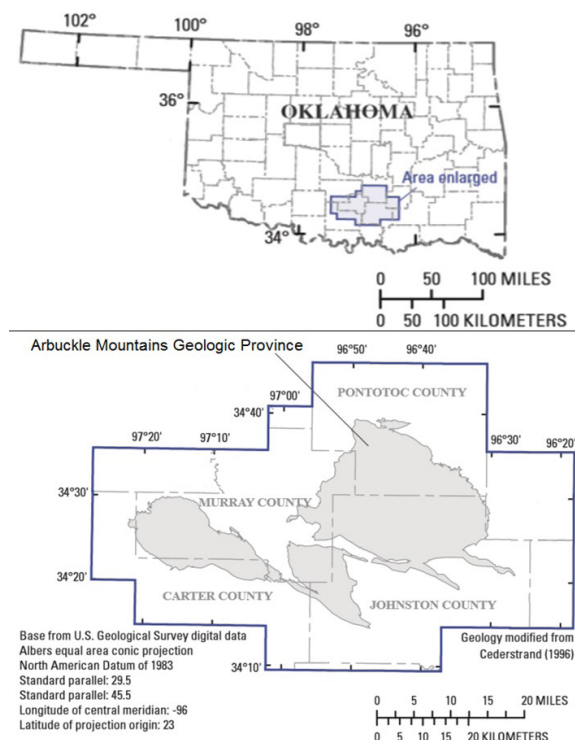
Figure 1.
Map of Arbuckle Mountains geological province in shaded area. Map modified from Christensen et al. (2011).

This paper reviews the different structural and geochemical environments in which these hypogenic caves may have developed and discusses the effectiveness of the roles each of these environments might have had on the development of hypogenic caves and paleokarst features. In hypogenic systems, different mechanisms may operate simultaneously or in sequence, making it difficult or impossible to discern which has contributed most to hypogene speleogenesis (Klimchouk, 2014), so determining anything conclusive may be beyond the scope of this paper.

Hypogenic Caves and Paleokarst Features

Paleokarst features in the Arbuckle Mountains first generated interest in 1987 when a well in the Cottonwood Creek oil field encountered a solution-enlarged fracture or cavern in an Upper Arbuckle subcrop during drilling at a depth of approximately

2,600 m when the bit dropped nearly 6 m (Johnson 1991, Puckett et al. 2009). The discovery of oil within this karst feature led to many studies of the karst and paleokarst features, such as Becker (1988) who attributed the origins to submarine processes. In 1993, the Annual Permian Basin Section—SEPM Field Trip was hosted in the Arbuckle Mountains with an emphasis on paleokarst. Several paleokarst features were described and their origins and alteration were attributed to hydrothermal activity during the Pennsylvanian-Permian based on hydrothermal oxygen isotope signatures in the veins and halos around paleokarst features studied in road cuts along Interstate 35 (Wilson, 1993; Fritz, 1993). It is thought that these ascending hydrothermal fluid events were multi-episodic and may be related to hydrocarbon migration (Lynch and Al-Shaieb, 1991).

On the Arbuckle anticline, paleokarst features are only found north of the Chapman Ranch Fault,
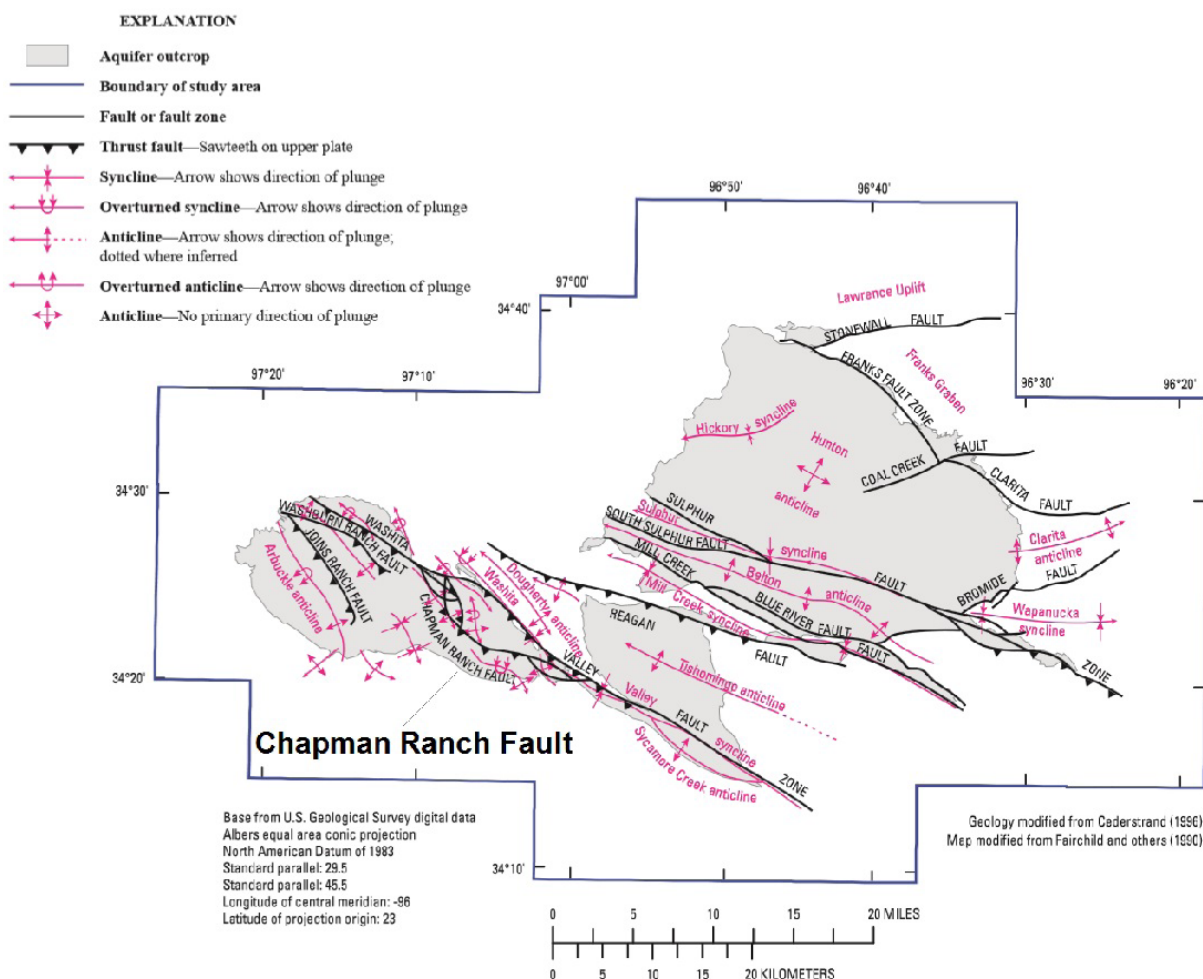
Figure 2.
Structural geologic map showing the trend of the Chapman Ranch Fault modified from Christensen et al. (2011).

indicating that the features likely formed as a result of orogenic processes rather than eogenetic karsting during sedimentation, since such features are not found throughout the anticline but where deformation and faulting was most severe. Chemical Remnant Magnetization (CRM) studies by Elmore (2001) suggested that basinal or orogenic-type fluids migrated laterally through paleoaquifers and vertically through faults/fractures during multiple flow events that spanned a time interval of approximately 60 Ma during the Late Paleozoic. Many of the paleokarst features are filled with terra rosa clays or cements and thought to have been buried during the Permian.

The existence of hypogenic caves in the Arbuckle Mountains was suggested by Christensen et al. (2011) and were confirmed in part through morphological investigations conducted in 2013 and 2014 by Blackwood (2014) using criteria discussed by Klimchouk (2007). The first scientific publication on the caves in the Arbuckle Mountains by Curtis (1959) looked at 11 caves and noted four of them as being the "dry type," as playing no apparent role in the storage or transport of groundwater. Morphological investigations of these caves has since confirmed them to hypogene in origin. It is thought that the hypogenic caves formed during the same time as the paleokarst features, but were either never buried or have since been exhumed (Blackwood et al., 2015). In the Devil's Garden Cave System near Falls Creek (Figure 3), a passage terminates into cemented terra rosa clays common of paleokarst. The Devil's Garden Cave System contains many classic signatures of a hypogenic cave, such as wall and ceiling features commonly produced by ascending fluids.

Figure 3.
Paleokarst feature in a terminating passage in the Devil's Garden Cave System. (Photo by Stacy Gantt-Blackwood, 2011)

Developmental Settings

The following settings have been documented in the Arbuckle Mountains and may have or are currently contributing to the development of hypogenic cave and karst features.

Basinal and Orogenic Fluids through Deep Fractures

The Arbuckle Mountains are heavily folded and faulted, and many of the faults extend to basement. Vertical displacements of more than 2,300 m have been measured from well logs and cuttings (Allen and Neman, 2012), while major strike-slip faults have lateral displacements over 60 km (Scheirer and Scheirer 2006). Evaluations of vertical fracturing from geophysical and thermal datasets by Halihan et al. (2009) indicate that many of the faults and other fractures extending to the bottom of the aquifers may be acting as conduits for the rapid vertical circulation of groundwater throughout the geologic units, eliminating any geothermal gradient within the Arbuckle aquifers.

Significant vertical fracturing was observed and drilling evidence suggests the permeability of the aquifers increases with depth. Bore-hole temperature data shows that the groundwater is actually 0.5°C colder at depth than at the water table. In order for the groundwater to cool the rocks and fluid samples 10-15°C below the expected temperature, and maintain a gradient near zero, fluids must be ascending and descending through the aquifer rapidly. It is expected that this zone of vertical circulation extends to basement at a depth of approximately 1000 m. It is possible that this vertical connection may be stronger than the lateral connection between springs and wells (Halihan et al., 2009). During the Arbuckle-Simpson Hydrology Study (Christensen et al., 2011), the best MOD Flow modeling results were obtained when the vertical hydraulic conductivity was increased substantially (1,000 times greater). The improved results are thought to coincide with vertical flow through the Sulphur Fault, which may be masked beneath the Pennsylvanian confining unit.

Freshwater Flushing and Mixing with Brine and Petroleum Beneath Confining Units

The Arbuckle Mountains once contained brines and petroleum that have since been largely flushed from the aquifers (Puckett, 2009), although traces of hydrocarbons can still be detected in some freshly broken rock samples. Petroleum is now found in economical amounts, along with the brines, only where the Arbuckle rocks subcrop hundreds of meters beneath the Pennsylvanian rocks.

Wells drilled through the confining units at the flanks of the Arbuckle Mountains often flow as artesian and contain sulfide odors. Freshwater springs typically emanate up-gradient near the bases of the Arbuckle Mountains, but not capped by confining units. The area between these springs and wells is thought to indicate the location of the freshwater/brine transition zone at the edge of the freshwater system. These contrasts in water chemistry beneath confining units may be efficient to drive the disequilibrium and dissolution mechanisms (Klimchouk, 2007). Unpublished isopach maps constructed from well data by Geologist Robert Allen indicate vast aquifers of sulfur-rich water extending several kilometers from the flanks of the freshwater aquifers.

The Arbuckle Mountains are an eroded anticline. The rocks at the crest of the anticline once subcropped confining and semi-confining units that have since been eroded further and further from the crest. Outcrops in the Upper Arbuckle Group that were previously overlain by semi-confining units of the Simpson Group contain vast networks of solutionally widened joints, some of which are wide enough to allow human entry for direct exploration. These networks of joints resemble network mazes, which are commonly associated with hypogene speleogenesis (Palmer, 2007). It has been speculated that as erosion breached the Arbuckle Mountains, the rocks were altered by meteoric processes, perhaps facilitating hypogene speleogenesis as the freshwater infiltrated aquifers and/or petroleum reservoirs that contained petroleum and brine (Puckett et al., 2009). This process occurring beneath the semi-confining units would fit within the hypogenic hydrogeological model described by Klimchouk (2007). Morphological investigations within these caves have not been able to confirm whether or not these features are hypogenic as overprinting by descending water has been very effective in the vadose zone.

The development of paleokarst features within the Viola Limestone may be the most likely features to have formed as a result of petroleum and brine flushing beneath a confining unit. The Viola Limestone underlies the Sylvan Shale, an organic rich oil producing shale and effective aquitard. Almost all caves surveyed in the Viola Limestone contain hypogenic signatures.

Aggressive Agents
The caves of the Arbuckle Mountains are fairly well known for their seasonally high levels of atmospheric carbon dioxide (Palmer and Palmer, 2009). It is thought that the high levels of carbon dioxide are from decaying organic matter within caves containing passage geometries that inhibit effective air circulation (Badino, 2009). However, it is possible that some of the carbon dioxide could be carried from depth. Carbon dioxide and organic acids can be generated at high temperatures by the conversion of organic matter into petroleum can increase the porosity of carbonate rocks in oilfields (Kharaka et al., 1986).

The role of sulfuric acid in the Arbuckle Mountains is unclear, though hydrogen sulfide is common near the flanks of the Arbuckle Mountains and may form sulfuric acid if sufficient oxygen available. Gypsum is found in minimal amounts in water samples in wells and springs along the flanks of the Arbuckle Mountains (Christensen, 2009), and at least one of the hypogenic caves appears to have gypsum crystals in the walls near a rising shaft where a hydrogen sulfide odor is currently being investigated using lead acetate paper. Pyrite is also present in many of the formations in the Arbuckle Mountains, but it is not clear how much an affect it has on internal aggressiveness and dissolution in the Arbuckle Mountains.

Current Evidence for Upwelling Fluids
Aside from artesian springs modeled during the Arbuckle-Simpson Hydrology Study, Beard (2014) has been investigating the possibility of upwelling in a cave in the eastern Arbuckle Mountains. Though geochemical and morphological studies show little to no evidence of upwelling, perhaps due to strong epigenetic overprinting and dominating processes, geophysical studies show a deep vertical conductive feature extending well beneath the cave.

With regards to the hypogenic caves that were described by Curtis (1959) as "dry caves" and thought to no longer play a role in the storage and transport of groundwater; A flooding event apparently unrelated to surface recharge was observed in December 2014 (Blackwood 2014) when water upwelled from the drain of White Woman Cave (Figure 4) to flood the cave 1 m deep. The flood removed dirt from the walls and left an obvious water-level line throughout the cave. Photo comparisons indicated that the cave had flooded to the same level in the past based on a barely discernable water-level line, but such events may be incredibly rare. A dated signature from 1952, written in carbide on a wall, was partially removed when carbide-coated dirt was washed away, indicating that the cave had probably not flooded to that level since that time. Since studies of paleokarst by Elmore (2001) suggested basinal or orogenic fluids as playing a role in locally altering the carbonates, a hypothesis for the upwelling fluid in White Woman Cave may be related to the recent spike in Oklahoma

earthquakes due to wastewater injection. One suggestion that water could have been squeezed up through the Washburn Ranch Thrust Fault, which runs very near to the cave, as a result of one of two earthquakes that occurred in the area around that time.
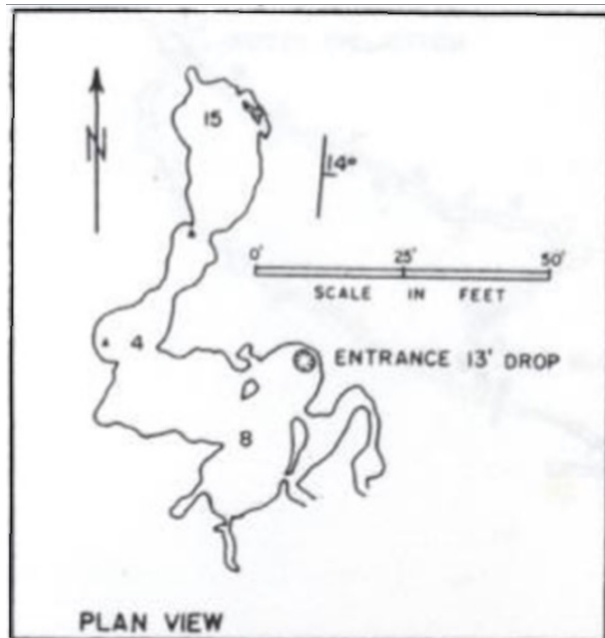

Figure 4.
Map of White Woman Cave (Curtis, 1959).

Discussion

The Arbuckle Mountains contain various settings favorable for the development of hypogenic karst. Although it is not for certain which process lead to the development of the known hypogenic caves, it is possible that they may have developed around the same time or simultaneously with the paleokarst features that are thought to have developed by hydrothermal fluids ascending vertically through fractures and are perhaps orogenic in nature. The groundwater temperatures at present remain nearly isothermal throughout the hydrostratigraphic units of the Arbuckle Group where studied, so the hydrothermal process that likely formed many of the paleokarst features is no longer active.

The hypogenic caves and paleokarst features on the north flank of the Arbuckle Mountains developed in chaotic settings, within rocks that are heavily folded and faulted. The large thrust faults penetrate the basement rocks where they have been studied in test wells. It is uncertain whether or not these features developed beneath confining units or if they developed entirely by fluids squeezed up through fractures or circulating convection currents.

The artesian settings occurring at the flanks of the Arbuckle Mountains are structurally similar to the settings at the Simpson-Arbuckle contact where the Simpson may be acting as a semi-confining unit to produce solutionally widened joints similar to hypogenic network mazes.

The aggressive agents may all play a role to varying degrees, but carbonic acid appears to be the dominant dissolving agent on the anticline, while the mixing of freshwater and brine may be the dominant dissolving agent near the base of the anticline. Biological degradation of hydrocarbons trapped in the rocks, as well of the oxidation of pyrite may also contribute, but the minute amounts of gypsum might indicate that their roles are relatively insignificant.

It is possible that these processes were multi-episodic and several developmental settings occurring simultaneously.

Acknowledgements

References

Al-Shaieb Z. 1993. Road Log, Permian Basin Section-SEPM Annual Field Trip, 1993, Arbuckle Mountains, Oklahoma. Paleokarst, Karst-Related Diagenesis, Reservoir Development, and Exploration Concepts: Examples from the Paleozoic Section of the Southern Mid-Continent. p. 8

Allen RW, Newman RL. 2012. The Arbuckles below your feet. Oklahoma Geological Survey presentation.

Badino G. 2009. The legend of carbon dioxide heaviness. Journal of Cave and Karst Studies 71 (1): 100-107.

Beard KS. 2014. Investigation of upwelling along the eastern boundary fault of the Arbuckle-Simpson aquifer. Geological Society of America South-Central Section—48th Annual Meeting. Abstract and presentation.

Becker RD. 1988. Stratigraphy and depositional characteristics of the bromide dense unit and viola limestone, subsurface Central Oklahoma [unpublished M.S. thesis]. Tulsa (OK): University of Tulsa.

Blackwood KW. 2014. Hypogenic karst in the Arbuckle Mountains. Proceedings of the Oklahoma Academy of Science, Vol 93 2013. p. 70.

Blackwood KW, Beard KS, Halihan T. 2015. Development and distribution of hypogenic caves and paleokarst features in the Arbuckle Mountains of south central Oklahoma, USA. American Association of Petroleum Geologists, Annual Convention and Exhibition, June 3, 2015, Denver, Colorado.

Christensen S, Osborn NI, Neel CR, Faith JR, Blome CD, Puckett J, Pantea MP. 2011. Hydrogeology and simulation of groundwater flow in the Arbuckle-Simpson aquifer, south-central Oklahoma. U.S. Geological Survey Scientific Investigations Report 2011-5029. p. 10, 11, 18-98

Christensen SC. 2009. Geochemical investigation of the Arbuckle-Simpson aquifer, south-central Oklahoma. U.S. Geological Survey Scientific Investigations Report 2009-5036. p. 26

Curtis NM. 1959. Caves in the Arbuckle Mountains area, Oklahoma: Oklahoma Geological Survey. Oklahoma Geology Notes 19 (2): 20-31.

Elmore RD. 2001. A Review of paleomagnetic data on the timing and origin of multiple fluid-flow events in the Arbuckle Mountains, Southern Oklahoma. Petroleum Geosciences 7 (3): 223-229. http://dx.doi.org/10.1144/petgeo.7.3.223

Halihan T, Mouri S, Puckett J. 2009. Evaluation of fracture properties of the Arbuckle-Simpson aquifer. Final Report for the Arbuckle-Simpson Hydrology Study. p. 1-60

Ham WE. 1973. Regional geology of the Arbuckle Mountains, Oklahoma. Oklahoma Geological Survey Special Publication 1. p. 1.

Johnson KS. 1991. Geologic overview and economic importance of late Cambrian and Ordovician rocks in Oklahoma. Late Cambrian-Ordovician Geology of the Southern Midcontinent, 1989 Symposium: Oklahoma Geological Survey Circular 92. p. 1-14

Kharaka Y, Law L, Carothers W, Goerlitz D. 1986. Role of organic species dissolved in formation water from sedimentary basins in mineral diagenesis. In Gautier DL, editor. Roles of organic matter in sediment diagenesis. Society of Economic Paleontologists and Mineralogists, Special Publication 38. p. 111-122. http://dx.doi.org/10.2110/pec.86.38.0111

Klimchouk AB. 2007. Hypogene speleogenesis: hydrogeological and morphogenetic perspective. Carlsbad (NM): National Cave and Karst Research Institute. p. 5-97.

Klimchouk AB. 2014. The methodological strength of the hydrogeological approach to distinguishing hypogene speleogenesis. Hypogene Cave Morphologies Special Publication. Carlsbad (NM): National Cave and Karst Research Institute. p. 5.

Lynch M, Al-Shaieb Z. 1991. Paleokarstic features and thermal overprints observed in some of the Arbuckle cores in Oklahoma. Arbuckle Group Workshop and Field Trip, Oklahoma Geological Survey, Special Publication 91-3.

Palmer AN. 2007. Cave geology. Dayton (OH): Cave Books.

Palmer AN, Palmer MV, Veni G. 2009. Caves and karst of the USA. Huntsville (AL): National Speleological Society. p.180

Puckett J, Halihan T, Faith J. 2009. Characterization of the Arbuckle-Simpson aquifer. Final report submitted to the Oklahoma Water Resources Board, Stillwater, Oklahoma State University School of Geology. p. 22, 24

Scheirer DS, Hosford Scheirer A. 2006. Gravity investigations of the Chickasaw National Recreation Area, south-central Oklahoma. U.S. Geological Survey Open-file Report 2006-1083. p. 40

Wilson JL. 1993. The Lower Ordivician Great American Bank of the Southwestern United States. In Keller DR, Reed CL. Paleokarst, karst-related diagenesis, reservoir development, and exploration concepts: examples from the Paleozoic section of the southern mid-continent: 1993 annual field trip guidebook, Permian Basin Section-SEPM, Arbuckle Mountains, Oklahoma. p. 41.

EVIDENCE OF HYPOGENIC KARST DEVELOPMENT IN THE TAURUS MOUNTAIN RANGE, TURKEY

C. Serdar Bayari
Hacettepe University, Dept. of Geological Eng.
Beytepe Campus, Ankara, 06800, Turkey, serdar@hacettepe.edu.tr

N. Nur Özyurt
Hacettepe University, Dept. of Geological Eng.
Beytepe Campus, Ankara, 06800, Turkey, nozyurt@hacettepe.edu.tr

Alexander Klimchouk
Institute of Geological Sciences
Natl. Academy of Science of Ukraine
55-b Gonchara Str., Kiev 01054 Ukraine, klim@speleogenesis.info

Koray Törk
Karst and Cave Research Unit
General Directorate of Mineral Research and Exploration
Dumlupınar Bulvarı 139, Ankara, 06800 Ankara, Turkey, cave@mta.gov.tr

Lütfi Nazik
Ahi Evran University, Dept. of Geography
Sahir Kurutluoğlu Cad. 100, Kırşehir, 40100, Turkey, lutfinazik@ahievran.edu.tr

Abstract
The Taurus Mountain Range extends between the Mediterranean Sea and the Central Anatolian Plateau of Turkey. It is made primarily of carbonate rocks exhibiting extensive karst development. Recent evidence and reassessments of available data revealed that hypogenic processes have contributed substantially to the development of karst in this area. Remarkable examples of hypogenic karst development along the range, from west to east, include the Antalya Travertine Plateau and Kırkgöz submerged cave system, giant collapse dolines (obruks), and deep karst development in high mountains that include carbonate-hosted ore deposits. Common properties of hypogenic karst in the range include high dissolved helium of mantle and crustal origin in groundwater, and proximity to extinct volcanic and/or tectonic structures. Evidence indicates that hypogenic karst formation in the range may or may not be associated with hydrothermal fluid migration during development. Additionally, earth tides appear to provide the energy needed for deep fluid migration.

Introduction
We use the term hypogenic karst development to denote the formation of solution void-conduit systems by fluids that recharge the soluble formation from below, independent of recharge from the overlying or immediately adjacent surface karst landscapes. The groundwater may be a cool discharge of a regional artesian system or a warm/hot hydrothermal fluid which may or may not be mixed with near-surface cool groundwater. Recent assessments (e.g. Özyurt and Bayari, 2014; Bayari and Özyurt, 2014) of available and new observations on karst development suggests that hypogenic karst formation in the Taurus Mountain Range is more widespread than previously thought. Understanding the mechanisms of hypogenic karst development is important in terms of water resources management, exploration of oil reservoirs and ore deposits, etc.

The Taurus Mountain Belt of southern Turkey is a part of the Alpine-Himalayan orogeny. The belt is composed of several major units. Each unit is made up mainly of Paleozoic to Mesozoic aged carbonate (i.e., mostly limestone and partly dolomite) formations. These units, once laying side by side in a 1500-km-wide epicontinental sea, were thrusted onto each other during the closure of the Tethys Ocean in the Cenozoic between the Eurasian Plate and northward-moving African and Arabian plates. The thrusting process resulted in the formation of Taurus Mountain Belt, which created

an orographic barrier about 200-km-wide between the Mediterranean Sea to the south and the Central Anatolian Plateau to the north. The Taurus Mountain Belt hosts some remarkable examples of hypogenic karst development, such as (a) the Antalya Travertine Plateau and Kırkgöz submerged cave system, (b) giant collapse dolines (obruks), and (c) deep karst development in high mountains that include carbonate-hosted ore deposits. Characteristic features of these areas and their relation to hypogenic karst development are presented briefly below. The common properties of hypogene karst development in these areas are also discussed.
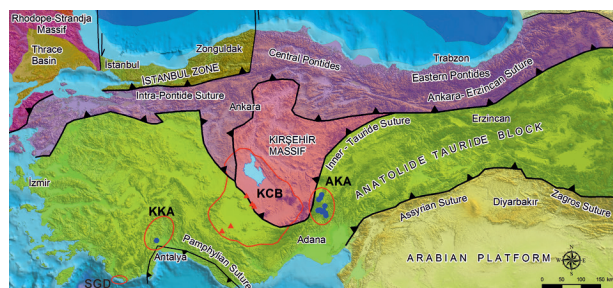

Figure 1.
Location of sites mentioned in text on the map of Turkey (after Özyurt and Bayari, 2014). KKA: Antalya Travertine Plateau, KCB: Central Anatolia obruks, AKA: Aladağlar Massif, SGD: Submarine groundwater discharge zone.

Antalya Travertine Plateau and Kırkgöz Submerged Cave System

The Antalya Travertine Plateau is located in southwestern Turkey on the southern flank of the Taurus Mountains. It is the largest freshwater travertine deposit in the world and has formed since the Upper Pliocene. It is made up of three quasi-horizontal benches called upper (Döşemealtı), lower (Varsak-Düden), and submarine plateaus. The upper and lower plateaus extend from 250-300 m and 50-150 m above mean sea level and comprise an area of about 650 km2. The thickness of the travertine in the upper and lower plateau is estimated as 50 m and 150 m, respectively. Two 50-m-high steep walls separate the upper and lower and lower and submarine plateaus. The submarine plateau is located 50-150 m below mean sea level and extends 2.5 km offshore.

Currently, the travertine formation is sustained by a number of karst springs scattered in the upper and lower plateaus. Among all, Kırkgöz (~Q = 18 m3/sec) and Düdenbaşı (~Q = 10 m3/sec) springs are the most prominent. A team of US and Turkish cave divers explored the submerged part of these springs in 1995 and found very large and deep dissolution cavities. One of the submerged cavities in the Kırkgöz system was

named "Stadium" based on its dimensions of >100 m by 60 m by 50 m (height-length-width). The Stadium was considered to be the largest submerged cavity in Asia (Kincaid, 1999). The same team discovered the main submerged feeder cavity of Düdenbaşı spring, which extends 65 m below surface at a length of 400 m. Both explorations were terminated due to the technical limitations of the diving equipment.

The presence of such a large freshwater travertine deposit and submerged cavities/feeders in the associated karst springs is apparently associated with hypogenic fluid migration through the large carbonate massif of the Taurus Mountains. In this part of the eastern Mediterranean, Rhodes Basin (-4,500 m), Finike Trough (-300 m) and Antalya Basin (-2,500 m) mark the extent of a suture zone between the Taurid Anatolid plate and the subducted plate of the southern branch of Neo-Tethys Ocean. Earthquakes with epicenters up to 160 km below surface indicate a continuing and relatively rapid subduction of a lithospheric plate which probably occurs along the suture zone. Such deep tectonic activities are also evidenced by the dissolved noble gas data obtained from the karst springs in the Antalya Travertine Plateau (Özyurt et al., 2000). Helium isotope ratios of these groundwaters indicate an apparent gas influx from mantle and crustal sources. Therefore, the formation of large submerged cavities and associated travertine deposits are very likely associated with the hypogenic fluids enriched by crustal and mantle carbon dioxide.
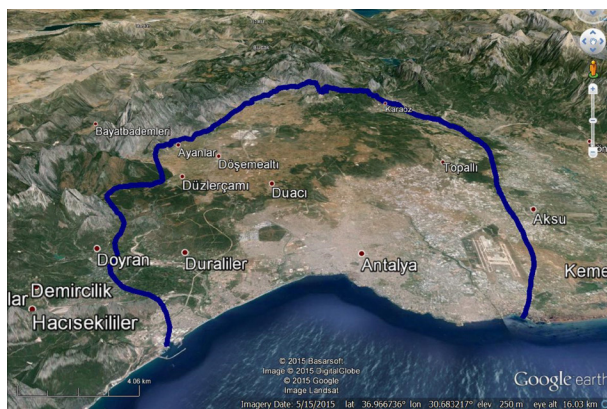

Figure 2.
Google Earth oblique view of the Antalya Travertine Plateau, looking north. The solid line defines the boundary of the plateau. Kırkgöz and Düdenbası springs are located at the northwest and center-south of the image, respectively. Upper and lower plateaus are differentiated by agricultural lands and rural lands, respectively.

Obruks—Giant Collapse Dolines in Central Anatolia

"Obruk" is the Turkish term for the collapse dolines commonly observed throughout the Taurus Mountain Range. However, much of the large-scale obruk development is also observed at the Obruk Plateau of the Konya closed basin located north of the central Taurids. The obruks have a characteristic upside-down truncated cone shape with surface diameters ranging from 30 m to 300 m. Depths of the obruks range from a few meters up to 150 m. Their formation still continues, and a few obruks have formed each year during the last decade.

Most of the closed basin tectonically belongs to the Taurid-Anatolid Plate, part of which is the Taurus Mountain Range. In this part of Turkey, ongoing extensional tectonic processes continued during the Cenozoic and led to the formation of this closed basin. Lithospheric thinning caused by the extensional tectonism resulted in asthenosphere rise that eventually led to volcanic activity which started in the Miocene and continued discontinuously until the beginning of the Holocene. Recent evidence shows that the formation of obruks is associated with the excessive geogenic carbon-dioxide uprising from the mantle and/or deep-seated carbonate rock which has been metamorphosed by mantle heat. Several areas in the closed basin use carbon-dioxide dissolved in groundwater for dry ice production. Recent data on dissolved gases, obtained from wells tapping regional cool groundwater, indicate an apparent mixture of mantle and crustal gas fluxes, which is in agreement with the carbon-13 signal of dissolved carbon-dioxide gas (Bayari et al., 2009a, 2009b). Özyurt and Bayari (2014) show that during the last 45,000 years, the groundwater's helium content originated mainly from the mantle and deep crustal, increasing along the regional flow path that extends from the Taurus Mountains to the terminal Salt Lake.

Aladağlar High-Mountain, Deep-Karst System

The Aladağlar Massif, located at the central eastern end of the Taurids, has been subject to extensive karst hydrogeological and morphological research. Like other parts of the Taurus Mountain Range, the massif is comprised entirely of carbonate nappes. With peaks exceeding 3,700 m in elevation and large karst springs (Q > 7 m3/sec, Özyurt, 2005) located down to 400 m a.s.l., the massif is one of the thickest karst aquifers of the world. Since the closure of the Neo Tethys Ocean around the Late Cretaceous–Early Tertiary Period, the basin had been covered by a thick ophiolite nappe cover until the Eocene. During this period, plutons intruded into the massif and brought the first hydrothermal fluids

Figure 3.
After Atlas Magazine, Kızören Obruğu is the largest obruk with a lake in the Konya closed basin. The 300-m diameter lake is a window to the local water table. In the front of this image are the ruins of a medieval inn along the Silk Road.

that precipitated the original carbonate-hosted sulfide deposits. Synchronously with this initial hypogenic and hydrothermal karst development, a left-lateral strike-slip fault (known as the Ecemiş Fault), marking another suture line between Taurid-Anatolid Plate and Kırşehir Metamorphics, moved the massif up to 60 km northeast since the Eocene. During this period, the massif was also uplifted and the impermeable ophiolite nappe cover was eroded almost completely. Removal of the ophiolite cover initiated the epigenic karst development as infiltrating recharge from surface found its way to the karst springs at lower elevations upon erosion of the overlying ophiolite cover.

During the Oligocene-Miocene period, tropical to subtropical conditions dominated the climate. Accordingly, oxygen-rich recharge from the surface started to convert the sulfidic metals into the carbonate minerals that are mined today. After the Miocene,

a warm pluvial climate dominated the massif. The increased elevation of the massif since the Oligocene, paired with the favorable climate, led to the development of deep sub-vertical karst systems until the Quaternary (Törk, 2008). During Quaternary glaciations, the massif was subject to dramatic glacial erosion that completely removed the preexisting epikarst zone. Today, the glacially scoured upper plateau of the Aladağlar massif abounds with decapitated shafts that are partly or wholly filled with glacial debris (Klimchouk et al., 2006).

One of the unfilled shafts discovered and explored during a seven-year Ukrainian-Turkish speleological field survey is 1,400-m-deep Kuzgun Cave (Klimchouk et al., 2006). The cave developed as a set of vertical shafts connected by narrow lateral meander passages. The cave provides excellent evidence of hypogenic and epigenic karst development throughout its history. In many places it cuts across large preformed hypogenic geode-like cavities, presumably hydrothermal, lined with a crust of columnar calcite crystals and partly filled with clay containing large spherical concretions.

The Aladağlar Carbonate Massif hosts large karst springs with discharges as high as 7 m3/sec, and its total mean annual discharge of karst groundwater is about 31 m3/sec (Özyurt and Bayari, 2008). Some of the springs have associated travertine deposits that form natural bridges over the main stream, the Zamantı River. Noble gas isotopes dissolved in spring water indicate mantle and crustal gas influx into the karst system (Özyurt and Bayari, 2014).

Figure 4.
Aladağlar Carbonate Massif. View to the peaks of the Aladağlar Carbonate Massif from the west. The highest peak is Demirkazik (3,756 m a.s.l.).

Earth-Tidal Pumping of Deep Karst Groundwater

Sustainable mineral dissolution, particularly in deep-burial environments and deep-seated confined flow systems, requires replacement of saturated pore fluid with unsaturated water. Such fluid movement requires energy beyond the limits of hydraulic force potential dictated by Earth's gravity. Earth tides provide an additional energy source for fluid migration in environments where gravitational hydraulic potential energy is not sufficient. Like sea tides, Earth tides are generated by the gravitational force of the moon and sun exerted on the Earth. Periodic variation of the lateral compression of the crust driven by Earth tides, combined with the vertical pressure exerted over the crust mainly by seasonal precipitation load, lead to the temporal compression and expansion of porous media. Such periodic compression and expansion forces help the pores "breathe" fluid in and out. The effect of earth tides is well-known in the oil industry and has also been observed in aquifers.

An approximate year-long record of high temporal resolution temperature and specific conductance observations, obtained from a submarine karst cave in the Mediterranean coast of southwestern Turkey, provides evidence on how groundwater discharges into the sea driven by Earth tides (Bayari and Özyurt, 2014; Bayari et al., 2011). Analysis of the periodic oscillations have shown that the deeply-circulating groundwater discharging from the large karst massif into the sea is controlled mainly by the combined effect of Earth tides and precipitation load upon the confined karst aquifer (Bayari and Özyurt, 2014) (Figure 5).
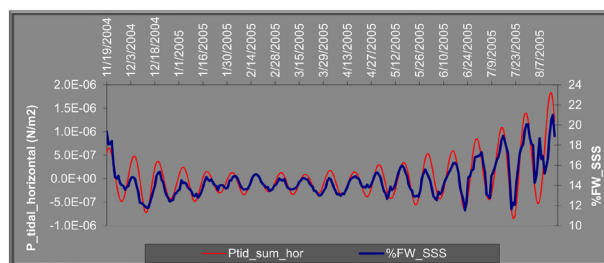

Figure 5.
Temporal salinity variation in submarine groundwater discharge from Mivini Cave and the synchronous horizontal component of total Earth tidal force exerted by the moon and the sun on Earth. The horizontal component of Earth tides compresses the crust to disturb its fluid content. About one-third of this force is exerted by the sun and two-thirds by the moon.

Conclusions and Outlook

Reassessment of the existing data and new observations on the isotopic composition of karst groundwater show that hypogenic karst development in the Taurus Mountain Range is more widespread than previously thought. Characteristic properties of the areas with hypogenic karst development include high mantle and crustal gas flux into the groundwater, large karst features like caves and collapse dolines, large travertine deposits associated with karst springs, and the presence of carbonate-hosted ore deposits.

Evidence indicates that hypogenic karst formation in the Taurus Mountain Range may or may not be associated with hydrothermal fluid migration. Moreover, Earth tides appear to provide the energy facilitating fluid migration in deep geological media where the hydraulic gradient is not sufficient.

Many carbonate formations in tectonically active regions of the world, like Turkey, have been subject to magmatic activity. Therefore, it seems very likely that hypogenic karst development by means of hydrothermal fluid circulation is a common process in such carbonate formations. However, apparent evidence of hydrothermal karst development may be erased by epigenic or hypogenic cool groundwater circulation that follows the hydrothermal period. Future studies should focus on the detection of hydrothermal minerals in carbonate rocks as a means of proving past hypogenic karst development. In current deep-circulating cool groundwater systems, helium and carbon isotopes dissolved in groundwater appear an effective tool for determining the contribution of deep components in the uprising flow.

References

Bayari CS, Özyurt NN. 2014. Earth tide, a potential driver for hypogenic fluid flow: observations from a submarine cave in SW Turkey. In: Klimchouk A, Sasowsky I, Mylroie J, Engel SA, Engel AS, editors. Selected Papers and Abstracts of the Symposium; 2014 Feb. 2-7; San Salvador Island, Bahamas. Karst Waters Institute Special Publication 18. Leesburg (VA): Karst Waters Institute. p. 20-24.

Bayari CS, Özyurt NN, Öztan M, Baştanlar Y, Varinlioğlu G, Koyuncu H, Ülkenli H, Hamarat S. 2011. Submarine and coastal karstic groundwater discharges along the Southwestern Mediterranean coast of Turkey. Hydrogeology Journal 19 (2): 399-414.
http://dx.doi.org/10.1007/s10040-010-0677-y

Bayari CS, Pekkan E, Özyurt NN. 2009a. Obruks, as giant collapse dolines caused by hypogenic karstification in central Anatolia, Turkey: analysis of likely formation processes. Hydrogeology Journal 17: 327-345.
http://dx.doi.org/10.1007/s10040-008-0351-9

Bayari CS, Özyurt NN, Kilani S. 2009b. Radiocarbon age distribution of groundwater in the Konya Closed Basin, central Anatolia, Turkey. Hydrogeology Journal 17: 347-365.
http://dx.doi.org/10.1007/s10040-008-0358-2

Kincaid T. 1999. Morphologic and fractal characterization of saturated karstic caves [Ph.D. thesis]. Laramie (WY): University of Wyoming. (In Turkish.)

Klimchouk A, Bayari S, Nazik L, Törk K. 2006. Glacial destruction of cave systems in high mountains, with special reference to the Aladaglar massif, Central Taurids, Turkey. Acta Carsologica 35 (2): 111-122.

Özyurt NN. 2005. Investigation of groundwater residence time in the Aladağ (Kayseri-Adana) karst aquifer [Ph.D. thesis]. Ankara (TR): Hacettepe University. (In Turkish.)

Özyurt NN, Bayari CS. 2014. Helium isotopes as indicator of current hypogenic karst development in Taurids Karst Region, Turkey. In: Klimchouk A, Sasowsky I, Mylroie J, Engel SA, Engel AS, editors. Selected Papers and Abstracts of the Symposium; 2014 Feb. 2-7; San Salvador Island, Bahamas. Karst Waters Institute Special Publication 18. Leesburg (VA): Karst Waters Institute. p. 77-81.

Özyurt NN, Bayari CS. 2008. Temporal variation of chemical and isotopic signals in major discharges of an Alpine karst aquifer in Turkey: implications with respect to response of karst aquifers to recharge. Hydrogeology Journal 16: 297-309.
http://dx.doi.org/10.1007/s10040-007-0217-6

Özyurt NN, Bayari CS, Tezcan L. 2000. Groundwater age dating in young groundwater by means of tritium/tritiogenic helium-3 method: springs of Antalya Travertine Plateau. Proceedings of the Earth Science and Mining Congress; 1998 Nov. 2-6; Ankara, Turkey. Ankara (TR): MTA Publications. p. 557-571. (In Turkish.)

Törk K. 2008. Effects of glaciation up on the karst development in Aladağlar (Niğde-Kayseri-Adana) [Ph.D. thesis]. Ankara (TR): Hacettepe University. (In Turkish.)

THE INFLUENCE OF SYNDEPOSITIONAL FAULTING AND BRECCIA ZONES ON HYPOGENE CAVE DEVELOPMENT AND MORPHOLOGY IN THE GUADALUPE MOUNTAINS, NEW MEXICO

Paul A. Burger

National Park Service
240 W 5th Avenue
Anchorage, AK, 99501, USA, paul_burger@nps.gov

Abstract

The Guadalupe Mountains are the exhumed remnants of a Permian reef complex that was uplifted beginning around 21 million years ago. The caves of the Guadalupe Mountains were formed by the mixing of deep-circulating meteoric water and hydrogen-sulfide-rich brine derived from surrounding oil and gas deposits. Cave development was controlled by fracture zones, faults, and structures associated with Permian and Tertiary tectonics.

Cave development shows strong linear trends that are correlative to broad structural trends in the Guadalupe Mountains and reflect fracturing, faulting, and folding during uplift. Some anticlinal features reflect deposition of Permian sediments across syndepositional faults. Many of these syndepositional faults can be observed in the caves and exhibit a strong influence on both overall passage trends and on passage character.

There are large breccia zones associated with syndepositional faults, forereef deposits, paleochannels, and paleokarst. In these areas, cave passages typically change from large, linear trunk passages to complex spongework mazes of smaller passages.

Introduction

The Guadalupe Mountains of southeastern New Mexico and West Texas host some of the most well-known and spectacular caves in the world, representing well over 320 km of mapped passages. There has been much written about the geologic origins of the caves and the role of hydrogen sulfide and microbes on cave development (Jagnow et al., 2000; Northup et al., 2000). While there has been some discussion on the vertical control of cave levels, mainly paleohydrology, and some on the controls on cave orientation, little has been written on the control of cave passage character and local morphology. The intent of this paper is to present observations on the relationship between faults, fault-related features, and breccia zones and cave passage location and morphology.

Geologic Setting

The Guadalupe Mountains (Figure 1) are the exhumed remnants of a Permian reef complex formed along the edge of an inland sea beginning around 254 Ma and exposed during middle to late Tertiary uplift and erosion (King, 1948; Newell et al., 1953; Hill, 1996). The massive member of the Capitan Formation was composed primarily of a calcareous sponge and algae framework with some bryozoans, bivalves, marine snails, and various microorganisms (Figure 2; King, 1948; Newell et al., 1953). The majority of the reef volume is made of marine cement which was almost contemporaneous with deposition, resulting in excellent preservation of the fossils and lack of wholesale diagenetic alteration of the limestone.
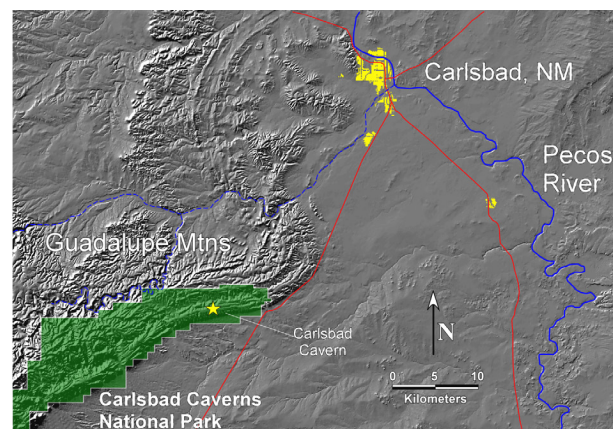

Figure 1.
Area map of Guadalupe Mountains and Carlsbad Caverns National Park.

During reef growth, large blocks of cemented material and other gravity-driven deposits were shed into the deeper water of the basin, forming the breccia or

foreslope member of the Capitan Formation, and are also characterized by early marine cementation (Newell et. al, 1953).
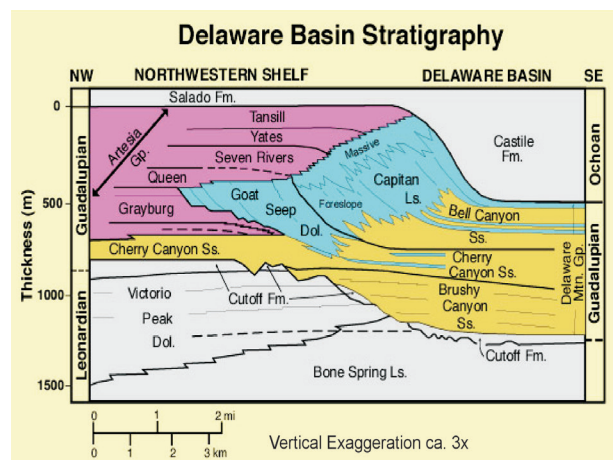

Figure 2.
General stratigraphy of the Guadalupe Mountains and Delaware Basin (after Scholle, 2008.)

On the shelf landward of the reef, alternating layers of carbonate siltstones (during lower sea level) and dolomite (during elevated sea level) were deposited in lagoonal environments that varied from unrestricted to restricted marine conditions. These deposits are represented by the backreef Seven Rivers, Yates, and Tansill formations (Newell et al., 1953).

Around 251 Ma, the connection between the inland sea and the open ocean began to close, leaving a thick sequence of evaporite deposits subsequently overlain by an accumulation of younger sediments through the early Tertiary (Hill, 1996). These younger sediments began to be eroded away during the development of the Laramide-aged Alvarado Ridge 35-38 Ma. This ridge was a broad topographic feature that extended from southern Wyoming through western Texas and into northern Mexico (Eaton, 1987). During Basin and Range extension beginning around 21 Ma, the Alvarado Ridge was broken into smaller structural blocks, including the Guadalupe Mountains. Neither of these tectonic periods resulted in major deformation, but caused minor tilting (less than 10°) and fracturing of the Permian rocks. It was these fractures that became major regional pathways for fluid flow and cave development.

Speleogenesis

The Guadalupe Mountains possess few characteristics of karst areas. There are few sinkholes and karst springs and the lack of surface stream flow is more a

reflection of the area being desert than the presence of subterranean pathways for the water. Early explanations of cave development focused on underground streams and traditional models of carbonic acid speleogenesis. The presence of large deposits of speleogenetic gypsum and other unusual mineral deposits coupled with the lack of fluvial features led researchers to develop a hypogenic cave development model involving sulfuric acid dissolution (Egemeier, 1971, 1987). Early researchers suggested oxidation of pyrite from the backreef units as the acid source (Jagnow, 1979). More recent studies have shown that sulfuric acid is related to the oxidation of hydrogen sulfide generated from the oil and gas deposits surrounding the Guadalupe Mountains (Davis, 1980; Hill, 1987; Jagnow et. al., 2000).

Initial fracture enlargement and solution of the Permian rocks took place as the result of strong groundwater flow from the upland areas of the Alvarado Ridge developed between 35 and 38 million years ago (DuChene and Cunningham, 2006). Beginning 12-15 million years ago, enlargement of initial pathways was concentrated where upwelling of deep-circulating hydrogen-sulfide-rich brine derived from surrounding oil and gas deposits (Polyak et al., 1998; Palmer and Palmer, 2000). Exposure to circulating oxygen from the surface resulted in aggressive, subaerial sulfuric acid speleogenesis. Large, irregular rooms and three-dimensional spongework passages were formed at or near the water table (Palmer and Palmer, 2000).

The vertical distribution of cave passages was controlled by changing groundwater flow conditions caused by uplift and faulting of the catchment area (Polyak et al., 1998; DuChene and Cunningham, 2006) and downcutting of the Pecos River Valley. Changes in hydrologic conditions lowered the mixing zone with time, creating distinct cave development levels identified by many authors (Jagnow, 1979; Hill, 1987; Polyak et al., 1998). Klimchouk (2007) also described the influence of paleohydrology on the geomorphic character of hypogene caves in the Guadalupes related to zones of differing permeability.

Eventually, the water table was lowered enough that sulfuric acid dissolution ceased and the open passages became partially filled with secondary carbonate minerals, breakdown collapse, and in some cases secondary fill originating from the surface.

Structural and Facies Influences on Cave Development

Jagnow (1979) was the first investigator to compile a comprehensive list of potential influences on cave

development. Major factors included joints, base levels, and stratigraphic position. He considered "sandstone dikes," teepee structures, and faults to be minor factors. Hill (1987) conducted detailed studies in the context of these factors and expanded the list to include some general observations about the significance of paleohydrology.

As more cave passages have been discovered and mapped, these concepts have been expanded and refined, particularly with regards to lithologic controls (DuChene and Cunnigham, 2006; Palmer and Palmer, 2000; Burger, 2009).

General Fault and Fracture Influence on Cave Development

The major faults and structures of the Guadalupe Mountains have been well documented since the earliest days of geologic mapping in the area (King, 1948; Hays, 1964). The influences of these faults on regional fracture patterns and cave development were noted by Jagnow (1979) and Hill (1987) as broad controls on cave orientation.

Major faults and folds in the Guadalupe Mountains were influenced by sediment compaction in the Permian, and Permian to Tertiary tectonics. The east-northeast trend reflects the development of fractures parallel to the shelf margin and developed as a result of sediment loading during deposition, as the massive reef overstepped reef talus. The north-northwest trend is younger, and relates to later uplift associated with the growth of the Alvarado Ridge (DuChene, 2009, written communication).

Jagnow (1979) generated radial histograms for more than 50 caves over the course of his work. He noted that there was strong correlation between the trends found in the caves and those linear features mapped on the surface by King (1948) and Hayes (1964). Jagnow divided the joints into major and minor trends based on the relative amounts of cave development seen along those trends. All researchers have noticed prominent trends roughly parallel to the reef orientation (even as the trend of the reef changes over distance) and a second set roughly orthogonal to the first. Jagnow (1979) also noted that the prominent set appearing to control cave and passage development shifted from reef-parallel to reef-perpendicular west of the Huapache Monocline, a major fold thought to represent sediment draping over a deep-rooted structural feature.

Similar relationships between regional structural trends and Lechuguilla Cave passage orientation have also been well documented (Jagnow, 1989; Palmer

and Palmer, 2000; Burger, 2009). While the timing of some of the structures in the Guadalupe Mountains is still problematic (Hill, 1996), there is clear influence of the structure and fracture patterns on overall cave development (Figure 3).

Previous researchers developed histograms based on tracing passages on cave maps and from limited fracture mapping within the passages. Recent surveys provide large digital data sets that are conducive to broader, statically robust analyses. Since survey shots through a cave vary around the trend of the passage where the mapping is being conducted, this data can be used to characterize all passage orientations, not just the obvious primary ones.

Most of the fractures are vertical to just subvertical, but Queen (1981) noted dissolution pockets aligned with steeply-inclined fractures, attributing them to possible Laramide tectonics. Steeply-inclined fissure passages are common in the Guadalupe Caves, notably the Rift and the route to Lake of the White Roses in Lechuguilla Cave and the Four O'Clock staircase in Virgin Cave. However, the exact structural controls on these features have not been determined and not all are aligned along the mapped dominant fracture trends.
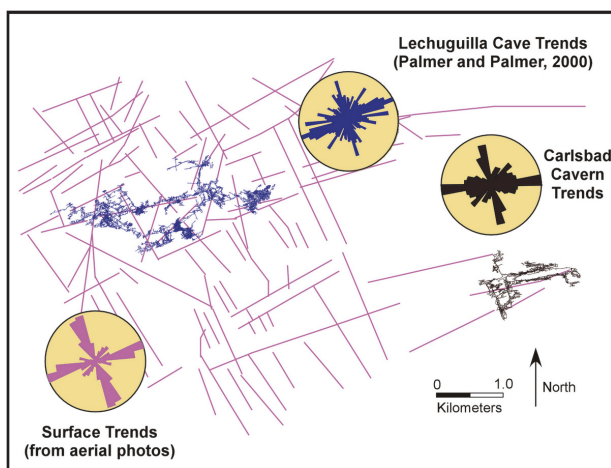
Figure 3.
Surface and cave structural trends.

Local structures can also strongly influence cave development. Dry Cave on Mckittrick Hill west of Carlsbad appears to be developed around the center of a dome in the backreef (Figure 4). Dips measured at points throughout the cave show a consistent trend away from a central high point (Allison and Stockton, 2009). This feature may be a bioherm, patch reef, or other positive feature underlying the backreef sediments (Noe and Mazzullo, 1994).

Syndepositional Faults

Queen (1981) was the first to publish observations of faults and fault-related features (i.e., chaotic breccias) in Carlsbad Cavern. He noted evidence of early karstification along those trends, but no comprehensive study has been published that investigates the influence of these features on cave development in general and on passage character specifically.
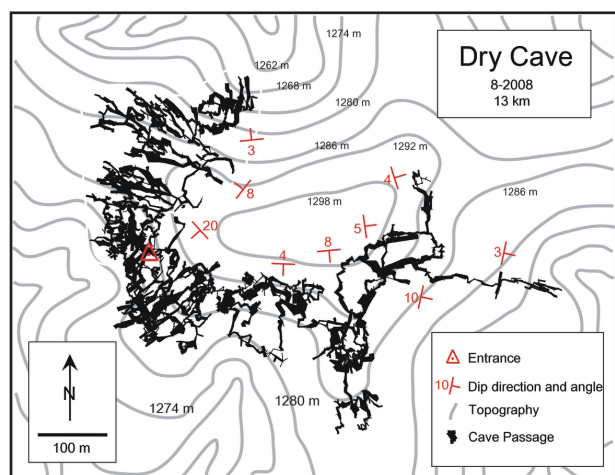
Figure 4.
Dry Cave showing bedrock orientations (Allison and Stockton, 2009).

The identification of smaller-scale faults has been problematic. Inside the caves, the bedding can be obscured by secondary speleothem growth, ferromanganese deposits, breakdown, and other speleogentic features. On the surface, their expression is subtle and has only recently been identified. Steep, basin-dipping clinoforms and outcrops with shelfward-dipping bedding have been observed in backreef units since some of the earliest detailed stratigraphic studies (i.e., Newell et al., 1953; Smith, 1973; Pray and Esteban, 1977; Hurley, 1989) with wide-ranging hypotheses to explain their origin. Hurley (1989) credited the informal term "fall in" structures for these structures to Lloyd Pray.

Detailed studies putting rock units into a sequence stratigraphic framework (Tinker, 1996 and 1998; Kerans and Tinker, 1999) allowed researchers to develop a more comprehensive understanding of these features. Using changes in unit thickness and detailed mapping of near-vertical features, Hunt and others (2002) determined that the majority of these features were syndepositional faults (also Kosa, 2003; Kosa et al., 2000; Kosa and Hunt, 2006). The faults they mapped are

dip slip with displacement of up to 30 m parallel to the shelf margin, and are segmented vertically and laterally. They dip steeply shelfward and basinward, and grew incrementally during deposition of the Yates and Tansill formations (Figure 5).

They also found there was episodic development of paleokarst along the syndepositional faults concurrent with sediment accumulation on the shelf (Kosa et al., 2000). These paleocavern systems can have more than 270 m of vertical relief, extend at least 1.2 km along strike, and are typically less than 10 m wide, but some are up to 90 m wide. The paleocaverns can extend more than 110 m below the top of the reef facies. They found these solution-modified syndepositional faults extend to at least 33 km along strike from Slaughter Canyon.
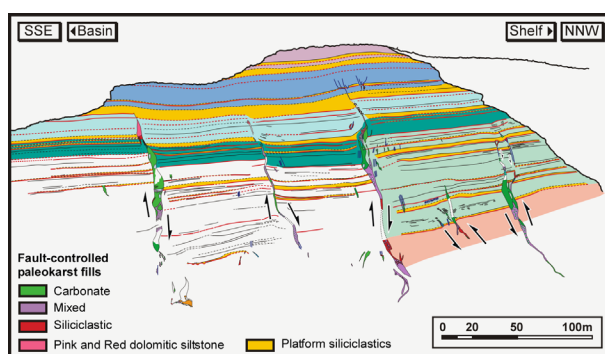
Figure 5.
Profile view of Slaughter Canyon outcrop showing variable fill types in solution-modified syndepositional faults (from Kosa and Hunt, 2006). Also note the way bedding appears to drape over fault tips, resembling shallow antiforms.

Kosa and others (2006) identified seven main lithologies associated with paleocavern development: (1) limestones and limestone breccias, (2) microspar-lithified breccias, (3) carbonate-rich breccias, (4) reworked and remnant breccias, (5) beige dolomitic siltstone–sandstone and associated breccias, (6) pink dolomitic siltstone–sandstone and associated breccias, and (7) spar-cemented breccias.

The relationship between the paleocavern deposits and the backreef sequence stratigraphy provides evidence for incremental fault growth and multiple episodes of dissolution, brecciation, collapse, deposition, cementation, and dolomitization within the paleocaverns during Capitan times.

The expressions of these faults important to this study are:
- Offset bedding and areas bound by faults
- The draping of upper backreef units across the faults, appearing as local anticlinal forms
- The fill of open fractures with shelf sediment, the Neptunian or sandstone "dikes" of previous studies (note: I will use the term Neptunian fissures for these features to avoid the potentially misleading term "dike" more often associated with igneous intrusions)
- Early dissolution breccias and paleocavern formation (Kosa and Hunt, 2006; Simo et al., 2006) oriented along the features

Recent research has also shown that early fluid movement along these faults has favored local dolomitization (Simon et al., 2015). This reinforces earlier observations of dolomitization along fracture zones in the reef and forereef units (Melim and Scholle, 1989). This process has created zones of more resistant rock associated with these faults, leading to the development distinct resistant topographic "fins" that can be seen throughout the Guadalupes. The correlation between syndepositional faults and the resistant fins may provide some explanation for the observed coincidence between cave development and these features as documented by Jagnow (1979).

Observations of Fault Control on Cave Development

While many of these structural features can be observed in outcrop and on aerial photographs, their influence on cave development is best mapped in the subsurface. The most extensive caves in the Guadalupe Mountains are Carlsbad Cavern (50 km long, Figure 6) and Lechuguilla Cave (222 km long, Figure 7), both within the boundary of Carlsbad Caverns National Park. Carlsbad Cavern penetrates the Tansill, Yates, and Capitan formations. Lechuguilla Cave penetrates the Yates, Seven Rivers, and Capitan formations and possibly the Goat Seep and Queen formations (Palmer and Palmer, 2000). Both caves provide access to extensive three-dimensional views of the geology and allow for direct observation of geologic structure and features that have influenced cave development. Many of the features seen in these two caves can be observed in other caves throughout the Guadalupe Mountains, but Carlsbad and Lechuguilla will be used as representative examples. Other outstanding examples of fault influenced development are discussed below.

Lechuguilla Cave

The entrance of Lechuguilla Cave has long been thought to have formed along the crest of a small anticline (Jagnow, 1989). Breccia seen in the entrance pit and
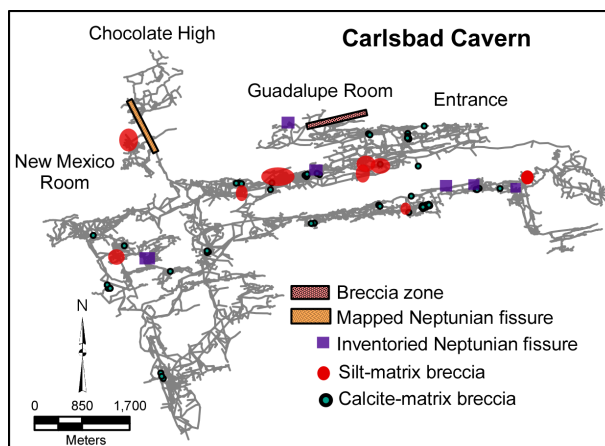
Figure 6.
Plan view of Carlsbad Cavern.

throughout the entrance series of the cave suggests that passage development is controlled by a syndepositional fault that is represented by an antiform near the cave entrance and by breccia deposits within the cave.
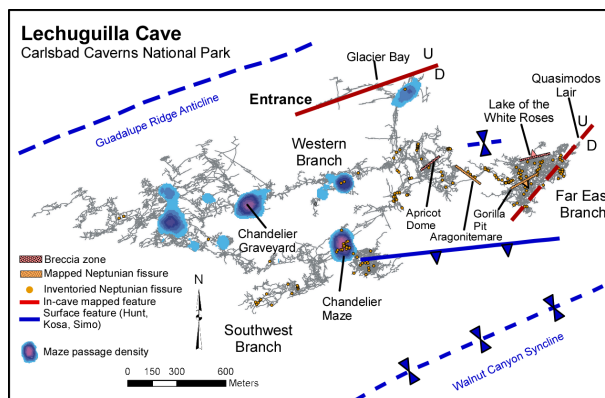
Figure 7.
Plan map of Lechuguilla Cave.

Boulder Falls, the first major pit in the cave was mapped to coincide with a vertical breccia feature (Palmer and Palmer, 2000). An obvious fault can be seen in the wall in Glacier Bay. When traced along the axis of this room, this fault appears to be aligned with the trend of the entrance series (Figure 8). The coincidence in orientation of these features suggests they are related to one significant fault that can be traced from the Entrance to Glacier Bay, a horizontal distance of over 470 m. The surface expression of this fault was also mapped by Hunt and others (2002) after being mapped in the cave.

This is the only place where distinct, offset bedding has been observed inside Lechuguilla Cave, but that is

likely the result of limited exposures, secondary mineral deposition, and weathering product development. Early karstification along these faults has resulted in large breccia zones, across which it is impossible to trace bedding.

The Firefall Hall—Quasimodos Lair in the Far East section of Lechuguilla (Figure 9) is a major passage that cuts 122 m vertically through formational boundaries from the Capitan all the way up into the backreef. At the upper terminus of the room, it is clear that the passage has developed along a significant fault (Figure 8). The boundary between the fault and the adjoining calcite-cemented breccia is sharp and linear. This fault has no expression on the surface above the cave but has clearly influenced passage development. It shows both the difficulty in using surface mapping to predict cave development and illustrates the usefulness of the underground exposures accessible in Guadalupe Mountain caves.

Figure 9.
Fault Breccia in Quasimodos Lair, Far East, Lechuguilla Cave. Photo by Paul Burger.

If these fissures do represent syndepositional faults, then there are places where it is possible to observe significant influence on cave development in Lechuguilla, particularly along the steep, vertical connections between cave levels (Figure 6). Several examples are given below.

The Aragonitemare Climb between the Moby Dick Room and the Far East follows a Neptunian fissure. The climb varies from 2 to 10 m wide and cuts through more than 100 m of strata.

Apricot Dome, the vertical route between the Rustcicles area and Hoot-n-Holler Hall from the Capitan Formation into the Seven Rivers, is formed along a Neptunian fissure that grades downward into a tabular breccia body. The vertical route continues upwards into Ghost Town, but bedrock details are obscured by secondary deposits. This feature is the likely pathway for minerals from the more iron-rich Yates and Seven Rivers formations that were carried downward to form the Rustcicles, iron-oxide-rich stalactites likely formed beneath the water table.

Figure 8.
Fault exposed in Glacier Bay (oblique view) with person for scale near arrow point. Photo courtesy of Gene Cooper, Four Chambers Studio; photo by Stan Allison, NPS.

While directly observable instances of faults are rare, associated features and facies can be seen throughout both long caves in the park. Hunt and Kosa (2002) found that all of the Neptunian fissures mapped on the surface were related to syndepositional faulting.

Gorilla Pit, the main route between the upper Far East and the Outback in Lechuguilla Cave, is aligned with a Neptunian fissure that descends from the Seven Rivers down into the Capitan and appears more as a tabular breccia body lower.

In Carlsbad Cavern (Figure 5), the route from the New Mexico Room up into Chocolate High follows the trend of Neptunian fissures from the Capitan up into the Yates backreef. One of the largest rooms in the cave, The Guadalupe Room appears to align with a tabular breccia

body that can only be traced vertically for 25 m along one wall, so it is not possible to see how its character varies with depth.

Lechuguilla and Carlsbad Cavern have many locations where there are single, fissure-like connections between larger, well-developed levels and it is expected that with more detailed mapping, more of these features will be found to correlate with Neptunian fissures and related tabular breccia bodies.

Ogle Cave (Figure 10) is located about 400 m shelfward of the Yates platform margin and was strongly influenced by faulting. Neptunian fissures located near the entrance were first described by Jagnow (1979) and were later attributed to fill by Ogallala-aged sediments into fissures that had opened during the Cretaceous (Hill, 1987).

The area that contains the cave was called the Ogle Cave Fault Zone by Hunt and others (2002). Later work by Resor and others (2011) mapped this feature for more than 13 km along strike, bounding a 170-200-m-wide graben, down-dropped 20-30 m below the surrounding platform. The fault system consists of 2-3 high angle (~80° dip) normal faults that extend more than 200 m down dip. They found that the fault segments vary in strike by more than 25°, roughly paralleling the present day erosional scarp that reflects the Permian platform depositional margin.

The cave's 100-m-deep entrance shaft is located on the westernmost cluster of these faults. The main trunk passage continues for 450 m south to where it dramatically changes character. The passage beyond continues as a very narrow vertical fissure aligned with a prominent fracture zone running at approximate 160°, the overall trend of the cave. The main trunk-sized passage then continues for 150 m at a higher level, but the controlling fracture set appears to be offset to the east.

The large room to the west of the main trunk would correspond to the approximate location of the southern bounding fault of the graben as mapped by Resor and others (2011). A prominent south-dipping breccia zone was mapped near the beginning of this room and likely represents an expression of one of the features in the fault zone.

Breccia Zones

The controls on overall orientation and large-scale patterns are generally understood with respect to structure (see discussion above), vertical location (Jagnow, 1979; Hill; 1987; Polyak, 1998; DuChene, 2000; Palmer and Palmer, 2000), and related to formational boundaries (Jagnow, 1989; DuChene, 2000; Burger, 2009). There has been little study on the controls of actual passage character and morphology in Guadalupe Mountain caves.

Local character changes and influence of teepee structures have been documented (Queen, 1981; Jagnow, 1979; Burger, 2009) and appear to be limited to cave passages developed in the Yates Formation. More widespread, however, is the influence of breccia zones
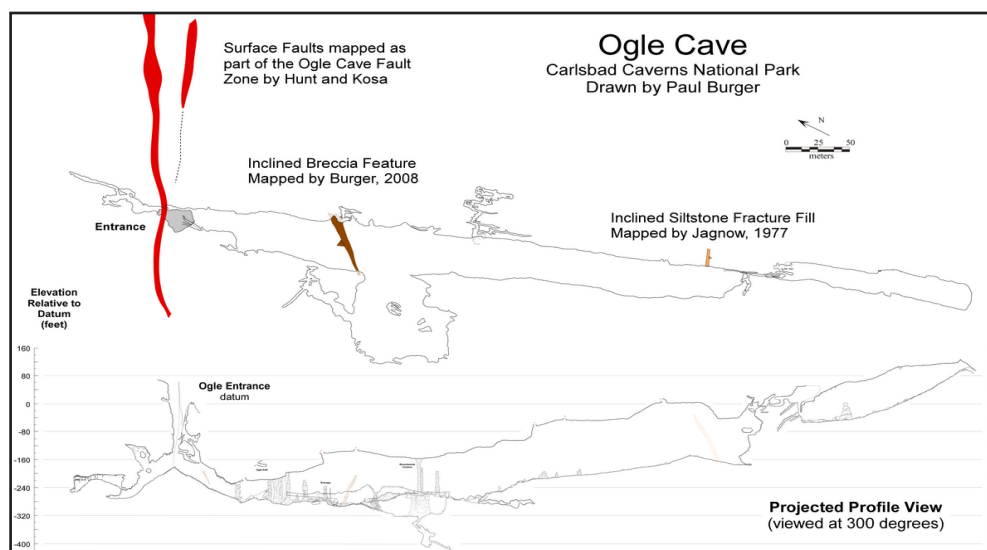

Figure 10.
Plan and profile of Ogle Cave, showing major mapped structural features.

that can frequently cross formational boundaries. As discussed in the previous section, there are breccias associated with early dissolution of syndepositional faults. These tend to be linear and generally less than 10 m wide (though they may range up to 90 m). There are several other mechanisms that can produce breccia zones under the geologic conditions present in the Capitan Reef and Guadalupe Mountains.

This discussion will focus only on two outstanding examples of breccia control of cave development—Lechuguilla Cave and Virgin Cave—though there are many other examples in the Guadalupes.

Lechuguilla Cave

As part of the mapping of Lechuguilla Cave, speleologic inventories are conducted, gathering bedrock data for each survey station. DuChene (2000, 1996) classified the breccia bodies found in Lechuguilla Cave based on his detailed mineral inventory (now integrated into a broader, more general inventory database). The breccia bodies were divided into depositional breccias, related to the growth of the Permian Reef and part of the bedrock, and speleogenetic breccias, related to the development of the cave. The depositional breccias were subdivided into mosaic and chaotic types and characterized to aid in the identification of their possible depositional environments. The resulting data, collected from more than 14,730 individual points, shows a strong correlation between the presence of breccia and dense mazes in some areas (Figure 6).

One of the most distinct areas where this can be seen is the Chandelier Maze in the Southwest Branch of the cave. The LeBarge Borehole, a tunnel nearly 15 m in diameter, ends abruptly to the west at the edge of a dense three-dimensional maze area extending for more than 300 m from east to west. This maze area ends to the west, where the breccia zone stops and intact bedrock continues. Here the Prickly Ice Cube Room continues as a single large passage 30 m wide with 100 m of vertical range. The maze area ends to the south against a steeply inclined passage leading to one of the deepest points in the cave. Breccia can be seen distinctly on the footwall of this feature but rarely on the hanging wall.

The route down to Lake of the White Roses in the Far East part of Lechuguilla Cave is a steeply descending fissure. The hanging wall of this passage is a breccia with subangular clasts up to 20 cm wide. The footwall contains no breccia. This fissure is not oriented parallel to the main reef trend and is unlikely to represent the contact between the massive and forereef members of the Capitan Formation. More likely, this fissure

represents dissolution along a linear fracture or fault developed prior to the onset of speleogenesis.

Many of the other spongework maze passages that did not appear as clearly in the density gradient mapping are formed in the distinct calcite-matrix breccias classified by Jagnow (1989) and DuChene (2000) as being part of the forereef facies.

Virgin Cave

Virgin Cave, in the Lincoln National Forest, has been mapped to just under 5 km. The main trend of the front section of the cave is oriented along a linear, near-vertical, tabular breccia body. It is approximately 217 m long and up to 46 m wide, and is oriented northeast-southwest (Figure 11). Development within this body consists of spongework maze passages formed in breccia fill with clasts more than 2 m in diameter.

Passages outside of this zone are more linear and follow regional fracture trends. Individual stratigraphic units cannot be traced across this feature so it is uncertain whether this feature is a fault, an enlarged fracture, or paleokarst. While the origin of the breccia is not clear, the breccia zone has had a profound influence on cave passage character.

The change in passage character is likely the result of a difference in overall solubility. The breccia zones contain a much higher proportion of insoluble materials. In these maze areas, thick deposits of silica, iron, and manganese are common. During speleogenesis, the aggressive waters were not nearly as effective at wholesale dissolution of the rock.
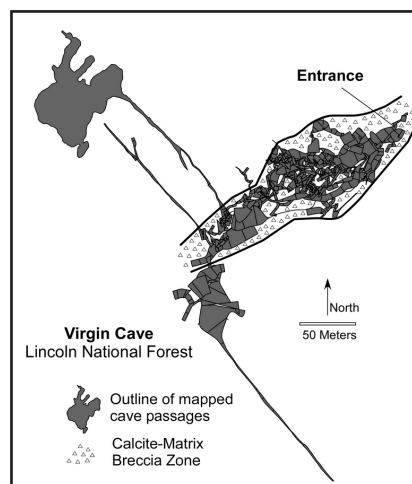

Figure 11.
Plan map of Virgin Cave, showing large breccia zone where cave is developed as a spongework maze.

The relationship between these breccia zones and passage morphology is important. Understanding the flow regimes through these zones has broader implications on characterizing fluid flow (water, oil, gas, etc.) through these types of deposits in deeply buried karst.

Conclusions

The influence of regional structure and lithology on cave development in the Guadalupes has been well-documented, though we are only beginning to understand the timing and persistence of these features. More localized structures have not had nearly as much attention, but are important to understanding where caves developed and why they developed specific characteristics.

Syndepositional faults originated during Permian time and have had a significant influence on fluid flow, diagenesis, and cave development since that time. Features such as Neptunian fissures and fault-associated breccias are important influences on passage character and have been vital to facilitating vertical fluid flow during cave development and for downward movement of minerals as the water table lowered.

Breccia bodies associated with primary deposition, faults, early karstification, and other processes have had a local strong influence on later fluid flow and passage development, especially with regards to the formation of dense maze areas.

More detailed mapping of these breccia zones to characterize their morphology and extent is needed to fully gauge their influence on speleogenesis. Detailed mapping is also needed to determine the orientation, vertical and lateral variability, and extent of Neptunian fissures, especially in the longer caves.

It is important to understand these influences not only on the speleogenesis of Guadalupe caves, but on some of the natural variability seen in buried karst systems that formed under similar conditions.

References

Allison SD, Stockton AJ. 2009. Exploration in Dry Cave 2005-2009, Guadalupe Mountains, New Mexico. Proceedings of the 2009 International Congress of Speleology. Huntsville (AL): National Speleological Society.

Burger PA. 2009. Structural and facies control of hypogenic karst development in the Guadalupe Mountains, New Mexico, USA. NCKRI Symposium 1: Advances in Hypogene Karst Studies. Carlsbad (NM): National Cave and Karst Institute. p. 60-70.

Davis DG. 1980. Cave development in the Guadalupe Mountains: a critical review of recent hypotheses. NSS Bulletin 42 (3): 42-48.

DuChene HR. 1996. Interim Report, April 1 – September 30, 1996. Lechuguilla Cave Geological and Mineralogical Inventory Project. Unpublished Report to Carlsbad Caverns National Park. 22 p.

DuChene HR. 2000. Bedrock features of Lechuguilla Cave, Guadalupe Mountains, New Mexico. Journal of Cave and Karst Studies 62 (2): 109-119.

DuChene H, Cunningham KI. 2006. Tectonic influences on speleogenesis in the Guadalupe Mountains, New Mexico and Texas. In: New Mexico Geological Survey, 57th Field Conference Guidebook, p. 211-217.

Eaton GP. 1987. Topography and origin of the Southern Rocky Mountains and Alvarado Ridge. In: Coward M, Dewey JF, Hancock L, editors. Continental extension tectonics. Geological Society Special Publication 28. p. 355-369. http://dx.doi.org/10.1144/gsl.sp.1987.028.01.22

Egemeier SJ. 1987. A theory for the origin of Carlsbad Cavern. NSS Bulletin 49 (2): 73-76.

Egemeier SJ. 1971. A comparison of two types of solution caves. Unpublished report to Carlsbad Caverns National Park, April 12.

Hayes PT. 1964. Geology of the Guadalupe Mountains: US. US Geological Survey Professional Paper 446.

Hill CA. 1996. Geology of the Delaware Basin – Guadalupe, Apache, and Glass Mountains, New Mexico and Texas. Society of Economic Paleontologists and Mineralogists, Permian Basin Section, Publication 96-39.

Hill CA. 1987. Geology of Carlsbad Cavern and other caves in the Guadalupe Mountains, New Mexico and Texas. New Mexico Bureau of Mines and Mineral Resources Bulletin 117.

Hunt DW, Fitchen WM, Kosa E. 2002. Syndepositional deformation of the Permian Capitan reef carbonate platform, Guadalupe Mountains, New Mexico, USA. Sedimentary Geology 154: 89-126. http://dx.doi.org/10.1016/S0037-0738(02)00104-5

Hurley NF. 1989. Facies mosaic of the lower Seven Rivers Formation, McKittrick Canyon, New Mexico. In: Harris PM, GA Grover, editors. Subsurface and outcrop examination of the Capitan Shelf Margin, northern Delaware Basin. Society of Economic Paleontologists and Mineralogists, Core Workshop No. 13, p. 325-346. http://dx.doi.org/10.2110/cor.89.13.0325

Jagnow DH, Hill CA, Davis DG, DuChene HR, Cunningham KI, Northup DE, Queen JM. 2000. History of the sulfuric acid theory of speleogenesis in the Guadalupe Mountains, New Mexico. Journal of Cave and Karst Studies 62 (2): 54-59.

Jagnow DH 1989. The geology of Lechuguilla Cave, New Mexico. In: Harris PM, Grover GA, editors. Subsurface and outcrop examination of the Capitan shelf margin, northern Delaware Basin. Society of Economic Paleontologists and Mineralogists Core Workshop No. 13: 459-466.

Jagnow DH. 1979. Cavern development in the Guadalupe Mountains. Columbus (OH): Cave Research Foundation.

Kerans C, Tinker SW. 1999. Extrinsic stratigraphic controls on development of the Capitan reef complex. In: Saller AH, Harris PM, Kirkland BL, Mazzullo SJ, editors. Geologic Framework of the Capitan Reef Tulsa, OK, SEPM Special Publication No. 65. p. 15-36. http://dx.doi.org/10.2110/pec.99.65.0015

King PB. 1948. Geology of the southern Guadalupe Mountains, Texas. US Geological Survey Professional Paper 215.

Klimchouk AB. 2007. Hypogene speleogenesis: hydrogeological and morphogenetic perspective. National Cave and Karst Research Institute Special Paper #1. National Cave and Karst Institute. Carlsbad, New Mexico.

Kosa E, Hunt DW. 2006. Heterogeneity in fill and properties of karst-modified syndepositional faults and fractures: upper Permian Capitan platform. Journal of Sedimentary Research 76: 131-151. http://dx.doi.org/10.2110/jsr.2006.08

Kosa E. 2003. Heterogeneity in the structure, diagenesis and fill of syndepositional faults in carbonate strata: Upper Permian Capitan Platform, Guadalupe Mountains, New Mexico, USA [Ph.D. thesis]. Manchester (GB): University of Manchester. 384 p.

Kosa E, Hunt DW, Roberts G, Fitchen WM, Bockel-Rebelle MO. 2000. Temporal and spatial variability in the fill and diagenesis of syndepositional fault zones, Permian Capitan reef platform, Slaughter Canyon, Guadalupe Mountains, New Mexico: implications for platform development, diagenesis and connectivity of Yates reservoirs [abs.]. In: Ahr WM, Harris PM, Morgan WA, Somerville ID, Stanton RJ, Jr., editors. Permo-carboniferous carbonate platforms and reefs. SEPM-IAS Research and Field Conference, Programs and Abstracts Volume; Tulsa (OK): SEPM (Society for Sedimentary Geology). p. 95.

Melim LA, Scholle PA. 1989. Dolomitization model for the forereef facies of the Permian Capitan Formation, Guadalupe Mountains, Texas-New Mexico. In: Harris PM, Grover GA, editors, Subsurface and Outcrop Examination of the Capitan Shelf Margin, Northern Delaware Basin: Tulsa, OK, SEPM Core Workshop No. 13. p. 407-413. http://dx.doi.org/10.2110/cor.89.13.0407

Newell KJ, Fischer AG, Whiteman AJ, Hickox JE, Bradley JE. 1953. The Permian reef complex of the Guadalupe Mountains region, Texas and New Mexico. San Francisco (CA): W.H. Freeman and Co.

Noe SU, Mazzullo SJ. 1994. Patch reef-dominated outer shelf facies along a non-rimmed platform, middle to upper Tansill Formation, northern Guadalupe Mountains, New Mexico. West Texas Geological Society Bulletin 33 (5): 5-11.

Northup DE, Dahm CN, Melim LA, Spilde MN, Crossey LJ, Lavoie KH, Mallory LM, Boston PJ, Cunningham KI, Barns SM. 2000. Evidence for geomicrobiological interactions in Guadalupe caves. Journal of Cave and Karst Studies 62 (2): 80-90.

Palmer AN, Palmer MV. 2000. Hydrochemical interpretation of cave patterns in the Guadalupe Mountains, New Mexico. Journal of Cave and Karst Studies 62 (2): 91-108.

Pray LC, Esteban M, editors. 1977. Upper Guadalupian Facies, Permian Reef Complex, Guadalupe Mountains, New Mexico and West Texas—Road logs and locality guides (1977 Field Conference Guidebook). Midland (TX): Permian Basin Section, SEPM Publication No. 77-16, Vol. 2. 194 p.

Polyak VJ, WC McIntosh, Güven N, Provencio P. 1998. Age and origin of Carlsbad Cavern and related caves from $^{40}Ar/^{39}Ar$ of Alunite. Science 279 (20): 1919-1922. http://dx.doi.org/10.1126/science.279.5358.1919

Queen JM. 1981. A discussion and field guide to the geology of Carlsbad Caverns: preliminary report to the National Park Service for the 8th International Congress. 64 p. (Unpublished.)

Resor PG, Hunt DW, Flodin E. 2011. Three-dimensional geometry of platform-scale fracture systems, Guadalupe Mountains, New Mexico, U.S.A. (abs). American Association of Petroleum Geologists. AAPG Annual Convention and Exhibition, Houston, Texas.

Rush J, Kerans C. 2010. Stratigraphic response across a structurally dynamic shelf: the latest Guadalupian composite sequence at Walnut Canyon, New Mexico, U.S.A. Journal of Sedimentary Research 80 (9): 808-828. http://dx.doi.org/10.2110/jsr.2010.073

Simo JA, Van Alstine JM, Hunt D, Taberner C, Thurmond J, Piccoli L. 2006. Fracture-controlled karsted carbonate platform tops, Rattlesnake Canyon, Guadalupe Mountains, New Mexico, U.S.A. (abs). American Association of Petroleum Geologists. AAPG Annual Convention and Exhibition, Houston, Texas.

Simon R, Kerans C, Zahm C. 2015. Syndepositional fault control on dolomitization of a steep-walled carbonate platform margin, Yates Formation (Permian), Guadalupe Mountains, New Mexico (abs). American Association of Petroleum Geologists. AAPG Annual Convention and Exhibition, Denver, Colorado.

Smith DB. 1973. Geometry and correlation along Permian Capitan Escarpment, New Mexico and Texas: discussion. American Association of Petroleum Geologists Bulletin 57 (5): 940-945.

Tinker SW. 1998. Shelf-to-basin facies distributions and sequence stratigraphy of a steep-rimmed carbonate margin: Capitan depositional system, McKittrick Canyon, New Mexico and Texas. Journal of Sedimentary Research 68 (6): 1146-1174. http://dx.doi.org/10.2110/jsr.68.1146

Tinker SW. 1996. Building the 3-D jigsaw puzzle: applications of sequence stratigraphy to 3-D reservoir characterization, Permian Basin. American Association of Petroleum Geologists Bulletin. 80: 460-485.

SULFURIC ACID CAVES OF ITALY: AN OVERVIEW

Ilenia Maria D'Angeli
Department of Biological, Geological, and Environmental Sciences
Via Zamboni 67
40126 Bologna, Italy, ilenia.dangeli@alice.it

Jo De Waele
Department of Biological, Geological, and Environmental Sciences
Via Zamboni 67
40126 Bologna, Italy, jo.dewaele@unibo.it

Sandro Galdenzi
Viale Verdi, 10
60035 Jesi, Italy, galdenzi.sandro@tiscali.it

Giuliana Madonia
Department of Earth and Marine Sciences
Via Archirafi 22
90123 Palermo, Italy, giuliana.madonia@unipa.it

Mario Parise
National Research Council, IRPI
Via Amendola 122-I
70126 Bari, Italy, m.parise@ba.irpi.cnr.it

Leonardo Piccini
Department of Earth Sciences
Via La Pira 4
50121, Firenze, Italy, leonardo.piccini@unifi.it

Marco Vattano
Department of Earth and Marine Sciences
Via Archirafi 22
90123 Palermo, Italy, marco.vattano@unipa.it

Introduction

The general geodynamic situation of Italy is quite complex. The land has undergone several stages of formation, compressed between the African and the Eurasian continents. The phase of extensional tectonics governed by the rollback of continental terrains (Corsica, Sardinia, Balearic Islands, Kabylies blocks, and Calabria) caused the generation of the Apennine chain, which crosses northwest to southeast and is the backbone of Italy's mainland. The structure of the Apennine chain contains many thrusts, horst and graben structures, and deep faults, as well as the widespread presence of mainly Mesozoic carbonate outcrops. This has caused the formation of deep karstic circulation systems, as evidenced by the abundance of hydrothermal springs and associated travertine deposits. Furthermore, the presence, at depth, of both hydrocarbon reservoirs and Triassic gypsum deposits is responsible for the presence of rising waters rich in H_2S.

Since the late 1980s, cave systems in the Frasassi Canyon and Monte Cucco, with their important gypsum deposits, undoubtedly showed that sulfuric acid played an important role in the creation of voids (Galdenzi, 1990), similar to what was described for the Guadalupe Mountains in New Mexico. Afterwards, many other caves throughout the country were found to be formed by the sulfuric acid speleogenesis, making Italy one of the most important countries in the world for the concerns of SAS caves.

KARST AREAS AND HYPOGENE SULPHURIC ACID CAVES OF ITALY

1 Mt Pisani	11 Montecchio	21 Fiume Coperto
2 Tassare-Mt Nerone	12 Parrano	22 Mt Lattari
3 Mt Rotondo	13 Pozzi della Piana	23 S. Cesarea Terme
4 Mt Cucco	14 Triponzo	24 Capo Palinuro
5 Frasassi	15 Acquasanta Terme	25 Mt Sellaro
6 Faggeto Tondo	16 Cittareale	26 Cassano allo Ionio
7 Mt di Campiglia	17 Buco del Pretaro	27 Terme Luigiane
8 Mt. Civitello	18 Mt Soratte	28 Phaff
9 Mt Cetona	19 Pozzo del Merro	29 S. Barbara
10 Roselle	20 Subiaco	30 Corona 'e Sa Craba

	31 Monte Inici
	32 Acqua Fitusa
	33 Mt Kronio
	34 Acqua Mintina

Figure 1.
Italian karst areas and the hypogene SAS karst systems (modified from Sivelli & De Waele, 2013, Speleologia 68, special issue printed for the 16th ICS Brno. GIS elaboration by M.L. Garberi).

In the past few years, detailed studies involving geomorphology, mineralogy, and geochemistry have been carried out in some of these caves. Sulfuric acid caves have been discovered from many regions along the Apennine chain (Tuscany, Umbria, Marche, Latium, Campania, and Calabria), and also from Apulia, Sicily, and Sardinia.

Here we give a review of the state-of-the-art knowledge on known hypogene SAS caves in Italy, as well as ongoing studies in selected areas.

Overview of Studies

Caves resulting from sulfuric acid have been known for almost a century (Triponzo caves, Principi, 1931). While some typical mineral deposits were studied in the 1980s (Cala Fetente caves on Capo Palinuro, Forti, 1985), the study of the mechanisms responsible for the formation of these caves and their typical morphologies started half a century later (Galdenzi and Menichetti, 1989). The first studies mainly focused on the Umbrian and Marche Apennines, around the cave systems of Frasassi-Grotta Grande del Vento (Galdenzi, 1990) and

the nearby Faggeto Tondo Cave (Forti et al., 1989). A general overview of hypogenic caves in Central Italy was brought a few years later (Galdenzi and Menichetti, 1995). This important review paper was comprised of a set of cave locations in which the presence of sulfates was a clear indication of sulfuric acid speleogenesis. These included the ones of Parrano, Pozzi della Piana, Acquasanta Terme, Cittareale, and Monte Soratte, in addition to the aforementioned caves.

A few years later, sulfuric acid caves were found in Calabria (Monte Sellaro, Cassano allo Ionio, Terme Luigiane (Galdenzi, 1997), while more and more detailed studies continued to be carried out in Umbria (Menichetti, 2011), especially the Monte Cucco System (Menichetti et al., 2007), Monte Soratte (Mecchia, 2012), Acquasanta Terme caves (Galdenzi et al., 2010), and especially in Frasassi Caves (Galdenzi et al., 1997; Galdenzi, 2001; Forti et al., 2002; Galdenzi et al., 2008; Galdenzi, 2009, 2012).

Microbiological studies started in the last two caves in 2005 (Macalady et al., 2006, 2007, 2008; Jones, 2008, 2010), bringing very interesting results. These studies also shed light on the speleogenetic role of microorganisms in Frasassi (Jones et al., 2015).

Other sulfuric acid caves have been recognized in the last few years. In Sardinia, the formation of many mine caves can be ascribed to this type of speleogenesis (De Waele et al., 2013a), while Montecchio Cave was studied in detail in Tuscany (Piccini et al., 2015). In Sicily, several caves host gypsum deposits or have typical SAS morphologies, such as Acqua Fitusa, Monte Inici, and Monte Kronio caves (Vattano et al., 2013; De Waele et al., 2014b). Typical SAS morphologies have also been described from epigenic caves in Veneto, in which the local oxidation of pyrite caused the formation of sulfuric acid (Tisato et al., 2012). Further caves are awaiting more detailed studies but are surely related to rising H_2S-rich waters (De Waele et al., 2014a).

References

De Waele J, Forti P, Naseddu A. 2013a. Speleogenesis of an exhumed hydrothermal sulphuric acid karst in Cambrian carbonates (Mount San Giovanni, Sardinia). Earth Surface Processes and Landforms 38: 1369-1379.
http://dx.doi.org/10.1002/esp.3375

De Waele J, Galli E, Piccini L, Rossi A. 2013b. Descrizione morfologica e mineralogica della grotta ipogenica sulfurea di Montecchio (Grosseto, Toscana). In: Cucchi F, Guidi P, editors. Atti del XXI Congresso Nazionale di Speleologia "Diffusione delle conoscenze"; 2011, 2-5 June; Trieste. p. 380-386.

De Waele J, Galdenzi S, Madonia G, Menichetti M, Parise M, Piccini L, Sanna L, Sauro F, Tognini P, Vattano M, Vigna B. 2014a. A review on hypogenic caves in Italy. In: Klimchouk AB, Sasowsky ID, Mylroie J, Engel S, Summers Engel A, editors. Hypogene cave morphologies. Selected papers and abstracts of the symposium held February 2 through 7, 2014; San Salvador Island, Bahamas. Karst Waters Institute Special Publication 18. Leesberg (VA): Karst Waters Institute. p. 28-30.

De Waele J, Plan L, Audra P, Vattano M, Madonia G. 2014b. Sulfuric acid water table caves (Grotte du Chat / Acqua Fitusa /Bad Deutsch Altenburg + Kraushöhle). In: Klimchouk AB, Sasowsky ID, Mylroie J, Engel S, Summers Engel A, editors, Hypogene cave morphologies. Selected papers and abstracts of the symposium held February 2 through 7, 2014; San Salvador Island, Bahamas. Karst Waters Institute Special Publication 18. Leesburg (VA): p. 31-35.

Forti P. 1985. Le mineralizzazioni della grotta di Cala Fetente (Salerno, Campania). Mondo Sotterraneo 1985 (1-2): 41-50.

Forti P, Galdenzi S, Sarbu SM. 2002. The hypogenic caves: a powerful tool for the study of seeps and their environmental effects. Contintental Shelf Research 22: 2373-2386.
http://dx.doi.org/10.1016/S0278-4343(02)00062-6

Forti P, Menichetti M, Rossi A. 1989. Speleothems and speleogenesis of the Faggeto Tondo Cave (Umbria, Italy). In: Hazslinszky T, Takacsne BK, editors. Proceedings 10th International Congress of Speleology, Budapest, Vol. 1: p. 74-76.

Galdenzi S. 1990. Un modello genetico per la Grotta Grande del Vento. In: Galdenzi S, Menichetti M, editors. Il carsismo della Gola di Frasassi. Memorie Ist. It. Spel. II (4): 123-142.

Galdenzi S. 1997. Initial geological observations in caves bordering the Sibari plain (southern Italy). Journal of Cave and Karst Studies 59: 81-86.

Galdenzi S. 2001. L'azione morfogenetica delle acque sulfuree nelle Grotte di Frasassi, Acquasanta Terme (Appennino marchigiano-Italia) e di Movile (Dobrogea-Romania). Le Grotte d'Italia V (2): 49-61.

Galdenzi S. 2009. Hypogene caves in the Apennines (Italy). In: Klimchouk AB, Ford DC, editors. Hypogene Speleogenesis and Karst Hydrogeology of Artesian Basins. Special Paper 1. Simferopol (UA): Ukrainian Institute of Speleology and Karstology. p. 101-116.

Galdenzi S. 2012. Corrosion of limestone tablets in sulfidic ground-water: measurements and speleogenetic implications. International Journal of Speleology 41 (3): 149-159.
http://dx.doi.org/10.5038/1827-806X.41.2.3

Galdenzi S, Maruoka T. 2003. Gypsum deposits in the Frasassi caves, Central Italy. Journal of Cave and Karst Studies 65: 111-125.

Galdenzi S, Menichetti M. 1989. Evolution of underground karst systems in the Umbria-Marche Appennines in central Italy. In: Hazslinszky T, Takacsne K, editors. Proceedings 10th International Congress Speleology, Budapest, 3: p. 745-747.

Galdenzi S, Menichetti M. 1995. Occurrence of hypogenic caves in a karst region: examples from central Italy. Environmental Geology 26: 39-47. http://dx.doi.org/10.1007/BF00776030

Galdenzi S, Menichetti M, Forti P. 1997. La corrosione di placchette calcaree ad opera di acque sulfuree: dati sperimentali in ambiente ipogeo. Proceedings of the 12th International Congress of Speleology, La Chaux-de-Fonds, Switzerland 1: p. 187-190.

Galdenzi S, Cocchioni F, Filipponi G, Selvaggio R, Scuri S, Morichetti L, Cocchioni M. 2010. The sulfidic thermal caves of Acquasanta Terme (central Italy). Journal of Cave and Karst Studies 72 (1): 43-58. http://dx.doi.org/10.4311/jcks2008es0056

Galdenzi S, Cocchioni M, Morichetti L, Amici V, Scuri S. 2008. Sulfidic ground-water chemistry in the Frasassi caves, Italy. Journal of Cave and Karst Studies 70: 94-107.

Jones DS, Tobler D, Schaperdoth I, Mainiero M, Macalady J. 2010. Community structure of subsurface biofilms in the thermal sulfidic caves of Acquasanta Terme, Italy. Applied Environmental Microbiology 76: 5902-5910. http://dx.doi.org/10.1128/AEM.00647-10

Jones DS, Lyon EH, Macalady JL. 2008. Geomicrobiology of biovermiculations from the Frasassi cave system, Italy. Journal of Cave and Karst Studies 70: 78-93.

Jones DS, Polerecky L, Galdenzi S., Dempsey BA, Macalady JL. 2015. Fate of sulfide in the Frasassi cave system and implications for sulfuric acid speleogenesis. Chemical Geology 410: 21-27. http://dx.doi.org/10.1016/j.chemgeo.2015.06.002

Macalady JL, Dattagupta S, Schaperdoth I, Jones DS, Druschel GK, Eastman D. 2008. Niche differentiation among sulfur-oxidizing bacterial populations in cave waters. ISME Journal 2: 509-601. http://dx.doi.org/10.1038/ismej.2008.25

Macalady JL, Jones DS, Lyon EH. 2007. Extremely acidic, pendulous microbial biofilms from the Frasassi cave system, Italy. Environmental Microbiology 9: 1402-1414. http://dx.doi.org/10.1111/j.1462-2920.2007.01256.x

Macalady JL, Lyon EH, Koffman B, Albertson LK, Meyer K, Galdenzi S, Mariani S. 2006. Dominant microbial populations in limestone-corroding stream biofilms, Frasassi cave system, Italy. Applied and Environmental Microbiology. 72: 5596-5609. http://dx.doi.org/10.1128/AEM.00715-06

Mecchia M. 2012. Indizi di speleogenesi ipogenica nelle grotte del Monte Soratte. Notiziario dello Speleo Club Roma 16: 58-69.

Menichetti M. 2009. Speleogenesis of the hypogenic caves in Central Italy. In: White WB, editor. Proceedings of the 15th International Congress on Speleology, Kerrville: p. 909-915.

Menichetti M. 2011. Hypogenic caves in western Umbria (Central Italy). Acta carsologica 40 (1): 129-145.

Menichetti M, Chirenco MI, Onac B, Bottrell S, 2007. Depositi di gesso nelle grotte del Monte Cucco e della Gola di Frasassi. Considerazioni sulla speleogenesi. In: Atti Congresso Nazionale di Speleologia, Iglesias: p. 308-325.

Piccini L, De Waele J, Galli E, Polyak VJ, Bernasconi SM, Asmerom Y. 2015. Sulphuric acid speleogenesis and landscape evolution: Montecchio cave, Albegna river valley (Southern Tuscany, Italy). Geomorphology 229: 134-143. http://dx.doi.org/10.1016/j.geomorph.2014.10.006

Principi P. 1931. Fenomeni di idrologia sotterranea nei dintorni di Triponzo (Umbria). Le Grotte d'Italia 5: 1-4.

Sivelli M, De Waele J. editors 2013. A journey across speleological Italy. Map in Scale 1:1,500,000, Società Speleologica Italiana, attached to Speleologia 68.

Tisato N, Sauro F, Bernasconi SM, Bruijn RHC, De Waele J. 2012. Hypogenic contribution to speleogenesis in a predominant epigenic karst system: a case study from the Venetian Alps, Italy. Geomorphology 151/152: 156-163. http://dx.doi.org/10.1016/j.geomorph.2012.01.025

Vattano M, Audra P, Benvenuto F, Bigot JY, De Waele J, Galli E, Madonia G, Nobécourt JC. 2013. Hypogenic caves of Sicily (southern Italy). In: Filippi M, Bosak P, editors. Proceedings of the 16th International Congress of Speleology; 2013 19-27 July, Brno; Volume 3: p.144-149.

DEEP PHREATIC INFLUENCE ON THE ORIGIN OF CAVES AND KARST IN THE CENTRAL APPALACHIAN GREAT VALLEY

Daniel H. Doctor

U.S. Geological Survey
12201 Sunrise Valley Drive, MS926A
Reston, Virginia, 20191, dhdoctor@usgs.gov

Wil Orndorff

Virginia Dept. of Conservation and Recreation, Natural Heritage Program
8 Radford Street
Christiansburg, VA 24073, Wil.Orndorff@dcr.virginia.gov

Abstract

Conceptual models of karst development in the central Appalachian Great Valley have previously focused on shallow phreatic and vadose processes of epigenic karstification. We propose an alternative hypothesis of deep phreatic (hypogenic) karst development as a major contributor to speleogenesis in the region encompassing the Shenandoah River drainage basin, Virginia and West Virginia. The central Great Valley karst is formed within a thick sequence of folded and faulted Paleozoic carbonate rocks that reside within a structural synclinorium, yielding a modern artesian carbonate aquifer system. Evidence for modern deep (>300 m) circulation of meteoric waters within a regional artesian aquifer include (1) high yield wells and voids in carbonate rocks at depths greater than 300 m (1000 ft) below land surface, (2) springs with supra-ambient temperatures, (3) springs of relatively constant discharge and chemistry elevated above base level with decades-old groundwater as the predominant fraction in the young component, and (4) biological evidence for a karst system that has been dissected into compartments by uplift and incision. An examination of several larger caves in the region indicates that many initially formed under fully phreatic conditions guided by geologic structures. Many (but not all) of these caves have been subsequently invaded by vadose waters as a result of erosion and exhumation. Those not so affected are relict phreatic caves, bearing no relation to modern drainage patterns. Features suggesting that deep phreatic processes dominated the development of these relict caves include (1) cave passage morphologies indicative of ascending fluids, (2) cave plans of irregular pattern, reflecting early maze or ramiform development, (3) a general lack of cave breakdown and cave streams or cave stream deposits, and (4) sparry calcite wall and pool coatings within isolated caves intersecting the local water table, and within unroofed caves at topographic locations elevated well above base level. The conceptual premise promulgated here is that deep circulation and upwelling of meteoric waters initiated preferential porosity within restricted areas in the geologic past, and that these zones were guided by geologic structure and diagenesis to become favorable for cavern formation. Episodes of deep karstification were likely separated by long periods of geologic time, encompassing multiple phases of sedimentary fill and excavation within caves, and reflect a complex history of deep fluid migration that set the stage for later, shallow speleogenesis that continues today.

Introduction

The history of karst studies in the United States arguably has its roots in the central portion of the Appalachian Great Valley of Virginia, within the watersheds of the James and Shenandoah Rivers (Figure 1). The classic studies on the origin of limestone caves by William Morris Davis (1930) and J. Harlan Bretz (1942) made specific references to several Shenandoah Valley caves, and addressed the problem primarily on the basis of passage morphologies, thus instigating a decades-long debate over the depth of cave formation in the Appalachians (Palmer, 2007a; White, 2007). In spite of the previous research devoted to the Shenandoah Valley region, its caves and karst have eluded interpretation within classical speleogenetic models that have been developed since (e.g., Davies, 1960; Palmer, 1975; Ford and Ewers, 1978), and continue to present a challenge to the field of karst research.

In this paper, we present a review of existing literature in order to construct a more complete hydrogeologic framework within which to interpret the processes of speleogenesis and karstification in the central
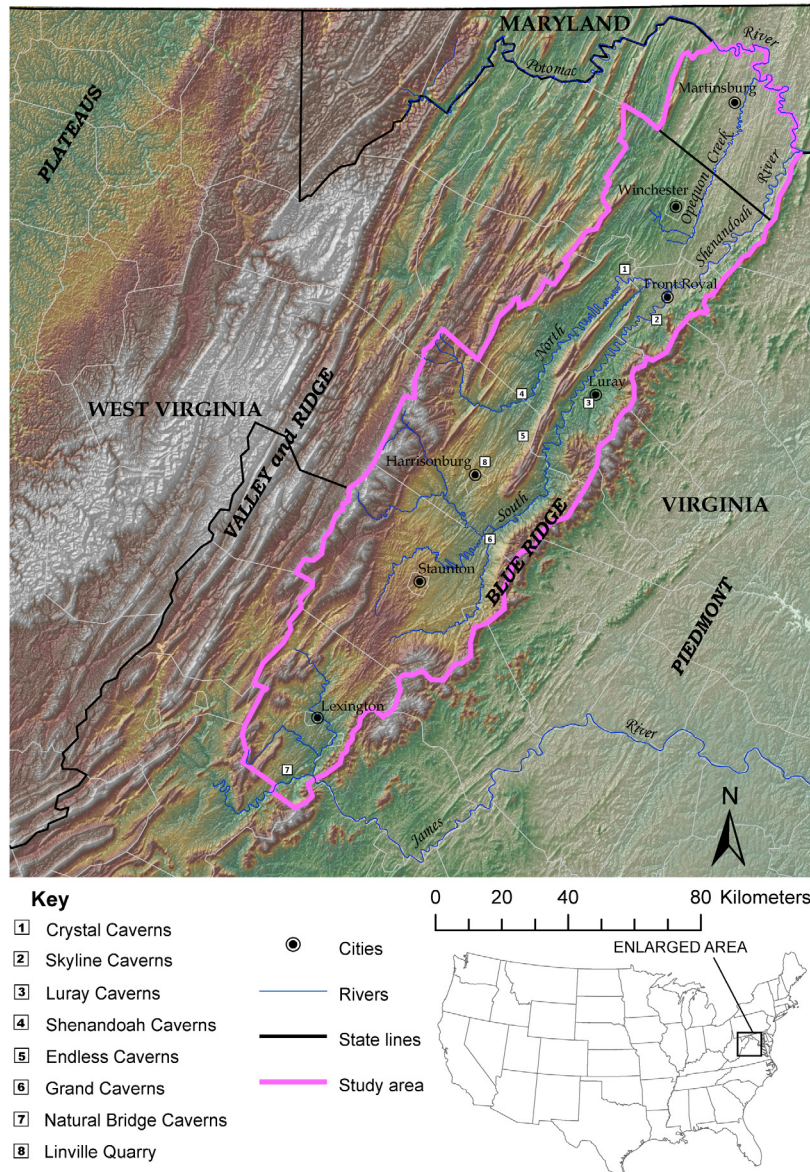
Figure 1.
Map of the central Appalachian region with the Great Valley study area outlined. Locations of larger caves mentioned in the text are shown in the numbered boxes.

Appalachian Great Valley (AGV). Details on the individual caves mentioned here and their respective geologic settings can be found in recent field guides by Doctor et al. (2014, 2015). We conclude that the hydrogeologic framework suggests an early influence of deep phreatic groundwater circulation on speleogenesis in this area, supported by our observations of cave morphology, regional hydrogeology, and regional geology. We adhere to the definition of hypogene speleogenesis provided by Klimchouk (2007) as "the formation of caves by water that recharges the soluble formation from below, driven by hydrostatic pressure or other sources of energy independent of recharge from the overlying or immediately adjacent surface." Although we prefer to associate our conceptual use of the term hypogenic with the source of the water being *per ascensum* (Ford, 1995) rather than with the source of solutional aggressivity being deep-seated (Palmer, 1991; 2011), we do not find the two interpretations of the term mutually exclusive in our study area. The solution of carbonate rock to form caves at depth likely occurred due to mixing corrosion between carbonate-type waters, or in isolated cases, from the oxidation of sulfide minerals in siliciclastic and igneous rocks

adjacent to carbonates. Not all caves in our study area were influenced by deep phreatic speleogenetic processes; we focus on a select number that appear to have been so influenced, and among these we find the history of speleogenetic processes widely varied. Our conceptual model envisages a complex history of phreatic and vadose conduit formation caused by a combination of (1) early proto-conduit formation by deeply circulating hydrothermal fluids, later exploited by near-surface meteoric waters for cave development, (2) deep circulation of meteoric waters that rise again along geologic structures to form caves through chemical corrosion induced by cooling of rising waters and mixing with shallow waters, and (3) enlargement and modification of phreatic solution conduits through denudation and invasion resulting from erosion and surficial karstification, often enhanced by thick surficial sedimentary cover. This conceptual model stands in contrast to the prevailing conceptual model of the Appalachian Great Valley karst as being predominantly fluviokarstic in origin, and has implications for water resource management and the geomorphic development of the Great Valley region as a whole.

Ancient and Modern Carbonate Thermal Springs in the Virginia Valley and Ridge

Within carbonate aquifers, deep groundwater circulation generally results in warm and hot springs and their associated mineral deposits. Although sparse, important geologic evidence for ancient warm springs within the Shenandoah Valley does exist. For example, Nolde and Giannini (1997) reported layered deposits composed of chalcedony and microcrystalline quartz at two sites in Virginia, one within the Shenandoah Valley near the town of Broadway in Rockingham County, and another to the south and west within the Warm Springs anticline in Bath County (Figure 2). Nolde and Giannini (1997) interpreted these deposits as siliceous sinter formed within ancient warm springs based upon the mineralogy and chemistry of the deposit, and on the presence of the modern warm springs in the vicinity. At the Broadway site, Nolde and Giannini (1997) report hydrothermally altered outcrops at the top of the Beekmantown Group that extend into the New Market Limestone and Edinburg Formation. The Broadway site is characterized by numerous solution features in outcrops, orange-red to pink vesicular alteration rinds on outcrop surfaces, large sinkholes, and at least one known cave. The cave is small (<30 m total length), with passages occluded by collapse and sedimentary fill. The cave lies along bedrock strike 500 m north of the sinter deposit, and contains lithified sedimentary fill cemented primarily with calcite. Another larger cave is located about 2 km

along strike to the southwest of the sinter deposit, within an abandoned quarry in the town of Linville. Linville Quarry Cave contains a bauxite-like deposit of sediment that is lithified with late-stage calcite cement. The calcite invades clay pisoliths composed primarily of illite and kaolinite, and fills small vugs in the cemented sediment (Doctor et al., 2014). Petrographic examination revealed a scalenohedral habit to the calcite cement, likely indicating a hydrothermal origin.

The siliceous sinter deposits in the Warm Springs anticline area of Bath County are similar in chemical and mineralogical composition to the Broadway sinter deposit, affording a direct comparison of karstification processes in these seemingly disparate regions. Two hypotheses concerning the origin of heat in the spring waters of the Warm Springs region are (1) a cooling magmatic pluton at depth, and (2) deep circulating groundwater controlled by geologic structures. Heat flow data indicates that a normal geothermal gradient of 25ºC/km exists in the flat-lying rocks of the Appalachian Plateau (Perry et al., 1979). In contrast, a shallow geothermal gradient of about 10ºC/km exists in the core of the Warm Springs anticline—where surface hot springs up to 40ºC are known to exist—indicating substantial circulation of meteoric water at depth; the elevated temperatures have not been attributed to a cooling magmatic body (Perry et al., 1979; Hobba et al., 1979). The depression of the geothermal gradient is likely the result of enhanced percolation of cooler surface waters to depths of at least 300 m (Perry et al., 1979). A numerical modeling study of groundwater flow in the Warm Springs anticline region has shown that circulation to depths of up to 5 km is theoretically possible, with the constraints that (1) the discharge area is within a zone of enhanced hydraulic conductivity, (2) a horizontal zone of enhanced permeability exists at depths between 3 and 5 km, and (3) the recharge area is characterized by relatively low permeability (Severini and Huntley, 1983). While this porous-media groundwater model has known limitations for representing flow within a karstified fractured rock aquifer, it demonstrates that thermal convection is sufficient to produce 40ºC hot springs at the surface without invoking a cooling magmatic body at depth. These results are supported by a study of spring water chemistry, which indicates that greater than 95% of the dissolved solids consist of Ca^{2+}, Mg^{2+}, HCO_3^-, and SO_4^{2-} (Helz and Sinex, 1974).

More recent modeling of coupled heat flow and geochemical reactions along deep circulating flow in fractured carbonate rock has shown that buoyant convection cells develop that serve to enhance mixing
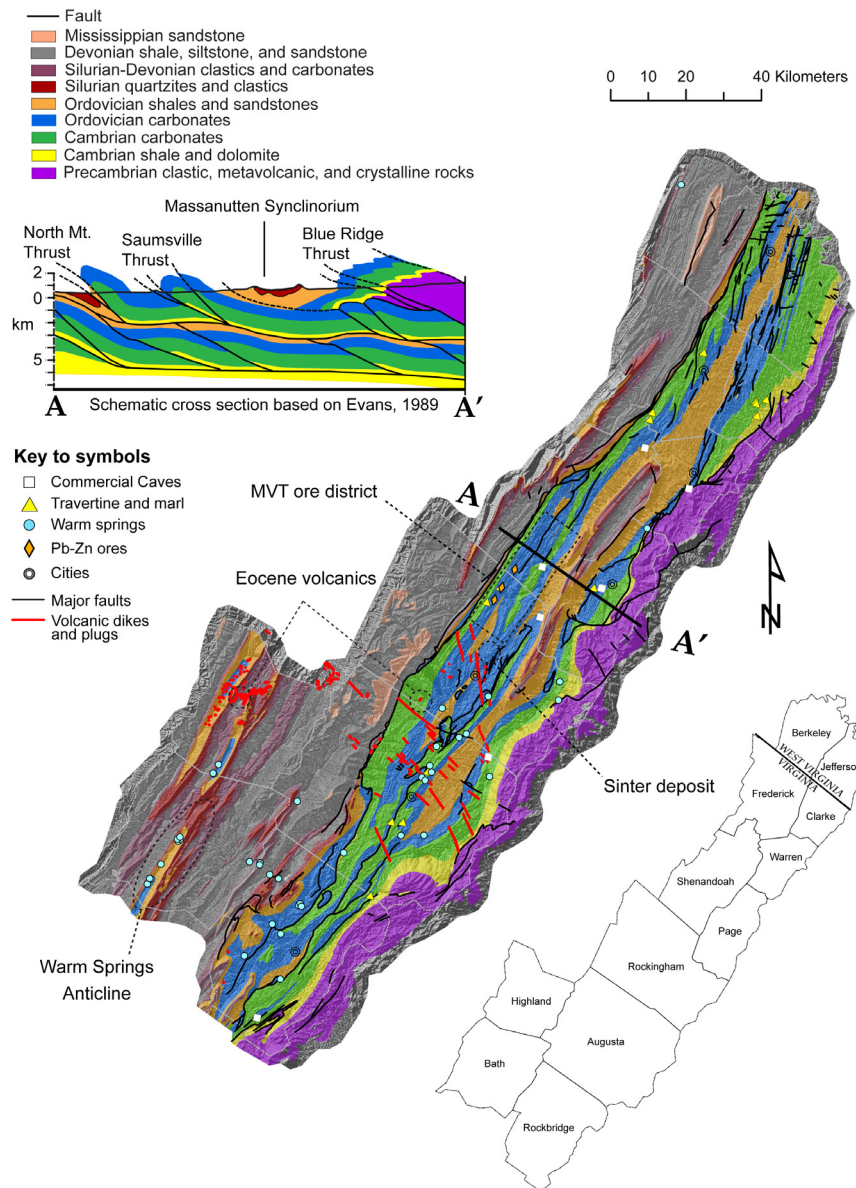
Figure 2.
Generalized geologic map and cross section of the study area.

between deep and shallow water to induce solutional conduit formation at depth (Chaudhuri et al., 2009, 2013).

Modern Hydrology of the Shenandoah Valley Karst

The carbonate aquifer of the Great Valley in Virginia and West Virginia is characterized by a large component of rising, artesian flow. The karstic aquifer discharges to numerous springs that range in flow rate across three orders of magnitude. Cady (1936) reports 95 springs in the Shenandoah Valley with discharge ranging from 27 to 29,000 m^3/day, and average flow of 363 m^3/day. Some larger springs exhibit a delayed response to rainfall

events, with long hydrograph recession periods and muted chemical variability (Vesper et al., 2008; Doctor et al., 2011). Spring discharge accounts for 60% to 90% of stream flow (Harlow et. al, 2005), thus most streams in the karst areas of the Valley are gaining rather than losing. Circulation of groundwater through conduits exceeds depths of 1000 ft (300 m), as evidenced by a small number of high-yield deep wells; most wells are finished less than 100 m below land surface and yield between 3.6-600 L/min (Cady, 1936).

Constraints on the maximum depth of karst groundwater circulation are provided by geologic structure and water

temperatures of springs. Reeves (1932) identified at least 15 thermal springs in the Shenandoah Valley (Figure 2), and defined thermal springs as those that maintain temperatures above the mean ambient temperature of 12.8ºC across seasonal cycles; however, true hot springs have temperatures that are a minimum of 5ºC above ambient (White, 1965). One of these, Dices Spring, showed a constant temperature of 17.9±0.04°C (n =13,400) from the period of June 2011 to December 2012 (Doctor et al., 2014). As already described above, a zone of truly hot (>30ºC) carbonate waters exists in Bath County, Virginia, south and west of the Shenandoah Valley, and these hot springs have been interpreted to gain their heat from deep circulation (>3 km) of meteoric water along fractures and faults (Perry et al., 1979). Given the presence of ancient warm spring deposits and modern warm springs, hydrothermal activity appears to have played at least a local role in ancient karst development in the Shenandoah Valley.

Geologic controls on groundwater flow strongly influence spring discharge and geochemistry in the Great Valley, and temporal geochemical variability is often muted (Vesper et al., 2008; Doctor et al., 2015). Larger perennial springs often occur along faults, and many lie above base-level streams. A comparison of the elevation of a number of perennial springs to the elevation of the nearest confluence of the spring run with a trunk surface stream indicate that springs lie an average of 26 m above local base level (Figure 3). Upward flow gradients in wells occur particularly where cross-strike faults and joints intersect either bedding planes or strike-parallel faults (McCoy and Kozar, 2008; Doctor et al., 2014).

Recent age-dating of well and spring waters throughout the Great Valley of Virginia and in the vicinity of Shenandoah National Park has provided important insight into the hydrologic function of the karst. The ages are based upon measured concentrations of chorofluorocarbons (CFCs), tritium/helium-3, sulfur hexafluoride (SF6), and associated gas and water chemistry and stable isotopic composition (Plummer et al., 2000; Plummer et al., 2001). For example, Hudson Spring in the town of Luray (near Luray Caverns) showed a tritium/helium-3 groundwater age of 24.4 ±0.8 years for the young component; however, the mean age would have to be significantly older. If interpreted as a binary mixture, the water from Hudson Spring is a mixture of about 1/3 water with an average age of 24 years and 2/3 of older (pre-1960s) water. Similarly, two wells in the Conococheague Limestone located approximately 20 km south of Luray showed tritium/helium groundwater ages for the majority of the young

component of 40 and 29 years (Plummer et al., 2000). The tritium and helium isotope data for these samples collectively indicate mixtures of tritiated post-1960s water and much older water, but no evidence for a deep mantle source of helium has been documented.
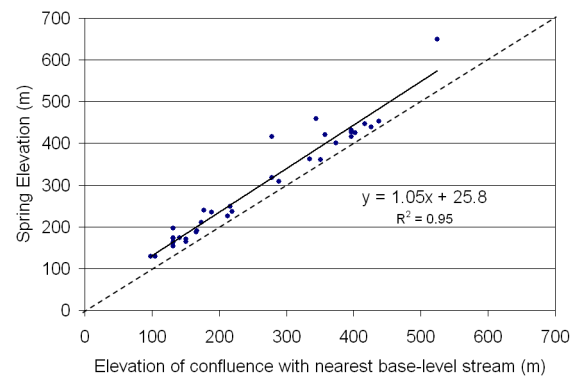
Figure 3.
Elevations of perennial springs compared to elevations of major base-level streams in the Shenandoah Valley. Note that the springs are all elevated above base-level streams by approximately 26 m, on average.

Dye Trace Results

In the mountainous regions of the Valley and Ridge Province, west and southwest of the Shenandoah Valley, characterizing and delineating karstic drainage basins can often be achieved through dye tracing. Springs generally discharge at or very near base level, travel times between the sink points and springs range from a few hours to usually not more than two weeks, and drainage is generally convergent, except near basin divides (Wright, 1985; Idstein, 1992). In contrast, dye tracing in the Shenandoah Valley is generally less straightforward for delineating groundwater basins. Many of the larger springs of the Shenandoah Valley discharge at elevations ranging from 10 to 60 m above the modern base level, as defined by the Shenandoah River and its tributary forks (Figure 3). These larger, elevated springs occur along and support the flow of most perennial surface streams (Harlow et al., 2005). Dye traces up-gradient of these springs yield long travel times, high dilutions, and divergent flow (Jones, 1987, 1991, 1997; Kozar et al., 2007). In a quantitative dye tracing study near Winchester, Virginia, water sampling for dye was supplemented by water chemistry analyses (Doctor et al., 2011). The trace took place during the largest snowmelt event on record, punctuated by heavy rainfall. In spite of the large changes in spring discharge, the resulting chemical time series obtained at the spring showed remarkably little variation. Dye

recovery was muted and prolonged, indicating a large phreatic groundwater reservoir contributing to the spring discharge that is relatively well-buffered against rapid infiltration, behavior that is in contrast to typical spring responses in the Appalachian lowland plateaus.

These observations are consistent with a conceptual model of geologic structures that compartmentalize the aquifer (Orndorff and Hutchins, 2007; Weary et al, 2007; Vesper et al., 2008). Jones (1987, 1991) described the karst system as a diffuse flow aquifer with water moving through a network of fractures, faults, and bedding plane partings enlarged by dissolution. Wright (1990) concurred, saying that "mixed diffuse-flow and conduit-flow conditions occur in the valley region, but diffuse-flow conditions predominate." Nevertheless, large caves are found throughout the Valley that appear to be decoupled from the modern hydrologic flow system.

Travertine-Depositing Springs

Numerous springs and groundwater seeps within streams in the Shenandoah Valley are saturated with calcium carbonate. As a result, tufa, travertine, and marl accumulate on riffles or waterfalls in stream beds (Figure 2). CO_2 loss from stream outgassing and uptake by in-stream growth of photosynthesizing biota (algae, diatoms, moss) causes precipitation of calcium carbonate (Hubbard et al, 1985; Herman and Hubbard, 1990). Travertine-depositing springs and streams are commonly associated with faults. Travertine-depositing springs often have water temperatures that are ambient or only mildly warmer, and PCO_2 values that are as high as 2 orders of magnitude greater than atmospheric. According to the classification of Pentecost (2005), the tufa and travertine deposits fall into the category of meteogene source waters with ambient or super-ambient temperatures, and a soil source of carbon dioxide. The $\delta^{13}C$ values of dissolved inorganic carbon (DIC) are -12‰ to -10‰ (PDB) (Herman and Hubbard, 1990), and fall within the range of values expected for closed-system carbonate rock dissolution with soil CO_2, indicating that the majority of dissolution occurred under closed-system conditions (Deines at al., 1974). In contrast, a travertine-depositing warm spring (Falling Spring) located outside of the Shenandoah Valley in the highlands to the southwest shows more elevated $\delta^{13}C$ values of dissolved inorganic carbon (-3‰ PDB) (Herman and Hubbard, 1990), indicative of a greater degree of isotopic exchange with the rock (Gonfiantini and Zuppi, 2003), isotopic fractionation due to CO_2 outgassing (Doctor et al., 2008a), or a source of CO_2 more enriched in ^{13}C than soil CO_2 (Herman and Hubbard, 1990).

Generation of the high PCO_2 values in calcite-saturated groundwater can occur through several mechanisms, such as (1) oxidation of soil organic matter and plant root respiration at shallow depth, (2) degassing from cooling magmatic or volcanic bodies, (3) decarbonation metamorphic reactions at great depth, (4) thermochemical or biochemical oxidation of hydrocarbons at depth, and (5) biologically mediated hydrogen sulfide oxidation generating sulfuric acid for carbonate dissolution (Hill, 1995; Engel et al., 2004; Pentecost, 2005). No evidence exists in our study area for degassing cooling magmas or metamorphic decarbonation reactions occurring at depths, thus these sources of CO_2 can be ruled out. Oxidation of soil organic matter occurs near or at the surface, thus PCO_2 values would have to be preserved at springs by having open-system equilibrium conditions in zones of high rates of soil organic matter oxidation. Given the $\delta^{13}C$ values of DIC indicative of closed-system conditions, a relatively deeper occurrence of carbonate solution seems likely. Acidity generated by the oxidation of sulfides in shales is probable; higher sulfate concentrations in springs are generally associated with those having chemistry and temperatures indicative of deeper flow (Doctor et al., 2014). The depth to which carbonate solution takes place in the modern system is as yet unresolved.

Biological Evidence for Deep Groundwater Basins

The distribution and genetic divergence of the Madison Cave Isopod, *Antrolana lira (Cirolanidae)* (Bowman, 1964), provides insight into and raises questions about the Cenozoic and perhaps Mesozoic history of the Shenandoah Valley. The species is a phreatobyte, and is restricted to living within karst aquifers. Throughout the world, fresh water cirolanid isopods are known only from karst aquifers with an obvious present or historic connection to the marine environment (Holsinger et al., 1994). *Antrolana lira*, endemic to the Shenandoah Valley, is the only species for which such a historic connection is not well-documented in the geologic record. Holsinger et al. (1994) proposed that a Cretaceous marine embayment brought marine water into contact with carbonate rocks of the Shenandoah Valley via the water gap at the confluence of the Potomac River and Shenandoah River at Harpers Ferry (Figure 1). However, Naeser et al. (2006) used fission-track dating of detrital zircons to show that sediment with a Valley and Ridge provenance is present in the Atlantic Coastal Plain only in mid-Oligocene and younger strata, meaning that the Harpers Ferry water gap probably did not exist during the Cretaceous. Hutchins et al. (2010) reported that the Madison Cave

Isopod colonized the karst aquifer of the Shenandoah Valley several tens of millions of years ago, based on divergence and mutation rates of the species. Hutchins et al. (2010) compared mitochondrial DNA of *Antrolana lira* from across its range, and determined that at least three distinct genetic populations existed, separated by approximately 9-12% for the portion of genome examined. Assuming that the species represents a single invasion of the karst aquifer by marine cirolanids, the habitat must have been subsequently dissected, thus isolating individual populations that began to diverge genetically at least several million years ago (Hutchins et al., 2010).

Orndorff and Hutchins (2007) suggested that the isolation of the individual isopod populations was due to landscape dissection by uplift and downcutting of a regionally extensive karst aquifer during formation of the modern river drainage network. Both insoluble bedrock formations and modern river valleys appear to form barriers to migration of *Antrolana lira*, the latter perhaps due to filling of underlying conduits with sediment. Also, because of its marine origins, the existence of *Antrolana lira* implies that at some point a marine-freshwater interface existed within the Shenandoah drainage basin. However, sedimentary evidence of that interface is absent, and was likely removed by Miocene and later erosion.

The important implication provided by studies of *Antrolana lira* is that a regionally extensive karst system existed long before the development of the modern river drainage. This hypothesis is consistent with phreatic rather than vadose formation of caves of the Shenandoah Valley, except in the vicinity of entrenched modern rivers. This hypothesis means that the former base-level conditions of the modern river systems provided conditions for modification of a previously existing network of solution cavities and conduits that formed under phreatic conditions.

Cave Elevations and Potential Base-Level Control on Karst Development

Davies (1960) argued in support of the dominance of base-level control on passage development within the folded and faulted Appalachian Valley and Ridge by correlating tiers of larger passages with elevations of river terraces on the surface in the vicinity of base-level streams. However, these correlations were not precise, and it is probable that in many cases preexisting deep passages had been graded to terrace levels by sedimentation and enlarged during periods of stable base level. For example, Davies (1960) used Grand Caverns

to support his conceptual model, but did not have knowledge at the time that Madison Saltpeter Cave and Steger's Fissure extend well below the present level of the Shenandoah River (Kastning, 1995). Nevertheless, Davies (1960) did consider that, "In the initial stages of solution primitive tubes, pockets, and similar solution features are developed at depth in the groundwater. … The product of this stage is a series of random, non-integrated, immature openings."

The role of base-level control on cave development in the Shenandoah Valley was further explored by White and White (1974). They presented evidence for the correspondence between passage development and erosional levels at the surface within the greater Potomac River drainage basin; however, for the Shenandoah Valley, the results were equivocal given the data available at the time. White and White (1974) demonstrated that (1) the elevation profile of cave development closely parallels the present day elevation profile of the Shenandoah River, but (2) the peaks in cave distribution were not coincident between the North Fork and South Forks of the Shenandoah River. Revisiting the analysis of White and White (1974) after several decades of additional cave discovery, we have plotted the elevations of cave entrances along the profile of the Shenandoah River (Figure 4), as well as the frequency distribution of cave entrance elevations through the Shenandoah Valley (Figure 5). The data shown in Figure 4 indicates that cave entrances exist across a wide range of elevations throughout the Shenandoah Valley, and do not necessarily show elevational control that parallels the river profile. Figure 5 validates the conclusion by White and White (1974) that there is a lack of accordance between cave elevations in the North Fork and South Fork watersheds. Interestingly, taking all of the cave elevation data together reveals a clear bi-modal distribution between the North and South Fork drainages. When the overall distribution is grouped by counties located within the respective watersheds, one sees a series of overlapping, near-Gaussian distributions with peaks that progressively decrease in elevation moving downstream in the respective drainage, with greater numbers of caves in the upstream, headwater regions (Figure 5). This pattern seems to indicate an overall lack of control by erosional surfaces or dominant periods of base-level stability, and instead points to the control that steeper hydraulic gradients may exert on excavation of early-formed caves existing across a range of elevations. Lithologic variations and local relief likely also exert controls on elevations of cave passages, particularly in the headwater regions of the watersheds.
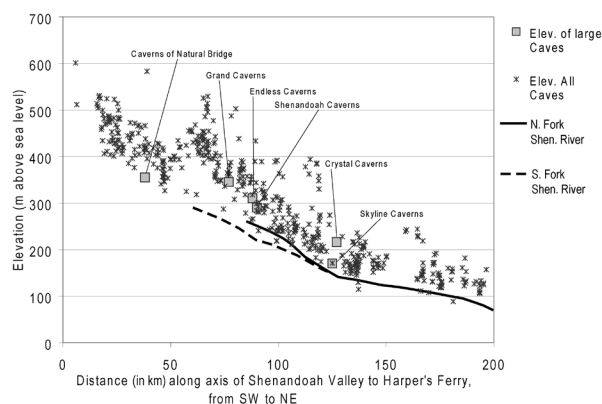
Figure 4.
Profile of cave elevations in relation to the channel of the Shenandoah River. Cave elevations roughly parallel the profile of the river; however, caves exist at numerous elevations and tend to be more abundant in headwater areas, indicating a lack of control by erosional surfaces or dominant periods of base-level stability.

Conceptual Models for Deep Karst Development

In light of the geologic and hydrologic context provided above, we evaluate prior conceptual models for cavernous karst development applicable to the central Appalachian Great Valley, and introduce a new conceptual model here.

Our general conclusion is that caves already existing far below base level are exposed through denudation of the land surface rather than created by periods of stable base level corresponding to erosional surfaces. The caves showing horizontal extension but largely phreatic morphologies likely were formed well below the water table in a zone of mixing between confined rising waters and shallow unconfined aquifer water. Certainly, some new caves are actively forming or enlarging near to incised surface streams where groundwater gradients steepen. However, for the most part, caves occur both in the uplands and in the valleys and do not show distributions corresponding to valley-wide elevational tiers. As river incision lowers base level, cavern-development processes progress from phreatic, to water table, to vadose, with varying degrees of water table and vadose development overprinting the initial phreatic forms (Worthington, 2005). The conceptual model of caves largely forming at or near base level does not apply well to caves that exist far from base-level streams (e.g., Crystal Caverns, Shenandoah Caverns) or those that exist adjacent to base-level streams yet show no

evidence of stream deposits (e.g., Grand Caverns), and thus lack the evidence needed to invoke the mechanism described for their formation. According to the four-phase model of karst evolution in dipping carbonate strata put forth by Ford and Ewers (1978), fracture frequency controls development of phreatic loops within conduits that connect focused recharge from the surface (sinking streams) through deep conduits to outlet springs at base level. In this model, lower fissure frequency (state 1) promotes deeper conduit development, and horizontality in passage development is controlled by the water table during stable periods of base level (Ford and Williams, 2007). This model seems to have limited applicability in the Shenandoah Valley given that (1) sinking streams are relatively uncommon except where colluvium covers carbonates on the flanks of ridges, and (2) it does not account for caves located within isolated hills on the land surface with no obvious surface flow inlets or outlets.

Fracture frequency is high in these rocks due to folding and faulting, which would tend to preclude development of deeper flowpaths according to the Ford and Ewers (1978) model. However, the total carbonate package is thick within the Appalachian Great Valley (>3 km; Figure 2), and faults frequently bringing siliciclastic units into contact with the carbonates. Steeply dipping bedding planes, faults, and extensional fracture zones account for the availability of deep flow paths (Doctor et al., 2015).

A somewhat different conceptual model of deep phreatic loops was proposed by Worthington (2001). In this model, the decrease in viscosity that accompanies normal geothermal heating of downward migrating groundwater allows for long (several km) flowpaths to develop in proportion to their depth. Worthington (2001, 2004) also explored the dependence of other factors on flow depth, and concluded that the controlling factors were flow path length and stratal dip; however, these empirical models do not deal specifically with the problem of flow path genesis. Although calcite solutional capacity is replenished through cooling of water as it rises (e.g., Dublyansky, 2000), this is not sufficient to form caves in the absence of other sources of acids or mixing with waters of different geochemical composition (Andre and Rajaram, 2005). Perhaps just as significant is the increase in calcite solubility with depth that results from greater hydrostatic pressure under closed system conditions; however, the effect of mixing corrosion is more likely. The analytical modeling work of Gabrovšek (2000) showed that isolated conduit formation along deep flow paths is promoted by mixing corrosion between deep and shallow meteoric fluids of

contrasting partial pressure of CO_2, and buoyancy-driven convection within mixing zones (Chaudhuri et al., 2009; 2013) Thus, mixing of shallow and deep waters—both of meteoric origin—is a plausible means of producing caves well below the water table.
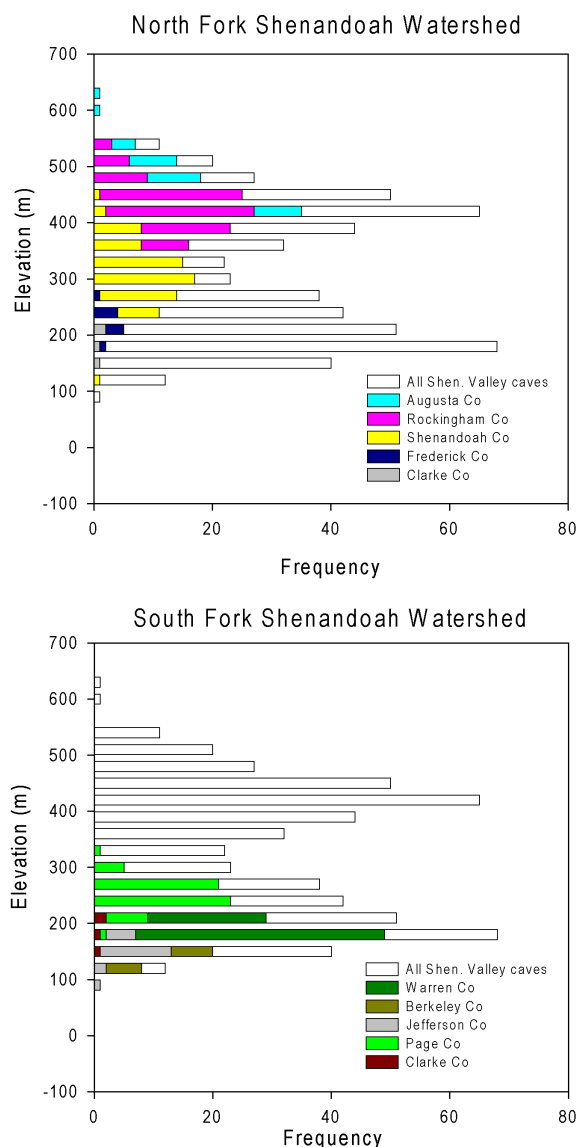

North Fork Shenandoah Watershed

South Fork Shenandoah Watershed

Figure 5.
Histograms of cave elevations within the North Fork and South Fork Shenandoah River watersheds. Peak elevations in overlapping normal distributions grouped by county become lower moving downstream, showing a lack of any dominant elevational tiers. Caves are exposed, excavated and enlarged by river down-cutting rather than formed during periods of stable base level.

Our conceptual model begins with the initiation of karst porosity at depth through upwelling and migration of hydrothermal fluids, possibly related to fluid migration during orogenesis and Mississippi Valley Type (MVT) ore deposition (Herbert and Young, 1956), ancient volcanism (Southworth et al., 1993), or some other diagenetic process. These aggressive fluids may have initiated conduit porosity (generally ranging from a few millimeters to tens of centimeters) within restricted areas of geologic structure conducive to enhancement of localized flow systems. This phase of proto-conduit development was followed by subsequent conduit growth through circulation of meteoric waters from the land surface.

Enlargement of proto-conduits took place at depth along sub-horizontal zones, perhaps corresponding to horizons of increased hydrostatic pressure, and/or within mixing zones controlled by localized convective cells (Chaudhuri et al., 2013), but located well beneath the water table. As denudation proceeded, initially deep caves became uncovered and exposed. Carbonate rocks that had been dolomitized and/or silicified in preferential fracture zones by early hydrothermal fluids became slightly more resistant to surficial weathering than surrounding rock, ultimately hosting caves that reside within isolated hills on the land surface (Doctor et al., 2014). In some cases, the caves become incorporated into a flow system that largely fits into the conceptual models of Ford and Ewers (1978) and Worthington (2001) discussed above, with the condition that initial conduit formation was promoted by aggressive fluid migration to create proto-conduits in the rock in zones guided by local geologic structures (Doctor et al., 2014, 2015).

A final, late stage of cavern development observed within caves in the Shenandoah Valley is one of free-surface stream development within certain caves, indicating complete incorporation of the preexisting cavern into an integrated epigenic flow system. Large caves in the Shenandoah Valley that appear to have resulted from this late-stage of passage development include Endless Caverns and Skyline Caverns. Integration of these initial hypogenic conduits and/or caves within a near-surface karst system is fortuitous, and largely controlled by geologic structures that cause aquifer compartmentalization and/or promote surface stream invasion into preexisting caverns. Some caves appear to largely preserve an initial mode of early hypogenic formation, with minimal overprinting from epigenic karstification, such as Luray Caverns (Hack and Durloo, 1977) and Grand Caverns (Doctor et al., 2014). Other caves indicate that proto-conduit

development largely preceded the majority of cavern formation, perhaps existing orders of magnitude longer in the subsurface than the timescale needed for cave development (e.g., Crystal Caverns at Hupp's Hill). Still others appear to have evolved to a stage in which epigenic processes of cave development now dominate, such as Skyline Caverns (Doctor et al., 2015) and Endless Caverns (Bretz, 1942).

Summary and Conclusions

The geologic and hydrologic framework of the northern Great Valley indicates that the karst has formed through deep-phreatic solutional processes over time spans of tens of millions of years. Although paleokarst horizons are known to exist within the overall stratigraphic section (e.g., within the post-Sauk and post-Kaskaskia unconformities; Palmer and Palmer, 2011), these horizons do not exhibit preferential cave development in the Appalachian Great Valley. The caves we describe, for example, occur in all ages of exposed carbonate units, from Cambrian through Middle Ordovician.

Several large caves in the Shenandoah Valley exhibit morphologic features that can be interpreted as resulting from ascending phreatic fluids such as feeder tubes, cupolas, and rising wall and ceiling channels, blind passage terminations, and joint control of passage orientation (Klimchouk, 2009). By themselves, these features are not conclusive evidence for hypogenic cave origin, as a floodwater explanation for their development has also been suggested (e.g., Palmer 1975; Palmer, 2011). However, most of the Shenandoah Valley caves lack an obvious genetic relation to sinking surface streams. Caves that likely were initiated via hypogenic processes contain maze-like passages formed along intersecting joints and bedding planes with vertical extent upwards of 20 m, and lack evidence of floodwater formation such as coarse-grained sediment fills, organic matter detritus, or scallops that would indicate high velocity flow regimes. Large, phreatic caves likely formed as a result of buoyant convection and mixing corrosion between deep upwelling waters and shallow infiltrating waters in structurally favorable zones (adjacent to faults, along fold axes, or within fold noses) through long periods of geologic time, with regional karst development spanning the entire Cenozoic Era. Field and petrographic evidence shows that carbonate rocks hosting certain relict phreatic caves were dolomitized and/or silicified by early hydrothermal fluid migration in these preferential zones. Evidence for past episodes of early hydrothermal fluid flow include silicification and dolomitization of carbonates along faults and associated with igneous intrusive rocks, as well as ancient deposits of siliceous sinter and calcite.

Sub-water table stream flow evidently overprints the maze character of certain cave passages, yet no indication of a modern free surface stream exists (e.g., Luray Caverns, Grand Caverns, Crystal Caverns). Where free surface streams do exist, the impact of a cave stream on passage enlargement appears localized in a few passages, with a lack of floodwater features in the upper levels (e.g., Skyline Caverns).

Caves in the folded rocks of the Appalachian Valley and Ridge that are largely horizontal in their extent have been interpreted as being developed within a few tens of feet proximal to the water-table (Davies, 1960). However, many caves were either wholly or partially filled with very fine-grained silt and clay sediment for part of their history, even in passages that show no indication of having been occluded by collapse, causing difficulty in assessing the true vertical extent of cavern development. Water table modification of preexisting passages has resulted in grading of passages with sediment fill as well as horizontal enlargement by phreatic and free-surface cave streams. Meteoric waters migrating at depth along geologic structures that mix with waters from a shallow karst aquifer system may enhance mixing corrosion near to, but below, the water table, thus enabling horizontal cavern development under phreatic conditions. Solution by mixing corrosion is well known when the fluids exhibit strong contrasts in PCO_2 (Bögli, 1964; Wigley and Plummer, 1976). Such rising waters may have stagnated within structural traps—particularly along fold axes and within the noses of plunging anticlines—ponding to produce caverns through slow circulation and mixing corrosion (Figure 6). In areas where cross-strike faults, joints, and lineaments intersect thrusts or fold axes the waters may emerge as tufa and travertine-depositing springs and seeps. The total depth of circulation of the modern system may be only several hundred meters, such as in the case of the mildly warm springs in the Shenandoah Valley; however, true hot springs in the Warm Springs region indicate depths of circulation up to a few kilometers is ongoing. Continued landscape erosion causes cavern drainage and collapse, especially near to base-level streams where downcutting permits subsurface piracy of surface tributary streams that flow toward base level through the exposed caverns. As surface karstification continues, the intersection of the hypogenic and epigenetic flow systems results in flow integration within a structurally compartmentalized carbonate aquifer.

Certain large caves of the Valley tend to occur immediately adjacent to the Shenandoah River, where river downcutting exposed and drained phreatic

passages, subjecting them to varying degrees of vadose modification, including formation fill and surface stream capture. On opposite ends of the spectrum of epigenic modification are Grand Caverns and Skyline Caverns. Grand Caverns shows next to no evidence of epigenic modification, whereas Skyline Caverns exhibits significant vadose modifications resulting from surface stream capture; however, the uppermost passages greatly reflect long-lived phreatic conditions.

Numerous caves in the Shenandoah Valley intersect the modern phreatic water table, frequently exposing the surface of a chemically saturated reservoir with calcite rafts. Examples include Madison Saltpetre Cave, Grand Caverns and Crystal Caverns. Cave streams are relatively rare in the Shenandoah Valley, and are best developed in caves like Skyline Caverns, Ogdens Cave (Doctor et al., 2008b) and Endless Caverns where surface stream capture has occurred.

Groundwater ages within some springs in the carbonate units are on the order of one to two decades. This is not to say that the spring waters do not have a component

of very recent water. All of the groundwater ages represent a mixture of groundwater components of multiple residence times, and as such great disparity between ages of the components is expected. However, the fraction of very young water is small in cases where groundwater ages are obtainable, as is evidenced in the gas chemistry of the springs. It is noteworthy that many of the spring waters even yield to age-dating methods using gas equilibration techniques in a karst setting. This indicates that air-water exchange one might expect to take place in karst does not impact many of the larger springs in the Valley, and that closed-system evolution of groundwater along deep flowpaths is occurring.

Landscape denudation exposes the phreatically formed caves. The elevations of the entrances to exposed caves in the Valley follow the downcutting of the Shenandoah River, indicating their progressive exposure as erosion lowers the land surface (Figure 5). At depths greater than 1000 ft (300 m), solutional conduits are encountered by wells, while voids near the water table periodically flood and drain as sinkhole ponds. Sinkholes are widely distributed throughout all carbonate units in
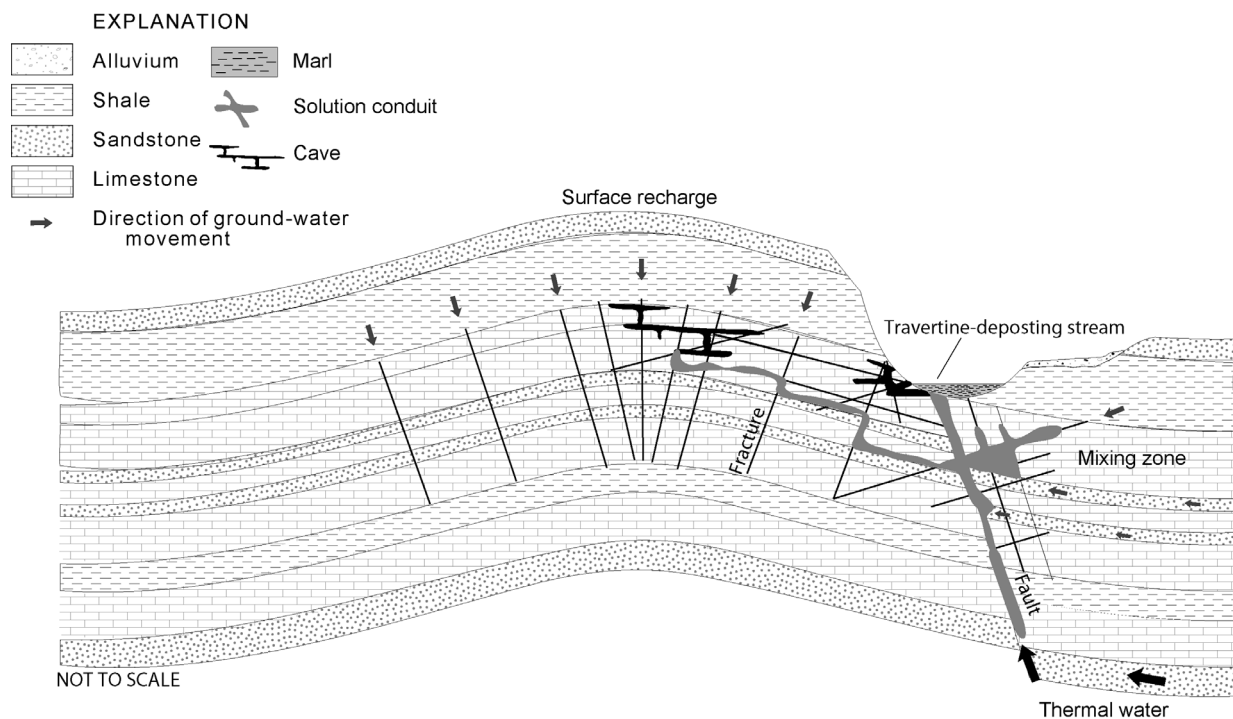
Figure 6.
Schematic illustration of isolated phreatic maze cave development within a mixing zone localized near to a fault. Rising water along the fault intersects the shallow karst aquifer, and creates cavernous porosity in the mixing zone. If rising fluids were initially hydrothermal, alteration of the bedrock along fractures may result in slightly more resistance to weathering, and result in a cave located within a hill on the land surface.

the Shenandoah Valley; however, clustering of their distribution is controlled by the fold and fault structures of the bedrock units (Hack, 1965; Hubbard, 1983; Orndorff and Goggin, 1994; Doctor et al., 2008b).

Although very few data currently exist that can be used to directly constrain the ages of caves in the Shenandoah Valley, the Gray fossil site in eastern Tennessee provides a minimum age of late Miocene to Paleocene (>5.3 million years) to the equivalent Great Valley karst further to the south (Zobaa et al., 2011). The site is a paleo-sinkhole that filled with fine clay, and was a deathbed of numerous species of Miocene megafauna. As a result of erosion, the clay sediment forms a low positive hill on the land surface, within which the fossils are preserved. Such evidence compels consideration of speleogenetic processes that have occurred deep in the geologic past. Although the cave passages are controlled by preexisting structures, the major episodes of speleogenesis occurred sometime after major orogenic deformation ceased. While neo-tectonism has affected cave morphology to varying degrees through facilitating capture of surface streams and truncation of cave passages by incision, many caves in the Shenandoah Valley show little modification of their hypogene origins.

Recognition of hypogenic karst systems formed in association with hydrothermal fluid migration through folded and faulted rocks in active tectonic regions is globally widespread. Such settings include the hydrothermal karst of the Transdanubian Range in Hungary (Dublyansky, 2000), and the eastern Tiber River basin in the central Appenines of Italy (Minissale et al., 2002), among others. Less common are hypogenic caves described in passive tectonic margins, such as within the ancient fold-thrust belt of the Appalachians. However, Auler and Smart (2003) describe hypogenic caves in eastern Brazil that they believe formed as a result of sulfuric acid produced by pyrite oxidation at relatively shallow depths.

The Appalachian orogenic belt has a long and complex history, exposing rocks and structures that record three Paleozoic orogenies, Mesozoic rifting to form the modern Atlantic Ocean, and the recently recognized Cenozoic uplift that continues to this day. These mountains and valleys also host world-class karst. Given the recent advances in the knowledge of ages of caves and karst in the Appalachian region, prior interpretations of cave formation have not looked far enough into the geologic past for an explanation of the speleogenesis. Enhancement of cavernous porosity formed at depth is the likely result of mixing between rising and infiltrating

waters as well as surface lowering through erosion and cavern modification by invading streams. This process has resulted in caves both atop ridges and in the valleys, and an unusually deep karst aquifer in the Shenandoah Valley.

Acknowledgments

References

Andre BJ, Rajaram H. 2005. Dissolution of limestone fractures by cooling waters: early development of hypogene karst systems. Water Resources Research 41 (1): W01015.
http://dx.doi.org/10.1029/2004WR003331

Auler AS, Smart PL. 2003. The influence of bedrock-derived acidity in the development of surface and underground karst: evidence from the Precambrian carbonates of semi-arid northeastern Brazil. Earth Surface Processes and Landforms 28: 157-168.
http://dx.doi.org/10.1002/esp.443

Bögli A. 1964. Mischungskorrsion,ein Beitrag zur Verkarstungs-problem [Mixing corrosion, a contribution to the karst problem]. Erdkunde 18 (2): 83-92.
http://dx.doi.org/10.3112/erdkunde.1964.02.02

Bowman TE. 1964. *Antrolana lira*, a new genus and species of troglobitic cirolanid isopod from Madison Cave, Virginia. International Journal of Speleology 1 (1): 229-236.
http://dx.doi.org/10.5038/1827-806X.1.1.18

Bretz JH. 1942. Vadose and phreatic features of limestone caves. Journal of Geology 50 (6, Part 2): 675-811.
http://dx.doi.org/10.1086/625074

Cady RC. 1936. Ground-water resources of the Shenandoah Valley, Virginia. Virginia Geological Survey Bulletin 45, 137 p. 2 plates.

Chaudhuri A, Rajaram H, Viswanathan H, Zyvoloski G, Stauffer P. 2009. Buoyant convection resulting from dissolution and permeability growth in vertical limestone fractures. Geophysical Research Letters 36 (3): L03401.
http://dx.doi.org/10.1029/2008GL036533

Chaudhuri A, Rajaram H, Viswanathan H. 2013. Early-stage hypogene karstification in a mountain hydrologic system: a coupled thermo-hydro-chemical model incorporating buoyant convection. Water Resources Research 49 (9): 5880-5899. http://dx.doi.org/10.1002/wrcr.20427

Davies WE. 1960. Origin of caves in folded limestone. Bulletin of the National Speleological Society 22 (1): 5-18.

Davis WM. 1930. Origin of limestone caverns. Geological Society of America Bulletin 41: 475-628. http://dx.doi.org/10.1130/GSAB-41-475

Deines P, Langmuir D, Harmon R. 1974. Stable carbon isotope ratios and the existence of a gas phase in the evolution of carbonate groundwaters. Geochimica et Cosmochimica Acta 38 (7): 1147-1164. http://dx.doi.org/10.1016/0016-7037(74)90010-6

Doctor DH, Farrar NC, Herman JS. 2011. Interaction Between shallow and deep groundwater components at Fay Spring in the Northern Shenandoah Valley Karst. USGS Karst Interest Group Proceedings, Fayetteville, Arkansas, April 26-29. U.S. Geological Survey Scientific Investigations Report 2011-5031, p. 25-34.

Doctor DH, Kendall C, Sebestyen SD, Shanley JB, Ohte N, Boyer EW. 2008a. Carbon isotope fractionation of dissolved inorganic carbon (DIC) due to outgassing of carbon dioxide from a headwater stream. Hydrological Processes 22 (14): 2410-2423. http://dx.doi.org/10.1002/hyp.6833

Doctor DH, Weary DJ, Orndorff RC, Harlow GE, Kozar MD, Jr., Nelms DL. 2008b. Bedrock structural controls on the occurrence of sinkholes and springs in the northern Great Valley karst, Virginia and West Virginia. Proceedings of the 11th Multidisciplinary Conference on Sinkholes and Engineering and Environmental Impacts of Karst, Tallahassee, Florida, September 23-26, p. 12-22. http://dx.doi.org/10.1061/41003(327)2

Doctor DH, Orndorff W, Maynard J, Heller MJ, Casile, GC. 2014. Karst geomorphology and hydrology of the Shenandoah Valley near Harrisonburg, Virginia. In: Bailey CM, Coiner LV, editors. Elevating geoscience in the southeastern United States: new ideas about old terranes. Field Guides for the GSA Southeastern Section Meeting, Blacksburg, Virginia, 2014. Geological Society of America Field Guide 35: 161-213. http://dx.doi.org/10.1130/2014.0035(06)

Doctor DH, Weary DJ, Brezinski DK, Orndorff RC, Spangler LE. 2015. Karst of the Mid-Atlantic region in Maryland, West Virginia, and Virginia. In Brezinski DK, Halka JP, Ortt RA, Jr., editors. Tripping from the fall line. Field Excursions for the GSA Annual Meeting, Baltimore, 2015. Geological Society of America Field Guide 40: 1-60. http://dx.doi.org/10.1130/2015.0040(11)

Dublyansky YV. 2000. Hydrothermal speleogenesis in the Hungarian karst. In Klimchouk AB, Ford DC, Palmer AN, Dreybrodt W, editors. Speleogenesis: evolution of karst aquifers. Huntsville (AL): National Speleological Society. p. 298-303.

Engel AS, Stern LA, Bennet PC. 2004. Microbial contributions to cave formation: new insights into sulfuric acid speleogenesis. Geology 32 (5): 369-372. http://dx.doi.org/10.1130/G20288.1

Evans MA. 1989. The structural geometry and evolution of foreland thrust systems, northern Virginia. Geological Society of America Bulletin, 101: 339-354. http://dx.doi.org/10.1130/0016-7606(1989)101<0339:TSGAEO>2.3.CO;2

Ford DC. 1995. Paleokarst as a target for modern karstification. Carbonates and Evaporites 10 (2): 138-147. http://dx.doi.org/10.1007/BF03175399

Ford DC, Williams P. 2007. Karst hydrogeology and geomorphology. Chichester (GB): John Wiley & Sons Ltd. http://dx.doi.org/10.1002/9781118684986

Ford DC, Ewers RO. 1978. The development of limestone cave systems in the dimensions of length and breadth. Canadian Journal of Earth Sciences 15: 1783-1798. http://dx.doi.org/10.1139/e78-186

Gabrovšek F. 2000. Evolution of early karst aquifers: from simple principles to complex models. Ljubljana (SI): Založba ZRC.

Gonfiantini R, Zuppi GM. 2003. Carbon isotope exchange rate of DIC in karst groundwater. Chemical Geology 197 (1-4): 319-336. http://dx.doi.org/10.1016/S0009-2541(02)00402-3

Hack JT. 1965. Geomorphology of the Shenandoah Valley, Virginia and West Virginia, and origin of the residual ore deposits. U.S. Geological Survey Professional Paper 484. 84 p. 3 plates.

Hack JT, Durloo LH. 1977. Geology of Luray Caverns Virginia. Virginia Division of Mineral Resources Report of Investigations 3. 43 p. 1 plate.

Harlow GH, Orndorff RC, Jr., Nelms DL, Weary DJ, Moberg RM. 2005. Hydrogeology and groundwater availability in the carbonate aquifer system of Frederick County, Virginia. U.S. Geological Survey Scientific Investigations Report 2005-5161. 30 p.

Helz GR, Sinex SA. 1974. Chemical equilibria in the thermal spring waters of Virginia. Geochimica et Cosmochimica Acta 38 (12): 1807-1820. http://dx.doi.org/10.1016/0016-7037(74)90164-1

Herbert P, Jr., Young RS. 1956. Sulfide mineralization in the Shenandoah Valley of Virginia. Virginia Division of Geology Bulletin 70. 58 p.

Herman JS, Hubbard DA, Jr., 1990. A comparative study of travertine-marl-depositing streams in Virginia. In: Herman JS, Hubbard DA, Jr., editors. Travertine-marl: stream deposits in Virginia. Richmond (VA): Virginia Division of Mineral Resources Publication 101. p. 43-64.

Hill CA. 1995. H_2S-related porosity and sulphuric acid oil field karst. Memoir, American Association of Petroleum Geologists 63: 301-306.

Hobba WA, Jr., Fisher DW, Pearson FJ, Jr., Chemerys JC. 1979. Hydrology and geochemistry of thermal springs of the Appalachians. U.S. Geological Survey Professional Paper 1044-E. 36 p. http://dx.doi.org/10.2172/6741577

Holsinger JR, Hubbard DA, Jr., Bowman TE. 1994. Biogeographic and ecological implications of newly discovered populations of the stygobiont isopod crustacean Antrolana lira Bowman (Cirolanidae). Journal of Natural History 28: 1047-1058. http://dx.doi.org/10.1080/00222939400770551

Hubbard DA, Jr. 1983. Selected karst features of the northern Valley and Ridge province, Virginia. Virginia Division of Mineral Resources Publication No. 44. 1 sheet (scale 1:250,000).

Hubbard DA, Jr., Giannini WF, Lorah MM. 1985. Travertine-marl deposits of the Valley and Ridge Province of Virginia: a preliminary report. Virginia Minerals 31 (1): 1-16.

Hubbard DA, Jr., Herman JS, Bell PE. 1990. Speleogenesis in a travertine scarp: observations of sulfide oxidation in the subsurface. In Herman JS, Hubbard DA, Jr., editors. Travertine-marl: stream deposits in Virginia. Richmond (VA): Virginia Division of Mineral Resources Publication 101. p. 177-184.

Hutchins B. 2007. Genetic Divergence Among Populations of the Madison Cave Isopod, Antrolana lira. 2007 National Speleological Society Convention Program with Abstracts, p. 77.

Hutchins B, Fong DW, Carlini DB. 2010. Genetic population structure of the Madison Cave isopod, Antrolana lira (Cymothoida: Cirolanidae) in the Shenandoah Valley of the eastern United States. Journal of Crustacean Biology 30 (2): 312-322. http://dx.doi.org/10.1651/09-3151.1

Idstein PJ. 1992. Investigation using fluorescent dyes and continuous groundwater monitoring of the sources and transfer mechanisms that contribute to the Cathedral Hall passage cave stream: Unthanks Cave, Lee County, Virginia [unpublished Master of Science thesis]. Richmond (KY): Eastern Kentucky University. 83 p.

Jones WK. 1987. Overview of the ground-water resources of Clarke County, Virginia with emphasis on the carbonate aquifers west of the Shenandoah River, in Clarke County ground-water protection plan. Lord Fairfax Planning District Commission, p. 7.1-7.22.

Jones WK. 1991. The carbonate aquifer of the Northern Shenandoah Valley of Virginia and West Virginia. In Kastning EH, Kastning KM, editors. Proceedings of the Appalachian Karst Symposium; 1976 March 23-26; Radford, Virginia. p. 217-222.

Jones WK. 1997. Karst hydrology atlas of West Virginia. Special Publication No. 4. Charles Town (WV): Karst Waters Institute.

Kastning EH, III. 1995. Evolution of a karstic groundwater system, Cave Hill, Augusta County, Virginia: a multi-disciplinary study. In Beck BF, editor. Karst geohazards. Rotterdam (NL): Balkema. p. 141-148.

Klimchouk A. 2007. Hypogene speleogenesis: hydrogeological and morphogenetic perspective. Special Paper No. 1,. Carlsbad (NM): National Cave and Karst Research Institute. 106 p.

Klimchouk A. 2009. Morphogenesis of hypogenic caves. Geomorphology 106: 100-117. http://dx.doi.org/10.1016/j.geomorph.2008.09.013

Kozar MD, McCoy KJ, Weary DJ, Field MS, Pierce HA, Schill WB, Young JA. 2007. Hydrogeology and water quality of the Leetown area, West Virginia. U.S. Geological Survey Open File Report 2007-1358. 99 p., 6 appendices.

Minissale A, Kerrick DM, Magro G, Murrell MT, Paladini M, Rihs S, Sturchio NC, Tassi F, Vaselli O. 2002. Geochemistry of Quaternary travertines in the region north of Rome (Italy): structural, hydrologic and paleoclimatic implications. Earth and Planetary Science Letters 203: 709-728. http://dx.doi.org/10.1016/S0012-821X(02)00875-0

McCoy KJ, Kozar MD. 2008. Use of sinkholes and specific capacity distributions to assess vertical gradients in a karst aquifer. Environmental Geology 54: 921-935.
http://dx.doi.org/10.1007/s00254-007-0889-1

Naeser ND, Naeser CW, Newell WL, Southworth S, Weems RE, Edwards L. 2006, Provenance studies in the Atlantic coastal plain: what fission-track ages of detrital zircons can tell us about the erosion history of the Appalachians. Geological Society of America Abstracts with Programs 38 (7): 503.

Nolde JE, Giannini WF. 1997. Ancient warm springs deposits in Bath and Rockingham Counties. Virginia. Virginia Minerals 43 (2): 9-16.

Orndorff RC, Goggin KE. 1994. Sinkholes and karst-related features of the Shenandoah Valley in the Winchester 30' x 60' quadrangle, Virginia and West Virginia. U.S. Geological Survey Miscellaneous Field Studies Map MF-2262 (scale 1:100,000).

Orndorff WD, Hutchins B. 2007. Evolution of the karst aquifers of the Shenandoah Valley, Virginia and West Virginia. National Speleological Society Convention, Marengo, IN, Program with Abstracts. p. 110.

Palmer AN. 1975. The origin of maze caves. National Speleological Society Bulletin 37 (3): 56-76.

Palmer AN. 1991. Origin and morphology of limestone caves. Geological Society of America Bulletin 103 (1): 1-21.
http://dx.doi.org/10.1130/0016-7606(1991)103<0001:OAMOLC>2.3.CO;2

Palmer AN. 2007a. Cave geology and speleogenesis over the past 65 years: role of the National Speleological Society in advancing the science. Journal of Cave and Karst Studies 69 (1): 3-12.

Palmer AN. 2011. Distinction between epigenic and hypogenic maze caves. Geomorphology 134: 9-22.
http://dx.doi.org/10.1016/j.geomorph.2011.03.014

Palmer AN, Palmer MV. 2011, Paleokarst of the USA: a brief review. In Kuniansky EL, editor. U.S. Geological Survey Karst Interest Group Proceedings, Fayetteville, Arkansas, April 26-29. U.S. Geological Survey Scientific Investigations Report 2011-5031, p. 7-16.

Pentecost A. 2005. Travertine. Berlin (DE): Springer-Verlag.

Perry LD, Costain JK, Geiser PA. 1979. Heat flow in western Virginia and a model for the origin of thermal springs in the folded Appalachians. Journal of Geophysical Research 84 (B12): 6875-6883.
http://dx.doi.org/10.1029/JB084iB12p06875

Plummer LN, Busenberg E, Böhlke JK, Carmody RW, Casile GC, Coplen TB, Doughten MW, Hannon JE, Kirkland W, Michel RL, Nelms DL, Norton BC, Plummer KE, Qi H, Revesz K, Schlosser P, Spitzer S, Wayland JE, Widman PK. 2000. Chemical and isotopic composition of water from springs, wells, and streams in parts of Shenandoah National Park, Virginia, and vicinity, 1995-1999. U.S. Geological Survey Open File Report 00-373. 70 p.

Plummer LN, Busenberg E, Böhlke JK, Nelms DL, Michel RL, Schlosser P. 2001. Groundwater residence times in Shenandoah National Park, Blue Ridge Mountains, Virginia, USA: a multi-tracer approach. Chemical Geology 179 (1-4): 93-111.
http://dx.doi.org/10.1016/S0009-2541(01)00317-5

Reeves F. 1932. Thermal springs of Virginia. Virginia Geological Survey Bulletin 36. 56 p., 2 plates.

Severini AP, Huntley D. 1983. Heat convection in Warm Springs Valley, Virginia. Groundwater 21 (6): 726-732.
http://dx.doi.org/10.1111/j.1745-6584.1983.tb01943.x

Southworth CS, Gray KJ, Sutter JF. 1993. Middle Eocene intrusive igneous rocks of the central Appalachian Valley and Ridge Province—setting, chemistry, and implications for crustal structure. Evolution of Sedimentary Basins—Appalachian basin, U.S. Geological Survey Bulletin 1839, Chapter J, 24 p.

Vesper DJ, Grand RV, Ward K, Donovan JJ. 2008. Geochemistry of a spring-dense karst watershed located in a complex structural setting, Appalachian Great Valley, West Virginia, USA. Environmental Geology.

Weary DJ, Doctor DH, Orndorff RC, Harlow GE, Jr. 2007. Structural control of spring locations in the northern Shenandoah Valley, Virginia and West Virginia: interpretation of geologic controls on ground-water flow paths in folded and faulted carbonate rocks. Geological Society of America Abstracts with Programs 39 (2): 99.

White DE. 1965. Thermal waters of volcanic origin. Geological Society of America Bulletin 68: 1637-1658.
http://dx.doi.org/10.1130/0016-7606(1957)68[1637:TWOVO]2.0.CO;2

White WB. 2007. A brief history of karst hydrogeology: contributions of the NSS. Journal of Cave and Karst Studies 69 (1): 13-26.

White WB. 2009. The evolution of Appalachian fluviokarst: competition between stream erosion, cave development, surface denudation, and tectonic uplift. Journal of Cave and Karst Studies, 71 (3): 159-167.
http://dx.doi.org/10.4311/jcks2008es0046

White WB, White EL. 1974. Base-level control of underground drainage in the Potomac River basin. Fourth Conference on Karst Geology and Hydrology Proceedings, West Virginia Geological and Economic Survey, p. 41-53.

Wigley TML, Plummer LN. 1976. Mixing of carbonate waters. Geochimica et Cosmochimica Acta 40 (9): 989-995. http://dx.doi.org/10.1016/0016-7037(76)90041-7

Worthington SRH. 2001. Depth of conduit flow in unconfined carbonate aquifers. Geology 29 (4): 335-338. http://dx.doi.org/10.1130/0091-7613(2001)029<0335:DOCFIU>2.0.CO;2

Worthington SRH. 2004. Hydraulic and geological factors influencing conduit flow depth. Cave and Karst Science 31: 123-134.

Worthington SRH. 2005. Evolution of caves in response to base-level lowering. Cave and Karst Science 32 (1): 3-12.

Wright W. 1985, Hydrology of the Skydusky Hollow Cave System. In Zokaites C, editor. Underground in the Appalachians: a guidebook to the 1995 Convention of the National Speleological Society. Huntsville (AL): National Speleological Society. p. 26-29.

Wright WG. 1990, Groundwater hydrology and quality in the valley and ridge and blue ridge physiographic provinces of Clarke County, Virginia. United States Geological Survey Water Resources Investigations Report 90-4134. 61 p.

Zobaa MK, Zavada MS, Whitelaw MJ, Shunk AJ, Obohikuenobe FE. 2011. Palynology and palynofacies analyses of the Gray Fossil Site, eastern Tennessee: their role in understanding the basin-fill history. Palaeogeography, Palaeoclimatology, Palaeoecology 308 (3-4): 433-444. http://dx.doi.org/10.1016/j.palaeo.2011.05.051

HYPOGENE IMPRINTS IN COASTAL KARST CAVES FROM MALLORCA ISLAND (WESTERN MEDITERRANEAN): A REVIEW OF THE CURRENT KNOWLEDGE ON THEIR MORPHOLOGICAL FEATURES AND SPELEOGENESIS

Joaquín Ginés
Federació Balear d'Espeleologia
C/ Uruguai s/n. Palma Arena
07010 Palma de Mallorca, Illes Balears, Spain, jginesgracia@yahoo.es

Joan J. Fornós
Grup de Geologia i Paleontologia, Dept. Biologia, Universitat de les Illes Balears
Ctra. de Valldemossa km 7.5
07122 Palma de Mallorca, Illes Balears, Spain, joan.fornos@uib.es

Francesc Gràcia
Federació Balear d'Espeleologia
C/ Uruguai s/n. Palma Arena
07010 Palma de Mallorca, Illes Balears, Spain, xescgracia@yahoo.es

Antoni Merino
Federació Balear d'Espeleologia
C/ Uruguai s/n. Palma Arena
07010 Palma de Mallorca, Illes Balears, Spain, tonymerinoj@gmail.com

Bogdan P. Onac
School of Geosciences, University of South Florida
4202 E. Fowler Ave., NES 107
Tampa, FL 33620, USA, bonac@usf.edu

Angel Ginés
Federació Balear d'Espeleologia
C/ Uruguai s/n. Palma Arena
07010 Palma de Mallorca, Illes Balears, Spain, agines.gracia@yahoo.es

Abstract

Among the abundant caves existing in the southern and eastern coasts of Mallorca Island (western Mediterranean), a few of them exhibit solutional features and deposits presumably related to hypogene basal recharge. The caves were formed in calcarenites whose ages range from Upper Miocene (Tortonian reef deposits) to Middle Pleistocene (eolianites) which form a fringing postorogenic belt, mainly deposited over Mesozoic folded and thrusted carbonate deposits. The hydrogeological setting corresponds to an unconfined coastal aquifer in very porous eogenetic rocks, with important lateral and vertical permeability variations related to different facies affected by coastal karst processes. Six caves containing hypogene evidences are distributed in three different coastal areas: the Llucmajor Upper Miocene platform, the Campos Plio-Pleistocene basin, and the Portocristo Upper Miocene littoral fringe. The first two areas are spatially coincident with geothermal anomalies reported in southern Mallorca, which are associated to important SW-NE faults.

The observed cave features or speleogens include a suite of solutional rising forms embracing, among others, subvertical feeder-like conduits and small ascending wall channels of variegated morphologies and dimensions. Sediments and black crusts rich in Fe and Mn oxides are frequent along with some uncommon

minerals (barite, celestine, chamosite, and strontianite) and multicolor alteration deposits, documenting a deep recharge rising into the unconfined and oxygenated littoral groundwater. No evidences of sulfuric acid speleogenesis are present in Mallorcan caves. From the speleogenetic point of view, the studied caves must be considered as complex littoral caves, in which the imprints of hypogene processes are evident but intermingled with other morphogenetic vectors like coastal mixing processes and a substantial meteoric recharge. This specific hydrogeological environment, where contrasting waters of very different geochemistry occur (meteoric input, coastal mixing, and deep basal recharge), has favored the development of extensive caves that show significant differences with respect to the conventional model of coastal karst speleogenesis. It is worth mentioning that the lithological variability of the involved eogenetic rocks introduces additional complexity to these phenomena, affecting both the hydrological behavior of the coastal aquifers and the planimetric pattern of the resulting caves.

Introduction

In recent years, hypogene speleogenesis has arisen as a new paradigm that explains the formation of a substantial amount of karst caves developed in a diversity of geological settings (Klimchouk, 2007, 2009). Growing interest has led to abundant contributions on the matter, presented in several specific conferences on hypogene speleogenesis (Klimchouk & Ford, 2009; Stafford et al., 2009; Otoničar et al., 2013; Klimchouk et al., 2014). The wideness of this research field is really important, embracing different lithologies and well-differentiated geochemical processes (sulfuric acid speleogenesis, cooling of thermal waters, and mixing processes). The complexity of this topic includes terminological issues on the exact meaning of the term "hypogenic", as it is discussed in detail in several references (Palmer, 2007; Mylroie & Mylroie, 2009; Dublyansky, 2014; Klimchouk, 2014).

Within this broad scenario, the references to hypogenic processes in coastal karst areas are very scarce. Thus, Mallorca Island (western Mediterranean) is a convenient place to evaluate and discuss the contribution of deep-seated processes in littoral speleogenesis. Karst caves are abundant all along the island, mainly in its eastern and southern coasts and in a context of eogenetic karstification. The vast majority of these caves show morphological features compatible with a coastal mixing origin, such as spongework caves extensively affected by collapse, documented for example in Ginés & Ginés (2007) and Ginés et al. (2013). Among these numerous caves, a few of them display some features pointing

towards the involvement of hypogenic processes in their formation, as first stated in the case of the extensive cave system of Cova des Pas de Vallgornera (Ginés et al., 2008, 2009). The present paper tries to critically review the role of hypogene speleogenesis in the coastal karstification of the island, on the basis of the up-to-date knowledge on these specific morphogenetic features in some Mallorcan caves.

Abridged Geological Setting

In general terms, Mallorca is built by folded Mesozoic to Middle Miocene rocks that are discordantly covered and flanked by slightly deformed Upper Miocene to Pleistocene sediments. Carbonate rocks are represented almost continuously since the Middle Triassic, and were affected by a compressive and thrusting tectonic phase lasting from the Paleogene to the Middle Miocene (Fornós & Gelabert, 1995; Fornós et al., 2002). Therefore, Mallorcan mountains are the NE continuation of the Alpine Betic thrust and fold belt that configures the southern part of the Iberian Peninsula.

From the physiographical point of view, the island is composed of two more or less parallel mountain ranges (Serra de Tramuntana and Serres de Llevant), along with some small hills in its central part. Graben-like depressed areas are developed on the foreland of these folded ranges, being filled with sediments of Upper Miocene to Quaternary ages. These post-tectonic deposits are disposed around the folded areas, forming a continuous littoral platform that stretches along the southern and eastern coasts of the island, the so-called Migjorn karst region (Figure 1). The litho-stratigraphy of this region is mainly constituted by an Upper Miocene Reef Complex (Late Tortonian-Early Messinian; Fornós et al., 2002), but also are locally present relatively thick Plio-Quaternary rocks (shallow marine to littoral Pliocene sediments and Pleistocene eolianites), which are filling preferentially some areas, like the Campos basin in the southernmost end of the island.

It is worth mentioning the existence of geothermal activity in southern Mallorca, particularly associated with Neogene extensional faults that are responsible for the geometry of the above-mentioned Campos basin. The faults delimitating this graben-type structures permit the hydraulic connection between Mesozoic deep reservoirs and the unconfined aquifers existing in the Upper Miocene and Plio-Quaternary rocks (López & Mateos, 2006; López, 2007). The principal geothermal anomalies occur in the Llucmajor platform (exploitation wells with groundwater temperature near 50ºC) and the Campos basin (Figure 1), where baths located in

Font Santa de Sant Joan and documented since the 15th century exploit hot waters (37ºC).
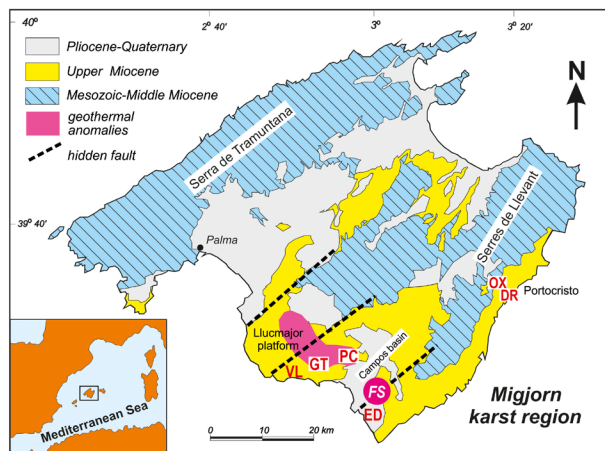

Figure 1.
Simplified geological map of Mallorcan Island with the location of the caves and geographical sites referred in the text.
VL: Cova des Pas de Vallgornera, GT: Cova de sa Guitarreta, PC: Pou de Can Carro,
FS: Font Santa de Sant Joan, ED: Es Dolç,
OX: Cova de s'Ònix, DR: Coves del Drac.

Caves Containing Hypogene Features

The Migjorn karst region is undoubtedly the richest cave area in Mallorca with more than a hundred significant coastal caves, formed principally in Upper Miocene calcarenites by coastal mixing processes (Ginés et al., 2013). From morphological and topographical point of view, they are not strictly "flank margin caves" as described by Mylroie & Carew (1990); in this respect, endokarst phenomena in the Migjorn region include complex and long caves, in which breakdown mechanisms have largely destroyed and masked the initial speleogenetic phases (Ginés & Ginés, 2007). Historical caves like the world-famous Coves del Drac, explored in 1896 by Edouard A. Martel, are located in this region and have greatly contributed to tourism of the island.

Only six caves of the referred area show evidence suggesting the involvement of hypogene speleogenesis on their formation. In any case, there is no evidence of sulfuric acid speleogenesis; but the majority of the considered caves are located in the vicinity of the geothermal anomalies described in the southern half of Mallorca (López, 2007). Basically, the caves can be grouped in three geographical subunits: the Llucmajor platform, the Campos basin, and the eastern coastal fringe near Portocristo village (Figure 1).

Llucmajor Upper Miocene Platform

Within this extensive flat area lies the Cova des Pas de Vallgornera, the most important cave of the Balearic Islands with a development exceeding 78 km (Merino et al., 2014). It is a quite complex coastal cave whose pattern and morphology is strictly controlled by the lithology of the Upper Miocene reefal carbonates that show sharp facies variations both laterally and vertically. Generally speaking, in the seaward part of the cave spongework passages and mazes are dominant together with important breakdown phenomena, corresponding to the very permeable reef front facies (Figure 2); in contrast, joint-guided galleries and conduits are common in the less permeable carbonate rocks of the back reef facies (Ginés et al., 2014).
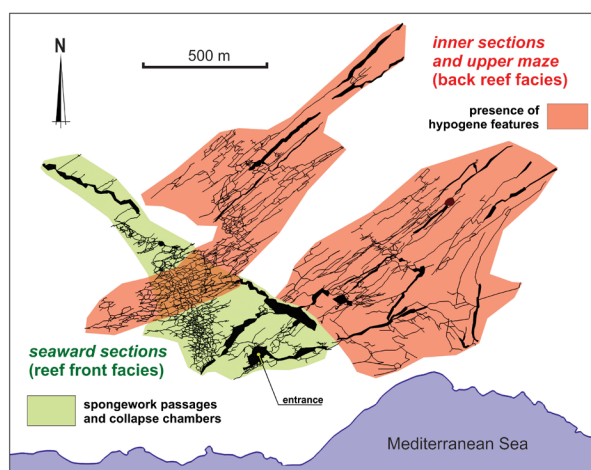
Figure 2.
The lithological control over the pattern of Cova des Pas de Vallgornera.

Particularly in the upper maze and inner passages that form the landward part of Cova des Pas de Vallgornera, features of a possible hypogene origin were first described a few years ago (Ginés et al., 2008), and subsequently documented with more detail in several papers (Ginés et al., 2009; Gràcia et al., 2009; Merino & Fornós, 2010; Fornós et al., 2011; Ginés et al., 2014). These features consist of solutional morphologies of rising flow that include—as the most diagnostic forms—feeder-like vertical or lateral conduits in the floor of the passages (Figure 3A), and very abundant and variegated solutional ascending channels carved in wall and ceilings (Figure 3B and 3C); the width of these rising flow runnels range from a few millimeters to a few decimeters. Frequently, the feeder-like features are present in the form of narrow slots in the floor of some maze areas and galleries. Conspicuous solution alveoli cover extensive areas of the ceilings and overhanging walls, developed owing to the high porosity of the rock (Figure 3B).
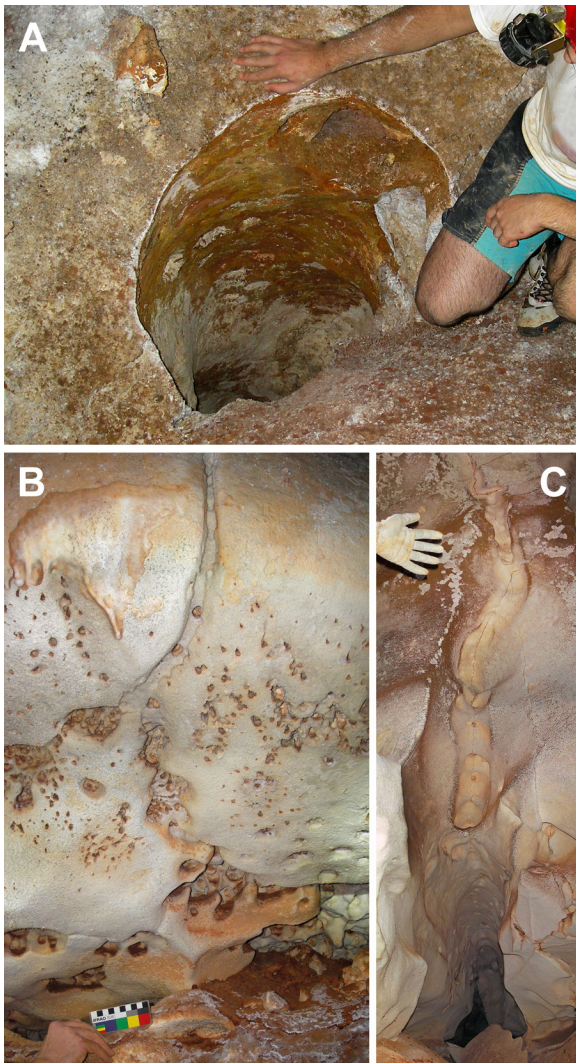
Figure 3.
Hypogene speleogens in Cova des Pas de Vallgornera. (A) feeder-like vertical conduit. (B) anastomosing rising channels and solutional alveoli. (C) ascending channel developed from a lateral feeding point. (Photos: A. Merino).

Crusts and sediments rich in Fe and Mn oxides and hydroxides are present in the landward inner sections of the cave, along with some uncommon mineral deposits (barite, celestine, chamosite, strontianite, nordstrandite, etc.) presumably linked to a deep hypogene recharge (Merino et al., 2009; Onac et al., 2014).

Regarding the genesis of the cave system, three speleogenetic vectors have been invoked: coastal mixing dissolution, a substantial meteoric recharge, and a hypogenic basal recharge (Ginés et al., 2009, 2014). The concurrence of a strongly contrasting geochemistry between the three invoked speleogenetic vectors could

explain the development of this extensive maze cave (Palmer, 2011). Chronologically, the main phases in the formation of Cova des Pas de Vallgornera probably correspond to the Middle Pliocene or even earlier, considering the vertebrate remains recovered inside the cave (Bover et al., 2014).

The hypogene deep recharge, postulated in this case, can be related to the geothermal phenomena documented in the area (López & Mateos, 2006), with groundwater at temperatures exceeding 50ºC near the Llucmajor village. Currently, the abundant phreatic pools in Cova des Pas de Vallgornera do not show temperature anomalies (mean water temperature is 20ºC). However, Cova de sa Guitarreta (Figure 1), a cave that reaches groundwater whose temperature is 27.1ºC (Merino et al., 2011), is in the vicinity. Cova de sa Guitarreta does not show hypogene diagnostic features and consists of a major collapse chamber, probably generated by the dissolution in depth associated to a basal geothermal recharge to the unconfined aquifer.

Campos Plio-Pleistocene Basin

Towards the southeast, the Llucmajor platform connects with the Campos basin, a graben-like slightly subsiding area filled with Plio-Quaternary sediments. In the western flank of the basin there is an interesting cavity known as Pou de Can Carro (Figure 1). It is a rather vertical cave, 45 m in depth, that reaches the water table of the unconfined coastal aquifer (Merino et al., 2011). The temperature of the phreatic waters show a feeble thermal anomaly, with values around 23.6ºC. The lower part of the cave consists of a breakdown chamber developed in Upper Miocene reefal calcarenites, but the upper 15 m of the cave were formed in reddish Pliocene eolianites. This upper section is composed of a nice assemblage of spherical voids and cupolas, 1 to 2 m wide, that are vertically connected all the way to the surface. The cave was excavated along an important fracture by condensation-corrosion processes leading to the particulate disaggregation of the Pliocene eolianites.

The Font Santa de Sant Joan is located in the eastern flank of the Campos basin. The Font Santa de Sant Joan is the only commercial thermal baths in Mallorca, with waters of 37ºC. Located to the south is a recently explored underwater cave called Es Dolç (Figure 1). Es Dolç has a development of more than 4 km (Gràcia et al., 2014) and a rather lineal planimetric pattern, with short extensions scattered along the main passage. The cave discharges brackish waters directly to the sea, having two more collapse entrances located inland in a coastal flat landscape with an elevation less than 15 m.
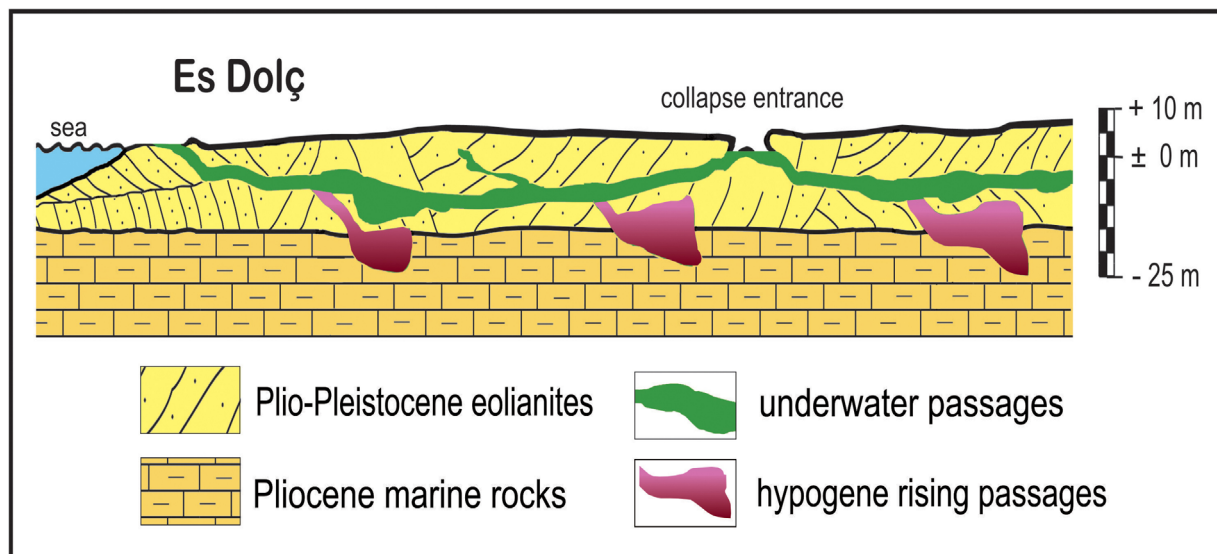
Figure 4.
Schematic profile of Es Dolç cave system showing the lithostratigraphical context of the underwater passages (vertical scale approx. x2; modified from Gràcia et al., 2014).

One of the most interesting aspects of Es Dolç is related to the fact that the cave develops mainly in Plio-Pleistocene eolianites, with its lower passages reaching the underlying Pliocene marine rocks (Gràcia et al., 2014).

Regarding the hypogene speleogens, there are solutional rising features like tiny and sharp ascending dissolution channels (Gràcia & Fornós, 2014), but the most striking morphologies are several ascending passages that begin from the underlying Pliocene rocks and rise until they connect with the main conduit in the Plio-Pleistocene eolianites (Figure 4). Some of these feeder-like features are quite spectacular, as visible in The Crater—a collapse morphology affecting vertical conduits underneath (Figure 5). Apart from the described hypogene imprints, Es Dolç has a noticeable drainage functionality of the littoral brackish aquifer. No thermal anomalies are observed in its phreatic waters, in spite of being relatively close to the Font Santa baths.

Portocristo Upper Miocene Littoral Fringe

The eastern coastal belt in the outskirts of Portocristo village stretches as a narrow fringe of Upper Miocene calcarenites with a maximum width of 3 km. Cova de s'Ònix opens in this area, relatively inland (2 km from the coastline). Its lowermost chambers reach the Jurassic folded basement, where some sea-level controlled pools occur. The cave shows some hypogene related imprints worth mentioning (Merino et al., 2011). Narrow dissolution ascending channels are present in the overhanging walls; on the other hand, this site

is the only place in Mallorca where folia occur in a narrow band located +2.9 m a.s.l. and related to the last interglacial sea level (Tuccimei et al., 2006).

Closer to the coastline opens the internationally renowned show cave of Coves del Drac (Figure 1). This endokarstic phenomenon was previously interpreted as fully representative for the coastal caves along the eastern littoral of Mallorca (Ginés & Ginés, 2007). Recent underwater explorations have extended the development of the cave to more than 6.5 km (Gràcia, 2015, personal communication), with over 4 km of subaqueous passages. There are diving and surveying tasks currently in progress at this site, which have recognized numerous hypogene features in the submerged sections of the cave.

The hypogene speleogens documented in Coves del Drac are mainly solutional rising channels, from a few millimeters to some centimeters in width, carved in the overhanging walls or ceilings of the underwater passages and chambers (Figure 6). Many of these rising channels are really striking because of the contrast between the whitish trajectory of the ascending dissolution runnels and the black-coated walls created by Fe- and Mn-rich crusts (Figure 6B).

This part of the eastern coastal fringe of Mallorca is not associated to current geothermal activity and, moreover, the cave pattern of Coves del Drac is clearly from spongiform to ramiform (Palmer, 2007) without a clear drainage functionality. Regarding its speleogenesis, the
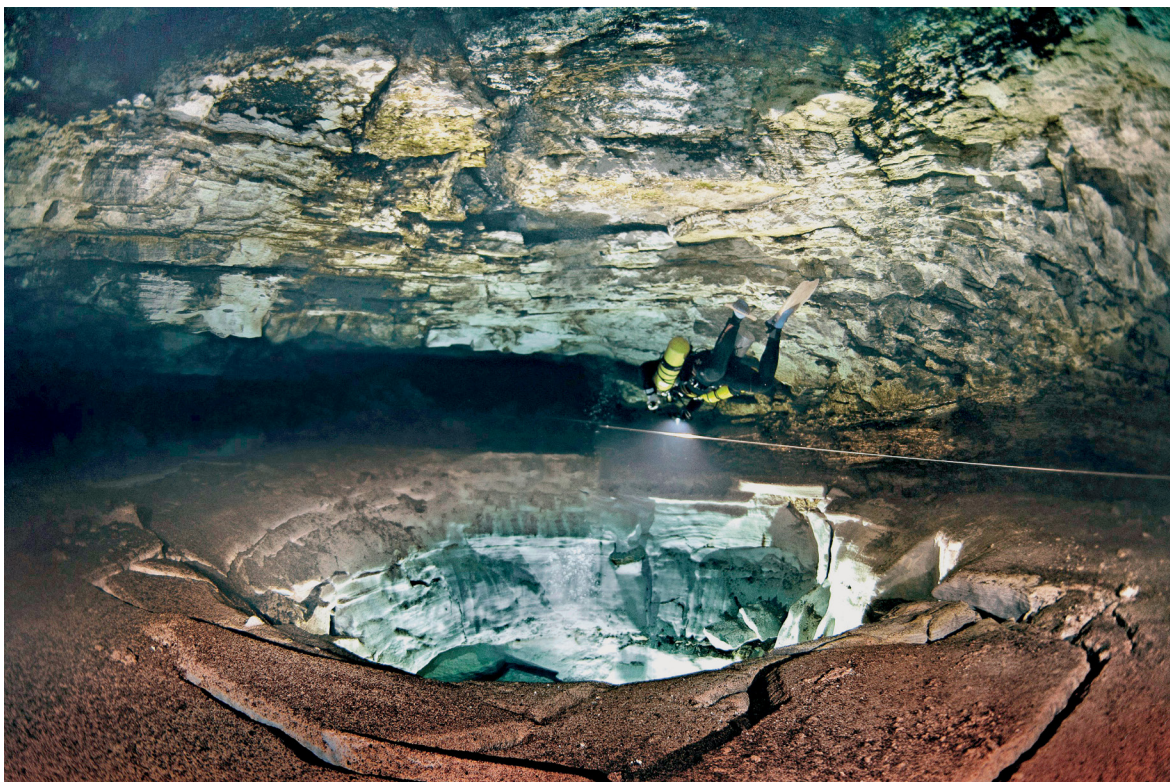
Figure 5.
Passage known as The Crater in the underwater passages of Es Dolç. It is a collapse feature leading to subvertical feeder-like conduits in the Pliocene rocks at its bottom. The ceiling of the gallery corresponds to Plio-Pleistocene eolianites. (Photo: Grup Nord de Mallorca).

hypogene imprints in this cave—although abundant—are not significant in terms of the generated volume of voids; it seems that these imprints are limited to slightly reshaping the walls and ceilings of the passages.

Discussion and Conclusions

Nowadays we think that there is no doubt about the existence of hypogene imprints in some coastal caves of southern and eastern Mallorca. The majority of caves referred in this paper are closely related to the geothermal anomalies documented in the southern half of the island (López & Mateos, 2006; López, 2007). At the current state of knowledge, there is no evidence of sulfuric acid speleogenesis.

Exclusively in the case of Pou de Can Carro, its present-day morphology is mostly conditioned by hypogene speleogens: namely, the spectacular array of condensation-corrosion spherical voids and cupolas that form the upper part of the cave as a result of the weak thermal character of the unconfined aquifer (Merino et al., 2011). In other localities, like Es Dolç and Cova des Pas de Vallgornera, the morphological suite of rising flow (Klimchouk, 2009) is well-represented, being the

ascending channels of diverse dimensions the most diagnostic features (Ginés et al., 2014; Gràcia & Fornós, 2014). Feeder-like vertical to subvertical conduits and/or slots are abundant in the floor of the passages in both caves.

Specifically in Cova des Pas de Vallgornera, there have been reports of uncommon minerals (barite, celestine, chamosite, strontianite, nordstrandite, etc.) that support the contribution of a deep hypogene recharge in the genesis of this extensive speleological system (Merino et al., 2009; Onac et al., 2014). These minerals seem to be associated to Fe- and Mn-rich black crusts or coatings, although such deposits are also present in other underwater coastal caves of the island without reported hypogene features.

The speleogenetic mechanisms probably include at least three different but complementary pathways: coastal mixing, deep hypogene recharge, and a substantial meteoric recharge as evidenced in specific cases (such as Cova des Pas de Vallgornera and Es Dolç). In the eastern littoral fringe near Portocristo, hypogene imprints are evident in two caves (Coves del Drac and

Figure 6.
Solutional ascending channels in the underwater passages of Coves del Drac. (A) narrow channel developed from a subdued wall pocket (Photo: A. Cirer). (B) Rising channels carved on the walls and ceiling contrast with the Mn- and Fe-rich black coatings (width of the image: 1 m. Photo: F. Gràcia).

Cova de s'Ònix), but it is not clear if this particular speleogenetic vector can be generalized to the coastal caves of the area or are exclusively minor and local morphological retouches of limited relevance. In this specific geographical unit, the association to geothermal phenomena does not exist today, but the recharge from the underlying Jurassic folded basement is a fact.

Regarding chronological issues, these hypogene speleogenetic phases have occurred from the Middle Pliocene, as documented by the paleontological remains in Cova des Pas de Vallgornera (Bover et al., 2014), to Pleistocene times, as it occurs in Es Dolç, whose passages are mainly developed in recent eolianites (Gràcia et al., 2014).

Finally, the incidence of the lithological variability of the involved eogenetic rocks is highly remarkable. This introduces additional complexity to the coastal karstification, affecting both the hydrological behavior of the littoral aquifers and the planimetric pattern of the caves formed in this particular setting.

Acknowledgements

References

Bover P, Valenzuela A, Guerra C, Rofes J, Alcover JA, Ginés J, Fornós JJ, Cuenca-Bescós G, Merino A. 2014. The Cova des Pas de Vallgornera (Llucmajor, Mallorca): a singular deposit bearing an exceptional well preserved Early Pleistocene vertebrate fauna. International Journal of Speleology 43 (2): 175-192. http://dx.doi.org/10.5038/1827-806X.43.2.6

Dublyansky YV. 2014. Hypogene speleogenesis - discussion of definitions. In: Klimchouk AB, Sasowsky I, Mylroie JE, Engel SA, Engel AS, editors. Hypogene cave morphologies. Leesburg (VA): Karst Waters Institute. Special Publication 18. p. 1-3.

Fornós JJ, Gelabert B. 1995. Lithology and tectonics of the Majorcan karst. In: Ginés A, Ginés J, editors. Karst and caves in Mallorca. Palma de Mallorca, Spain: Endins 20 / Monografies de la Societat d'Història Natural de les Balears 3. p. 27-43.

Fornós JJ, Merino A, Ginés J, Ginés A, Gràcia F. 2011. Solutional features and cave deposits related to hypogene speleogenetic processes in a littoral cave of Mallorca Island (western Mediterranean). Carbonates and Evaporites 26 (1): 69-81. http://dx.doi.org/10.1007/s13146-010-0040-3

Fornós JJ, Pomar L, Ramos-Guerrero E. 2002. Balearic Islands. In: Gibbons W, Moreno T, editors. The Geology of Spain. London (GB): The Geological Society. p. 327-334.

Ginés A, Ginés J. 2007. Eogenetic karst, glacioeustatic cave pools and anchialine environments on Mallorca Island: a discussion of coastal speleogenesis. International Journal of Speleology 36 (2): 57-67. http://dx.doi.org/10.5038/1827-806X.36.2.1

Ginés A, Ginés J, Gràcia F. 2013. Cave development and patterns of caves and cave systems in the eogenetic coastal karst of southern Mallorca (Balearic Islands, Spain). In: Lace MJ, Mylroie JE, editors. Coastal karst landforms. Dordrecht (DE): Springer. Coastal Research Library vol 5. p. 245-260. http://dx.doi.org/10.1007/978-94-007-5016-6_11

Ginés J, Fornós JJ, Ginés A, Merino A, Gràcia F. 2014. Geologic constraints and speleogenesis of Cova des Pas de Vallgornera, a complex coastal cave from Mallorca Island (Western Mediterranean). International Journal of Speleology 43 (2): 105-124. http://dx.doi.org/10.5038/1827-806X.43.2.2

Ginés J, Ginés A, Fornós JJ, Gràcia F, Merino A. 2008. Noves observacions sobre l'espeleogènesi en el Migjorn de Mallorca: els condicionants litològics en alguns grans sistemes subterranis litorals. Endins 32: 49-79.

Ginés J, Ginés A, Fornós JJ, Merino A, Gràcia F. 2009. On the role of hypogene speleogenesis in shaping the coastal endokarst of southern Mallorca (Western Mediterranean). In: Klimchouk AB, Ford DC, editors. Hypogene speleogenesis and karst hydrogeology of artesian basins. Simferopol (UA): Ukrainian Institute of Speleology and Karstology. Special Paper 1. p. 91-99.

Gràcia F, Fornós JJ. 2014. Les morfologies de dissolució hipogèniques i de la zona de mescla litoral a Es Dolç (Colònia de Sant Jordi, Ses Salines, Mallorca). Endins 36: 97-112.

Gràcia F, Fornós JJ, Gamundí P, Clamor B, Pocoví J. 2009. Morfologies de corrosió a la part submergida de la Cova des Pas de Vallgornera. Sector Antic, sector de Gregal i sector de les Grans Sales. Endins 33: 73-98.

Gràcia F, Clamor B, Gamundí P, Cirer A, Fernández JF, Fornós JJ, Ginés A, Ginés J, Uriz MJ, Munar S, Vicens D, Ginard A, Betton N, Vives MA, Jaume D, Mas G, Perelló MA, Cardona F, Timar-Gabor A. 2014. Es Dolç (Colònia de Sant Jordi, ses Salines, Mallorca). Cavitat litoral amb influències hipogèniques excavada a les eolianites quaternàries i als materials del Pliocè. Endins 36: 69-96. Palma de Mallorca.

Klimchouk AB. 2007. Hypogene speleogenesis: hydrogeological and morphogenetic perspectives. Carlsbad (NM): National Cave and Karst Research Institute. Special Paper 1. 106 p.

Klimchouk AB. 2009. Morphogenesis of hypogenic caves. Geomorphology 106: 100-117. http://dx.doi.org/10.1016/j.geomorph.2008.09.013

Klimchouk AB. 2014. The methodological strength of the hydrogeological approach to distinguishing hypogene speleogenesis. In: Klimchouk AB, Sasowsky I, Mylroie JE, Engel SA, Engel AS, editors. Hypogene cave morphologies. Leesburg (VA): Karst Waters Institute. Special Publication 18. p. 4-12.

Klimchouk AB, Ford DC, editors. 2009. Hypogene speleogenesis and karst hydrogeology of artesian basins. Conference Proceedings; Chernivtsi, Ukraine: Ukrainian Institute of Speleology and Karstology, Special Paper 1. 292 p.

Klimchouk AB, Sasowsky I., Mylroie JE, Engel SA, Engel AS, editors. 2014. Hypogene cave morphologies. Conference Proceedings; San Salvador Island, Bahamas: Karst Waters Institute, Special Publication 18. 103 p.

López JM. 2007. Las manifestaciones hidrotermales del sur de Llucmajor, Mallorca [research report]. Palma de Mallorca, Spain: Departament de Ciències de la Terra, Universitat de les Illes Balears. 132 p.

López JM, Mateos RM. 2006. Control estructural de las anomalías geotérmicas y la intrusión marina en la plataforma de Llucmajor y la cubeta de Campos (Mallorca). Las aguas subterráneas en los países mediterráneos. Instituto Geológico y Minero de España, Madrid. Serie Hidrogeología y Aguas Subterráneas 17: 607-613.

Merino A, Fornós JJ. 2010, Los conjuntos morfológicos de flujo ascendente (morphologic suite of rising flow) en la Cova des Pas de Vallgornera (Llucmajor, Mallorca). Endins 34: 85-100.

Merino A, Fornós JJ, Onac BP. 2009. Preliminary data on mineralogical aspects of cave rims and vents in Cova des Pas de Vallgornera, Mallorca. In: White WB, editor. Proceedings 15th International Congress of Speleology; Kerrville (TX): National Speleological Society. Vol 1. p. 307-311.

Merino A, Ginés J, Fornós JJ. 2011. Evidències morfològiques de processos hipogènics a cavitats de Mallorca. In: Gràcia F, Ginés J, Pons GX, Ginard A, Vicens D, editors. El carst: patrimoni natural de les Illes Balears. Palma de Mallorca, Spain: Endins 35 / Monografies de la Societat d'Història Natural de les Balears 17. p. 165-182.

Merino A, Mulet A, Mulet G, Croix A, Kristofersson A, Gràcia F, Perelló MA. 2014. Cova des Pas de Vallgornera, (Mallorca, Spain): history of exploration and cave description. International Journal of Speleology 43 (2): 95-104. http://dx.doi.org/10.5038/1827-806X.43.2.1

Mylroie JE, Carew JL. 1990. The flank margin model for dissolution cave development in carbonate platforms. Earth Surface Processes and Landforms 15: 413-424. http://dx.doi.org/10.1002/esp.3290150505

Mylroie JE, Mylroie JR. 2009. Diagnostic features of hypogenic karst: is confined flow necessary? In: Stafford KW, Land L, Veni G, editors. Advances in hypogene karst studies. Carlsbad (NM): National Cave and Karst Research Institute Symposium 1. p. 12–26.

Onac BP, Fornós JJ, Merino A, Ginés J, Diehl J. 2014. Linking mineral deposits to speleogenetic processes in Cova des Pas de Vallgornera (Mallorca, Spain). International Journal of Speleology 43 (2): 143-157. http://dx.doi.org/10.5038/1827-806X.43.2.4

Otoničar B, Gostinčar P, Gabrovšek F, editors. 2013. Hypogene speleogenesis (between theory and reality...). 21st International Karstological School "Classical Karst", Guide Book & Abstracts; Postojna (SI): Karst Research Institut ZRC SAZU. 98 p.

Palmer AN. 2007. Cave geology. Dayton (OH): Cave Books. 454 p.

Palmer AN. 2011. Distinction between epigenic and hypogenic maze caves. Geomorphology 134 (1): 9-22. http://dx.doi.org/10.1016/j.geomorph.2011.03.014

Stafford KW, Land L, Veni G, editors. 2009. Advances in hypogene karst studies. NCKRI Simposium 1; Carlsbad (NM): National Cave and Karst Research Institute. 182 p.

Tuccimei P, Ginés J, Delitala C, Ginés A, Gràcia F, Fornós JJ, Taddeucci A. 2006. Last interglacial sea level changes in Mallorca island (Western Mediterranean). High precision U-series data from phreatic overgrowths on speleothems. Zeitschrift für Geomorphologie 50 (1): 1-21.

HYPOGENIC SPELEOGENSIS AND PETROLEUM

HYPOGENE KARST ASSOCIATED WITH PETROLEUM RESOURCES IN PECOS COUNTY, TEXAS

Kevin W. Stafford
Stephen F. Austin State University
Department of Geology
P.O. Box 13011, SFA Station
Nacogdoches, TX 75962-3011, staffordk@sfasu.edu

Melinda S. Faulkner
Stephen F. Austin State University
Department of Geology
P.O. Box 13011, SFA Station
Nacogdoches, TX 75962-3011, mgshaw@sfasu.edu

Abstract
Pecos County is located in the Trans-Pecos region of west Texas and comprises the transition from the Central Basin Platform (CBP) to the Sheffield Channel. The climate is semi-arid and most surface streams are ephemeral, with the Pecos River providing the only perennial source of water other than isolated karst springs found throughout the county. The region is the southern extension of the Permian Basin and is well-known for hydrocarbon production. The Yates Field, positioned at the southeastern tip of the CBP in eastern Pecos County, and several small oil fields, scattered along the southern margin of the CBP throughout central Pecos County, attest to widespread petroleum resources in the area.

Known cave and karst features are relatively sparse throughout the region; however, those that are known commonly exhibit morphological features consistent with hypogene speleogenetic origins. Many of the caves contain secondary minerals that further support hypogene speleogenesis coupled with migration of light hydrocarbons ascending vertically through strata. While isolated hypogene karst features are not uncommon throughout the Trans-Pecos region, the best evidence of hypogene speleogenesis coupled with petroleum resources comes from studies of the Yates Field, a karstic petroleum reservoir, and studies of Amazing Maze Cave (a multi-story maze cave).

Yates Field has been known as a karstic petroleum reservoir since the early twentieth century when early drilling operations commonly encountered bit drops and developed wells exhibited sustained high flow rates. Early models for describing the karst of the Yates Field suggested that porosity represented eogenetic paleokarst

formed by syndepositional subaerial exposure. In the last decade, recent advances in speleogenetic theories have led to the reinterpretation of the Yates Field porosity as having formed by hypogene processes within Guadalupian strata of the San Andres, Grayburg, Queen, and Seven Rivers formations. Evidence for hypogene porosity origins include: (1) spatial distribution of karst based petrophysical log analyses; (2) zones of vertical brecciation with associated uranium enrichment; and (3) secondary mineralization including native sulfur, sulfide minerals, and diagenetic albite. The spatial distribution of karst porosity suggests that the proximal Pecos River, which has been at its current location since the early Cenozoic, provided the potentiometric driver for the forced convection component that drove hypogene dissolution within Guadalupian carbonates of the Yates Field. Free convection was enhanced by slightly elevated geothermal gradients associated with Basin and Range extension.

Amazing Maze Cave (AMC) was developed in Cretaceous carbonates of the Fort Terrett Formation of the Fredericksburg Group. This multi-story maze cave is positioned over the southern margin of the CBP and is underlain proximally by hydrocarbon reservoirs of the Taylor Link, Walker, and White Baker oil fields that produce from Guadalupian strata similar to that of the Yates Field. AMC is a rectilinear maze cave formed across at least four distinct stratigraphic horizons and includes more than seven kilometers of mapped passages. Morphometric features associated with rising fluids are common throughout the cave, as well as extensive deposits of secondary gypsum. Additional secondary minerals—including alunite, natroalunite, carnotite, and native sulfur—support speleogenetic origins associated with sulfuric acid-rich fluids, while

sulfur isotope analyses supports speleogenetic models similar to those proposed for the well-documented hypogene caves of the Guadalupe Mountains.

Karst porosity of the Yates Field and AMC both represent hypogene karst features that have been intercepted by anthropogenic processes. Vertical seepage of hydrocarbons into the Pecos River fueled the initial development of the Yates Field, which ultimately led to widespread documentation of karst porosity in associated Guadalupian carbonates. Similarly AMC was an incidental discovery as construction of Interstate 10 in 1970s intercepted the main level of the maze cave during road construction. Both of these hypogene systems did not have natural entrances prior to anthropogenic activity; therefore, it is probable that hypogene processes are far more common within the region but their discoveries await additional incidental breaching events.

THE POTENTIAL ROLE OF HYPOGENE SPELEOGENESIS IN THE LOWER FLORIDAN AQUIFER AND SUNNILAND OIL TREND, SOUTH FLORIDA, USA

Thomas A. Herbert

Lampl Herbert Consultants, Inc.
P.O. Box 10129
Tallahassee, Florida 32302-2129, taherbert@lampl-herbert.com

Sam B. Upchurch

SDII Global Corporation
4509 George Road
Tampa, Florida 33634, flwaterdoc@gmail.com

Abstract

The South Florida Basin is a deeply subsiding basin in the southern third of the Florida peninsula. This basin includes strata of Jurassic to Quaternary age. The Sunniland Trend is a more-or-less linear trend of oil-producing strata of Cretaceous (Aptian) age. The oil is produced from rudistid shoal mounds or knolls developed on a flexure that extends in a southeast direction from Lee to Dade counties.

Similarly, the lower Floridan aquifer, which is within Paleogene sediments in southern Florida, contains highly permeable zones ("boulder zones") that are currently utilized for subsurface wastewater disposal.

Both systems stratigraphically fit Klimchouk's model for evaporite-bounded circulation systems with breccias, conduits, and other evidence of speleogenesis.

This paper describes these two systems and the evidence for hypogene speleogenesis that currently exists. Finally, it suggests that consideration of conduit systems developed by sulfuric-acid-related hypogenesis may enable better petroleum exploration and waste disposal models.

Introduction

A fortuitous combination of karst-like conditions in the Cretaceous and Paleogene strata of southwestern Florida has rendered oil development of the Sunniland Trend, a series of small, but highly productive, oil fields in southwest Florida feasible with minimal disposal costs for brine waters produced with the oil. The oil is recovered from the Cretaceous (Aptian) Sunniland Formation along a trend (Figure 1) of rudistid knolls and breccia deposits at an average depth of 3,500 m (11,500 ft.) below sea level. In spite of the small aerial extent

of these knolls, these isolated plays have consistently produced oil with wells remaining productive for decades. Recognition of the potential for stratigraphic trap development associated with hypogenesis may increase interest in this mature trend.
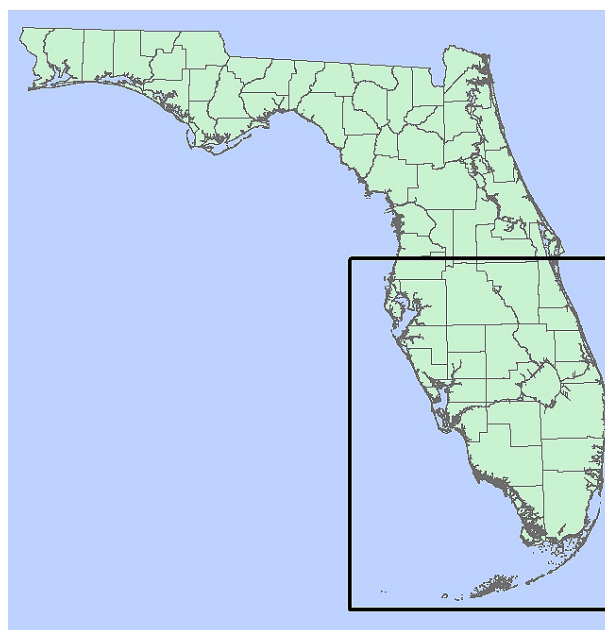
Figure 1.
Location of the Sunniland Trend and the "boulder zone" in southwest Florida. Extent of the "boulder zone" from Miller (1990).

Disposal of the brine separated from the petroleum fluids is a major cost item for most oil fields, but in south Florida an injection zone that is well confined and below the underground source of drinking water provides efficient and cost-effective disposal. Brine injection is into saline water within the lower Floridan aquifer,

Table 1.

Hydrostratigraphic relationships of the lower Floridan aquifer system and Sunniland Formation in southern Florida. Both horizons (shaded cells) have probably been subjected to hypogene karst processes. Data sources: Miller, 1986; Huddlestun et al., 1988; Pollastro et al., 2001; and others.

Epoch	Formation		Lithology	Hydro-stratigraphic Unit	Unit Thickness (meters)
Holocene	Undifferentiated		Quartz sand, silt, clay, shell	Surficial aquifer system	0 - 100
Pliocene	Tamiami Formation		Silt, sandy clay, shell, limestone		0 - 30
Miocene to Late Oligocene	Hawthorn Group	Peace River Formation	Interbedded sand, silt, gravel, clay, limestone, dolostone, phosphatic sand	Intermediate aquifer and confining unit	180 - 275
		Arcadia Formation	Sandy limestone, shell beds, dolostone, phosphatic sand, silt, clay		
Early Oligocene	Suwannee Limestone		Limestone	Upper Floridan aquifer	210 - 370
Late Eocene	Ocala Limestone		Limestone		
Middle Eocene	Avon Park Formation		Limestone, dolostone		150 - 240
			Dolostone, gypsum/anhydrite	Middle confining unit	
Early Eocene	Oldsmar Formation		Dolostone, gypsum/anhydrite	Lower Floridan aquifer	430 - 550 Incl. Boulder Zone (120±)
Paleocene	Cedar Keys Formation		Dolostone, dolomitic limestone		
			Massive anhydrite	Sub-Floridan confining unit	370±
Albian through Maastrichtian	Pine Key Formation		Limestone and dolostone		835±
	Naples Bay Group		Alternating layers of limestone, dolostone, anhydrite	Possible hypogenic karst systems	760±
	Big Cypress Group				
Aptian	Ocean Reef Group	Rattlesnake Hammock Fm.			
		Lake Trafford Fm.	Upper: Limestone, dolostone; lower: anhydrite	Upper confining beds	45±
		Sunniland Fm.	Limestone, anhydrite	Proposed hypogene karst system	75 - 85
	Glades Group	Punta Gorda Anhydrite	Anhydrite	Lower confining beds	245±
		Lehigh Acres Formation	Dolostone, shale	Poss. hypogene karst systems	195±
Additional Cretaceous and Jurassic strata underlie the Glades Group sediments.					

notably a series of horizons in Paleocene and lower Eocene strata known as the "boulder zone." Injection is efficient and driven by gravity. This horizon also appears to be a result of hypogenetic karst processes.

Both the production zones in the Cretaceous strata and the brine injection zones in the "boulder zone" lie in strata that physically correspond with the conditions suggested by Klimchouk (2007, 2009) for sulfuric-acid-related hypogene speleogenesis. In this paper, we briefly describe the geological conditions in the production and injection zones and the basis for our conceptualization of the porosity networks in each as hypogene conduits. We begin with a description of the lower Cretaceous Sunniland Trend and conclude with a description of the "boulder zones" that occurs in Paleogene strata.
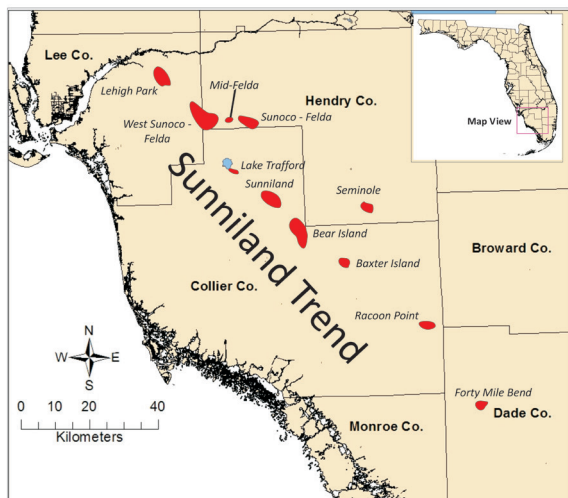
Figure 2.
Location of oil fields within the Sunniland Trend in southwest Florida.

The Lower Cretaceous Sunniland Formation

Location and Oil Production

The Sunniland Trend (Figure 1) is located in southwest Florida. The 11 individual fields (Figure 2) occur in a northwest-southeast linear trend that corresponds with a series of rudistid knolls (Mitchell-Tapping and Mitchell-Tapping, 2003) that have developed along a hinge line in the south Florida Basin. Southwest of the Trend, lower Cretaceous strata dip to the southwest.

Production in the Sunniland Trend began in the early 1940s from the upper part of the Sunniland Formation, a porous, early Cretaceous limestone with abundant rudistid fragments and breccia. Peak production was reached in the mid-1970s at 2.40×10^6 L (17,000 barrels day^{-1}). As of 2014, 1.9×10^{10} L (1.2×10^8 barrels, bbls) have been produced with the most productive wells yielding 6×10^8 L (4×10^6 bbls) each, and 40 wells have produced $>1.6 \times 10^8$ L ($>1 \times 10^6$ bbls) each.

Stratigraphy

Within the Sunniland Trend, the Sunniland Formation is at about 3,500 m (11,500 ft.) below sea level. It is underlain by the Lower Cretaceous Punta Gorda Formation (Tables 1 and 2), a massive limestone and anhydrite formation that serves as a lower confining unit for the Sunniland Formation and, probably, the circulation system that we believe created a hypogene karst system in the overlying Sunniland Formation. The reservoir seal across the Trend is the Lake Trafford Formation, a similar massive sequence of anhydrite and dense limestone.

The Sunniland Formation is up to 75 m (250 ft.) in thickness (Huddlestun et al., 1988). The unit has been subdivided into five informal stratigraphic units (Table 2; Applegate and Pontego, 1984; Mitchell-Tapping and Mitchell-Tapping, 2003). It is within these five facies that we believe hypogenic speleogenesis has significantly enhanced formation porosity and hydraulic conductivity.

The basal unit (Mitchell-Tapping and Mitchell-Tapping, 2003; Unit 5) consists of two major transgressive marine lithosomes. The lower basal facies is a fossiliferous limestone with abundant fractures and breccia zones. This horizon, locally known as the "rubble zone", is petroliferous. The Lake Trafford Field (Figure 2), a one-well field, has produced commercial oil quantities from this facies.

The second facies of Unit 5, which overlies the "rubble zone", is informally known as the "black shale." This unit is not shale; rather it is a dense, argillaceous "black limestone" with abundant organics. Because of its significant organic content and geochemical arguments (Applegate and Pontigo, 1984; Palacas, 1978a, 1978b; Palacas et al., 1981, 1984), this limestone unit is thought to constitute the source strata for the Sunniland oil fields, either within or adjacent to the Trend. The black limestone facies appears to coincide with a worldwide anoxic event in the Cretaceous sea, a source for prolific fields in carbonate units fringing the Gulf.

Unit 4, which overlies Unit 5 (Table 2), is a low porosity limestone to dolomitic limestone. This unit may serve as a semi-confining unit for fluid migration.

Unit 3 (Table 2) is a shallow, intertidal limestone (Mitchell-Tapping and Mitchell-Tapping, 2003) that has produced oil in one field. Mitchell-Tapping and Mitchell-Tapping (2003) reported evidence of hypersaline solutions associated with "phreatic" conditions in this facies. We interpret the "phreatic conditions" to represent evidence of dissolution and brecciation.

Unit 2 (Table 1) is a fragmental, intertidal limestone with abundant rudistid "debris mounds" (Mitchell-Tapping, 1987; Mitchell-Tapping and Mitchell-Tapping, 2003). Mitchell-Tapping and Mitchell-Tapping (2003) also reported evidence of phreatic conditions in this facies of the Sunniland. Unit 2 is a major oil-production zone in the West-Felda Field (Figure 2).

Finally, Unit 1, the primary oil producer in the Sunniland Trend, is a fossiliferous limestone deposited

Table 2.

Stratigraphic relationships of lithosomes within the Sunniland Formation (Lower Cretaceous) of southwest Florida. Descriptions modified from Applegate and Pontigo (1984) and Mitchell-Tapping and Mitchell-Tapping (2003).

Formation	Facies[1]	Lithology	Average Thickness (meters)	Function
Lake Trafford Formation		Limestone, anhydrite	46	**Upper confining unit**
Sunniland Formation	1	Molluscan limestone with anhydrite blebs in upper-most part, partly oolitic, bioturbated; regressive phase deposition	25	Primary oil production zone
	2	Intertidal limestone with rudistid fragments forming debris mounds	20	Phreatic environment with subaerial "leaching" near end of deposition (Mitchell-Tapping and Mitchell-Tapping, 2003); **primary oil production zone** in West-Felda field
	3	Shallow, intertidal limestone	10	According to Mitchell-Tapping & Mitchell-Tapping (2003) phreatic and hypersaline conditions existed near end of deposition; **primary oil production zone** in the Felda fields
	4	Light brown to cream limestone, occasionally dolomitic	15	Low porosity, low permeability; possible confining stratum
	5	Dense, argillaceous lime-stone; dark colored; "organically rich"	12	Considered a **possible source rock** for Sunniland oil
		Fossiliferous, transgressive limestone; fractured with common breccia masses; petroliferous odors common	15	Production in the Lake Trafford Field; termed the "**Rubble Zone**" because of fractures and rubble encountered during drilling; possible source rock for Sunniland oil
Punta Gorda Formation		Massive anhydrite with salt stringers	180 - 250	**Lower confining unit**
[1] Facies from Mitchell-Tapping and Mitchell-Tapping, 2003				

under marine regression conditions according to Mitchell-Tapping and Mitchell-Tapping (2003). The facies shows evidence of bioturbation and deposition of secondary anhydrite.

The unit that overlies the Sunniland Formation is the Lake Trafford Formation (Table 2), a massive limestone and anhydrite stratum that serves to confine the stratigraphic traps in Units 1 and 2 of the Sunniland Formation.

Petroleum Sources and Maturity

The petroleum from the Sunniland has been studied extensively. As noted above, the source of the petroleum is thought to be either local or down-dip southwest of the trend, and from within hydrocarbon-rich limestone (Palacas, 1978a, b; Palacus et al., 1984; Palacas et al., 1987). Applegate and Pontego (1984) also thought that the source of the petroleum was local. They characterized the petroleum from the Sunniland as "moderately immature" to "moderately mature."

Thermal maturity increases with depth, as does the total organic carbon content. Palacas (1978) noted that the average organic content was 0.41 percent. Clearly, there is ample carbon to serve as an energy source for microbial transformation of sulfur compounds and petroleum.

There is an issue with the maturity of the petroleum that may point to an efficient conduit system for petroleum migration. Mitchell-Tapping (2002) argued that the oil is too mature for the current bottom-hole temperatures in Sunniland wells. He noted that the bottom-hole temperatures are less than the published minimum temperatures for hydrocarbon generation. Griffin et al. (1977) studied the heat flow from three deep oil test wells in south Florida and found that the geothermal gradient was low, which would limit thermal maturation. In addition, the average organic carbon content is at, or near, the threshold for hydrocarbon production (Dowdle and Cobb, 1975).

Palacas et al. (1984, p. 477) noted that lower Cretaceous limestone in the eastern Gulf of Mexico had staining and residual asphalt that appeared to represent a "post-migration alteration product of a mature oil that has migrated from source rocks deeper in the section, or from stratigraphically equivalent … [strata]…down-dip…." The petroleum was found to be compositionally similar to the Sunniland petroleum.

If the maturity and organic-carbon content constraints are valid, there appears to be an unaccounted for petroleum-migration path operative in the Sunniland Trend oil fields.

Exploration Strategies and Possible Hypogene Speleogenesis

Exploration Strategies
Based on these stratigraphic relationships, the Sunniland Formation is considered by many to be a "self-sourcing" oil-bearing formation. Unit 5, especially the hydrocarbon-rich carbonate unit, is considered to be the petroleum source, and stratigraphic closures in units 1 through 3 form the traps. Data presented by Mitchell-Tapping (2002) and Palacus et al. (1984) suggest that the source rocks down dip from the Sunniland fields may be the hydrocarbon source.

Current exploration models search for low-relief structural traps seen on seismic data based on closure in the upper units along a hinge or fold within the regional Cretaceous strata of the South Florida Basin. This strategy is largely based on the stratigraphic

model developed by Mitchell-Tapping (1987) and Mitchell-Tapping and Mitchell-Tapping (2003). Thus, the exploration targets are structural traps developed in small "knolls" formed by accumulations of fragmented rudistid limestone on a regional hinge line. To our knowledge, no attempt has been made to develop exploration models based on stratigraphic traps associated with conduit networks or hydrocarbon migration mechanisms offered in a model relying on hypogene speleogenesis.

Evidence Suggestive of Hypogene Speleogenesis
As noted by the production figures presented above, the amount of recoverable oil and ease of extraction seem high relative to the size and distribution of the fields within the Sunniland Trend, particularly from low-relief structural features.

Detailed examination of the production and distribution of wells within the fields suggests that some form of conduit flow and secondary stratigraphic trap development exists. Within fields in the Trend, closely spaced wells result in a pattern of highly variable production with wells that have produced 10^8 L of oil in close proximity to dry or low-recovery wells. Within the fields, intervals of no core recovery or weight-of-drill string gaps are commonly described in drilling logs. This information combined with the concerns about source strata and geothermal temperatures suggest a more complicated system than has previously been described. Simply considering the entrained fluids as a karst-facilitated circulation system rather than connate water may account for the lower than expected geothermal gradient.

Improvements in 3-D seismic imaging and processing may provide the impetus for continued development of combination structural/stratigraphic plays in the Trend. From a commercial standpoint, the Sunniland may yield significantly more oil with detailed seismic evaluation (Applegate, 1991).

The stratigraphy associated with the Sunniland Formation is consistent with the conditions proposed by Klimchouk (2007, 2009) for hypogene speleogenesis. The formation is confined above and below by anhydrite. There is evidence of fluid movement within the formation with the petroleum categorized as "sour crude." Produced formation water releases an odor of H_2S upon degassing in the oil-water separator. The reports of widespread breccias and "phreatic conditions" (Mitchell-Tapping and Mitchell-Tapping, 2003) suggest the possibility of sulfuric-acid-related speleogenesis.

Abundant brecciated horizons in Units 1, 2, and 5 are consistent with collapse as hypogene conduiting developed. The Unit 1 and 2 breccias may be syndepositional rather than speleogenetic, but reports of evidence of "phreatic conditions" may also suggest dissolution in a hypogene system. Alternatively, syndepositional brecciation may have facilitated later speleogenetic enhancement of the breccias and conduits.

Also, the Sunniland Trend is but a small look-alike subset of a series of Albian/Aptian (Cretaceous) oil fields that surround the Gulf of Mexico (Carrasco-V, 2003), including several giant fields. Moore (2001), for example, discusses the historic Golden Lane oil fields of northeastern Mexico, including the breccias within which much oil was recovered. While to our knowledge no one has attributed these fields to hypogene speleogenesis, they, too, have stratigraphic relationships that compare favorably with Klimchouk's criteria. The mid-Cretaceous anoxic event appears to correlate across the Gulf of Mexico region as the carbon source.

Finally, Paull and Dillon (1980), Paull and Neumann (1987), Commau et al. (1987), Chanton et al. (1993), Robb (1990), and Hine (1997) discuss brine seeps near the base of the continental slope off Florida in both the Atlantic Ocean and Gulf of Mexico. The seeps offshore of southwestern Florida are at about 3,270 m (10,700 ft.) below sea level and are in Cretaceous limestone. They are characterized by relatively cool water. These seeps appear to occur at the same stratigraphic position as the Sunniland. According to these authors, the seeps appear to be locations of developing karst as a result of dissolution, causing sapping at the base of the continental margin.

Chanton et al. (1993) characterized limestone dissolution at the seeps as being a result of mixing seawater and sulfate-depleted brine derived from the Cretaceous sediments. Two sulfide sources were suggested to explain the isotopic compositions of sedimentary pyrite at the seeps. These are (1) a ^{34}S-enriched source derived from the Florida platform and (2) a ^{34}S-depleted component derived from microbial reduction of seawater sulfate. As a result of these microbial-driven reactions, the seeps support populations of chemotrophic organisms.

In summary, there is evidence of sulfur-driven geochemical reactions in pore or conduit waters within the Cretaceous sediments in the vicinity of the Sunniland Trend. This—combined with stratigraphic sequencing of anhydrite and fractured limestone strata consistent with Klimchouk's model, evidence of collapse and

brecciation, and a distribution of oil production suggestive of large conduits—suggests that hypogene speleogenesis may be responsible for development of the "plumbing" system that has resulted in migration of oil into the structures forming the Sunniland fields.

The Paleogene Lower Floridan Aquifer

The Lower Floridan aquifer occurs within the Floridan aquifer system, a major regional aquifer in Florida. By definition, the Lower Floridan aquifer occurs where regional confining units consisting of gypsum and anhydrite form effective aquitards that isolate the aquifer from the overlying and underlying strata (Southeastern Geological Society, 1986). In the South Florida Basin, the Lower Floridan aquifer is deeply buried and groundwater is generally saline.

Stratigraphic Relationships

The lower confining unit of the Lower Floridan aquifer (Table 1) consists of either (1) glauconitic, calcareous, argillaceous to arenaceous strata that range in age from late Eocene to late Paleocene or (2) massively bedded anhydrite in the lower Paleocene strata (Miller, 1986; Southeastern Geological Society, 1986).

The upper confining unit of the Lower Floridan aquifer (Table 2), the "middle confining unit" of the Floridan aquifer system, consists of fine-grained dolostone and limestone with significant interstitial gypsum and anhydrite. This unit includes part of the lower Avon Park and Oldsmar formations of Eocene age. The gypsum and anhydrite lower the bulk permeabilities of these horizons. Stewart (1966) and Navoy (1986) concluded that the evaporite minerals were primary and that they were present at the time of carbonate deposition. They also noted some fracture and fossil filling by evaporite minerals. Stewart (1966) and Navoy (1986) also observed that evaporite nodules have central cores of anhydrite and rims of gypsum. According to Hickey (1990), evaporite inclusions constituted about 10 to 30 percent of the host rock in central Florida. Hickey (1981, 1982, 1990) and Navoy (1986) concluded that the evaporite-rich strata are not laterally continuous.

Porosity in the Lower Floridan Aquifer

The dolostone within the Lower Floridan aquifer is fractured, and one or more high permeability "boulder zones" have developed (Winston, 1995). The informal name "boulder zone" is related to the property of the fractured dolostone to roll around and be abraded into rounded rocks by rotary drilling.

As a result of fracturing and possible dissolution, the boulder zones are extremely permeable. As such, they

have become targets for wastewater injection, including injection of brines derived from the Sunniland oil fields. In most cases, including southwest Florida, injection can be accomplished by gravity flow alone. In south Florida, there are as many as nine or ten "high permeability" zones within the lower Floridan aquifer (Maliva et al., 2001) where the receiving zone below 640 m (2,100 ft.) has the salinity of seawater or greater (>=10,000 mg/l).

Controversy exists as to whether the Lower Floridan aquifer has been subjected to dissolution-related karstification. There is no question that void spaces in the boulder zones can be huge. For example, there was a 27 m (96 ft.) drill-bit drop in Sun Oil Company's Red Cattle 32-2 well in the Felda Field (Kohout, 1965, 1967; Burke, 1967). This cavity extended from 768.7 to 796.1 m (2,522 to 2,612 ft.) below land surface. Maliva et al. (2001) attributed this rod drop to a fracture in the dolostone.

Vernon (1970) attributed "cavernous" porosity in the boulder zones to calcite dissolution with concomitant dolomite precipitation. Puri and Winston (1974) described the boulder zones as an intricate network of vugs and large cavities. The boulders were thought to have dropped from the roofs of caverns. Miller (1990) thought that the boulder zones represent caverns that are interconnected by pipes or solution tubes. Winston (1995) argued that boulder-producing zone(s) contain cavities and wall-collapse zones.

More recently, Safko and Hickey (1992) and Duerr (1994) examined borehole video logs and geophysical logs in the Lower Floridan aquifer. They concluded that the porosity of the boulder zone is a result of fracturing, not dissolution of the dolostone.

Maliva et al. (2001) investigated Class I injection well sites in southwest Florida and concluded that the dolostones of the boulder zones are regional diagenetic features occurring at varying depths and stratigraphic positions. In many areas, discontinuous anhydrite cement occludes fracture networks in the Oldsmar Formation. The presence of anhydrite as a cement in fractured dolostone suggested that the dolomitization and fracturing of the host strata preceded precipitation of the anhydrite.

Hypogene Origin of the Boulder Zones

The stratigraphy of the Lower Floridan aquifer compares favorably with Klimchouk's (2007, 2009) criteria for hypogene speleogenesis. The upper and lower confining strata include gypsum or anhydrite, and there is a well-developed groundwater circulation system associated with breccias and fractures that may have been enlarged by dissolution.

Water contained within the Lower Floridan aquifer is chemically similar to seawater, probably owing to the groundwater circulation system that currently exists within the aquifer (Kohout, 1965). The water is sulfur-rich, with abundant sulfate (Haberfield, 1991) and detectable hydrogen sulfide.

Other Evidence of Possible Karst Hypogenesis in the Lower Floridan Aquifer

As is the case with the Sunniland Formation, there is minimal direct evidence at this time to suggest that ongoing or former hypogenesis has enhanced the porosity of the Lower Floridan aquifer. However, others have suggested its existence based on geophysical or geochemical studies that reveal evidence of deep seated dissolution.

Randazzo (1997) speculated that hypogene speleogenesis had enhanced porosity in the Lower Floridan aquifer based on the abundance of sulfate mineralization in the aquifer water.

Cunningham and Walker (2009) and Cunningham (2013, 2015) utilized seismic methods to identify deep-seated collapse zones associated with sinkhole-like depressions offshore of the Miami area of southern Florida. They attributed these collapse features to hypogenic processes within the deep Floridan aquifer. Given the coastal offshore location of these collapse features, it is unclear whether they are a result of flank-margin speleogenesis as a result of groundwater mixing or of sulfuric-acid speleogenesis.

Onshore, there are several relatively deep cenotes in southern Florida. Little Salt Spring, a cenote approximately 150 km northwest of the northern limits of the Sunniland Trend, has been found to contain anoxic, sulfide-rich groundwater discharging from a vent at 73 m (240 ft.) depth (Yang et al., 2008). This water is mixing with shallow, oxic water and forming dissolved sulfate. While the cenote is 75 m (245 ft.) deep, the bottom is a collapse debris cone and no one knows how deep the collapse-filled aven extends. The presence of the vent opens the possibility that the cenote is a deep-seated collapse rather than a feature limited to the Upper Floridan aquifer, within which the cenote's known extent lies. Similar cenotes in the Yucatan Peninsula of Mexico have been attributed to sulfur reduction-oxidation origins (Stoessell et al., 1993; Schmitter-Soto et al., 2002; Socki et al., 2002).

Based on these lines of evidence, we suggest that the boulder zone and related high porosity zones in the Lower Floridan aquifer may also be a result of hypogene speleogenesis. If so, the sulfate-rich Cretaceous and Paleogene strata may represent a series of stacked and potentially interrelated hypogene systems.

The Upper Floridan aquifer is influenced by these systems and the gypsum/anhydrite that lies at its base (Table 1).

Sulfur Behavior in the Upper Floridan Aquifer

Evidence of sulfuric-acid related speleogenesis in the Upper Floridan aquifer (Table 1) is lacking. Upper Floridan water is often sulfur-rich, with a calcium-sulfate hydrochemical facies near the aquifer base and H_2S-rich water in numerous locations. This water has been extensively studied (Rightmire et al., 1974; Rye et al., 1981; Sacks, 1996; Sacks and Tihansky, 1996) and the consensus is that the sulfate near the base of the Upper Floridan is derived by dissolution of gypsum and/or anhydrite and by dedolomitization reactions at the contact with the middle confining unit (Table 1). The H_2S is derived by microbial reduction of the sulfate in portions of the aquifer with abundant carbon.

Therefore, while upward leakage of groundwater through the middle confining unit (Table 1) cannot be ruled out, it does not appear that deep-seated hypogene speleogenesis is currently a significant process in the Upper Floridan aquifer. Speleogenesis as a result of the mixing of waters, however, has almost certainly participated in karst development in coastal portions of the upper Floridan aquifer.

Conclusions

It is unfortunate that so little data concerning water chemistry and the nature of conduiting in Florida's deeply buried carbonate strata exists. However, there is tantalizing evidence that both Florida's Cretaceous and Paleogene strata have undergone hypogenic speleogenesis. If the existing evidence is correct, there is, or was, a stacked series of hypogene-speleogenesis systems. Each of which has the potential for interacting with the one above by leakage through fractures and/or gaps in the evaporite beds that contain the systems.

We suggest that a hypogene speleogenetic model may be an advantageous paradigm for expanding petroleum exploration for both structural and stratigraphic traps in the South Florida Basin and for evaluating the boulder zones as targets for wastewater injection.

References

Applegate AV, Pontigo FA. 1984. Stratigraphy and oil potential of the Lower Cretaceous Sunniland Formation on south Florida. Tallahassee (FL): Florida Geological Survey Report of Investigation No. 89.

Applegate AV. 1991. Drilling in South Florida, video documentary in the possession of the authors.

Burke RG. 1967. Sun whips Florida's boulder zone. Oil and Gas Journal 65: 126-127.

Carrasco-V B. 2003. Paleokarst in the marginal Cretaceous rocks, Gulf of Mexico. In: Bartolini C, Buffler RT, Blickwede JF, editors. The circum-Gulf of Mexico and Caribbean: hydrocarbon habitats, basin formation, and plate tectonics. Tulsa (OK): American Association of Petroleum Geologists Memoir 79. p. 169-183.

Chanton JP, Martens CS, Paull CK, Coston JA. 1993. Sulfur isotope and porewater geochemistry of Florida escarpment seep sediments. Geochimica et Cosmochimica Acta 57 (6): 1253-1266. http://dx.doi.org/10.1016/0016-7037(93)90062-2

Commeau RF, Paull JA, Commeau JA, Poppe LJ. 1987. Chemistry and mineralogy of pyrite-enriched sediments at a passive margin sulfide brine seep: abyssal Gulf of Mexico. Earth and Planetary Letters 82 (1-2): 62-74. http://dx.doi.org/10.1016/0012-821X(87)90107-5

Cunningham KJ. 2013. Marine seismic-reflection data from the southeastern Florida Platform: a case for hypogenic karst (abs.). International Association of Hydrogeologists, Proceedings, International Symposium on Hierarchical Flow Systems in Karst Regions, p. 59.

Cunningham KJ. 2015. Seismic-sequence stratigraphy and geologic structure of the Floridan aquifer system near "boulder zone" deep wells in Miami-Dade County, Florida. US Geological Survey Scientific Investigations Report 2015-5013.

Cunningham KJ, Walker C. 2009. Seismic-sag structural systems in Tertiary carbonate rocks beneath southeastern Florida, USA: evidence for hypogenic speleogenesis? In: Klimchouk A, Ford D, editors. Hypogene speleogenesis and karst hydrogeology of artesian basins. Special Paper 1. Simferopol (UA): Ukrainian Institute of Speleology and Karstology. p. 151-158.

Dowdle WJ, Cobb WM. 1975. Static formation temperature from well logs – an empirical method. Journal of Petroleum Technology 27: 1326-1330. http://dx.doi.org/10.2118/5036-PA

Duerr AD. 1994. Types of secondary porosity of carbonate rocks in injection and test wells in southern peninsular Florida. US Geological Survey Water-Resources Investigations Report 94-4013.

Griffin GM, Reel DA, Pratt RW. 1977. Heat flow in Florida oil test holes and indications of oceanic crust beneath the southern Florida-Bahamas Platform. In: Smith DL, Griffin GM, editors. The geothermal nature of the Floridan Plateau. Tallahassee (FL): Florida Bureau of Geology Special Publication No. 21.

Haberfeld JL. 1991. Hydrogeology of effluent disposal zones, Floridan aquifer, south Florida. Ground Water 29 (2): 186-190. http://dx.doi.org/10.1111/j.1745-6584.1991.tb00509.x

Hickey JJ. 1990. An assessment of the flow of variable-salinity ground water in the middle confining unit of the Floridan aquifer system, west-central Florida. US Geological Survey Water-Resources Investigations Report 89-4142.

Hill CA. 1995. H_2S-related porosity and sulfuric acid oil-field karst. In: Budd DA, Sailer AH, Harris PM, editors. Unconformities and porosity in carbonate strata. American Association of Petroleum Geologists Memoir 63, p. 301-306.

Hine AC. 1997. Structural and paleoceanographic evolution of the margins of the Florida Platform. In: Randazzo AF, Jones DS, editors. The geology of Florida. Gainesville (FL): University Press of Florida. p. 169-216.

Huddlestun PF, Hunter ME, Scott T, Chowns TM, Lloyd JM. 1988. Southern Florida, CSD 140, Col. 31. In: Lindberg FA, editor. Gulf Coast Region, Correlation of Stratigraphic Units of North America (COSUNA) Project. Tulsa (OK): American Association of Petroleum Geologists.

Klimchouk AB. 1997. The role of karst in the genesis of sulfur deposits, Pre-Carpathian region, Ukraine. Environmental Geology 31 (1): 1-20. http://dx.doi.org/10.1007/s002540050158

Klimchouk AB. 2007. Hypogene speleogenesis: Hydrogeological and morphogenetic perspectives. Carlsbad (NM): National Cave and Karst Research Institute.

Klimchouk AB. 2009. Principal characteristics of hypogene speleogenesis. In: Stafford KW, Land L, Veni G, editors. NCKRI Symposium 1 Advances in Hypogene Karst Studies, p. 1-11.

Klimchouk A. 2014.The methodological strength of the hydrogeological approach to distinguishing hypogene speleogenesis. In: Klimchouk A, Sasowsky ID, Mylroie J, Engel SA, Engel AS, editors. Hypogene cave morphologies. Leesburg VA, Karst Waters Institute, Special Publication 18, p. 4-12.

Klimchouk A, Tymokhina E, Amelichev G. 2012. Speleogenic effects of interaction between deeply derived fracture-conduit flow and interstratal matrix flow in hypogene karst settings. International Journal of Speleology 41 (2): 161-179. http://dx.doi.org/10.5038/1827-806X.41.2.4

Kohout FA. 1965. A hypothesis concerning cyclic flow of salt water related to geothermal heating in the Floridan aquifer. Transactions of the New York Academy of Science 28: 249-271. http://dx.doi.org/10.1111/j.2164-0947.1965.tb02879.x

Kohout FA. 1967. Ground-water flow and the geothermal regime of the Floridan Plateau. Transactions of the Gulf Coast Association of Geological Societies 17: 339-354.

Maliva RG, Walker CW, Callahan EX. 2001. Hydrogeology of the lower Floridan aquifer "boulder zone' of southwest Florida. In: Missimer TM, Scott TM, editors. Geology and hydrology of Lee County, Florida. Tallahassee (FL), Florida Geological Survey. Special Publication No. 49.

Miller JA. 1986. Hydrogeologic framework of the Floridan aquifer system in Florida, and in parts of Georgia, Alabama and South Carolina. US Geological Survey Professional Paper 1403-B.

Miller JA. 1990. Ground water atlas of the United States: Segment 6, Alabama, Florida, Georgia, South Carolina. US Geological Survey Hydrologic Atlas 730-G.

Mitchell-Tapping HJ. 1987. Application of the tidal mudflat model to the Sunniland Formation of south Florida. Transactions, Gulf Coast Association of Geological Societies 37: 415-426.

Mitchell-Tapping HJ. 2002. Exploration analysis of basin maturity in the South Florida sub-basin. Transactions, Gulf Coast Association of Geological Societies 52: 753-764.

Mitchell-Tapping HJ, Mitchell-Tapping AM. 2003. Exploration of the Sunniland Formation of southern Florida. Transactions, Gulf Coast Association of Geological Societies 53: 599-609.

Moore CH. 2001. Carbonate reservoirs. New York (NY): Elsevier.

Navoy AS. 1986. Hydrogeologic data from a 2,000-foot deep core hole at Polk City, Green Swamp area, central Florida. US Geological Survey Water-Resources Investigations Report 84-4257.

Palacas JG. 1978a. Preliminary assessment of organic carbon content and petroleum source rock potential of Cretaceous and lower Tertiary carbonates, South Florida Basin. Transactions, Gulf Coast Association of Geological Societies 28: 357-381.

Palacas JG. 1978b. Distribution of organic carbon and petroleum source rock potential of Cretaceous and lower Tertiary carbonates, South Florida Basin. US Geological Survey Open-File Report 78-140.

Palacas JG, Anders DE, King JD. 1984. South Florida Basin – prime example of carbonate source rocks of petroleum. In: Palacas JG, editor. Petroleum geochemistry and source rock potential of carbonate rocks. Tulsa (OK): American Association of Petroleum Geologists Studies in Geology 18: 71-96.

Palacas JG, Daws TA, Applegate AV. 1981. Preliminary petroleum source rock assessment of pre-Punta Gorda rocks (lowermost Cretaceous – Jurassic?) in south Florida. Transactions, Gulf Coast Association of Geological Societies 31: 369-376.

Palacas, JG, King JD, Claypool GE. 1984. Origin of asphalt and adjacent oil stains in lower Cretaceous fractured limestones, Deep Sea Drilling Project Leg 77. In: Buffler RT, Schlager W, Bowdler JL, Cotillon PH, Halley RB, Kinoshita H, Magoon LB, McNulty CL, Patton JW, Premoli Silva I, Avello Suarez O, Testarmata MM, Tyson RV, Watkins DK, editors. Initial reports of the Washington (DC): Deep Sea Drilling Project 77:477-488

Paull CK, Dillon WP. 1980. Erosional origin of the Blake Escarpment: an alternative hypothesis. Geology 8: 538-542.
http://dx.doi.org/10.1130/0091-7613(1980)8<538:EOOTBE>2.0.CO;2

Paull CK, Neumann AC. 1987. Continental margin brine seeps: their geological consequences. Geology 15: 545-548.
http://dx.doi.org/10.1130/0091-7613(1987)15<545:CMBSTG>2.0.CO;2

Pollastro RM, Schenk CJ, Carpentier RR. 2001. Assessment of undiscovered oil and gas in the onshore and state waters portion of the South Florida Basin, Florida – USGS Province 50. US Geological Survey Digital Data Series 69-A.

Puri HS, Banks JE. 1959. Structural features of the Sunniland oil field, Collier County, Florida. Transactions, Gulf Coast Association of Geological Societies 9: 121-130.

Puri HS, Winston GO. 1974. Geologic framework of the high transmissivity zones in south Florida. Florida Bureau of Geology Special Publication No. 20.

Randazzo AF. 1997. The sedimentary platform of Florida: Mesozoic to Cenozoic. In: Randazzo AF, Jones DS, editors. The geology of Florida. Gainesville (FL): University Press of Florida. p. 39-56.

Rightmire CT, Pearson, Jr. FJ, Back W, Rye RO, Hanshaw BB. 1974. Distribution of sulfur isotopes in ground waters from the principal artesian aquifer of Florida and the Edwards aquifer of Texas, United States of America. Vienna, International Atomic Energy Agency, Isotope techniques in groundwater hydrology, p. 191-207.

Robb JM. 1990. Groundwater processes in the submarine environment. In: Higgins CG, Coates DR, editors. Groundwater geomorphology: the role of subsurface water in Earth-surface processes and landforms. Boulder (CO): Geological Society of America. Special Paper 252, Chapter 12, p. 267-281.

Rye RO, Back W, Hanshaw BB, Rightmire CT, Pearson Jr. FJ. 1981. The origin and isotopic composition of dissolved sulfide in groundwater from carbonate aquifers in Florida and Texas. Geochimica et Cosmochimica Acta 45 (10): 1941-1950.
http://dx.doi.org/10.1016/0016-7037(81)90024-7

Sacks LA. 1996. Geochemical and isotopic composition of ground water with emphasis on sources of sulfate in the upper Floridan aquifer in parts of Marion, Sumter, and Citrus counties, Florida. US Geological Survey Water-Resources Investigations Report 95-4251.

Sacks LA, Tihansky AB. 1996. Geochemical and isotopic composition of ground water, with emphasis on sources of sulfate, in the upper Floridan aquifer and intermediate aquifer system in southwest Florida. US Geological Survey Water-Resources Investigations Report 96-4146.

Safko PS, Hickey JJ. 1991. A preliminary approach to the use of borehole data, including television surveys, for characterizing secondary porosity of carbonate rocks in the Floridan aquifer system. US Geological Survey Water-Resources Investigations Report, 91-4168.

Schmitter-Soto JJ, Comin FA, Escobar-Briones E, Herrera-Silveira J, Alcocer J, Suárez-Morales E, Elías-Gutíerrez M, Díaz-Arce V, Marín LE, Steinich B. 2002. Hydrogeochemical and biological characteristics of cenotes in the Yucatan Peninsula (SE Mexico). Hydrobiologica 467: 215-228.
http://dx.doi.org/10.1023/A:1014923217206

Socki RA, Perry, Jr. EC, Romanek CS. 2002. Stable isotope systematics of two cenotes from the northern Yucatan Peninsula, Mexico. Limnology and Oceanography 47 (6): 1808-1818.
http://dx.doi.org/10.4319/lo.2002.47.6.1808

Southeastern Geological Society. 1986. Hydrogeological units of Florida. Florida Geological Survey Special Publication 28.

Stewart, Jr. HG. 1966. Ground-water resources of Polk County. Florida Geological Survey Report of Investigations No. 44.

Stoessell RK, Moore YH, Coke JG. 1993. The occurrence and effect of sulfate reduction and sulfide oxidation on coastal limestone dissolution in Yucatan cenotes. Ground Water 31 (4): 566-575. http://dx.doi.org/10.1111/j.1745-6584.1993.tb00589.x

Vernon RO. 1970. The beneficial uses of zones of high transmissivities in the Florida subsurface for waste storage and waste disposal. Florida Bureau of Geology Information Circular No. 70.

Winston GO. 1995. The boulder zone dolomites of Florida, Volume 2, Paleogene zones of the southwestern peninsula. Miami (FL): Miami Geological Society.

White W. 1988. Geomorphology and hydrology of karst terrains. New York (NY): Oxford University Press.

Yang Y, Schaperdoth I, Albrecht H, Freeman KH, Macalady JL. 2008. Geomicrobiology and hopanoid content of a sulfidic subsurface vent biofilm, Little Salt Spring, Florida. American Geophysical Union Abstracts 1:0517.

ENGINEERING GEOHAZARDS IN HYPOGENE EVAPORITE KARST: CASTILE FORMATION, WEST TEXAS

Kevin W. Stafford

Stephen F. Austin State University
Department of Geology
P.O. Box 13011, SFA Station
Nacogdoches, TX 75962-3011, staffordk@sfasu.edu

Melinda S. Faulkner

Stephen F. Austin State University
Department of Geology
P.O. Box 13011, SFA Station
Nacogdoches, TX 75962-3011, mgshaw@sfasu.edu

Abstract

Hypogene karst processes have been widely documented throughout the Castile Formation outcrop area in Culberson County, Texas and Eddy County, New Mexico. Hypogene manifestations include typical and atypical cave development ranging from maze caves to vertically extensive, single-riser conduit features. Associated hypogene manifestations include vertical breccia pipes and blanket breccias, as well as commonly associated evaporite calcitization, selenitization, and native sulfur emplacement. The high solubility of gypsum promotes rapid surface denudation and erosional intersection of hypogene karst phenomena, which are not easily predictable based on surface manifestations prior to void breaches.

Ranch to Market Road 652 (RM 652) in northern Culberson County, Texas crosses the Castile Formation outcrop area from west to east. While the road was originally constructed in the 1950s for light rural traffic, recent advances in petroleum technology have pushed hydrocarbon exploration and extraction into the region, which significantly increases daily traffic and load. Numerous engineering problems have resulted, many of which are associated with original road construction, including common, small-scale road failures associated with road base compaction and subsidence. However, karst phenomena, including hypogene manifestations, are significant contributions to road failures. Breccia pipes commonly provide vertically transmissive zones that continue to subside locally, causing road failure. Isolated caves produce site-specific geohazards associated with road collapse and induce piping of soils from road subgrade. Cave-associated geohazards are coupled with both epigene and hypogene origins; however, hypogene caves have the potential to cause more significant road failures throughout the region. Secondary mineralization throughout the Castile and overlying Rustler formations complicates geohazards characterization.

Remote sensing and geophysical techniques can be coupled to characterize and delineate karst geohazards. Spatial analyses of aerial imagery and elevation models can be used to delineate regions of intense surficial manifestations of karst development as well as regions of secondary mineralization. Vegetation analyses provide insight into moisture content and gypsic soil development, enhancing delineation of localized karst phenomena while also serving as indicators of lithologic variation. Elevation models enable delineation of surface drainages and closed depressions for large-scale spatial analyses of surficial karst manifestations, which reveals regions of high-potential for interception and geohazards associated with clustering of hypogene karst features.

Ground Penetrating Radar (GPR) acquired along road transects (RM 652) provides evidence of shallow geohazard anomalies, including epigene and hypogene karst, as well as soil piping. While GPR is limited to less than three meters depth of resolution, it enables the differentiation of engineering-based geohazards associated with original construction and geology-based geohazards associated with karst processes. Results of GPR analyses enable the delineation of additional sites for resistivity-based analyses that produce greater depth of investigation.

By coupling shallow geophysical techniques with spatial analyses in gypsum karst terrains that host hypogene karst, potential geohazards can be reduced or avoided with proper engineering. Effective characterization of

hypogene and epigene karst geohazards can reduce the cost of construction and maintenance of roads and infrastructure in evaporite karst terrains. Delineation of the spatial extent, both laterally and vertically, of potential geohazards allows for specific engineering designs to be implemented for individual karst features, instead of requiring a universal solution that is applied to the entire region of focus.

HYDROTHERMAL KARST

DISCUSSION ON THE PROCESS OF DEEP KARST AND HYDROTHERMAL KARST

Yaoru Lu

Department of Geotechnical Engineering, Tongji University
No.1239 Siping Road
Shanghai, 200092, China, yrlu@tongji.edu.cn

Institute of Hydrogeology and Environmental Geology, Chinese Academy of Geological Sciences
No.268 North Zhonghua Street
Shijiazhuang, Hebei Province, 050061, China

Qi Liu

Department of Geotechnical Engineering, Tongji University;
Joint Research Center of Urban Environment and Sustainable Development, Ministry of Education
No.1239 Siping Road
Shanghai, 200092, China, liuqi472@163.com

Wei Zhang

Institute of Hydrogeology and Environmental Geology, Chinese Academy of Geological Sciences,
No.268 North Zhonghua Street
Shijiazhuang, Hebei Province, 050061, China, zhangwei1306@126.com

Abstract

Deep karst remains a major problem. This article discusses three kinds of karst: fossil karst, developed in China before the Yanshan Movement and filled in a later stage; Old Karst, developed and filled on high after Himalayan movement; and the undeveloped New Karst in the Quaternary. The deep karst of our discussion refers to the karst phenomena that has been developing since the Quaternary. These karst phenomena are controlled by local drainage datum planes in depths over several hundred meters or by distant drainage datum planes. Deep karst is often closely related to hydrothermal karst, which involves three conditions: deep water circulation, mixed water circulation, and development related to deep thermal sources. This paper explores the three types of thermal karst and then briefly discusses environmental influences and negative effects on deep karst development.

Introduction

Being widely distributed in China, karst is closely related to people's lives and economic development. Karst has both positive and negative effects. In particular, deep karst has some negative qualities that are often difficult to detect and study.

Kinds of Karst

Karst in China can be divided into three categories according to the geologic time and filling condition of their development: fossil or paleo-karst, Old Karst, and New Karst.

Fossil Karst or Paleo-Karst

Fossil karst or paleo-karst was developed in China before the Yanshan Movement and between the Archean and the Neogene. Early stages of this karst were filled and covered by later sediment. This karst developed in different periods and appears in different locations in south and north China. For instance, there is a period with abundant development of fossil karst in north China. From the Middle Ordovician to the Middle Carboniferous, the karst witnessed a 100-million-year period of discontinuous sedimentation called the North China Caledonian Fossil Karst. Figure 1 is a cross section sketch showing its evolution. Figure 2 is a cross section of fossil karst terrain (Lu, 1999).

Old Karst

Old Karst refers to karst that developed after the Yanshan movement and under the influence of the Himalayan movement. The karst developed in the uplift area of the Yanshan movement. It was not filled by the sediment layer of the Neogene period and continued to develop in later stages. The caves and the passages of the Old Karst could continue to develop, but are mainly distributed on in topographically high areas.
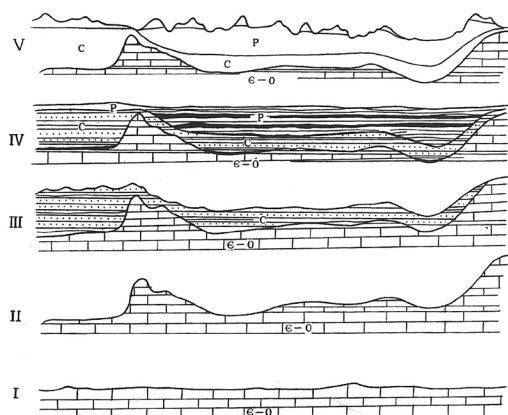
Figure 1.
Stages of development of the North China Caledonian Fossil Karst. (I) Exposure of Cambrian and the Ordovician carbonate rock and sediment; (II) Caledonian paleo-karst processes; (III) Post middle-to-late Carboniferous sedimentation and erosion; (IV) Post-Permian sedimentation; (V) Modern terrain (by Yanshan-Himalayan karst erosion).
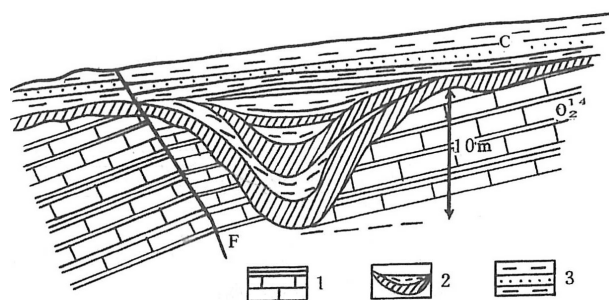

Figure 2.
Cross-section of the Caledonian Fossil Karst and alumina sediment around Heilongdong Ditch in Tianqiao section of the Yellow River. (1) Middle Ordovician carbonate shale; (2) Alumina and argillaceous sediment on paleo–karst depressions; (3) Middle Carboniferous sandstone and mudstone.

New Karst

New Karst refers to the karst developed after the Himalayan movement, and especially during the Quaternary period. At present, this is the main object for study in China, such as the Three Gorges area, characterized by intense downcutting from the end of Cretaceous to the Neogene E'Xi Stage (EX). Caves developed around the acting surface of the early karst is old karst; below SH acting surface are the new-karst caves. (Figure 3).

Deep Karst

Deep Karst mainly refers to the karst passages and cave systems developed from deep groundwater flow. The deep part of old karst caves and passages are hydrologic relicts located above the new karst system. There are three kinds of deep karst.

1. Karst systems controlled by the local erosion base surface. In very thick carbonate horizons, caves and passages resulting from the underground siphon drainage could reach depths of over several hundred meters or more under local river beds.
2. Karst systems controlled by distant river discharge, not by local rivers. These systems are developed in lower carbonate rocks. For the distant upper river, deep karst refers to karst caves controlled by the local lower river.
3. Hydrothermal deep karst. In some areas with abundant carbonate rocks, many karst features are produced by deep hydrothermal activity called hydrothermal karst. Generally, it could be divided into three types. A striking feature for the three types is the sedimentation caused by corrosion that relatively high temperature water has against carbonate rocks (Goldscheider et al., 2010.). Papers discussing hydrothermal karst are listed in References. Hydrothermal karst processes and patterns are shown in Figure 6.

The first two types of the deep karst are mainly based on the ambient temperature water processes (Figure 4). For the multilayer carbonate layer group, karst passages and caves developed in karst aquifers are all deep karst (Figure 5).

Some Discussion on Hydrothermal Karstification

Characteristics of hydrothermal karstification include:

1. Seepage water has a relatively high temperature and is always above 30°C.
2. It is rich in CO_2, which greatly speeds up dissolution. Some are also rich in SO_4.
3. Easy to generate dissolution and sedimentation. Karst channels are liable to change. The channel systems resulting from karstification by deep hydrothermal solution are close to the surface (Lu, 1987, 1988; Frumkin, 2015).
4. Hydrothermal karst water gushes from the surface and rapidly reduces its CO_2 partial pressure, and thus produces large travertine deposits.

Sources of CO_2 for deep karstification can be from upwelling CO_2 in the deep asthenosphere by pyrolysis
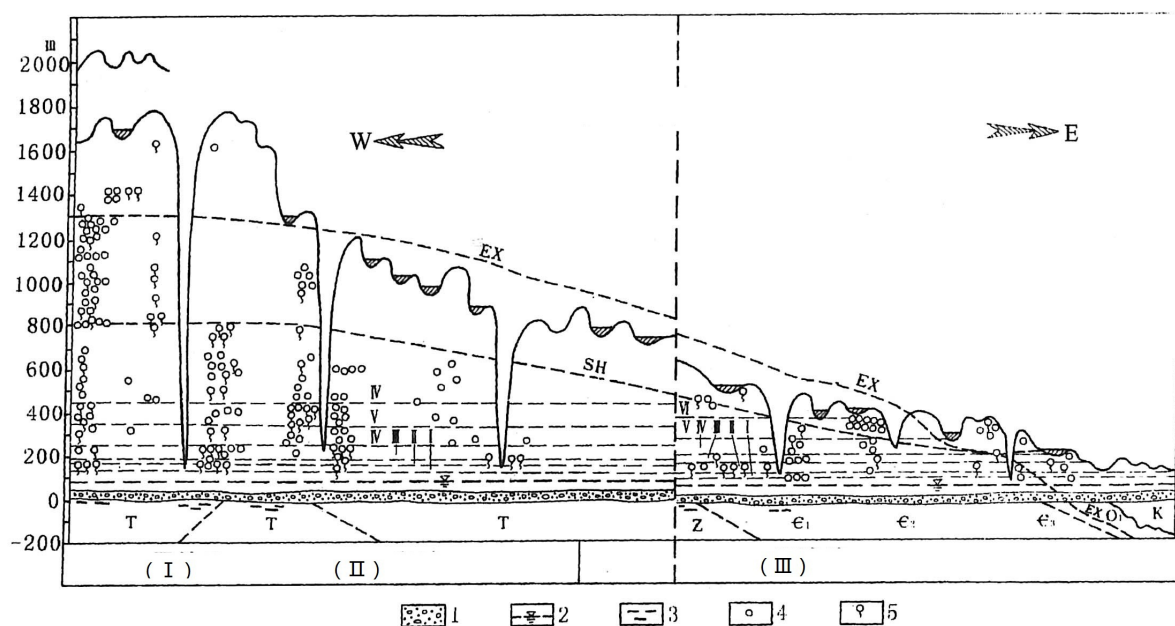
Figure 3.
Stages of karst development in the area with E'Xi stage (western Hubei Province) in the Three Gorges area (Lu, 1999, 2003). (1) Sand-gravel; (2) Water level of Yangtze River; (3) Cave unveiled below the riverbed; (4) Karst caves; (5) Underground rivers discharging as big karst springs; (EX) Lower limit of strong karstification zone from the end of the Cretaceous to the early Paleogene in western Hubei Province; (SH) Lower limit line of strong karstification in the Shanyuan Stage; (I-VI) Middle terrace in Yangtze River, Huangling anticline is omitted, and its western and eastern parts are connected by dotted lines; Three Gorges of Yangtze River (I) Qutang Gorge; (II) Wexia Gorge; (III) Xiling Gorge.
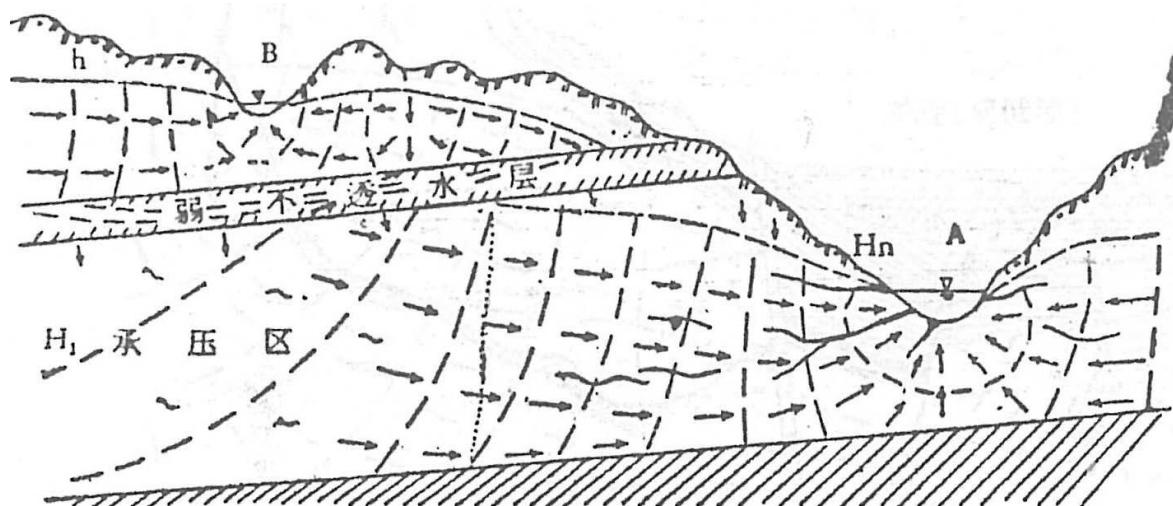

Figure 4.
Cross section of hydrodynamic conditions of double-layer karst (Lu, 1962). (A) Controlled by distant rivers. There are deep karst passage ways in high pressure areas; (B) Controlled by upper high rivers. The aquifers are not thick, and there is no deep karst.
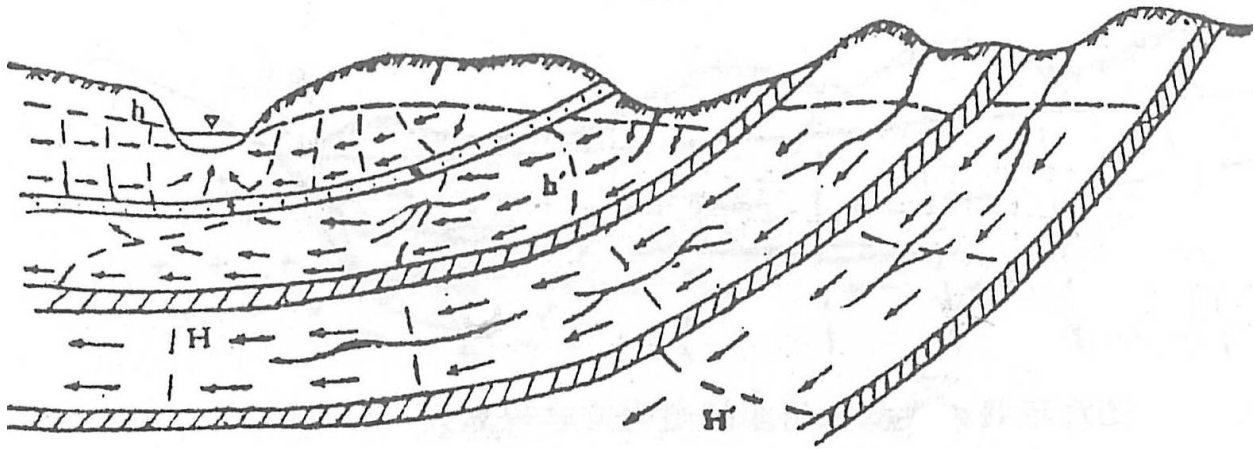
Figure 5.
Cross section of hydrodynamic condition of multi-aquifers.
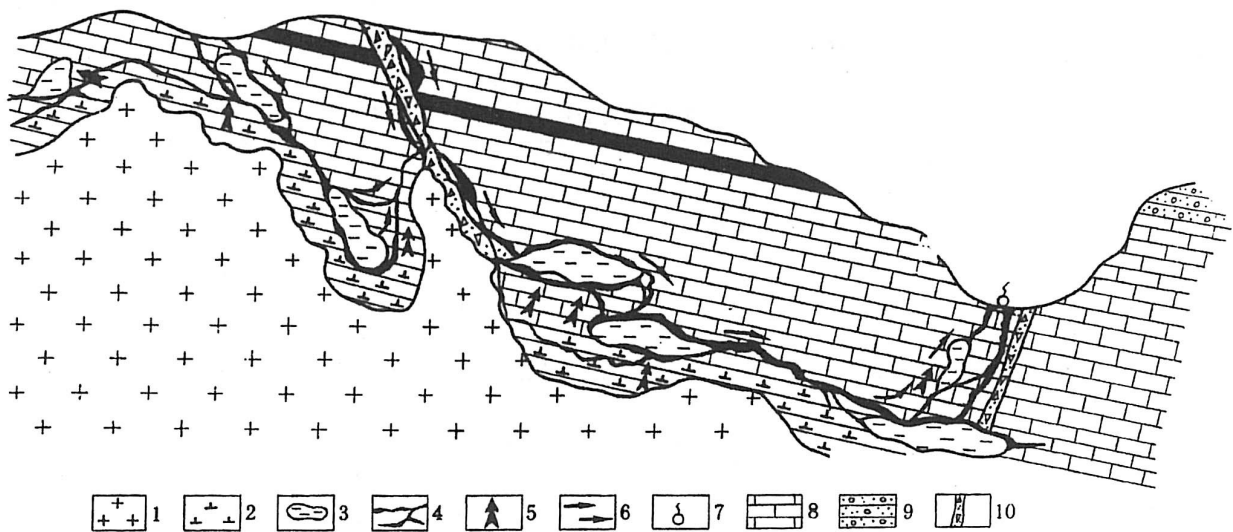
Figure 6.
Pattern of the hydrothermal karstification. (1) Igneous rock; (2) Hydrothermal metamorphic sediment; (3) Early hydrothermal karstification and relevant caves; (4) Late karst caves and passages (developed at ambient temperatures and atmosphere pressures); (5) Direction of hydrothermal processes; (6) Direction of karst water movement; (7) Hot spring; (8) Carbonate rocks; (9) Shale; (10) Fault.

of carbonate rocks deep in the earth, or from complex underground chemical/physical/biological functions.

There are three types of the hydrothermal solution, as follows.

Hydrothermal Solution Formed by Deep Water Cycle

The average geothermal gradient is 3°C per every 100 m of depth. The characteristics of some geothermal mineral water have been researched, particularly the conductivity of flow heat, heat flow unit, and geothermal gradient.

The relevant geothermal data of karst geothermal mineral water in Guizhou is shown in Table 1.

Table 1.
Some coefficients of thermal water in Guizhou.

Rock	CFU [w/(m °C)]	Geothermal gradient (°C /100 m)	HFU (×10⁻² w/ m²)
limestone	2.18～2.39	1.0～3.5	2.26～7.16
dolomite	2.89～3.06	2.0～3.5	3.39～8.71
sandstone	1.67～4.61	1.5～2.0	2.51～16.12

Note: CFU=conductivity of flow heat; HFU=heat flow unit.

For thermal mineral springs in areas such as Shijian, Zhijin, Guanling, Xingyi, Wuchuan, Zunyi, and Xifeng, as well as regions in Guizhou Province, the fact that the temperature is 35~56.5°C and the ^{3}H is 1.6~10.8(T、U), indicates deep-cycle thermal mineral water.

The hot spring in the marble in Taroko, Taiwan is also related to this deep cycle. Some thermal water isotopes of hydrogen and oxygen are compared in Table 2. While the ^{3}H of the shallow Taroko karst springs is 24.28± 4.97, the ^{3}H of the deep-cycle Wenshan Spring is less than 0.5.

Mixed-Cycle Hydrothermal Karst

Mixed-cycle hydrothermal karst refers to karst that consists of a mix of upper deep-cycle karst and water upwelling from deep hydrothermal sources (Figure 7) to show the mixed-cycle structure of dual water. The temperature variation of the underground water in Longyan, Fujian Province, shows that it results from the mixture of dual water by a drill hole (Figure 8).

Figure 9 shows the evolution of δ18O in water from samples of snow on Qomolangma Peak to deep karst water of the southeast coastal zone.

The chemical composition of the geothermal spring in Pamukkale, Turkey also shows that it results from the mixture of dual water.

Deep Hydrothermal Karst With Underground Thermal Sources

Deep underground, the intrusion of igneous rock may produce a heat source that results in karst development and corresponding mineralogical deposits. A brief analysis of hydrothermal karstification is shown in Figure 10.

A striking feature of the hydrothermal process is the production of skarn and other mineral resources in carbonate rocks. The processes of hydrothermal karst are comprehensively shown in Figure 11.

Environmental Problems of Deep Karst

Effect on Water Conservation Projects

When it comes to building reservoirs on local rivers, deep karst may lead to seepage below the dam foundation, around the dam, and outside the reservoir area. For example, a series of water power stations in China with dam heights of 45-230 m overlay significant passage development, some more than 200 m deep along faults. This required high-pressure curtain grouting, as well as many other treatments.

Tunnel Construction

The excavation of tunnels in karst areas can intersect deep karst groundwater at depths as great as 1,000 m. Flooding of mud and water has affected tunnels with lengths from 5 km to over 17 km in karstified regions.

One planned tunnel for express railways, about 35 km long and over 1,000 m deep, occurs in the deep zone where temperatures are always above 50°C. In this case, the tunnel needs to be rerouted through a zone where the temperature is below 45°C.

Deep Hydrothermal Karst and Ore Formation

According to our early experiments of corrosion where the temperature is above 75°C, hydrothermal processes are intensified by corrosion and flow diffusion. The process of hydrothermal karst in deep zones could precede mineralization to produce many mineral resources (Lu, 1986; Merce, 2004; Yurdal, 2006).

Being buried deep underground, these resources require new methods of exploration and exploitation. More in-depth research is also required on the effects that exploitation might have upon the surface environment.

Table 2.
Comparison of some isotopes in Taiwan.

Place	Wenshan hot spring	Kenidng sea water	Hengchun spring	Karst spring in Tailuge	Hulian marble spring	Surface water in Hualian
δD(‰, SMOW)	-74.0	-1.9	-13.2	-50.8	-19.9	-14.6
$\delta^{18}O$(‰, SMOW)	-10.73	-2.23	-2.85	-8.98	-6.77	-4.80
^3H(T.U.)	<0.50	29.56±5.49	28.15±4.21	24.28±4.97	34.18±3.15	40.25±5.01
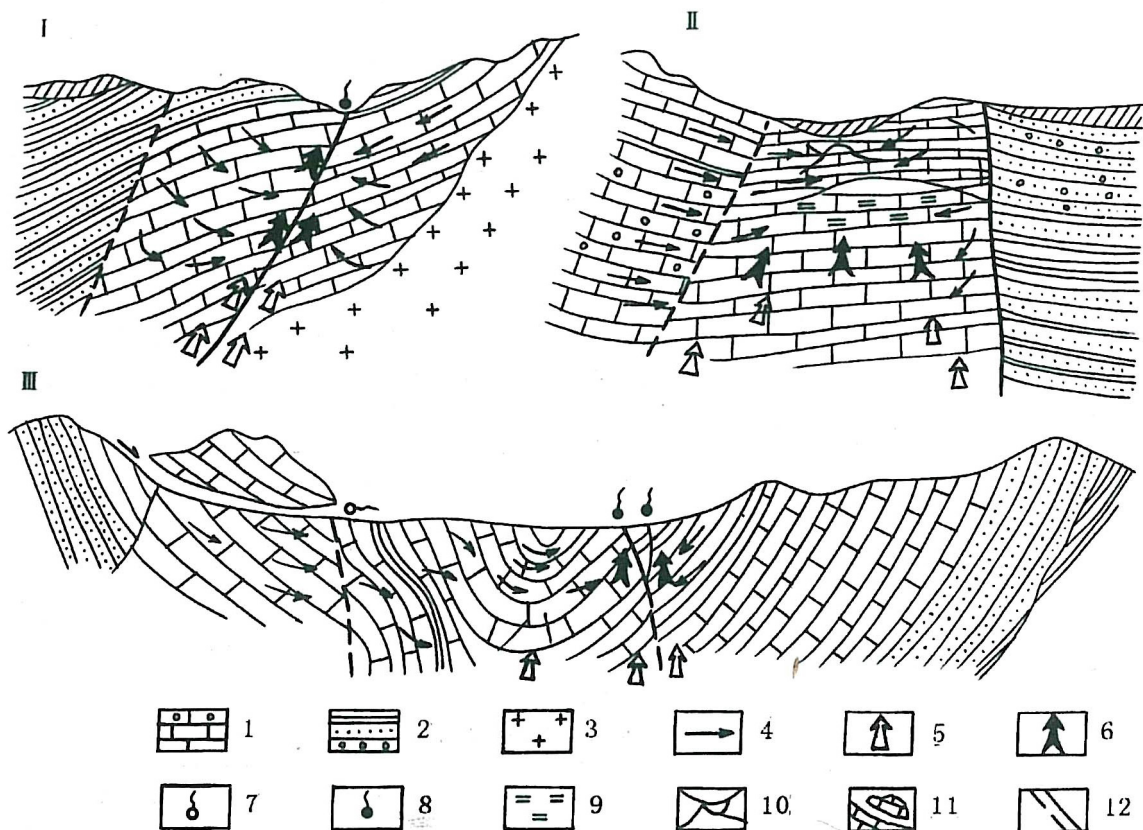
Figure 7.
Structure Pattern cross-section of the mixed-cycle of dual water. (I) Mixed-cycle pattern of dual water in a fault structure; (II) Half-sealed and weak-cycle pattern of mixed dual water in a fault structure; (III) Mixed-cycle pattern of dual water in folded structures; (1) Carbonate rocks; (2) Shale and conglomerate; (3) Igneous rock; (4) Direction of karst seepage water at ambient temperatures; (5) Direction of upward movement of deep hydrothermal solutions; (6) Mixed hydrothermal mineral water; (7) Karst water at ambient temperature; (8) Mixed karst hot springs; (9) Upper leaky confined unit with mixed hydrothermal mineral water; (10) Shallow cave karst channels; (11) Exit and entrance of karst subsurface river water; (12) Fault.
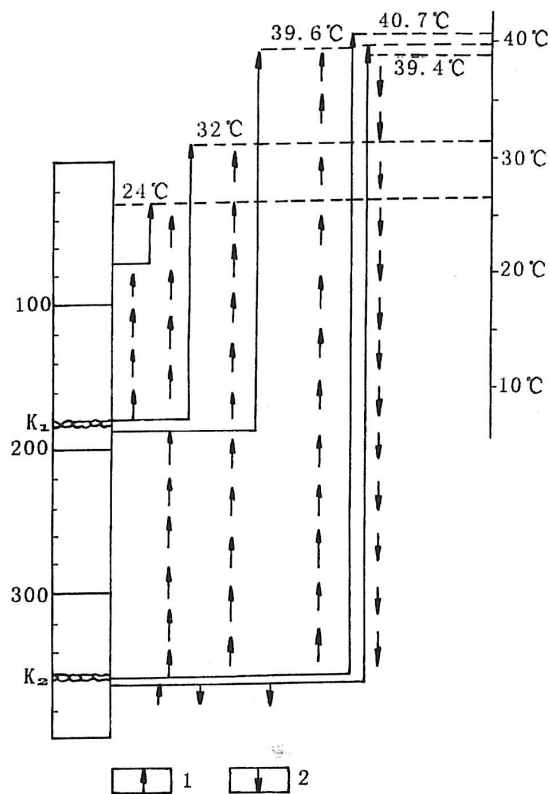
Figure 8.
Temperature variation of underground water in a borehole in Longyan, Fujian Province (based on data compiled by the hydrogeological engineering team from the Fujian Geology and Mineral Bureau). (1) Rising underground water; (2) Descending underground water; (K₁) Karst channels related to the source of the deep hot water; (K₂) Karst caves related to hot water.

Rational Exploitation of Deep Karst Fluid Resources

Serving as the storage space for hot mineral water or oil and gas, the space of a deep karst cave and passages determines its reserves. Such liquid resources are controlled by the size of the caves, fissures, and pores, and therefore, they have different volumes and various gases (Lu, 1997, 2001).

It must be pointed out that disasters such as explosions may occur due to the fact that the existence of the various gases always leads to the formation and mixture of three-phase matters, and in certain cave conditions, the gas mass can be compressed. Therefore, a more in-depth study on the negative effects of exploitation related to deep karst processes is needed.

Conclusion

The deep karst and hydrothermal karst are closely related. The result of deep karst processes should consider two factors. First, unlike the shallow surface with more known phenomena and relevant information, deep karst should be studied from the perspectives of heat, pressure, phase transition, and storage change of energy. Only in this comprehensive way, the characteristics of the deep karst process can be revealed, and their underground resources exploited rationally and efficiently. Second, more caution is needed to avoid deep karst environmental impacts and construction complications triggered by improper developments.
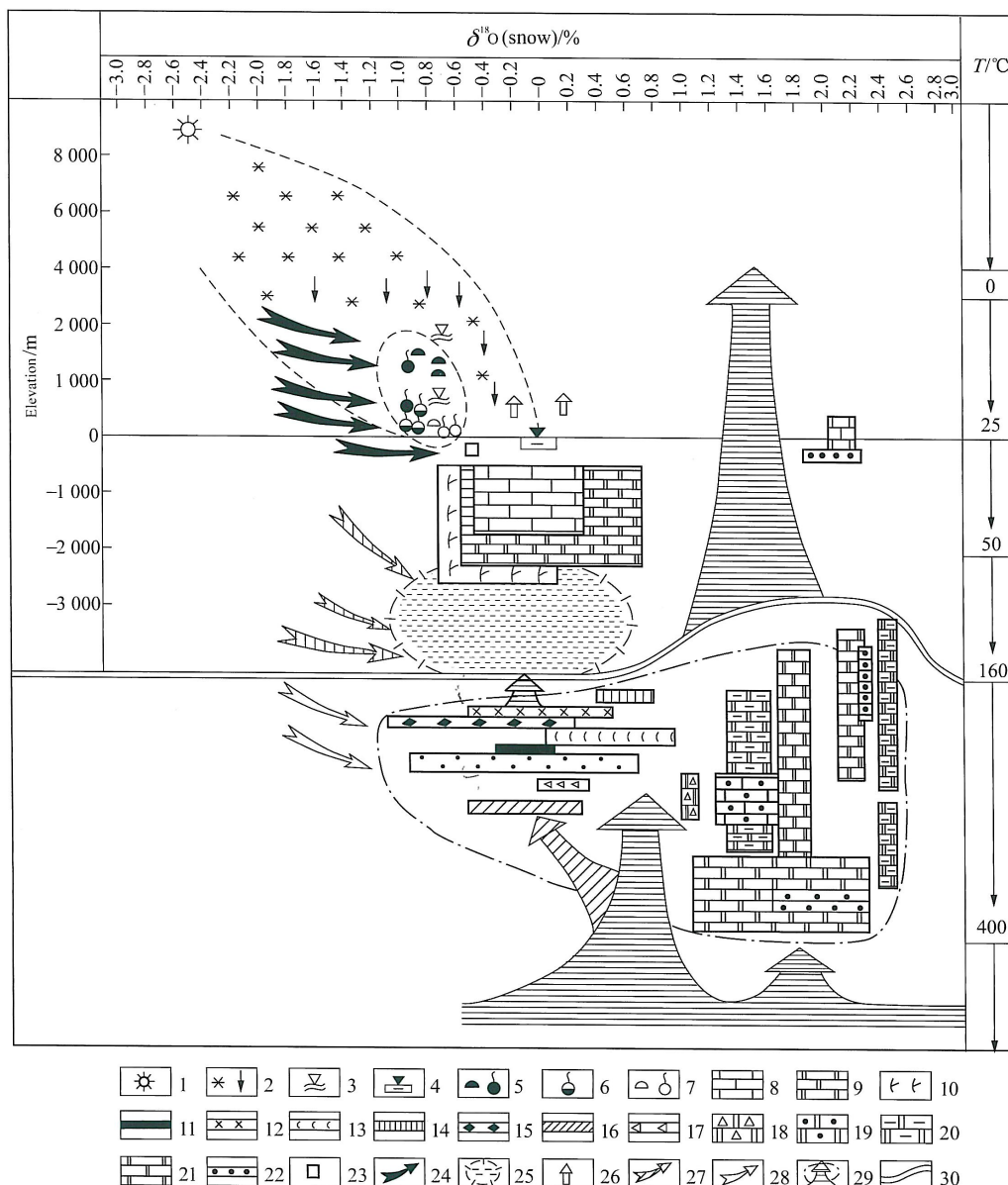
Acknowledgments

Figure 9.
*Analytical map of the δ¹⁸O of normal and hydrothermal karst water in some regions in China.
(1) New snow on Mt. Qomolangma; (2) Rain and snow in regions from Tibet to Beijing and
Shanghai; (3) River water; (4) Normal sea water; (5) Karst groundwater and springs in the Mt. E'mei
region of Sichuan; (6) Karst spring water in Jinan, Shandong; (7) Underground river and spring in
Hangzhou and Tonglu, Zhejiang; (8) Normal limestone; (9) Normal dolomite; (10) Coral;
(11) Magnetite; (12) Mineral liquid; (13) Thermal liquid at mineralization stage; (14) Calcite
adjacent to iron ore; (15) Lead-zinc ore; (16) Calcite near uranium ore; (17) Dolomite-magnetite;
(18) Dolomite ore; (19) Mineralized dolomite; (20) Standard dolomite; (21) Standard limestone;
(22) Siderite; (23) Shallowly buried karst water in Shanghai (Lu, 2013); (24) Flow direction of shallow
karst water; (25) Deep karst brine and thermal mineral water; (26) Karst thermal spring and brine
spring; (27) Karst water flow in deep zones; (28) Percolating direction of upper karst water in
mineralization stage; (29) Hydrothermal invasion direction and boundary of mineralization belts;
(30) Boundary of karst thermal mineral deposits without depth limitations (Wang, 1983; Committee
of Isotopic Geochemistry, China Society of Mineral Chemistry,1982; Lu, 2013).*
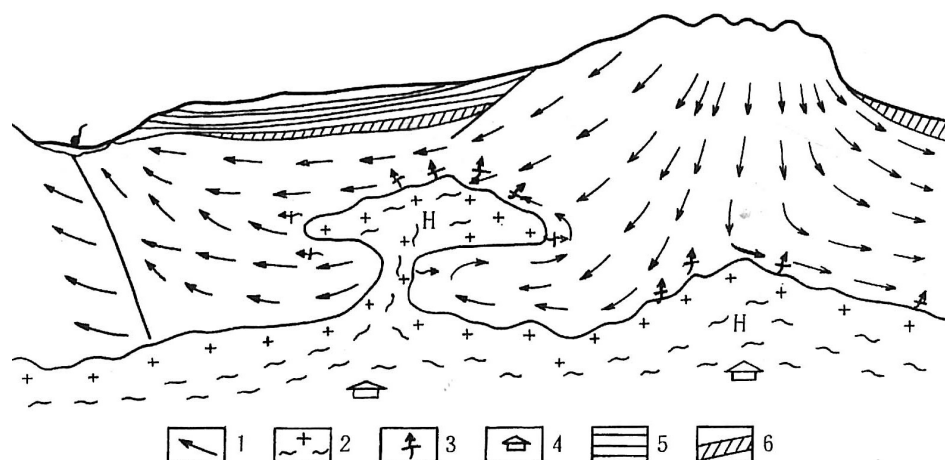
Figure 10.
Structure sketch of the heat source of igneous rocks. (1) Carbonate rocks and flow directions; (2) Igneous heat source and hydrothermal flow; (3) Heat conduction from the heat source; (4) Direction of deep hydrothermal flow; (5) Non-carbonate rocks; (6) Heat insulating unit; (7) Talus. (Lu, 1999)
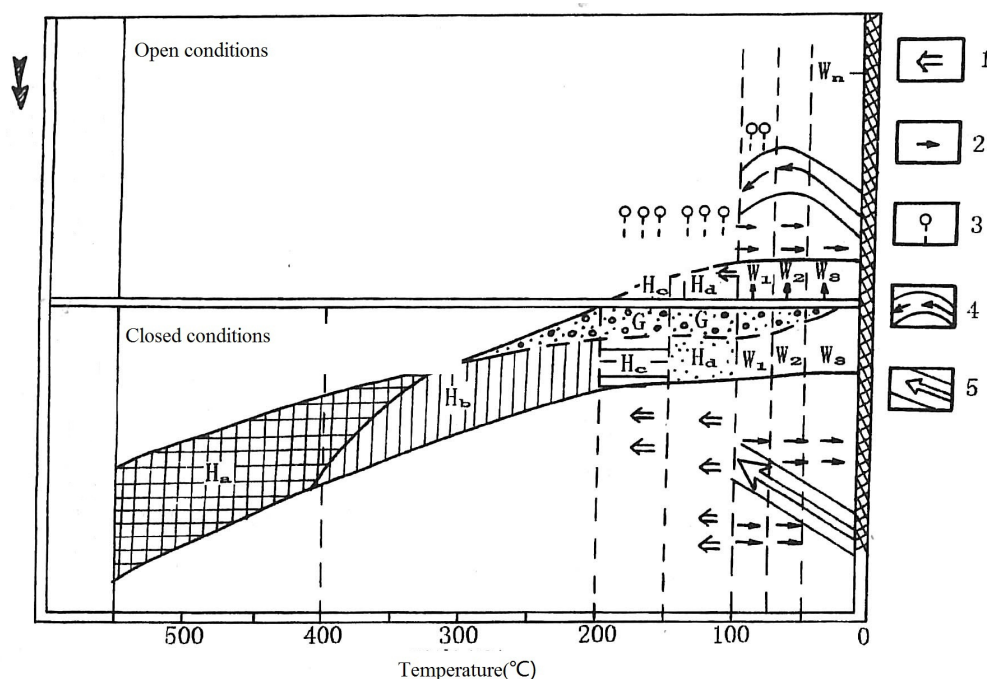
Figure 11.
Summary of hydrothermal karstification. (H_a)Corrosion – metamorphic–differentiation metallogenic belt with extremely high temperature hydrothermal solution; (H_b) Corrosion-liquid metallogenic belt with middle high temperature hydrothermal solution; (H_e) Corrosion-travertine sedimentary belt with middle temperature hydrothermal solution; G - Enrichment zone of gas distribution; (W_n) Karst water at ambient temperature; (W_1) High temperature karst groundwater; (W_2) Medium high temperature karst groundwater; (W_3) Low thermal temperature karst groundwater; (1) Mixture of ambient temperature water; (2) Mixture of hydrothermal solution; (3) Gasification; (4) Relation curve of corrosion rate of the open environment and temperature; (5) Relation curve of corrosion rate of the closed environment and the closed environment and temperature.

References

Committee of Isotopic Geochemistry, China Society of Mineral Chemistry. 1982. Compilation of the 2nd National Symposium on isotopic geochemistry. Guiyang (CN): Guiyang Qianling Printing Factory.

Corbella M, Ayora C, Cardellach E. 2004. Hydrothermal mixing, carbonate dissolution and sulfide precipitation in Mississippi Valley-type deposits. Mineralium Deposita 39 (3): 344-357. http://dx.doi.org/10.1007/s00126-004-0412-5

Frumkin A, Zaidner Y, Na'aman I. 2015. Sagging and collapse sinkholes over hypogenic hydrothermal karst in a carbonate terrain. Geomorphology 229: 45-57. http://dx.doi.org/10.1016/j.geomorph.2014.08.001

Genç Y. 2006. Genesis of the Neogene interstratal karst-type Pöhrenk fluorite–barite (± lead) deposit (Kırşehir, Central Anatolia, Turkey). Ore Geology Reviews 29 (2): 105–117. http://dx.doi.org/10.1016/j.oregeorev.2005.11.005

Goldscheider N, Mádl-Szőnyi J, Erőss N. 2010. Thermal water resources in carbonate rock aquifers. Hydrogeology Journal 18: 1303-1318. http://dx.doi.org/10.1007/s10040-010-0611-3

Lu Y. 1962. Primary research on karst hydro-dynamic condition (abs.). Papers Volume of National Conference. Beijing (CN): Scientific Press. (In Chinese.)

Lu Y. 1986. Karst in China: landscapes, types, rules. Chinese with English explanation. Beijing (CN): Geological Press.

Lu Y. 1987. Water resources in karst regions and their comprehensive exploitation and harnessing. In: Gardiner V, editor. International geomorphology, 1986, part II. Chichester (GB): John Wiley and Sons Ltd. p. 1151-1167.

Lu Y. 1988. Hydrogeological environments and water resources patterns in China. Proceedings of the IAH 21st Congress, Karst hydrogeology and karst environment protection. Beijing (CN): Geological Publishing House. p. 64-75.

Lu Y, Duan G. 1997. Artificially induced by hydrogeological effects and their impacts of environments on karst of North and South of China. Fei J and Krothe NC. Hydrogeology: Proceedings of the 30th International Geological Congress. Volume 22. Utrecht (NL): VSP. p. 113-120.

Lu Y. 1999. Research on the evolutions of karst hydrogeological environments and their engineering impacts. Beijing (BJ): Scientific Press.

Lu Y. 2001. Rational exploitation of resources and the prevention of geohazards in karst regions. Acta Geologica Sinica 75 (3):239-248. http://dx.doi.org/10.1111/j.1755-6724.2001.tb00526.x

Lu Y. 2003. Geo-ecology and sustainable development. Nanjing (CN): Hohai University Press.

Lu Y. 2013. Karst in China: a world of improbable peaks and wonderful caves. Beijing (CN): High Education Press.

Wang Y, Liu B, Chengye Z. 1983. Oxygen and carbon isotopic composition and diagenesis of carbonate rocks. Geological Review 29 (3): 278-284.

HERCULES AND DIANA HYPOGENE CAVES (HERCULANE SPA, ROMANIA): DISSIMILAR CHEMICAL EVOLUTIONS DOCUMENTED BY THEIR PRESENT-DAY THERMAL WATER DISCHARGES

Horia Mitrofan
"Sabba Ştefănescu" Institute of Geodynamics of the Romanian Academy
19-21 Jean-Louis Calderon Street
020032 Bucharest, Romania, horia.mitrofan@geodin.ro

Constantin Marin
"Emil Racoviţă" Institute of Speleology of the Romanian Academy
Calea 13 Septembrie 13
050711 Bucharest, Romania, constmarin@gmail.com

Ioan Povară
"Emil Racoviţă" Institute of Speleology of the Romanian Academy
Calea 13 Septembrie 13
050711 Bucharest, Romania, ipov.iser@gmail.com

Bogdan P. Onac
School of Geosceinces, University of South Florida
4202 E. Fowler Avenue, NES 107
Tampa, FL 33620, USA, bonac@usf.edu

"Emil Racoviţă" Institute of Speleology of the Romanian Academy
Clinicilor 5
400006 Cluj, Romania

Abstract
Hercules Cave and Diana Cave are two small caves situated some 600 m apart, for which a hypogene origin has been previously suggested. Thermal water discharges (up to about 54°C) are hosted by each cave, and were recently made the object of an eight-month chemical monitoring operation. By plotting the concentrations of several chemical species (Na, K, Ca, Sr, Mg, SiO_2, Br) against the concentration of the conservative anion Cl, it was found that both caves discharged a binary water mixture, which was derived from the same saline (and hot) parent-fluid and the same fresh (and cold) parent-fluid. This fact was substantiated mainly by the conservative behavior that Na and Br displayed both in Hercules and Diana Cave's spring waters. Alternatively, the original water mixture appears to have systematically experienced, before reaching the sampling point in Diana Cave, significant depletions in terms of K, Ca, Sr, and SiO_2, while no such depletions were recorded in Hercules Cave. Inferred depletion mechanisms include K^+-Na^+ cation-exchange and Ca, Sr and SiO_2 precipitation in minerals. Both processes could be favored by the possibility that upstream Diana Cave, water flow occurred slowly and in a diffuse manner through a network of cracks (likely across the shaly Iuta Layers). While the absence of analogous depletions at Hercules Cave was probably due to the fact that an extended network of penetrable passages presumably extended upstream the presently known length of that cave, such an underground environment is unlikely to favor precipitation of minerals or cation-exchange processes.

Introduction
The present study addresses the hydrochemical behavior displayed by two karst cavities—Hercules and Diana—both of which are located at Herculane Spa on Cerna Valley (Southern Carpathians, Romania). Extensive experimental datasets analyzed in the framework of several previous investigations (Onac et al., 2009, 2011, 2013; Wynn et al., 2010; Puşcaş et al., 2013) have strongly suggested a hypogene origin for these caves.

At present, both caves still host near-neutral pH NaCl-type thermal water discharges with temperatures up to about 54°C. Yet, until now, the corresponding spring waters have not been systematically and simultaneously monitored in terms of their hydrochemistry. Therefore, by filling this investigation gap, we aimed to elucidate the processes responsible for shaping the chemical character of the groundwater discharges, processes that could have been also involved in the corresponding hypogene speleogenesis.

Geological and Hydrogeological Setting

The concerned caves develop in a 200-250-m-thick stack of Late Jurassic–Early Cretaceous (J_3-K_1) limestones with cherts, underlain by sandstones and conglomerates of Early Jurassic (J_1) age, and overlain by the Late Cretaceous (K_2) shaly Iuta Layers (marly limestones and siltstones). Both cavities occur within the southeastern limb of a SW-NE oriented syncline (Figure 1). Karst water, supplied by several swallets located further northeast, is channeled southwestward along that syncline strike (Mitrofan et al., 2008; Povară et al., 2008). In the proximity of the two caves, there are also located (Figure 1) additional outlets (wells, impenetrable springs) that discharge thermo-mineral water, also of NaCl-type, frequently sulfide-rich, with TDS values up

to about 6 g/L and temperatures up to about 56°C.

For the Herculane Spa aquifers, hydrogen and oxygen stable isotopes' contents have been published by Crăciun et al. (1989), who had sampled three unspecified outlets with NaCl chemical types and discharge temperatures of 56-61.5°C. Studies were also published by Winn et al. (2010), who had sampled several thermal and non-thermal outflows, including the Hercules and Diana Caves. All data suggested that the discharged thermal fluids were basically of meteoric origin, and no significant alteration of the corresponding original isotopic signature had occurred as a result of metamorphic processes, which possibly acted along the hydrothermal flow paths.

This so-far acquired body of information seems insufficient for elucidating both the mechanisms involved in the heating of the discharged fluids and the origin of the water mineralization.

Data Collection and Processing

In the present study, discharge water samples for chemical analyses were collected from Hercules Cave and Diana Cave. The water sampling was performed from early June 2013 to mid-February 2014, twice a week at Hercules Cave and weekly at Diana Cave.
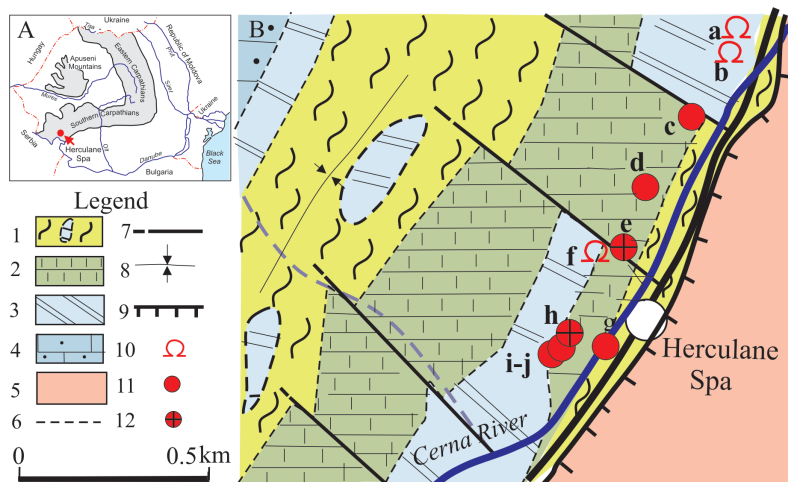
Figure 1.
(A) Location map of study area; (B) Sketch map illustrating the thermal water discharges' location and their associated geological setting.
Legend of symbols: (1) Black argillites with limestone olistoliths (K2); (2) Marly limestones and siltstones (Iuta Layers, K2); (3) Limestones with cherts (J3-K1); (4) Sandstones and conglomerates (J1); (5) Getic crystalline schists; (6) Geological boundary; (7) Fault; (8) Syncline; (9) Overthrust boundary; (10) Cave; (11) Thermo-mineral spring; (12) Well. The indicated outlets are: (a) Hercules Cave; (b) Despicatura Cave; (c) Apollo outlet; (d) Hebe spring; (e)– Diana well; (f) Diana Cave; (g) Venera outlets; (h) Neptun I+IV well; (i) Neptun II spring;(j) Neptun III spring.
The index map illustrates the location of the study region within Romania.

Nalgene High-Density Polyethylene bottles were used to store the collected samples. When collected, the samples were filtered using Thermo Scientific Chromacol Polyether Sulphone Syringe Filters (0.45 μm pore size). Suprapur (Merck) 65% nitric acid was used for the collected samples' pH adjustment.

The complete chemical analysis of all water samples was conducted in the Hydrogeochemistry Laboratory of the "Emil Racoviţă" Institute of Speleology. The techniques utilized for analyzing concentrations were as follows. The Na, K, Mg, Ca, and Sr concentrations were determined by the Dynamic Reaction Chamber – Inductively Coupled Plasma Mass Spectrometry technique (DRC-ICP-MS). The Cl, Br, and Si (expressed here as SiO_2) concentrations were determined in standard ICP-MS mode. Both approaches followed the USEPA (2007) standard. The determinations were carried out with a NexION 300S (PerkinElmer, Shelton, CT, USA) ICP-MS instrument, equipped with a S10 Autosampler. All solutions were prepared with ultrapure water (LaboStar TWF UV7 Ultrapure Water System, electric resistance 18.2 MΩ×cm).
Several lines of evidence (Bulgăr and Povară, 1978;

Povară and Marin, 1984; Mitrofan et al., 2015) had suggested that the Hercules Cave discharge was derived from the mixing of a cold freshwater flow component, with another hot, saline water component. Such a mixing pattern can be primarily investigated by plotting, against the concentration of the conservative anion Cl, the concentrations of several other chemical species (main cations, SiO_2, Br). The purpose of this approach is to establish if the latter species behaved conservatively as well; otherwise stated, if those constituents' concentration fluctuations in the Hercules Cave spring water were controlled only by variable mixing ratios between the two above-indicated flow components, or if other altering processes also intervened. Figures 2-4 plot the data-points corresponding to Diana Cave's spring flow concentrations, and—where available—results of chemical analyses conducted several decades earlier (Institutul de Balneologie şi Fizioterapie, 1973) at the two cave water discharges.

Figures 2 and 3 indicate that for most of the considered constituents of Hercules spring water (Na, K, Ca, Sr, SiO_2, Br), very good correlations with the Cl cation concentration can be outlined. Thus, the assumption that
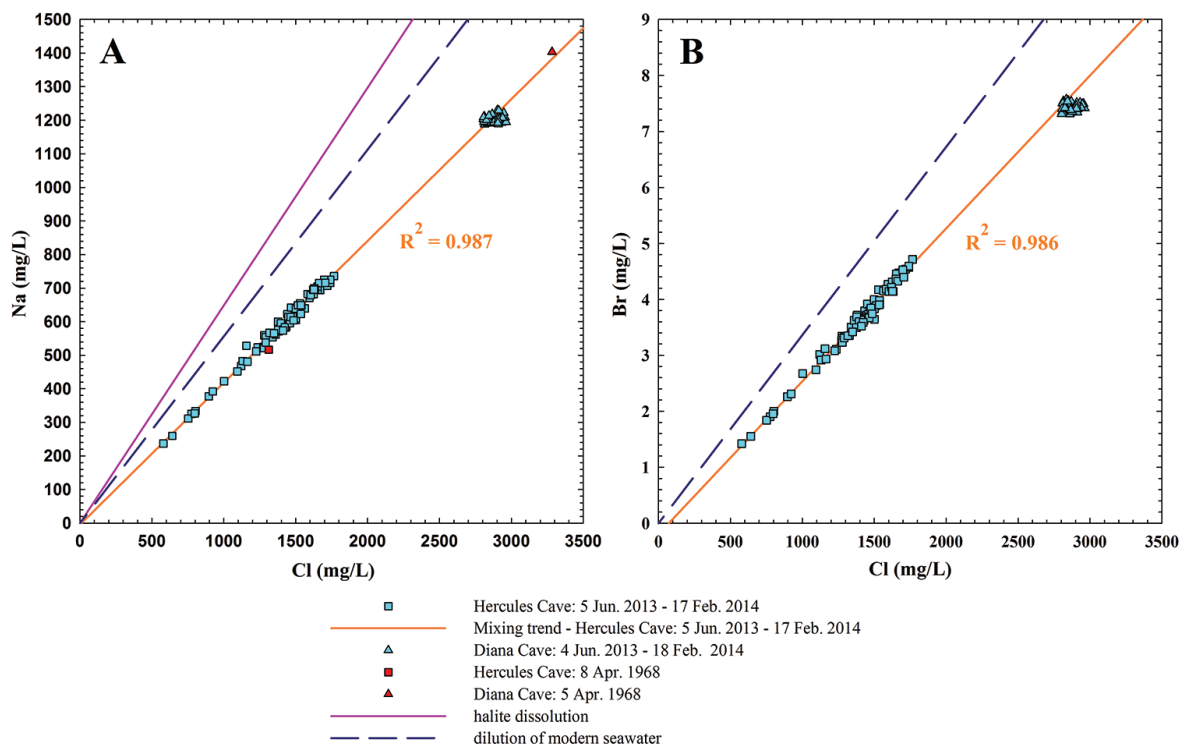

Figure 2.
Plots of Na (A) and Br (B) as a function of Cl. They indicate that both Hercules Cave and Diana Cave discharge a binary water-mixture derived from the same saline (and hot) and fresh (and cold) parent-fluids. Those two endmembers undergo virtually no time variations of their Na, Cl and Br contents.

the corresponding constituents behave conservatively is supported. Namely, concentrations are not altered by mechanisms other than variable mixing between a saline endmember, which has a virtually constant content of the concerned species, and a poorly mineralized groundwater, with fairly invariable concentrations as well.

Regression lines computed based exclusively on the concentrations of Hercules spring constituents (Figures 2 and 3, where the corresponding r^2 values are also indicated) were further used to assess whether the Diana spring water concentrations fell on the same regression lines, or if, alternatively, they were subject to significant shifts.

Results and Discussion

Figure 2A clearly indicates that the Na vs. Cl data-points fall on a mixing-line that is common to both Hercules and Diana Caves; the same also holds true for the Br vs.
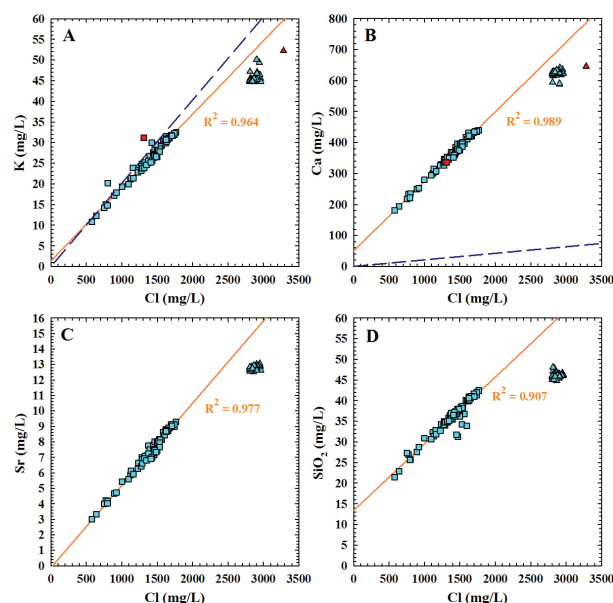

Figure 3.
Plots of K (A), Ca (B), Sr (C), and SiO2 (D) as a function of Cl (symbols as in Figure 2). In Hercules Cave, those constituents' contents were not altered by mechanisms other than variable mixing between the two endmembers (saline and fresh) of virtually constant concentrations. In contrast, it appears that after reaching the sampling point, the Diana Cave water-mixture had experienced significant depletions in terms of K (probably by cation-exchange) and of Ca, Sr and SiO2 (probably by mineral precipitation).

Cl data-points (Figure 2B). It hence results that the same saline and fresh parent fluids contribute to the binary water mixture discharged by both caves. In this respect, the only difference between the two cave discharges is the much wider range of dilutions exhibited by the Hercules Cave water, whose concentrations moreover are, each time, considerably smaller than those measured at Diana Cave.

Another inference derived from Figure 2 is that Na and Br behave conservatively not only in the Hercules Cave spring water, but also in the Diana Cave discharge.

Yet a similarly conservative behavior fails to be obeyed by other chemical species in the Diana Cave water flow. Specifically, before reaching the sampling point in Diana Cave, the original water mixture appears to have systematically experienced significant depletions in terms of K, Ca, Sr and SiO_2 (Figure 3A, B, C, and D). Mechanisms possibly responsible for this setting could involve:

- K^+-Na^+ cation exchanges (the possible Na^+ excess that would result from such a process being too small to be discerned in the Na vs. Cl plot of Figure 2A);
- precipitation of Ca (most likely involving associated Sr) and silica.

The distinct behavior recorded at Diana Cave might be a consequence of the fact that the cave was partly developed at the contact of an actual limestone body with the shaly Iuta Layers. It is therefore quite possible that upstream the cave, water flow occurred slowly and in a diffuse manner through a network of cracks, possibly across the shaly Iuta formation, where cation-exchange processes could be favored by the clayey environment. In contrast, although the currently known length of Hercules Cave is not much larger than that of Diana Cave (94 m and 22 m, respectively), there is a significant body of evidence (Mitrofan and Povară, 1992; Mitrofan et al., 2015), that suggests that an extended network of penetrable passages should continue upstream Hercules Cave. Accordingly, it seems unlikely that such an underground environment would favor processes that lead to significant depletions of the concerned constituents, by cation-exchange or mineral precipitation.

As already specified, in terms of their chemical species' contents, the two endmembers that contribute to the water mixture discharged by both the Hercules and Diana Caves, seem to undergo no time variations. Yet a different behavior is displayed by the Mg^{2+} cation, whose concentration in the freshwater flow-component

appears to be highly variable (Figure 4). This setting is highly conspicuous for the Hercules Cave discharge, where the freshwater fraction prevails; in contrast, the Mg concentration fluctuations are significantly dampened at Diana Cave, where the saline flow component results in a much larger contribution. It is important to stipulate that the Mg content of the involved saline endmember seems to be—as suggested by the overall pattern of the Mg vs. Cl diagram of Figure 4—extremely low. As for the rather elevated Mg concentration value determined in 1968 at Diana Spring, it is unclear whether it is indeed relevant or merely due to an analytical error.
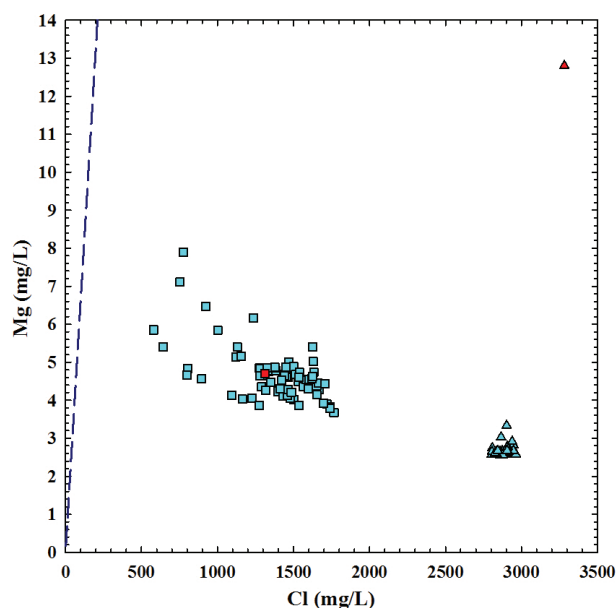

Figure 4.
Plot of Mg as a function of Cl (symbols as in Figure 2). It is suggested that the Mg concentration in the freshwater endmember is highly fluctuating. This setting is highly conspicuous for Hercules Cave, in which the freshwater fraction prevails; in contrast, significantly dampened fluctuations occur at Diana Cave, where a much larger contribution is due to the saline endmember, whose Mg2+ content appears to be extremely low.

As a result of the hydrochemical monitoring of the Hercules and Diana Caves' water discharges, it became possible to reliably assess ratios between the main constituents of the saline parent-water. In particular, it became clear that those ratios did not correspond to the ratios expected as a result of diluting modern seawater (e.g., the Na vs. Cl and Br vs. Cl plots of Figures 2A and B; the K vs. Cl and Ca vs. Cl plots of Figures 3A

and B; the Mg vs. Cl plot of Figure 4). As for the Na vs. Cl mixing trend (Figure 2A), it did not match the halite dissolution line either. Consequently, one must admit that the saline parent-water composition essentially resulted for water-rock interaction—a conclusion that is potentially relevant for the circumstances under which hypogene speleogenesis might develop.

Further evidence that these caves are of hypogene origin comes from detailed mineralogical and stable isotope analyses performed on the thermo-mineral waters and the minerals precipitated within them. The $\delta^{34}S$ values of the sulfate in the thermal waters of these two caves are extremely ^{34}S-enriched, while dissolved sulfide increases sharply (especially in Diana Cave) and the $\delta^{34}S$ values of dissolved sulfide take on the isotopic signature of the initial dissolved sulfate (Wynn et al., 2010). This fact is documented by the $\delta^{34}S$ of gypsum crusts (~19‰) in the cave sulfates of Diana and Hercules, which indicates a more complete sulfate-limited thermochemical sulfate reduction. The negative correlation between $\delta^{34}S$ and $\delta^{18}O$ values in the latter group of cave sulfates is consistent with increasing $H_2S:SO_4^{2-}$ ratios downstream (higher $\delta^{34}S$ values), and more anoxic conditions downstream (lower $\delta^{18}O$ values). This trend culminates in $\delta^{18}O$ values of SO_4^{2-} indicating near complete exclusion of O derived from O_2 in sulfate minerals from Diana Cave (Onac et al., 2011).

Of the two caves, Diana Cave is by far the richer and more diverse in terms of minerals (Onac et al., 2009). Abundant steam and H_2S rises from the thermal water to condensate on the walls and ceiling of the cave. The sulfuric acid produced by H_2S oxidation/hydrolysis causes a strong acid-sulfate weathering of the bedrock, generating in combination with Al^{3+} and Na^+ from the marls and thermal water, a paragenesis that includes native sulfur, bassanite, epsomite, halotrichite group minerals, alunite, anhydrite, tamarugite, and rapidcreekite. The last three sulfates have their type locality in this carbonate cave environment (Diaconu, 1974; Puşcaş et al., 2013; Onac et al., 2013).

Conclusions

The chemical composition of the thermal spring waters discharged by the Hercules and Diana hypogene caves was monitored for about eight months. It consequently became possible to ascertain that a common mixture between two endmembers (saline and fresh) supplied both indicated outlets. The contents of most chemical species in the two endmembers were invariable in time; one exception was the Mg^{2+} cation, whose concentration in the freshwater flow-component appeared to be highly fluctuating.

In Hercules Cave, the constituents' concentrations were only altered by the variable mixing between the saline and fresh endmembers. However, in Diana Cave, it appears that before reaching the sampling point, the original water mixture systematically experienced significant depletions in terms of K (probably by cation-exhange) and of Ca, Sr, and SiO_2 (probably by mineral precipitation). Both of these indicated processes could be favored by the possibility that upstream Diana Cave, the water flow occurred slowly and in a diffuse manner through a network of cracks, likely across the shaly Iuta Layers. The absence of analogous depletions at Hercules was probably due to the fact that an extended network of penetrable passages presumably extended upstream the presently known length of that cave, such an underground environment being unlikely to favor precipitation of minerals or cation-exchange processes.

Another significant issue clarified by the hydrochemical monitoring operation addressed the nature of the saline parent-water composition. It was ascertained that it was essentially a result of water-rock interaction—such a conclusion being potentially relevant for the circumstances under which hypogene speleogenesis might develop.

Acknowledgements

References

Bulgăr A, Povară I. 1978. Separation of karstic thermal springs discharge components as based on the analysis of discharge and temperature variations measured at the exurgence. Travaux de l'Institut de Spéologie "Emile Racovitza" 17: 209-214.

Crăciun P, Barnes I, Bandrabur T. 1989. Stable isotopes in hydrogeothermal structures in Romania. Studii Tehnice şi Economice, Institutul Geologie şi Geofizică, Seria E, 15: 17-39.

Diaconu G. 1974. Quelques considérations sur la présence de l'anhydrite dans la grotte "Pestera Diana" (Băile Herculane-Roumanie). Travaux Institute Spéologie "Emile Racovitza" 13: 191-194.

Institutul de Balneologie şi Fizioterapie. 1973. The mineral waters and therapeutic muds in the Socialist Republic Romania, Vol. IV. Bucureşti (RO): Editura Medicală. (In Romanian.)

Mitrofan H, Povară I. 1992. Delineation of a thermal water carrying karstic conduit by means of thermometric measurements in the Băile Herculane area (Romania). Theoretical and Applied Karstology 5: 139-144.

Mitrofan H, Povară I, Mafteiu M. 2008. Geoelectrical investigations by means of resistivity methods in karst areas in Romania. Environmental Geology 55 (2): 405-413.
http://dx.doi.org/10.1007/s00254-007-0986-1

Mitrofan H, Marin C, Povară I. 2015. Possible conduit-matrix water exchange signatures outlined at a karst spring. Groundwater 53: 113-122.
http://dx.doi.org/10.1111/gwat.12292

Onac BP, Sumrall J, Tămaş T, Povară I, Kearns J, Dârmiceanu V, Vereş D, Lascu C. 2009. The relationship between cave minerals and H_2S-rich thermal waters along the Cerna Valley (SW Romania). Acta Carsologica 38 (1): 27-39.
http://dx.doi.org/10.3986/ac.v38i1.135

Onac BP, Wynn JG, Sumrall JB. 2011. Tracing the sources of cave sulfates: A unique case from Cerna Valley, Romania. Chemical Geology 288 (3-4): 105-114.
http://dx.doi.org/10.1016/j.chemgeo.2011.07.006

Onac BP, Effenberger HS, Wynn JG, Povară I. 2013. Rapidcreekite in the sulfuric acid weathering environment of Diana Cave, Romania. American Mineralogist 98: 1302-1309.
http://dx.doi.org/10.2138/am.2013.4452

Povară I, Marin C. 1984. Hercules thermomineral spring. Hydrogeological and hydrochemical considerations. Theoretical and Applied Karstology 1: 183-194.

Povară I, Simion G, Marin C. 2008. Thermo-mineral waters from the Cerna Valley Basin (Romania). Studia UBB Geologia 53 (2): 41-54.
http://dx.doi.org/10.5038/1937-8602.53.2.4

Puşcaş CM, Onac BP, Effenberger HS, Povară I. 2013. Tamarugite-bearing paragenesis formed by sulphate acid alteration in Diana Cave, Romania. European Journal of Mineralogy, 25 (3): 479-486.
http://dx.doi.org/10.1127/0935-1221/2013/0025-2294

USEPA. 2007. Method 6020A. Inductively Coupled Plasma-Mass Spectrometry. U.S. Environmental Protection Agency.

Wynn JG, Sumrall JB, Onac BP. 2010. Sulfur isotopic composition and the source of dissolved sulfur species in thermo-mineral springs of the Cerna Valley, Romania. Chemical Geology 271 (1): 31-43.
http://dx.doi.org/10.1016/j.chemgeo.2009.12.009

ENVIRONMENTAL EFFECTS OF RATIONAL UTILIZATION OF KARST GEOTHERMAL RESOURCES IN THE NORTH CHINA PLAIN

Wei Zhang
No.268, Zhonghua North Street, Xinhua District
Shijiazhuang City, Hebei Province, 050061, China, zhangwei1306@126.com

Guiling Wang
No.268, Zhonghua North Street, Xinhua District
Shijiazhuang City, Hebei Province, 050061, China, guilingw@163.com

Feng Liu
No.268, Zhonghua North Street, Xinhua District
Shijiazhuang City, Hebei Province, 050061, China, 542507283@qq.com

Abstract

As a clean energy resource, geothermal resources play an important role in protecting and improving the environment. This paper uses the well-known North China Plain, with a carbonate karst reservoir, to demonstrate how significant the geothermal resource is and to highlight essential environmental differences between karst geothermal resources and coal resources. After analyzing the different geothermal areas, the maximum allowable drawdown method and mining coefficient method are applied as tools for evaluating geothermal recoverable reserves. Evaluation procedures include researching geological characteristics; selecting an assessment method; and completing a final comprehensive evaluation. The evaluation results show that the karst geothermal resource for the North China Plain is 5.28×10^{17}J. The exploration and utilization of the karst geothermal resource will beneficially result in energy savings of coal resources of about 3×10^7t and emission reduction of carbon dioxide of about 7.17×10^7t.

Introduction

China is a country with large amounts of geothermal resources reserves. These geothermal resources, at medium and low temperatures, are mainly distributed in large sedimentary basins and the fault zones of mountains. Sedimentary basin reserves contain huge amounts of geothermal resources, which are the first choice for exploitation of geothermal resources at medium and low temperatures in China. However, there is a big problem with difficulties on reinjection of the hydrothermal fluids. Reinjection in sandstone reservoirs in most areas is not practical, but for geothermal reservoirs with karstic fissures in provinces and cities such as Tianjin and Xiongxian, development has been achieved at a certain scale. At present, mainly with a method of exploration and reinjection, the reinjection rate can reach more than 90%, which achieves sustainable development. When conditions for recharge and circulation are beneficial, reinjection is easy and the impact on environment is less. Making full use of the characteristics of karstic geothermal reservoirs and their rational development and utilization is important for reducing waste of resources, extending the life of production wells, and reducing environmental pollution.

I. Status of Development and Utilization of Geothermal Resources at Home and Abroad

As clean energy, geothermal resources can have a positive environmental effect. Based on the World Energy and Climate Policy Assessment, geothermal resources rank the highest among the four renewable energy sources of solar, wind, hydro, and geothermal (Kewen, 2013). Actively promoting the development and utilization of geothermal resources has important practical significance and long-term strategic significance in alleviating some of the pressure of energy supplies and other environmental problems.

Development and utilization of geothermal resources can be divided into two types: electric power generation and direct use. High temperature geothermal resources (more than 150°C) are mainly used for electric power generation. A report from an international energy conference published by the Electric Power Research Institute shows that the amount of the international geothermal resources calculated by two standard methods is 1.2×10^{13} GWh (EPRI, 1978). Medium temperature (90-150°C) and low temperature (25-90°C) geothermal resources are used directly in applications related to heating, refrigeration, medicine, tourism, industrial drying, farming, etc.

After long-term development, direct utilization of geothermal resources has gradually evolved from independent small-scale uses to large-scale projects. As of 2010, in 78 countries, geothermal resources' total installed capacity of direct use is 48,493MWt, and the use of energy is about 423,830 TJ/Year (117,740 GWh/Year) (Lund, 2010).

Long-term, the international use of geothermal resources is predicted with a direct use of geothermal resources capacity of 160.5GWt by 2020 (Bertani, 2010 and Goldstein et al, 2011). According to the trend of geothermal development, different equipment is suitable for the different temperatures of geothermal resources (Lund, 2006, 2010; Lund et al., 2005a, 2005b). According to statistics, there are currently 2,307 hot springs and 5,480 geothermal wells in China.

The utilization of geothermal exploitation is growing at an annual rate of nearly 10%. The direct use of geothermal energy in China in 2013 is 165,000TJ/Year. Among the uses of geothermal energy at medium and low temperature, heating accounts for 32.16%, tourism accounts for 31.83%, aquaculture accounts for 12.41%, farming accounts for 13.25%, industrial uses account for 0.33%, and other uses account for 10.02%.

II. Characteristics of the Geothermal Reservoir in North China Plain

The North China Plain is a large Mesozoic and Cenozoic sedimentary basin (Figure 1). The basement is composed of a set of complexly folded metamorphic rocks of Archean and Lower Proterozoic age. The cover layer is composed of two sets of sedimentary rocks: (1) Middle and Upper Proterozoic, and (2) Lower Paleozoic and Cenozoic. The former are marine carbonate rocks and the latter are terrestrial facies clastic rocks. Strata from the upper Ordovician to the lower Carboniferous are generally missing.

Under the Quaternary System deposits of the North China Plain, is a multi-layered geothermal reservoir, generally classified into two categories. These are Cenozoic porous geothermal reservoirs (porous geothermal reservoirs), composed mainly of terrestrial facies clastic sedimentary rocks; and Meso and Neoproterozoic carbonate rock karstic fissure geothermal reservoirs (bedrock geothermal reservoirs), composed mainly of marine deposits.

Porous geothermal reservoirs include the Neogene Minghuazhen and Guantao Formations, and Paleogene formations. The Neogene geothermal aquifer exists throughout almost the whole North China Plain. The
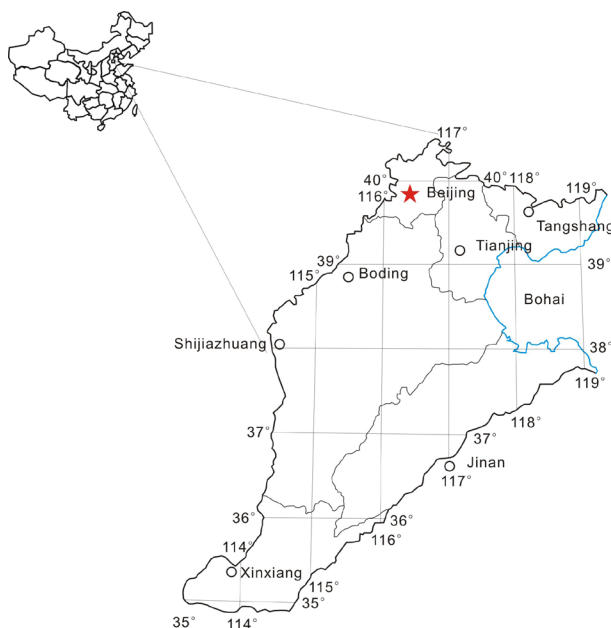

Figure 1.
The study area map.

Paleogene geothermal aquifer is distributed in the basins covered by the Neogene deposits.

Bedrock geothermal reservoirs include Paleozoic Ordovician and Cambrian rocks and the Mesoproterozoic Wumishan Formation of Jixian County. Geothermal reservoirs occur mainly in the uplift belts between the basins and in secondary uplifted areas in the basin interiors, where they are generally covered by younger rocks.

The Paleozoic Ordovician–Cambrian geothermal reservoir is generally distributed in uplifts in the region near Beijing, Tianjin, Bazhou, Ningjin, Leling, Zhanhua, and Guangrao. The elevation of the top surface of the reservoir is controlled by the basement tectonics. In Gaoqing, Zhanhua, and Guangrao, the buried depth of the reservoir top is 1,000-1,500 m below the ground surface, and in Beijing, Tianjin, and Leling, it is up to 2,000-3,000 m below the ground surface.

The degree of development of karstic fissures and the thickness of the weathering crust's development are variable because of effects of lithology, basement tectonics, and the buried depth of the rocks. In the area of Beijing, the karstified part of the reservoir is often used as a target stratum for groundwater production. It is an adequate geothermal reservoir as it has water-bearing conditions and good geothermal geological properties. This occurs when it is buried deeply and the overlying insulation layer is thick. The general performance of

this reservoir is of poor heat production ability and low calorific value is offered.
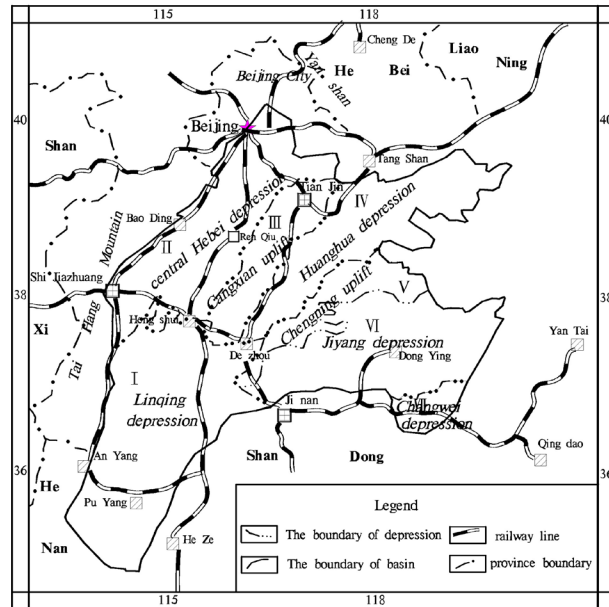

Figure 2.
Map of the tectonic zone.

The Wumishan geothermal reservoir in the Jixian System of the Proterozoic Erathem is found mainly in areas near Beijing, Tianjin, Cangxian, and Ningjin. It has burial depths of 800-2,000 m and a total thickness of more than 300-1,000 m. Due to different geological conditions in the study area, some exposed surfaces of the Wumishan Formation form bornhardts and in other areas the top of the formation may be buried deeper than 3,500 m. As the main aquifer of the Beijing and Tianjin area, it has the largest reserve of geothermal resources in Beijing, accounting for more than 90% in the Plain area. Due to the influence of repeat geological tectonic movement, Wumishan fissures develop well, creating conditions for karstification, and the rock has good water capacity and transmissivity.

III. Evaluation Method

The delineation of the area of each hydrothermal reservoir must meet the following two conditions: (1) it is not buried deeper than 4,000 m and has a temperature above 25°C, and (2) the water yield of single wells is more than 20m³/h.

In areas without control of well and other data, the extent of the geothermal reservoir is delineated by calculating the temperature based on published burial depths and using the average geothermal gradient of 25°C/Km. The results were limited to areas with calculated temperatures above 25°C.

1. The Calculation of Minable Quantity of Geothermal Fluid

When using the method of maximum allowable drawdown to calculate the minable quantity of geothermal fluid of a single well for a certain mining period (usually 100 years), the sum of the central drawdown of the calculation area and additional drawdown of mining of a single well is limited to not more than 100 m, the largest mining quantity obtained, as the minable quantity of geothermal fluid within the calculation area. The expression:

$$Q_{wk} = \frac{4\pi T S_1}{\ln(6.11\bar{t})} = \frac{4\pi T S_1}{\ln(\frac{6.11Tt}{\mu^* R_1^2})} \quad \text{...........................(1)}$$

$$Q_{wd} = \frac{2\pi T S_2}{\ln \frac{0.473 R_2}{r}} \quad \text{..(2)}$$

In the expression: Q_{wk}—minable quantity of geothermal fluid, m³/a; Q_{wd}—minable quantity of geothermal fluid of single well, m³/a; S_1—central drawdown of calculating area, m; S_2—additional drawdown of single well, m; R_1—radius of the mining area, m; R_2—radius of single well control, m; μ^*—elastic storativity of thermal reservoir; t —time of mining, a; T—transmissivity, m²/a; r— radius of pumping well, m.

For mining coefficient of the prospective area of geothermal exploitation, the value of the mining coefficient depends on the lithology of reservoir, development of pores and fissures, and the water supply situation; select large value with supply situation, and select small value without supply situation.

$$Q_{wk} = Q_R \cdot X \quad \text{..(3)}$$

In the expression: Q_R—storage of geothermal fluid, m³; X —minable coefficient.

2. The Calculation of Minable Heat of Geothermal Fluid

The expression for the calculation of minable heat of geothermal fluid is:

$$Q_p = Q_{WK} C_W \rho_w (T_1 - T_0) \quad \text{..........................(4)}$$

In the expression: Q_p— minable heat of geothermal fluid, kJ/d; Cw—specific heat of geothermal fluid, kJ/kg·°C; ρ_w—density of geothermal fluid, kg/m³; T_1—temperature of the geothermal reservoir, °C; T_0—temperature of the constant zone of subsurface temperature, °C.

3. Minable Quantity of Geothermal Fluid Considering the Condition Of Reinjection

For the geothermal field of basin type, as per mining for 100 years under the condition of reinjection, with the consumption of 15% of geothermal reserves, according to the radius influenced by the heat balance calculation and the allowable mining quantity, the formula is as follows:

$$Q_{allowable} = \frac{AQ_p}{\pi R^2} = \frac{0.15AH}{(1-\alpha\beta)tf}$$ ....(5)

$$R = \sqrt{1-\alpha\beta} \times \sqrt{\frac{Q_p tf}{0.15H\pi}}$$

$$\alpha = \frac{Q_r}{Q_p}$$

$$\beta = \frac{T_1 - T_0}{T_1 - T_0}$$

$$f = \frac{\rho_w C_w}{\varphi\rho_w C_w + (1-\varphi)\rho_r C_r}$$

In the expression: R—influenced radius under the condition of reinjection, m; P_w, P_r—density of geothermal water, density of rocks, kg/m³: Cw, Cr,—specific heat of geothermal water, specific heat of rocks, KJ/Kg. °C; φ—porosity of reservoir rock; t—time(select 100Y), 36,500, d; Q_p—water inflow of single well at 20m drawdown, m3/d; Q_r—quantity of reinjection, m³/d; T_1—temperature of the geothermal reservoir, °C; T_2—temperature of reinjection, 25°C; T_0—temperature of the constant zone of subsurface temperature, °C; α— reinjection rate; considering the lithology of the reservoir and development of pores and fissures, the porous media part of the geothermal reservoir is set at 30%, the karstic part of the of geothermal reservoir is set at 90%, and the fissure-type part of the geothermal reservoir is taken 50%; Q, allowable-minable quantity of under the condition of reinjection, m³/d; A—Evaluation area, m²; H— thickness of geothermal reservoir, m.

4. Evaluation of environmental effects

According to the allowable minable heat evaluated by geothermal resources, we can estimate the economic,

social, and environmental benefits. The saving of coal equivalent to the heat of the geothermal resources developed and used is calculated through the following expression:

$$M = \frac{Q}{2.93 \times 10^{10} \times 0.6} = \frac{Q}{1.758 \times 10^{10}}$$ ....(6)

In the expression: M—saving coal (use standard coal), t/a; Q—quantity of geothermal resources, J; 2.93×10^{10} is the unit conversion coefficient, heat of per ton of standard coal is 2.93×10^{10}J (calculated by calorific value of 7,000 kilocalorie per kilogram:1 kilocalorie=4,186.8joule); 0.6 is the geothermal efficiency ratio, calculate by heat efficiency 0.6 of coal-fired boiler.

The quantity of reducing coal emissions equivalent to the heat of geothermal resources developed and used is calculated in Table 1.

Table 1.
List of reducing emissions of standard coal.

Item	Formula	
carbon dioxide (CO_2, t/a)	(1)=2.386M	[a] Coal ash is not air emission, it belongs to emission of solid waste.
sulfur dioxide (SO_2, t/a)	(2)=1.7%M	
nitrogen oxide (NOx, t/a)	(3)=0.6%M	
Suspended dust (t/a)	(4)=0.8%M	
Coal ash (t/a)	(5)=10%M	

IV. Analysis of Environmental Effects

Geothermal energy, wind energy, solar energy, and biomass are classified as renewable energy. The World Energy Council (WEC, 2007) listed total installed capacity and annual electricity production of a variety of renewable energy sources in the world, and calculated the utilization coefficients of each (Capacity Factor). The utilization coefficient of geothermal power generation is the highest of the four energy sources (Table 2) (Fridleifsson et al., 2008).

Comparing CO_2 emissions in the life cycles of various types of energy power generation, wind power is the lowest, followed by geothermal power and nuclear power. Because of the energy used in the production process of PV panels, the solar electrical energy generation's life cycle equivalent emissions rises, while

the coal-fired power and natural gas power generation of conventional fossil fuel energy are 60 times and 30 times of the lowest emissions (Horne, 2013).

Table 2.
Comparison of world electric power from renewable energy in 2005. Table from Fridleifsson (2008).

	Installed capacity		Annual production of electricity		Capacity factor
	GWe	%	TWh/yr	%	%
Water power	778	87.5	2,837	89	42
Biomass	40*	4.5	183	5.7	52
Wind energy	59	6.6	106	3.3	21
Geothermal energy	8.9	1.0	57	1.8	73
Solar energy	4	0.4	5	0.2	14
Total renewable resources	890	100	3,188	100	41**

Compiled from the tables in the 2007 Survey of Energy Resources (WEC, 2007).
*The installed capacity for Biomass is not given in the WEC 2007 Survey of Energy Resources, but said "In excess of 40 GW" in the text. The capacity factor is thus uncertain.
**Weighted average.

Table 3.
Comparison of carbon dioxide equivalent emissions in life cycle of a million degrees of electricity of various kinds of energy.

Types of energy resources	CO_2 emission (tons)
Coal-burning power generation	974
Gas-fired power generation	469
Nuclear power	15
Hydropower	18
Biomass power generation	46
Wind generation	14
Solar electrical energy generation	39
Geothermal power generation	15

The minable heat of geothermal fluid of karstic geothermal resources of North Plain is 5.28×10^{17}J. The equivalent saving of coal is 3.00×10^7t, reduction of emissions of carbon dioxide is 7.17×10^7t, reduction of emissions of sulfur dioxide is 5.11×10^5t, reduction of emissions of nitrogen oxide is 1.80×10^5t, reduction of suspended dust is 2.40×10^5t, and coal ash is 3.00×10^6t.

If adopting mining well to well, under the condition of reinjection, the minable heat of geothermal fluid per year is 5.11×10^{19}J. This can greatly improve the geothermal resources availability, recover the heat production ability of the heat storage, keep the heat reservoir pressure, and achieve sustainable development and utilization. If adopting mining well to well in the karstic geothermal resources of North Plain, the amount of coal saved is 2.91×10^9t, reducing emissions of carbon dioxide to 6.94×10^9t, emissions of sulfur dioxide to 4.94×10^7t, and emissions of nitrogen oxide to 1.74×10^7t. Suspended dust is 2.32×10^7t and coal ash is 2.91×10^8t, which has additional positive effects on the environment.

Table 4.
List of the environmental benefits of developing and utilizing the karst geothermal resources of North Plain.

Item		Mining of single well	Reinjection of well to well
carbon dioxide (CO_2, t/a)		7.17	693.54.
sulfur dioxide (SO_2, t/a)		5.11	494.14
nitrogen oxide (NOx, t/a)		1.8	174.4
Suspended dust (t/a)		2.4	232.54
Coal ash	(t/a)	3	290.67

Conclusions
The characteristics of geothermal resources are green and beneficial to the environment. Developing and utilizing geothermal resources can reduce dependence on traditional fossil fuels, which can produce ash, slag, and sulfur dioxide and nitrogen oxide emissions. Reducing dependence on fossil fuels also reduces the cost of urban pollution controls. By using geothermal resources, the ecological environment can be protected effectively, which has obvious environmental benefits.

References

Bertani R. 2010. World update on geothermal electric power generation 2005-2009. Proceedings of the World Geothermal Congress 2010; Bali, Indonesia.

Electric Power Research Institute. 1978. Geothermal Energy Prospects for the Next 50 Years. Special report ER-611-SR.

Fridleifsson IB, Bertani R, Huenges E, Lund JW, Ragnarsson A, Rybach L. 2008. The possible role and contribution of geothermal energy to the mitigation of climate change. In: Hohmeyer O, Trittin T, editors. IPCC Scoping Meeting on Renewable Energy Sources; 2008 Jan. 20-25; Luebeck, Germany. p. 59-80.

Goldstein BA, Hiriart G, Tester JW, Bertani R, Bromley CJ, Gutiérrez-Negrín LC, Huenges E, Ragnarsson A, Mongillo MA, Muraoka H, Zui VI. 2011. Great expectations for geothermal energy to 2100. Proceedings 36th Workshop on Geothermal Reservoir Engineering; 2011 Jan. 31-Feb. 2; Stanford University, California. SGP-TR-191, p. 5-12.

Horne R. 2013. World outlook for geothermal electricity. Proceedings of the Second International Conference on Effective Development and Utilization of Geothermal Energy in Deep Formations; Beijing, China. University of Geosciences (Beijing).

Li Kewen. 2013. Comparison and Development among Geothermal Energy, Solar and Wind Power, Chinese High-temperature Geothermal Exploration and Development, p. 43-54

Lund JW. 2006. Direct heat utilization of geothermal resources worldwide 2005. Proceedings of the ASEG 2006 -18th Geophysical Conference. Extended Abstracts, 1: 1-15.

Lund JW. 2010. Direct utilization of geothermal energy. Energies 3: 1443-1471. http://dx.doi.org/10.3390/en3081443

Lund JW, Freeston DH, Boyd TL. 2005a. Direct application of geothermal energy: 2005 worldwide review. Geothermics, 34 (6): 691-727. http://dx.doi.org/10.1016/j.geothermics.2005.09.003

Lund JW, Freeston DH, Boyd TL. 2005b. World-wide direct uses of geothermal energy 2005. Proceedings of the World Geothermal Congress, Antalya, Turkey.

World Energy Council. 2007. Survey of Energy Resources, 427-437.

World Energy Council. 2010. World Energy and Climate Policy Assessment.

HYPOGENIC DRIVERS FOR ECOSYSTEMS

BIOTIC CHANGES IN A DEEP SULFIDIC OFFSHORE SINKHOLE

Haydn Rubelmann III
University of South Florida
4202 E. Fowler Ave. SCA 110
Tampa, FL, 33620, U.S.A., *rubelman@mail.usf.edu*

James R. Garey
University of South Florida
4202 E. Fowler Ave. ISA 2015
Tampa, FL, 33620, U.S.A., *garey@usf.edu*

Abstract

Jewfish Sink is an anoxic sinkhole located 1 km offshore from West Central Florida in the Gulf of Mexico. It was a submarine spring until 1962 when flow ceased due to a drought. Unlike the blue holes and black holes of the Bahamas, Jewfish Sink has a narrow 6 m opening that restricts light into the 45 m deep sink. Geochemical measurements were recorded over two time periods spanning a combined total of six years. Over that time, the anoxic bottom waters were stable and contained high levels of sulfide throughout most of the study. Analysis of environmental DNA from water samples within the sink demonstrated that sulfur reducers had the highest relative abundance compared to other functional guilds. Environmental DNA from the sink was studied at four depths at nine intervals over a two-year period. Denaturing Gradient Gel Electrophoresis (DGGE) was used to fingerprint 16S rRNA bacterial communities and dissimilatory sulfite reducing communities by targeting the 16S rRNA bacterial gene and the dsr gene associated with dissimilatory sulfite reducing bacteria and archaea. Water chemistry was also measured during this two-year study. The shallow regions of the sink were oxygenated, and deeper regions were anoxic. In the winter, the oxygenated regions extended much deeper into the sink than in the summer. Clines established themselves seasonally in the upper waters of the sink and developed unique bacterial communities that were different from communities in the deeper regions of the sink. Prokaryotes containing the dsr gene were found only in the deeper anoxic zones of the sink and dissimilatory sulfite reducing prokaryotes containing the dsr gene were found only in anoxic zones, becoming undetectable when a zone became oxygenated due to the movement of the oxycline. It took several months for the dissimilatory sulfite reducing communities to be reestablished when the oxycline moved back up the sink.

The lowest depth studied within the sink (40 m) remained stable chemically and biologically until a turnover event during an unusually cold winter occurred. This turnover event disrupted the biological communities at 40 m and led to a reestablished community comprised of different species than those found prior to the event. This finding suggests that the microbial communities are in a meta-stable state, and when perturbed, they may not return to their former state.
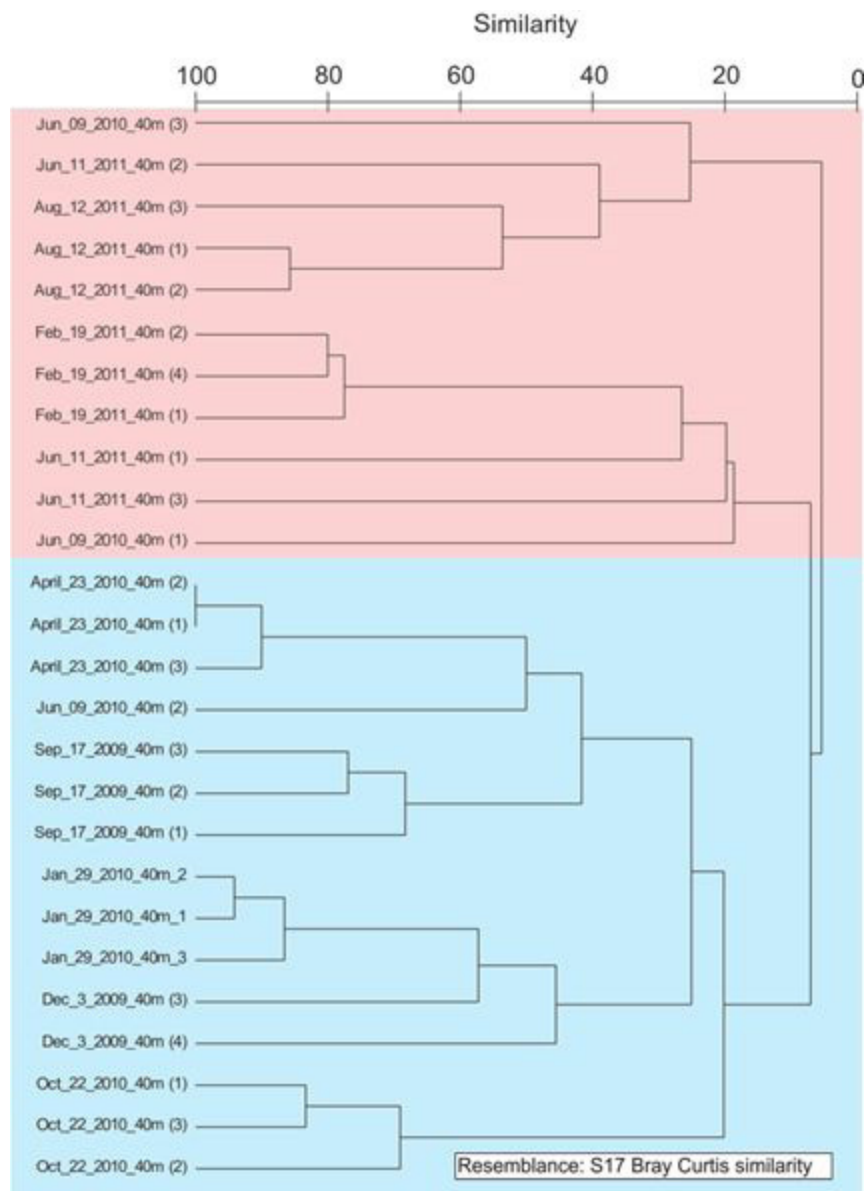
Figure 1.
Cluster analysis of prokaryotic communities at 40 meter sites showing major groupings pre- and post- turnover. The blue clade contains 40 meter fingerprints sharing at least 20% similarity observed prior to the turnover event on February 19, 2011. The red clade represents the community after the turnover event.

CHEMOAUTOTROPHICALLY-BASED SUBTERRANEAN ECOSYSTEMS

Serban M. Sarbu

"Emil Racoviţă" Institute of Speleology of the Romanian Academy
Calea 13 Septembrie 13, 050711 Bucharest, Romania, iserbansarbu@yahoo.com

Abstract

The process of photosynthesis is responsible for supplying most biological communities with energy and organic carbon. Alternatively, chemoautotrophically-based, rich, and diverse communities were discovered in the late 1970s around deep-sea thermos mineral vents. Their energy is supplied by bacteria that oxidize reduced inorganic compounds. In 1986, Movile Cave was discovered in Romania. Microbial mats consisting of sulfide-oxiziding, methanotrophic, and nitrifying bacteria are abundant in the cave, at the interface between the air and the anoxic waters rich in hydrogen sulfide, methane, and ammonia. Stable isotope studies confirmed that chemoautotrophic carbon fixation in these mats supplies the food for its unusually diverse aquatic and terrestrial invertebrate communities consisting entirely of endemic species. Several other chemoautotrophically-based underground ecosystems have been discovered and investigated since. Sulfur-oxidizing bacteria have been shown to supply the food base for subterranean invertebrate communities in the Frasassi Caves in Italy, Ayyalon Cave and Tabgha Spring in Israel, and Mellisotrypa Cave in Greece. All of these caves are of hypogenic origin and they contain sulfur-oxidizing acid-forming microbial mats that accelerate the process of limestone dissolution. Biological investigations in these caves have shown striking similarities between their subterranean communities. Interestingly, closely related sulfur-oxidizing filamentous bacteria have been identified living as ectosymbionts on the exoskeleton of Niphargus species (Amphipoda) in several of these ecosystems. Additionally, morphological and behavioral adaptations have been observed and are currently being studied in some of the aquatic invertebrates. Such features are presumed to be advantageous in coping with high concentrations of hydrogen sulfide, ammonia, and carbon dioxide and very low concentrations of oxygen present in these subterranean environments.

MESIC VEGETATION COMMUNITIES WITHIN THE OWL CREEK AND BEAR CREEK WATERSHEDS AS EVIDENCE OF UPWARD MIGRATION OF DEEP-SEATED KARST

Melinda S. Faulkner

Stephen F. Austin State University
Department of Geology
P.O. Box 13011, SFA Station
Nacogdoches, TX 75962-3011, mgshaw@sfasu.edu

Kevin W. Stafford

Stephen F. Austin State University
Department of Geology
P.O. Box 13011, SFA Station
Nacogdoches, TX 75962-3011, staffordk@sfasu.edu

Abstract

The Owl Creek and Bear Creek watersheds, located in Coryell County, are part of the surface drainage that flows into Belton Lake near the confluence of the Leon River. The creeks and their tributaries provide continuous surface and sub-surface flow responsible for downcutting and incision within the Owl Mountain Province on the eastern peninsula of the Fort Hood Military Installation. The Owl Mountain Province is characterized by a dissected plateau, with the Bear Creek watershed providing a solutionally widened valley that dissects the uplands. The Owl Creek watershed defines the northern extent of the Owl Mountain Province.

The landscape and its topography are largely controlled by the erosional behavior of the Lower Cretaceous limestones and marls of the Fredericksburg Group. The resistant Edwards caps the plateaus while the lower permeability of the Comanche Peak forces ascending fluids to flow laterally and spring out, incising slot canyons into the steep sided scarps. These canyons follow the trend of major conjugate joint sets where deep-seated fluids rise along solutionally widened flow paths to feed surface springs and seeps. Although the climate within the area can be characterized as sub-humid to semi-arid, continued erosion along the preferential flow paths has created north- and east-facing mesic slot canyons where forest species that grow best in cooler, wet habitats continue to thrive.

The habitats of the mesic, dissected portions of the study area are strongly influenced by floristic contributions from the eastern deciduous forests, including tall-grass prairie species. One such relict species, bigtooth maple, *Acer grandidentatum,* is a small deciduous hardwood tree indigenous to North America. It exists as a continuous population in the intermountain regions of the western United States from southern Idaho through the Wasatch Mountains of Utah. Smaller disjunct populations of *A. grandidentatum* can be found throughout the Southwest; Texas has several isolated populations located in the Guadalupe and Wichita Mountains in West Texas, and several counties within the Edwards Plateau of Central Texas. As temperatures warmed and water resources became focused along incising canyons across the Edwards Plateau and Lampasas Cut Plain, populations of *A. grandidentatum* were forced to respond to the changing climate. Over time, as moister climates shifted to the east, relict populations of Pleistocene vegetation, including *A. grandidentatum*, contracted to mesic slot canyons in Central and West Texas associated with springs and seeps where consistent moisture was more readily available.

Today, isolated populations of bigtooth maple, *A. grandidentatum,* continue to exist as Pleistocene relicts in sheltered incised canyons within the Owl Creek and Bear Creek watersheds in Coryell County. These stands are isolated from larger populations by several hundred miles, but continue to thrive as a result of continuous moisture associated with ascending fluids. Permeability varies greatly over the boundaries of the interbedded Comanche Peak and Edwards; the interfingered formations have likely created a semi-confined aquifer system where deeper seated fluids migrate upwards through low permeability strata along preferential flow paths and communicate with meteoric waters near the ground surface, maintaining the moisture regime vital to the continued existence of mesic vegetation communities in the incised canyons.

LOCAL CASE STUDIES IN SPELEOGENESIS

THE COMPLEX EVOLUTIONARY HISTORY OF HYPOGENE KARST SYSTEMS: AN EXAMPLE FROM THE GIANT MAZES OF NE BRAZIL

Augusto S. Auler
Instituto do Carste
Rua Aquiles Lobo 297
Belo Horizonte, MG, 30150-160, Brazil, aauler@gmail.com

Alexander Klimchouk
National Academy of Sciences
55-b Gonchara Str.
Kiev, 01054, Ukraine, klim@speleogenesis.info

Francisco H. R. Bezerra
Departamento de Geologia
Universidade Federal do Rio Grande do Norte
Natal, RN, 59078-970, Brazil, bezerrafh@geologia.ufrn.br

Caroline L. Cazarin
Centro de Pesquisa e Desenvolvimento Leopoldo A. Miguez de Mello
Petrobras
Rio de Janeiro, RJ, 21941-915, Brazil, cazarin@petrobras.com.br

Fabrizio Balsamo
Dipartimento di Fisica e Scienze della Terra "Macedonio Melloni"
Università degli Studi di Parma
Parco Area delle Scienze 157/A
Parma, I-43124, Italy, fabrizio.balsamo@unipr.it

Abstract

Hypogene caves are frequently generated at great depth, being subject to a much longer evolutionary history than epigenic caves before unroofing and surface removal takes place. Timescales since the onset of the main speleogenetic phase can be in the order of hundreds of millions of years, especially in areas of slow uplift rates. This allows for prolonged interaction between the cave and the dynamics of the surrounding environment. Post-speleogenetic modification processes can occur both in the phreatic and vadose zones, but tends to increase as the cave moves towards the surface, resulting in significant imprints in terms of conduit modification and mineral/sediment emplacement.

The hypogene karst of NE Brazil is exemplified by giant maze caves in a cratonic setting, such as Toca da Boa Vista and Toca da Barriguda. After the main speleogenetic phase, the wall bedrock was weathered in the phreatic zone, resulting in small cavities filled with calcite spar. Multiple episodes of sediment infilling took place in the lower portions of the caves, recorded in at least two magnetic reversals that, due to the difference in elevation between the sites, are probably not sequential, implying in minimum ages > 1 Myr. The transition to the vadose zone was accompanied by multiple paleoclimate oscillations and associated processes in the caves. Significant condensation corrosion caused retreat of the cave walls and weathering of surfaces of subaerial speleothems throughout the caves. Minimum average rates in corroded speleothems were estimated at 0.06 mm/kyr, which may imply in significant passage enlargement, given timescales of the order of million years. Speleothem deposition predates the limit of ^{230}Th dating method (ca. 600 kyr), including massive subaqueous deposition during late Pleistocene wet intervals. Peculiar mineralization and wall rock alteration due to bat guano occurred throughout the caves. The studied hypogene caves are valuable repositories of mineral and clastic deposits, accumulating a wealth of information about the geological and paleoenvironmental history of NE Brazil.

CONDENSATION CORROSION SPELEOGENESIS IN THE AMARGOSA DESERT AND THE TECOPA BASIN

Yuri Dublyansky
Institute of Geology, Innsbruck University
Innrain 52
Innsbruck, 6020, Austria, juri.dublyansky@uibk.ac.at

John Klenke
Nye County Nuclear Waste Repository Project Office
2101 E. Calvada Boulevard, Suite 100
Pahrump, NV 89048, USA, jklenke@co.nye.nv.us

Christoph Spötl
Institute of Geology, Innsbruck University
Innrain 52
Innsbruck, 6020, Austria, christoph.spoetl@uibk.ac.at

Abstract
Caves in the Devils Hole Ridge near Ash Meadows (Nevada) are thought to have been formed by extensional tectonics. Here, we summarize observations of the morphologies of caves formed by condensation corrosion above a moderately thermal aquifer in the Devils Hole Ridge as well as at a site near Shoshone (California). At Devils Hole, water of the regional aquifer has been saturated with respect to calcite (i.e., non-aggressive) for the last two to three million years, hence speleogenesis in phreatic zone has been impossible. Meanwhile, potential local catchments are very small and the climate is arid, which precludes epigene speleogenesis. Any solutional forms can therefore be uniquely attributed to condensation corrosion.

Introduction
The term "condensation corrosion" refers to the development of cavities in soluble rock, above the water table, through the action of water, which originates from condensation of water vapor on the rock walls. Aggressiveness with respect to carbonate rock is caused by the uptake of gases (CO_2 or H_2S) from the cave air into the condensate giving rise to acidic solutions. Characteristic solution forms, such as spherical and hemispherical niches, bell holes, etc., develop where free convection of cave air is involved. Advective air movement typically produces smaller-scale cave wall morphologies. The highest potential for free convection is expected in hypogene settings, where the water is thermal (enhanced evaporation) and contains elevated amounts of CO_2 and/or H_2SO_4 (enhanced aggressiveness of condensate with respect to the carbonate rock).

In most cases studied so far, condensation corrosion developed during the latest stages of hypogene (thermal) speleogenesis, when caves, initially formed under phreatic conditions, emerged into the vadose zone (e.g., Sarbu & Lascu, 1997; Audra et al., 2007). This created a situation characterized by (a) a significant free water surface available for evaporation, and (b) open air-filled space in which convective air movement can develop. In addition, thermal gradients are typically high above thermal lakes, promoting both air convection and moisture condensation. With the exception of several unusual caves in Hungary (e.g., Sátorkö-puszta and Batori caves) for which condensation corrosion could be the leading if not the only speleogenetic mechanism, condensation corrosion in most caves does not affect the cave gross morphology, but is only responsible for modifications of the meso- and micromorphology.

Importantly, the two types of speleogenesis occurring at radically different environments—phreatic dissolution and condensation corrosion under vadose conditions—produce similar solutional forms. This commonly leads to confusion and difficulties in interpreting speleogenetic processes

Geology and Hydrogeology
The area of interest belongs to the northern Great Basin region, which has experienced large-scale extension during the last 20 million years. The extension was not uniform throughout the region; the study area lies within the greatly extended domain (Wernicke, 1992). Hydrologically, the study area belongs to the Death
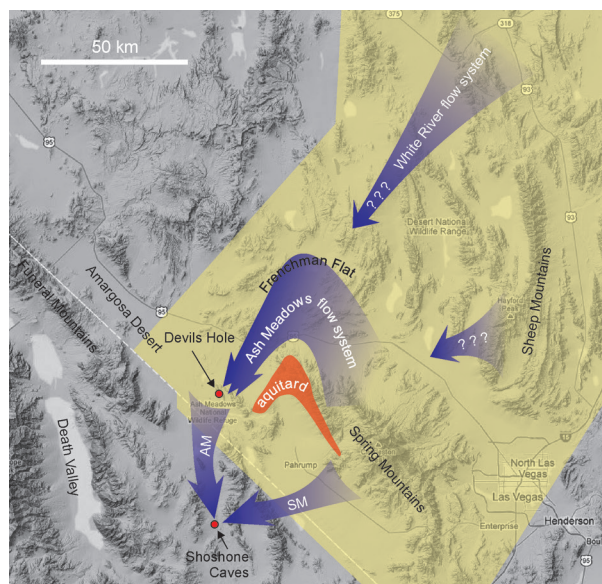
Figure 1.
Regional flow in the study area. The main flow path of the Ash Meadows Flow System is simplified from Winograd and Thordarson (1975). AM (Ash Meadow) and SM (Spring Mountain) are alternative flow paths proposed for the Tecopa Basin by Miner et al. (2007). The location of the carbonate corridor (colored yellow) is from Dettinger (1989), who did not map its extent beyond the Nevada-California border. Study sites are marked by red dots.

Valley regional groundwater flow system (DVRFS), a deep, fracture-controlled aquifer that encompasses approximately 100,000 km^2 of mountain ranges and low-elevation intermontane basins. Overall, groundwater in the DVRFS moves through permeable zones down hydraulic gradients from areas of recharge to regional areas of discharge. The topography produces numerous local subsystems within the major flow system. Water that enters the system in a recharge area may discharge in the nearest topographic low, or it may be transmitted to a regional discharge area.

Devils Hole Ridge is a small elongate mountain, approximately 3.0×0.7 km, built of Cambrian limestone (Bonanza King Formation), jutting out some 250 m above the floor of the southern Amargosa Desert. Immediately south of the Devils Hole Ridge lies the Ash Meadows oasis, the discharge area of the regional-scale (>12,000 km^2) Ash Meadows Groundwater Flow System. The latter is recharged by infiltration at the upper elevations of the Spring Mountains (about 3,600 m a.s.l., annual precipitation ~1,000 mm; Winograd et al., 1998). The water flows northwest toward Frenchman

Flat, merging with additional flow from the White River groundwater flow system along the way (Figure 1). From Frenchman Flat the water follows a high-transmissivity zone southward and ultimately discharges at the springs in the Ash Meadows oasis (Winograd and Thordarson, 1975). The curved flow path reflects the presence of an aquitard block at the northwestern end of the Spring Mountains (Figure 1).

The Shoshone site is located at the northern fringe of the Tecopa Basin. It represents a small hill, about 1.0×0.7 km, built of Cambrian limestone (Nopah Formation), rising about 80 m above the valley floor of the Amargosa river. The flow path bringing water to the basin is less certain. Current hydrogeological models of the DVRFS (e.g., Belcher, 2004; USGS, 2010) envisage a southwestward interbasin flow sourced from the Spring Mountains (Figure 1, SM). An alternative interpretation calls for a southward flow from the Ash Meadows-Amargosa Valley area (Figure 1, AM) along the Ash Meadows fault zone (e.g., Miner et al., 2007).

At both sites, caves are associated with steeply dipping extensional fractures. Aquifers tapped by the caves host moderately thermal water (34°C at Devils Hole and 30°C at Shoshone). This water is part of a regional groundwater flow system and has attained temperatures in excess of the mean annual air temperature that prevailed at the time and place of recharge (Miner et al., 2007). The carbonate aquifer tapped at both sites is not a simple artesian (confined) aquifer; due to the complex geologic structure of the area, it is confined by young and partly indurated sediments beneath valleys and unconfined beneath ridges.

Caves of the Devils Hole Ridge
Four caves are known in the Devils Hole Ridge.

The first, the famous Devils Hole, represents a nearly rectangular 23×7 m surface collapse into a steeply dipping fault-controlled fissure, which intersects the water table at 15 m below the land surface forming a 1.8×5.5 m pool. The water-filled part of this tectonic cave extends more than 140 m deep. The surface collapse represents a remnant of the subaerial chamber, which probably collapsed 50 to 60 kyr ago (Riggs, 1991). Another subterranean air-filled chamber, Browns Room, lies about 50 m northeast of Devils Hole; it is only accessible by SCUBA diving.

Devils Hole #2 cave (a.k.a. Devils Hole Cave) is located 200 m north of Devils Hole proper. It represents a NE-striking extensional fissure that intersects the water table at a depth of 43 m. The fissure was concealed at

the surface by an approximately 1.5-m-thick layer of carbonate-cemented alluvium/colluvium of Pliocene-Pleistocene age associated with a small WNW-trending wash on the eastern slope of the Devils Hole Ridge. The entrance to the cave opened when this indurated layer was breached from below by condensation corrosion. The cave consists of two chambers separated by a "plug" of collapsed blocks. The upper chamber is near-vertical, 5×15 m wide and 25 m high. The floor of the chamber is largely horizontal, and consists of the collapsed rocks. The lower chamber represents a tectonic fissure dipping approximately 60°, which intersects the thermal water table and continues underwater for more than 50 m.

Devils Hole Prospect is a cave located 50 m north of and about 12 m higher than Devils Hole proper. The entrance to the cave was opened during mineral prospecting, in the course of which indurated alluvium/colluvium material filling an approximately 1.5-m-wide fissure in the limestone, striking 220°, was removed. Unlike other caves in the Devils Hole Ridge, whose internal volume was created primarily by extensional tectonics, the Devils Hole Prospect Cave owes its enlargement almost exclusively to dissolution. The cave is carved in both Paleozoic limestone and indurated fault filling. Parts of the cave hosted by carbonate rocks show a characteristic solution-related morphology with abundant spherical niches, cusps, pendants, partitions, and cupolas. The same morphologies can be seen in the calcite-cemented fault-fill material.

The last unnamed cave is a collapse in alluvium, related to an extension fissure underneath, which occurs

approximately 1.1 km north of Devils Hole, as noted by Carr (1988). In 2014, the entrance was 2.5×1.5 m wide (Figure 2). Under an approximately 3-m layer of moderately indurated alluvium, an approximately 1-m-wide extension fissure opens in Cambrian limestone. The surface of the fissure is smoothed by dissolution. The fissure narrows and becomes impassable in both directions along strike as well as at a depth of about 10 m. The cave air is dry; there is presently no direct connection to the thermal water table beneath.

Caves Near Shoshone

Shoshone Cave was first described by Emerson (1951). Two caves, Upper and Lower Shoshone, were later reported as a habitat of the endemic whip-scorpion *Trithyreus shoshonensis* (Brigs and Hom, 1972). The authors noted that the survival of these scorpions would not be possible in the freezing winters of the Californian desert if not for the heating of cave by thermal groundwater.

Examining the site in February 2014, we found three caves, all opened or modified by mining operations. Similarly to Devils Hole Ridge, caves at Shoshone have characteristic "extension fissure" morphologies, modified by condensation-related dissolution.

Figure 2.
Unnamed cave in alluvium north of Devils Hole. The layer of alluvium penetrated by collapse (a) is about 3 m thick. The solution-widened fissure in Cambrian limestone underneath (b) is about 1 m wide; it narrows and becomes impassable about 10 m deeper.

Figure 3.
Lower Shoshone Cave. Solution morphology due to condensation corrosion in the upper part of the cave. Width of the solution channel is approximately 80 cm.
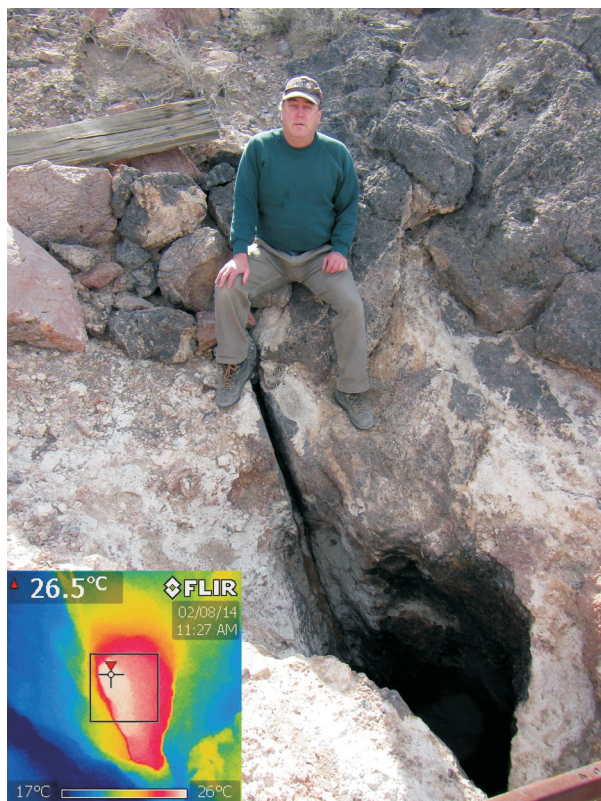
Figure 4.
Entrance to Upper Shoshone Cave. Insert: thermal image of the entrance taken using a FLIR i7 infrared camera, showing that warm air is exhaled from the cave.

The Lower Shoshone Cave was affected by mining operations (purportedly, prospecting for hematite). At the bottom, the cave intersects the slightly thermal (30°C) aquifer in a small, 1×1.5 m wide pond. The steep fissure continues below the water surface to unknown depth. A ca 1 cm thick mammillary calcite crust is present on some of the rock under water. Because of the large opening at the entrance, the outside cool air flows into the cave, lowering the temperature inside to 22-23°C (measured in February 2014) and lowering the humidity (i.e., non-condensing). The upper part of the cave, where the fissure is up to 5 m wide, features abundant solutional forms (Figure 3), including cupolas and pendants.

In places, cave walls show patches of white popcorn-like botryoidal calcite, deposited under subaerial conditions.

The Upper Shoshone Cave does not provide direct access to the water table, although it is clearly connected to it by impassable passages. The air temperature in the cave exceeds 26°C (Figure 4) and the humidity

at the time of visit was close to 100%, resulting in condensation. Near the entrance, condensation of humid air resulted in the growth of patches of green moss.

The walls of the caves are smooth, affected by solution, and commonly feature pendants, side wall cupolas, partitions, and rock bridges. Patches of subaerial popcorn calcite are present as well (Figure 5).

Figure 5.
Upper Shoshone Cave. Solution forms and a patch of subaerial popcorn (lower right corner). Picture taken looking down into the narrowing (impassable) continuation of the cave.

The Middle Shoshone Cave can be accessed through an artificially widened pit in the limestone and is equipped with a wooden ladder. The pit leads to a natural part of the cave which shows morphologies and deposits that are very similar to the other two Shoshone caves.

Monogenetic Solution Cavities

All the caves from Devils Hole Ridge and Shoshone site are associated with extensional fissures. In fact, in all but one (Devils Hole Prospect Cave), most of the cave volume can be attributed to tectonic extension, while dissolution can be held responsible for the meso- and micro-morphological features.

Figure 6.
Solution cavity in the Devils Hole ridge. Note the absence of a guiding fissure and calcite corallites coating the walls. Corallite from an adjacent cavity was dated to 413 ± 12 and 318 ± 8 kyr (Dublyansky and Spötl, 2015).

This does not hold true for smaller cavities found at both sites. Such cavities commonly develop in massive rock, lacking any guiding cracks or fissures. Cavities are exposed on bedrock slopes, and are truncated by slope retreat to different degrees: some of them open as small-diameter (7-10 cm) holes which widen inward, whereas others are truncated or even almost completely destroyed. The common morphological feature of these cavities is their near-circular cross-section in plan view. In vertical cross-section they show spherical, spheroidal (vertically elongated), and tubular shapes. The diameter of the cavities ranges between 10 and 130 cm. Many of them are filled with loose detrital deposits (silt, sand, and gravel). Most of the cavities have barren walls, but some host speleothems formed under subaerial conditions (corallites, popcorn; Figure 6).

The largest solution cavity formed without obvious relation to extension tectonics was observed at the Shoshone site (Figure 7). It is a fragment of a vertical cave channel with a complex cross-section (combination of circular and flattened tubes). At some point in time the cave was truncated by denudation and filled by detrital material.

Meso-Morphological Features Produced by Condensation Corrosion Speleogenesis

Initially, the origin of Devils Hole was attributed to solution enlargement of tectonic fractures (Winograd and Thordarson, 1975; Dudley and Larson, 1976). Subsequently, Riggs et al. (1994) posited a purely

Figure 7.
Solution cave exposed by retreat of the rock surface, Shoshone. The cavity was cleaned from detrital deposits.

tectonic (i.e., extensional) origin of the Devils Hole passages, a process they dubbed "tectonic speleogenesis." Condensation corrosion was identified as an agent responsible for partial destructions of calcite deposits in Browns Room, a subaerial chamber in Devils Hole (Riggs and Deacon, 2002). Subsequently, Dublyansky and Spötl (2015) described a wide spectrum of condensation corrosion-related morphological features in the Devils Hole Ridge. Our observations indicate that similar morphologies are also observed in the Shoshone caves.

Solution-Smoothed Walls
Solution-smoothed walls were observed in the upper chamber of Devils Hole #2, in Devils Hole Prospect and in all three Shoshone caves. The walls parallel to the strike of the fissures are uniformly affected by solution, creating smooth slightly undulating surfaces.

Flat Channels Along Fractures and Calcite Veins
Small channels with characteristic solution morphology, precluding any involvement of gravity-driven water flow, cut through both the bedrock limestone and the calcite veins on the eastern and western walls of the upper chamber of Devils Hole #2. The orientation of the channels coincides with the orientation of the chamber, which suggests that they developed along preexisting extensional fractures (and associated calcite veins).

Cupolas in Indurated Alluvium-Colluvium
The ceilings of the upper chambers of Devils Hole #2 and Devils Hole Prospect are composed of carbonate-cemented colluvium/alluvium. Dissolutional cupola-

like forms are present in the ceilings with the solution surfaces cutting uniformly across massive limestone bedrock as well as alluvium/colluvium consisting of cobbles, finer-grained material, and carbonate cement. Small cupola-shaped cavities (10 to 50 cm in diameter) in this heterogeneous material are locally separated by millimeter-thin partitions.

Horizontal Tubes

Two horizontal solution channels 3- to 7-m-long with a roughly isometric cross-section of 30-50 cm in diameter were found in the vertical walls of the Devils Hole #2 and Devils Hole Prospect caves. Although the development of horizontal channels is difficult to rationalize in the context of the condensation corrosion, we suggest that it is another morphological form related to this speleogenetic mechanism.

Punk Rock

The southern wall of the upper chamber of Devils Hole #2 shows a layer of soft powdery material, extending into the wall up to 2 cm and eventually passing into hard unaltered limestone. Despite its softness, the layer preserves the original structure and coloration of the bedrock. We propose that the "punk rock" alteration is a manifestation of condensation corrosion.

Pendants, Partitions, and Undulating Tubular Channels

These smaller and more elaborate solution morphologies were observed in Devils Hole Prospect and in the Upper and Lower Shoshone Caves (Figures 3 and 5).

Discussion

Condensation Corrosion: Dead or Alive?

Due to the very small potential of vadose recharge on the Devils Hole Ridge (surface area about 2 km2, vadose zone less than 250 m thick) epigenic speleogenesis was deemed to be largely impossible there, even under less arid climate conditions in the past. The Shoshone site seems to be equally or even less suitable for epigenic karst development. Its surface area is only about 0.7 km2, and the elevation above the valley floor does not exceed 80 m.

Condensation corrosion appears to be the only mechanism capable of producing solutional cavities in such locations. In Devils Hole Ridge, dissolution processes developed above a slightly thermal (34°C) aquifer, which has been slightly supersaturated with respect to calcite (i.e., incapable of bedrock dissolution) for the last several million years. The Shoshone caves are located above an aquifer with a temperature of 30°C.

On the basis of a microclimatic study, Dublyansky and Spötl (2015) concluded that condensation corrosion is not presently operational in any of the studied caves of Devils Hole Ridge. All these caves are presently open to the dry desert atmosphere, which drastically reduced the potential of condensation. Active development of the process elsewhere in the subsurface of the Devils Hole Ridge is entirely possible and even likely. At Shoshone, the Lower Cave is well ventilated and condensation corrosion no longer operational. In contrast, the Upper Shoshone cave has a tight entrance, restricting ventilation. Condensation is still active there, and can be observed on the walls near the entrance (Figure 8).

Figure 8.
Condensation droplets and moss near the entrance to Upper Shoshone Cave. The width of picture is approximately 7 cm.

Conditions Promoting Condensation Corrosion

Structural Conditions

One of the parameters controlling the amount of evaporation from a thermal water table (and, therefore, the amount of water available for condensation corrosion) is the surface area of the subterranean thermal lake. The potential of condensation corrosion increases with increasing evaporation surface. In many hypogene caves, condensation corrosion occurred during late stages of hypogene karstification above thermal lakes. As discussed above, at Devils Hole Ridge, subaqueous karstification can be ruled out because the water has been saturated with respect to calcium carbonate for perhaps as long as three million years. At both Devils Hole Ridge and Shoshone, the cavities occupied by the subterranean thermal lakes were created by extensional tectonics. Such lakes occur whenever open fractures intersect the thermal water table. Because the region

has remained in an extensional regime since the mid-Tertiary, such subterranean thermal water bodies are likely to be widespread and, by inference, condensation corrosion may have occurred (and likely still occurs) in many as yet unidentified locations.

In addition to creating evaporation surfaces, extensional fractures provide an open space above the thermal water table in which free air convection can develop. Extensional tectonics, collapse, and condensation corrosion operate in concert creating and enlarging the open space underground. As none of the processes has direct relationship to the Earth's surface, the result of this concerted action will remains unnoticed at the surface above these cavities, until the upward-propagating cavities intersect with the land surface due to denudation.

Thermal Conditions

A temperature gradient exists between the body of thermal water and the land surface. The aquifer underneath Devils Hole Ridge has maintained a nearly constant temperature of about 34°C for hundreds of thousands of years (Kluge et al., 2014; Tripati et al., 2015), meaning that the thermal conditions for condensation corrosion may have persisted for an equally long period of time. Extensional tectonic conditions could also create fractures that are open to the surface but do not intersect the thermal water table. Movement of cool air in such fractures provides additional cooling of the rock mass and leads to the development of a complex thermal field in the vadose zone of the rock including local thermal gradients in the bedrock, which are not vertical.

Microclimatic Conditions

The potential for and the intensity of condensation change with distance from the heat source (thermal lake). Condensation corrosion is least intensive near the thermal water table, where the difference in temperature between the thermal water pool and the surrounding rock is small. As the warm and moist air buoyantly moves upward along an open fracture, it cools. At a certain distance, its temperature may reach thermal equilibrium with the surrounding rock. Both buoyant movement and condensation will then no longer be possible. Additionally, the heat released due to condensation warms the rock surface, decreasing the local thermal air-rock gradient. For condensation to proceed, this heat must be removed through solid-state thermal conduction (Dreybrodt et al., 2005) and/or by downward flow of the condensate. It can be inferred, therefore, that there is a certain combination of parameters at which condensation corrosion is most intensive, and this combination is specific to each given cave configuration.

Condensation corrosion stops as soon as the conditions necessary for its operation cease to exist. One of the most efficient ways to stop condensation corrosion is to drastically change the microclimate inside the cave, for example, by enabling ventilation. In desert climatic conditions, such as at Devils Hole Ridge and Shoshone, condensation corrosion will slow down when a channel or cupola carves its way up through the rock and intersects with the land surface. Cool and dry air flow into the cave and mix with ascending warm and moist air decreasing its temperature and relative humidity. Condensation may terminate entirely if enough dry air enters the cave. In non-desert conditions, the downward flow of cool and moist air after the opening of the cave to the surface will not necessarily terminate condensation corrosion.

Acknowledgements

References

Audra P, Hoblea F, Bigot J-Y, Nobecourt J-C. 2007. The role of condensation-corrosion in thermal speleogenesis: study of a hypogenic sulfidic cave in Aix-Les-Bains, France. Acta Carsologica 36 (2): 185-194.
http://dx.doi.org/10.3986/ac.v36i2.186

Belcher WR, editor. 2004. Death Valley regional ground-water flow system, Nevada and California; hydrogeologic framework and transient ground-water flow model. United States Geological Survey Scientific Investigations Report 2004-5205.

Briggs TS, Hom K. 1972. A cavernicolous whip-scorpion from the northern Mojave Desert, California (Schizomida: Schizomidae). Occasional Papers of the California Academy of Sciences, No. 98.

Carr WJ. 1988. Geology of the Devils Hole area, Nevada. U.S. Geological Survey Open-File Report 87-560.

Dreybrodt W, Gabrovšek F, Perne M. 2005. Condensation corrosion: a theoretical approach. Acta Carsologica 34 (2): 317-348.

Dublyansky YV, Spötl C. 2015. Condensation-corrosion speleogenesis above a carbonate-saturated aquifer: Devils Hole Ridge, Nevada. Geomorphology 229: 17-29.
http://dx.doi.org/10.1016/j.geomorph.2014.03.019

Dudley WW, Larson JD. 1976. Effect of irrigation pumping on desert pupfish habitats in Ash Meadows, Nye County, Nevada. U.S. Geological Survey Prof. Paper 927.

Emerson D. 1951. Shoshone Cave. California Caver 3 (3): 2.

Faunt CC, D'Agnese FA, O'Brien GM. (2004). Hydrology. In: Belcher WR, editor. Death Valley regional ground-water flow system, Nevada and California—hydrogeologic framework and transient ground-water flow model. U.S. Geological Survey Scientific Investigations Report 2004–5205. pp. 141-163.

Kluge T, Affek HP, Dublyansky Y, Spötl C. 2014. Devils Hole paleotemperatures and implications for oxygen isotope equilibrium fractionation. Earth and Planetary Science Letters 400: 251-260. http://dx.doi.org/10.1016/j.epsl.2014.05.047

Maxey GB, Mifflin MD. 1966. Occurrence and movement of ground water in carbonate rocks of Nevada. National Speleological Society Bulletin 28 (3): 141-157.

Miner RE, Nelson ST, Tingey DG, Murrell MT. 2007. Using fossil spring deposits in the Death Valley region, USA to evaluate palaeoflowpaths. Journal of Quaternary Science 22: 373-386. http://dx.doi.org/10.1002/jqs.1077

Riggs AC.1991. Geohydrologic evidence for the development of Devils Hole, southern Nevada as an aquatic environment. In: Pister EP, editor. Proceedings of the Desert Fishes Council, Volumes 20 and 21. p. 47–48.

Riggs AC, Carr WJ, Kolesar PT, Hoffman RJ. 1994. Tectonic speleogenesis of Devils Hole, Nevada, and implications for hydrogeology and the development of long, continuous paleoenvironmental records. Quaternary Research 42: 241-254. http://dx.doi.org/10.1006/qres.1994.1075

Riggs AC, Deacon JE. 2002. Connectivity in desert aquatic ecosystems: the Devils Hole story. In: Sada DW, Sharpe SE, editors. Spring-fed wetlands: important scientific and cultural resources of the intermountain region, May 7-9, 2002, Las Vegas, NV. DHS Publication No. 41210.

Sarbu SM, Lascu C. 1997. Condensation corrosion in Movile cave, Romania. Journal of Cave and Karst Studies 59 (3): 99-102.

Tripati AK, Hill PS, Eagle RA, Mosenfelder JL, Tang J, Schauble EA, Eiler JM, Zeebe RE, Uchikawa J, Coplen TB, Ries JB, Henry D, 2015. Beyond temperature: clumped isotope signatures in dissolved inorganic carbon species and the influence of solution chemistry on carbonate mineral composition. Geochimica et Cosmochimica Acta 166: 344-371. http://dx.doi.org/10.1016/j.gca.2015.06.021

USGS (U.S. Geological Survey), 2010. Death Valley regional groundwater flow system, Nevada and California—hydrogeologic framework and transient groundwater flow model. Belcher WR, Sweetkind DS, series editors. U.S. Geological Survey, Professional Paper 1711.

Wernicke BP. 1992. Cenozoic extensional tectonics of the U.S. Cordillera. In Burchfiel BC, Lipman PW, Zoback ML, editors. The Cordilleran orogen—conterminous U.S. Geology of North America, Volume G-3. Boulder (CO): Geological Society of America. p. 553-581.

Winograd IJ, Riggs AC, Coplen TB. 1998. The relative contributions of summer and cool-season precipitation to groundwater recharge, Spring Mountains, Nevada, USA. Hydrogeology Journal 6: 77-93. http://dx.doi.org/10.1007/s100400050135

Winograd IJ, Thordarson W. 1975. Hydrogeologic and hydrochemical framework, South-Central Great Basin, Nevada-California, with special reference to the Nevada Test Site. U.S. Geological Survey Prof. Paper 712-C.

ACTIVE HYPOGENIC KARST IN ITALY

Sandro Galdenzi
Viale Verdi, 10, Jesi, 60035, Italy, galdenzi.sandro@tiscali.it

Marco Menichetti
University of Urbino
Pure and Applied Sciences Department,
Campus Scientifico Urbino, 61029, Italy, marco.menichetti@uniurb.it

Abstract
Hypogenic speleogenesis, dissolution by aggressive and deep-seated fluids, is the dominant cave formation process for the most important karst systems in Italy. Endogenic H_2S and CO_2 are the main corrosive agents of underground karst corrosion. Throughout the region, evidence of all end-members of karst processes can be found, from solution limestone caves to deposition of carbonate travertine. The redox reactions in the groundwater and in the atmosphere involve chemoautotrophic microbial activity. The presence of active hypogene branches in many caves permits a direct study of the karst-forming processes, as well as a comparison with resultant morphologies.

Introduction
Limestone karst speleogenesis is a morphological process involving the removal of mass from a host rock via an aggressive chemical agent transported by a fluid vector. Exogenous, soil-derived CO_2 is the chemical agent responsible for the formation of epigenic limestone caves, while endogenic agents are responsible for the corrosion seen during hypogenic cave speleogenesis (chemical, physical, or both; e.g., CO_2, H_2S, cooling, mixing, etc.). The fluid vector flowing through the rock mass could be water or a gas. The main difference between epigenetic and hypogenic speleogenesis, however, is related to the origin of the corrosive agents. Epigenic speleogenesis is a process that normally propagates downward from the surface through soil zone to depth through the subsurface drainage network. On the other hand, hypogene speleogenesis is related to the upward flow of deep-seated solutions generated at depths.

The Italian Peninsula is probably the world's best location to observe both the active and fossil hypogenic speleogenesis processes in different geological contexts (Galdenzi and Menichetti, 1989; Galdenzi, 2009; Menichetti, 2009) (Figure 1). All the end-members of the karst processes can be found here, from epigenetic limestone caves to hypogenic mazes to deposition of carbonate travertine. For more than a century of speleological research, many hypogenic limestone caves have been explored, mapped, and studied (Principi, 1931). In some of these cave systems, speleogenetic corrosional processes linked to the endogenic CO_2 and H_2S vents are active and directly observable.

Active and fossil hypogenic caves are known in the regions of Tuscany, Umbria, Marche, Latium, Campania, and Calabria. These caves are characterized by a variety of patterns and morphological sizes, including three-dimensional maze systems and deep shafts. In many cases, the caves are developed at several levels, which is related to the evolution of an external hydrographic network.

The local geological and structural features of the different areas, and the hydrology and groundwater flow modalities have led to the development of different cave morphologies.

Hydrogeological Framework
Analyses of the different morphological aspects of these karst systems in Italy have allowed the identification of primary formation processes within a geological and hydrogeochemical framework. Hypogene speleogenesis driven by deep-seated fluids is the cave formation processes for the most important karst systems in the Italian Apennines. Here, H_2S and endogenic CO_2 are the main agents of underground karst corrosion.
\
In many caves, hypogenic processes can be linked to the oxidation of H_2S that produces sulfuric acid as oxygen-rich groundwaters mix. In caves, the resulting limestone corrosion produces gypsum deposits that could be assumed to be indicators of hypogene speleogenesis. The cave morphologies show that the H_2S oxidation zone is not restricted to the shallow groundwater levels but can be extended to the deeper sections of the aquifer, which are fed by freshwater via a complex regional hydrogeological flow paths. Along the Peninsula, general low temperature CO_2 gas emissions are known,

with flow rates estimated at 10^{11} mol y^{-1} in proximity of the main outcrops of travertine deposits. The pCO_2 values of the groundwater range from 0.03 to 0.1 atm. This increases the solubility of $CaCO_3$ by an order of magnitude with respect to the soil pCO_2 typicall of epikarstic waters. The action of endogenic CO_2 in the cave formation, especially at lower temperatures, is not easy to detect, and the resulting cave morphology is not indicative of any specific cave formation process (Menichetti, 2011).

The travertine and tufa deposits represent the other end-member of karst processes as the product of the limestone dissolution by deep-seated fluids. These deposits form as a result of degassing of surfacing CO_2-rich groundwater containing >2 mmol L^{-1} calcium. Geothermal anomalies are particularly common along the Tyrrhenian side of the Peninsula (Figure 1). The cooling of thermal water during its ascent along conduits increases its CO_2 aggressiveness, with corrosion acting almost uniformly along fracture surfaces and producing a dramatic increase in hydrologic flow and karst void development.

The Hypogenic Caves

Along the Peninsula, karst is not homogeneously distributed, despite the presence of large limestone outcrops (Figure 1). In the Umbria-Marche Apennines area, the presence of major hypogenic caves is well-documented by several decades of research and exploration. Caves in this region are known for their vertical karst systems, such as Monte Cucco and Faggeto Tondo, and the maze systems of the still-active Frasassi Gorge and Acquasanta Terme caves. The main cave systems consist of a few tens of kilometers of solutional passages with galleries and shafts, which are characterized by large rooms, cupola and blind pits, anastomotic passages, bubble trails, roof pendants, knife edges, and phreatic passages (Galdenzi & Menichetti, 1995). The phreatic morphologies are widely diffuse in both active and fossil karst systems, indicating the important actions operated by aggressive gas during its ascent into the upper levels of the groundwater.

In the Lazio and Campania regions, where many Jurassic limestones experienced a Plio-Quaternary K-alcaline and calcalkaline volcanism, the hypogenic karst is marked by the presence of the Pozzo del Merro shaft and active large travertine deposits a few kilometers northeast of Rome. In these regions, high values of CO_2 and H_2S have been recorded in several cave systems.

In the southernmost regions, other hypogenic active karst systems have been identified at Capo Palinuro along the Tyrrhenian Sea coast. These systems are located in correspondence with several submarine H_2S vents in a setting where speleogenetic evolution is linked to sea level oscillations. In the northern Calabria region, hypogenic caves related to thermal sulfidic springs are known in three different areas, and active cave-forming processes occur in the Sibari area.

The Active Caves

The presence in many hypogenic caves of an active section permits a direct study of karst-forming processes as well as a comparison with the derived morphologies. In the whole Italian Peninsula, the main active cave-forming processes can be related to the oxidation of H_2S to sulfuric acid in the groundwater as well as in the atmosphere where the redox reactions involve chemoautotrophic microbial activity (Sarbu et al., 2000). Stratification and mixing of different waters with significant variations in chemistry, temperature, TDS and pH are well documented in almost all of the active caves., A significant amount of organic matter can grow in the sulfidic streams and close to the water table, as white filaments can be seen as meter-long seaweed-like structures in deep cave pools in Frasassi. The sulphur-oxidizing bacterial communities, which use H_2S as an energy source, support invertebrate life, producing a wholly chemoautotrophic aphotic ecosystem in the Frasassi sulfidic cave sections (Sarbu et al., 2000). The role played by these microbial communities in the limestone corrosion is not well understood. Data from the Frasassi caves show that oxidizing bacteria living in the cave streams do not play an active role in the production of acidity (Jones et al., 2015).

Close to the sulphidic streams, air moisture is rich in H_2S and CO_2, which is released from the groundwater and acts as a main agent of limestone-wall corrosion. The corrosion first appears on limestone as small white spots of about 1 cm in diameter. In these spots the calcium carbonate is replaced by gypsum, which can expand into a continuous rim of microcrystalline gypsum. At the limestone/gypsum interface, a sulphur-oxidizing bacteria biofilm plays an important role in the limestone corrosion. This biofilm, consisting of organic mucous matter, arranges in small formations like spider webs and thin "stalactites" with acid drops having pH <1 (Sarbu et al., 2000). The gypsum is often squashy and can easily fall in the floor, producing large deposits, as directly observed in the Acquasanta Caves.

This depositional mechanism can explain the large gypsum deposits in non-active hypogenic caves, also comprising the "gypsum glaciers" produced by post-depositional flow and accumulation. A similar origin

is consistent with stable isotope data. All gypsum deposits in M.Cucco, Frasassi Gorge, Pozzi della Piana, Acquasanta, and the Lepini Mountains have negative values of $\delta^{34}S$ ratio, which are compatible only with a derivation from H_2S released by groundwater. In the sulfidic groundwater, $\delta^{34}S$ is significantly different in sulphide (which is always negative) and dissolved sulphate (which is always highly positive).

The rate of limestone corrosion due to endogenic H_2S action on calibrated limestone slabs has been tested in a five-year experiment. The slabs were positioned in the sulphidic branch of the Frasassi cave system, both in air and water. The slab surface was replaced with gypsum at a rate of limestone corrosion of about 0.05 mm y^{-1} (Galdenzi et al., 1997). A subsequent experiment in groundwater showed that corrosion rate is influenced by flow dynamics and can increase to 1 mm y^{-1} with a weakly turbulent flow. A comparison of the measured corrosion rate with cave wall retreat has shown that active corrosion processes have acted at the same intensity throughout the caves' history (Galdenzi, 2012).

Modeling

Even though general speleogenetic reactions are known, the precise geological, hydrogeological, and geochemical conditions of their occurrence need to be documented. In particular, the reactions at the gas/water interface (H_2S, CO_2) and especially the role played by organic matter require further and more detailed research. Building a fluid flow model through a limestone mass could be one way to understand hypogenic karst processes and explore the relationship between lithology, tectonics, hydraulics, geochemistry, and geothermal setting.

A simple regional ground water flow model is critical to understanding heat and mass transport in hydrogeological systems related to active hypogenic caves. A multiphysics model that takes into account the hydraulic, thermal, and physical-chemical conditions of the Acquasanta Terme karst system indicates that a simple thermal convection at basin scale is not sufficient to explain the water temperature and geochemistry recorded in the sulphidic spring; an external heat source is necessary.

Conclusions

A more dynamic view of cave pattern development and evolution in space and time that will take into account the general altitude variations of the regional water table level together with episodic gas emissions needs to be considered.

The best conditions for hypogene cave development typically occur in small limestone outcrops covered by low-permeability units, in which fluids rising from depth can reach an oxidizing environment or mix with descending freshwater. However, some hypogenic caves also occur in open hydrogeologic massifs, where epigenic caves prevail, due to the high intensity of the corrosion.

Hypogenic caves generally have a multistage evolution related to the progressive incising of surface streams and the depression of the related base level. The great variety of examples in different geological settings offered by the Apennines make it a good place to evaluate the influence of geologic and geomorphic factors on hypogenic cave formation.

References

Galdenzi S. 2009. Hypogene caves in the Apennines (Italy). In: Klimchouk AB, Ford DC, editors. Hypogene speleogenesis and karst hydrogeology of artesian basins. Simperfol Ukrainian Institute of Speleology and Karstology, Special Paper 1: 101-115

Galdenzi S. 2012. Corrosion of limestone tablets in sulfidic ground-water: measurements and speleogenetic implications. International Journal of Speleology 4 (2): 25-35. http://dx.doi.org/10.5038/1827-806x.41.2.3

Galdenzi S, Menichetti M. 1989. Evolution of underground karst systems in the umbria-marche Apennines in Central Italy. Proceedings of the 10th International Congress of Speleology, Budapest, (3) p. 745-747.

Galdenzi S, Menichetti M. 1995: Occurrence of hypogenic caves in a karst region: examples from central Italy. Environmental Geology 26: 39-47. http://dx.doi.org/10.1007/BF00776030

Galdenzi S, Menichetti M, Forti P. 1997. La corrosione di placchette calcaree ad opera di acque sulfuree: dati sperimentali in ambiente ipogeo. Proceedings of the 12th International Congress of Speleology, (1) p. 187-190.

Jones DS, Polerecky L, Galdenzi S, Dempsey BA, Macalady JL. 2015. Fate of sulfide in the Frasassi cave system and implications for sulfuric acid speleogenesis. Chemical Geology 410: 21-27. http://dx.doi.org/10.1016/j.chemgeo.2015.06.002

Menichetti M. 2009. Speleogenesis of the hypogenic caves in Central Italy. Proceedings of the 15th International Congress of Speleology, p. 909-915.

Menichetti M. 2011. Hypogenic cave in Western Umbria (Central Italy). Acta Carsologica 40 (1): 129-145. http://dx.doi.org/10.3986/ac.v40i1.33

Principi P. 1931. Fenomeni di idrologia sotterranea nei dintorni di Triponzo (Umbria). Le Grotte d'Italia, 5: 1- 4.

Sarbu SM, Galdenzi S, Menichetti M, Gentile G. 2000. Geology and biology of the Frasassi Caves in Central Italy, an ecological multi-disciplinary study of a hypogenic underground ecosystem. In: Wilkens H, et al., editors. Ecosystems of the world. New York (NY): Elsevier. p. 359-378.
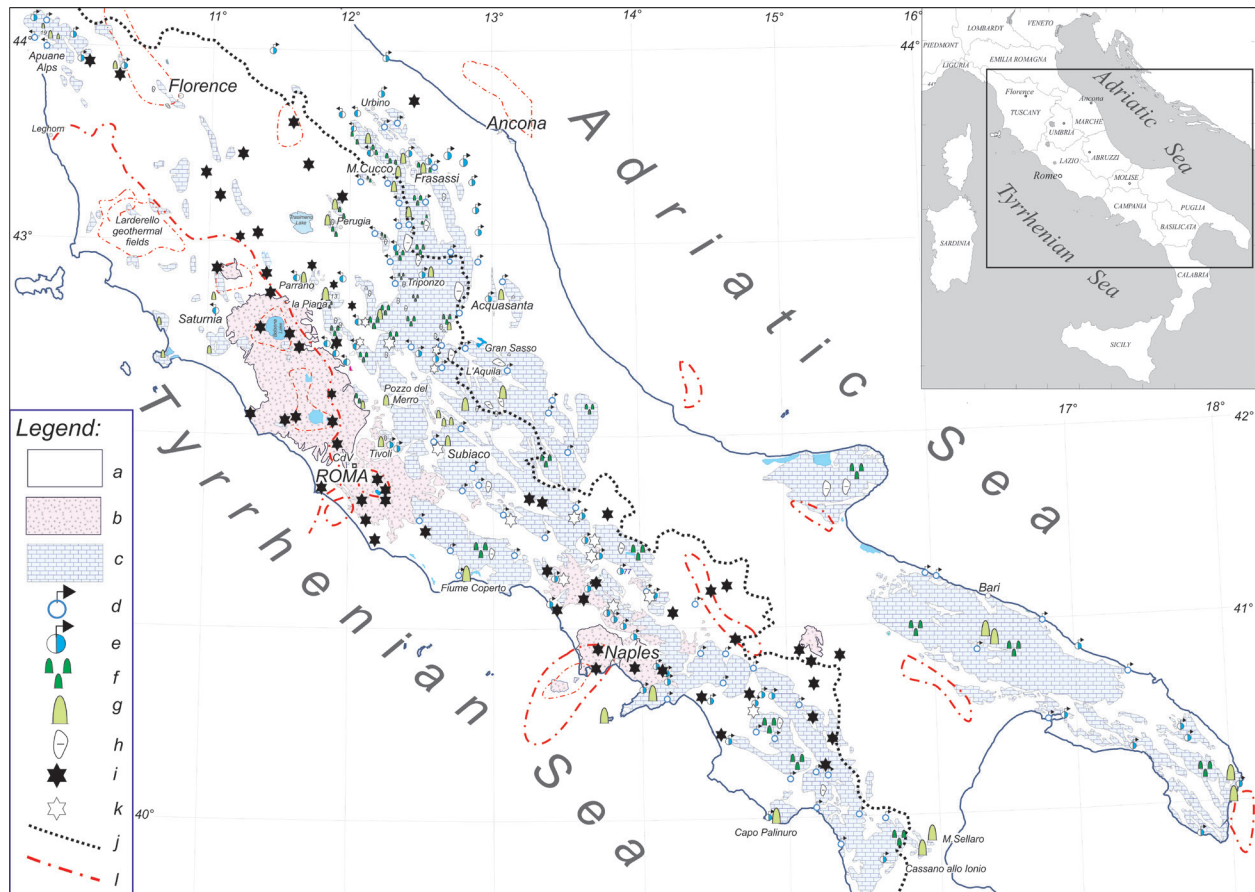
Figure 1.

Legend: (a) stratigraphic succession from Quaternary to Miocene; (b) Quaternary volcanic rocks; (c) the main calcareous stratigraphic succession from Jurassic to Miocene; (d) the main karstic spring; (e) the main mineralized spring; (f) important caves; (g) hypogenic caves; (h) close valley with karstic drainage; (i) CO_2-rich gas vent; (k) spring rich in CO_2 gas; (j) Apennines water divide; (l) geothermal heat flux, the thick dotted line indicates 100mW/m. In Larderello geothermal field, the heat flux reaches 400 mW/m.

STRUCTURAL CONTROL OF RELICT HYPOGENE KARST FEATURES IN THE OWL MOUNTAIN PROVINCE, FORT HOOD MILITARY INSTALLATION, TEXAS

Melinda S. Faulkner

Stephen F. Austin State University
Department of Geology
P.O. Box 13011, SFA Station
Nacogdoches, TX 75962-3011, mgshaw@sfasu.edu

Kevin W. Stafford

Stephen F. Austin State University
Department of Geology
P.O. Box 13011, SFA Station
Nacogdoches, TX 75962-3011, staffordk@sfasu.edu

Abstract

The Owl Mountain Province is a karst landscape with Lower Cretaceous Trinity and Fredericksburg Group carbonates found in outcrop and in the sub-surface. The area has been described as one of the high energy shoals that formed on the Comanche Platform behind the Stuart City Reef trend. These shoals—including Moffatt Mound, Nolan Creek Province, and Owl Mountain Province—were formed along the western flank of the Belton High, and are lithologically distinct from the main Edwards reef trend; the strata associated with these shoals formed in more restricted circulation waters and variances in depositional environments control the minor differences in lithology.

The Owl Mountain Province covers 89 km^2 and is located on the eastern peninsula of the Fort Hood Military Installation in Bell and Coryell Counties. It is bounded by Owl Creek to the north, Cowhouse Creek to the south, Belton Lake to the east, and the live fire range to the west. The topography is dominated by a broad, dissected plateau capped by the resistant, rudistid-rich Edwards limestone. Steep scarps along the edges of the plateau expose the Comanche Peak limestone; lower valleys along the creeks are mantled with thick soils derived over the Walnut Clay. Exposures along these scarps reveal significant karst development near the Comanche Peak and Edwards boundaries, surficial karst features associated with these plateaus include sinks and caves associated with upward stoping and collapse structures with significant overprinting by epigenic processes. Today, many of these cave features have been heavily overprinted by epigenic processes and impacted by anthropogenic surface modifications, therefore the identification and discussion of true hypogene features can be problematic.

Many of the surface and subsurface features are fracture-controlled, with both local and regional trends. Regional uplift during late Oligocene and early Miocene of the Edwards Plateau and Lampasas Cut Plain occurred as a result Balcones deformation. This uplift resulted in the development of conjugate joint sets within the Owl Mountain Province, exerting significant control on cave development and the trend of some sub-surface hydrologic flow regimes. Uplift along the Balcones front initiated rapid downcutting of existing drainage systems and as stream segments incised exposed rock, the intersection of fracture conduits with stream base level helped widen cavities and develop spring discharge outlets.

Along the scarps where the Edwards and Comanche Peak limestones are interbedded, varying permeabilities have partially confined hypogene and/or phreatic waters. These confining units have created potentiometric pressures and allowed preferential dissolution along ascending flow paths. Grottos and niches exposed in scarp faces along the trend of major conjugate joint sets could be remnant cave features exposed by block slope retreat. Tafoni and spongework structures indicate sluggish flow regimes within hypogenic systems. The poorly understood and complex interaction of the Edwards and Trinity aquifers within the Cut Plain has created a dynamic flow regime whereby ascending fluids could be partially responsible for the suite of features found in the known caves and exposed scarps.

Although today most of the known karst features are coupled to the surface, some of the caves within the Lampasas Cut Plain exhibit speleogenetic features that may be characteristic of ascending fluid migration,

indicating that at least part of the diagenetic history of these systems may have originated by pressurized fluids from below, with subsequent overprinting by meteoric waters. Geochemical analyses of springs within the Fort Hood Military Installation and the inter-fingering nature of the Comanche Peak and Edwards limestone occurring within these high energy shoals indicates a mixed fluid system where deeper seated phreatic or semi-confined hypogenic waters migrated upwards to maintain base flow as the landscape evolved. Since there are many conduits at the surface for direct recharge of both the Trinity and Edwards aquifers, the possibility of the Trinity Aquifer providing potentiometric pressure for ascending fluids is a potential driver for hypogenic speleogenesis within the Owl Mountain Province.

HYPOGENE CAVE MORPHOLOGY AT HIGH RESOLUTION: FULL 3-D SURVEY OF MÄRCHENHÖHLE (AUSTRIA)

Yuri Dublyansky
Institute of Geology, Innsbruck University
Innrain 52
Innsbruck, 6020, Austria, juri.dublyansky@uibk.ac.at

Andreas Roncat
Institute of Photogrammetry and Remote Sensing, Vienna University of Technology
Gußhausstraße 27-29/E120
Vienna, 1040, Austria, ar@ipf.tuwien.ac.at

Christoph Spötl
Institute of Geology, Innsbruck University
Innrain 52
Innsbruck, 6020, Austria, christoph.spoetl@uibk.ac.at

Peter Dorninher
Institute of Photogrammetry and Remote Sensing, Vienna University of Technology
Gußhausstraße 27-29/E120
Vienna, 1040, Austria, pdo@ipf.tuwien.ac.at

Abstract

The hypogene cave Märchenhöhle was mapped in 3-D by means of the laser scanning technique. The resulting triangulated model allowed detailed analysis of cave macro-, meso-, and micromorphology to be performed. Parts of the cave that would not be amenable to direct observations while in the cave (e.g., upper parts of large cave chambers and ceilings) could be studied at high resolution. The 3-D cave model-based morphogenetic analysis allowed identification of morphological features of hypogene speleogenesis at various scales and strengthened the attribution of the cave to a hypogene class.

Introduction

Mapping of caves is usually done using instruments such as (electronic) distance meters, compasses, and clinometers. Although computer support is available for data acquisition, processing, and drafting cave maps, there is still much manual work associated with this task (e.g., Plan and Xaver, 2010). As a result, the quality of the final map heavily depends on the experience and the cartographic skills of individual surveyors. It also relies on the surveyor's interpretation of which cave features are important to document.

In speleogenetic studies besides gross cave morphology, meso- and micromorphological features are of fundamental interest (Dublyansky, 2013). These smaller-scale features are typically not represented on the standard cave maps. For specialized morphogenetic maps, such features must be documented and interpreted on-site, and then represented on the final maps qualitatively (mostly as symbols).

Laser scanning has become the standard technique for medium- and large-scale surveying of topographic surfaces, and is being used increasingly in karst studies (Gallay et al., 2015; Idrees and Pradhan, 2016 and references therein). The technique allows unprecedented documentation of morphological features at different scales, ranging from macro (entire cave) to micro scales (i.e., cave wall relief). It offers the possibility to complement field observations on cave morphology with detailed studies following data processing. These studies may include parts of the cave that are not directly accessible in the field (e.g., upper parts of large chambers). This technique permits more detailed objective documentation (i.e., complete and non-selective visualization) and eventually quantitative morphogenetic observations and interpretations than possible when using conventional cave mapping techniques. Laser scanning is therefore a highly valuable tool in order to recognize hypogene caves by applying morphological criteria and differentiating them from epigene ones.

Study Site

Märchenhöhle (Fairy Tale Cave; Austrian cadastre # 1742/17) is located at the southern margin of the Northern Calcareous Alps, near Eisenerz (Styria, Austria). This 135-m-long cave opens near the crest of a limestone ridge at approximately 1,500 m a.s.l., some 900 m above the valley floor. The cave consists of several near-isometric chambers separated by relatively narrow openings. The lower parts of cave walls are coated with mammillary calcite (a.k.a. cave clouds). Above this crust, the internal surface of the cave exhibits a wealth of peculiar, smaller-scale corrosion features (e.g., funnel-shaped chambers with flat roofs; cupolas; cup-shaped pockets on inclined walls; etc.), suggestive of the hypogene speleogenesis.

The cave was identified as hypogene based on its location (high elevation, near the crest of a ridge). Gross morphology indicated no involvement of running water, as well as the presence of peculiar speleothems—cave clouds (Plan et al., 2009). Märchenhöhle was selected for the study due to its richness in morphological features attributable to hypogene speleogenesis.

The Instrument

We used a z+f Imager 5006i terrestrial laser scanner (Figure 1) operating according to the phase-measurement principle (Zoller+Fröhlich, 2015). The instrument is capable of recording 800 million points per scan in "Ultra High" scan mode (40,000 lines x 20,000 points per line) with a scan time of 27 min. The maximal range to be recorded is approximately 80 m. The maximum resolution results in a point spacing of 1.6 mm at a 10 m distance.

Scanning and Data Processing

The scanning campaign took place in July 2010. Field observations suggest that the near-entrance part of the cave has lost much of its initial meso- and micromorphology due to weathering and erosion. Accordingly, only the inner part of the cave was selected for scanning (Figure 2). In order to document the interior part of the cave, we acquired 11 scans with a total number of 1,600,000,000 recorded points (acquisition time 1 h).

Since the data was acquired from different positions, accurate determination of the relative positions and attitudes of the individual point clouds was necessary. This is known as "relative orientation" in photogrammetry and geodesy (Kraus, 2007) and as "co-registration" in the field of computer vision (Shapiro and Stockman, 2001). In our case, the relative orientation was established in a two-step approach: the relative
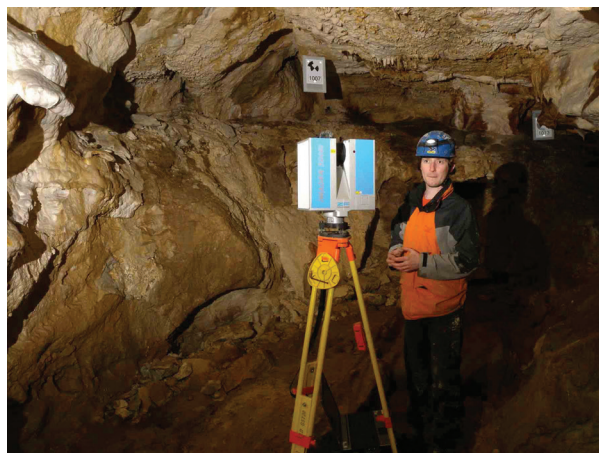

Figure 1.
A z+f Imager 5006i terrestrial laser scanner employed at Märchenhöhle. Two coded targets used for relative orientation of scans are visible in the background.

orientation was determined using coded targets (Figure 1) using the software of the scanner's manufacturer. It was refined using an ICP (iterative closest point; Besl and McKay, 1992) algorithm implemented in the Geomagic Studio software (Geomagic, 2015). The first step uses some distinct points in two scans with known point-to-point correspondence, whereas the latter makes use of the whole point clouds. Crude relative orientation with coded targets is needed for adequate performance of ICP.

Our study did not require an absolute georeference (i.e., position of the overall point cloud relative to a superior coordinate system such as national coordinate systems or WGS84). The local coordinate system was defined by taking the first scan position as the origin, defining the local plumb line (z axis) using the tilt sensor of the scanner and taking the scanner's horizontal 0° line as the y axis. A Cartesian right-handed coordinate system was uniquely determined in this way.

After the relative orientation, the point cloud underwent subsequent processing steps such as filtering, homogenization, and correction for systematic errors (Dorninger et al., 2008; Molnár et al., 2009; Nothegger and Dorninger, 2007). These steps were necessary to reduce the amount of data without losing significant details to enable the final 3-D modeling of the cave in reasonable processing time.

Results

Co-registration resulted in an overall 3-D point cloud covering the largest part of the cave. A floor plan of this

point cloud was compared to a map of the cave produced by traditional surveying in 1971. Although an absolute georeference was not available for both maps, they show good overall agreement (Figure 2).
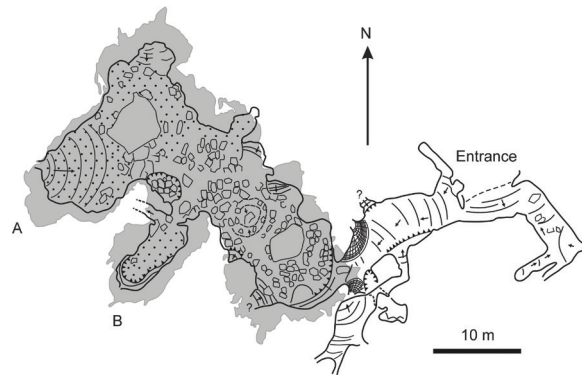

Figure 2.
Overlay of a map of Märchenhöhle and a floor projection of the recorded point cloud (grey). The two map images were manually adjusted. Two chambers are labeled A and B to assist with referencing in the other figures.

As a next step, horizontal profiles were derived from this point cloud. Each profile consists of the points located at a specific height ±5 cm. Color-coding of the single points according to their local height allows for the detection of horizontal or inclined structures (Figure 3). The profiles are available as GeoTIFF images and can thus be used for digitization in CAD software packages.
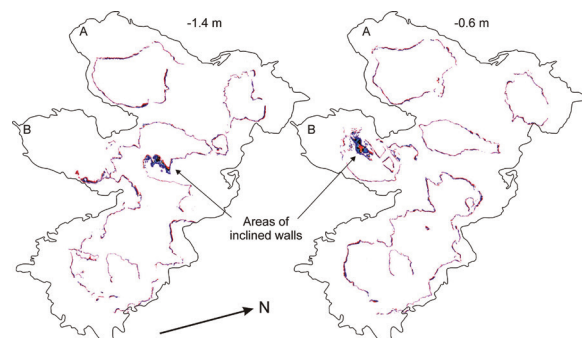
Figure 3.
Horizontal profiles of the point clouds at the local heights of -1.40 m (left) and -0.60 m (right). Blue color corresponds to the local height -5 cm, and red to the local height +5 cm. Black line shows the outline of the floor projection of the point cloud (cf. Figure 2).

The core result of this study was the derivation of a triangulated 3-D model of the cave (Figure 4). Whereas the original point cloud consisted of more than 109 points, the resulting 3-D model contains approximately 12×106 triangles. Although the point cloud was greatly reduced, sophisticated filtering allowed the accurate rendering of micromorphological features such as minor fractures and inclined pocketed walls (Figure 5).
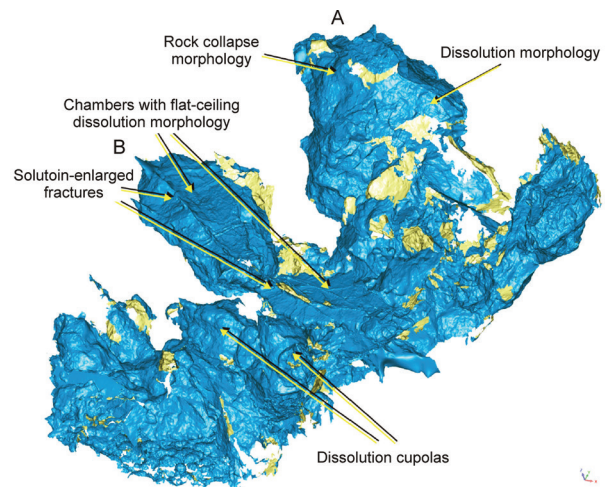

Figure 4.
Visualization of the triangulated 3-D model of Märchenhöhle. Note complex, compartmentalized gross morphology of the cave and rich meso- and micromorphology (selected features indicated by arrows). Outside surfaces of the model are rendered in blue, inner surfaces in yellow. The distance from the lower left to the upper right on the figure is 38 m.

Figure 4 shows the 3-D reconstruction of the cave's central chambers (viewed from outside). One shortcoming of the current results is the missing intensity and color information. Although intensity information was recorded by the scanner for each 3-D point, the intensity values must be calibrated before further use.

Figures 5 and 6 illustrate the advantages of the 3-D scanning. Ceiling and upper parts of the walls in two chambers of Märchenhöhle are shown, viewed from outside. When in the cave, these parts of the chambers can only be observed from a distance of several meters. Because of that, many of the morphological features are not visible on site. Examination of the 3-D model on the computer screen allows robust identification of features as small as a few centimeters. The software (Geomagic Studio) allows rotation of the model and viewing from different angles from outside and inside, which makes identification of features much easier than in case of "static" pictures.
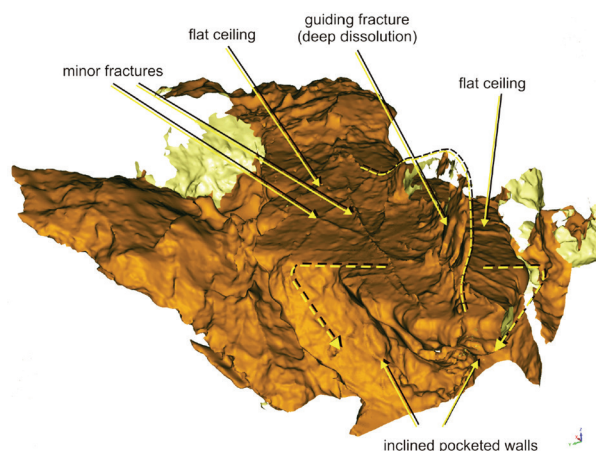
Figure 5.
Visualization of the triangulated 3-D model of one of the chambers (chamber B, cf. Figure 2) of Märchenhöhle. Note the complex morphology of the chamber and a wealth of the micromorphological features (minor solution-enlarged fractures, wall pockets) recognizable on the model surface. Distance across flat ceiling is approximately 8 m. View from SW.

Important morphological features that can be observed in Figure 5 are the flat horizontal ceiling and walls inclined inward at about 45° (funnel-shaped cross section). Such morphologies, known as *Laugdecke, Facetten,* and *Laughöhle*, are characteristic of near-stagnant phreatic conditions (Kempe, 1975; Lauritzen and Lundberg, 2000). They have been observed in another Austrian hypogene cave, Kozak Cave (Dublyansky, 2014; Spötl et al., 2016).

Figure 6 shows many interesting features, including two different varieties of notches: a sharp, wedge-shaped one and two others with rounded profiles. Importantly, there is an angular unconformity of about 20° between these notches, suggesting tectonic tilting of the host rock. One of the inclined walls in the chamber shown in Figure 6 shows a group of rounded solution pockets 10 to 20 cm in diameter, apparently produced by water dripping from the inclined ceiling above. This feature may be interpreted as indication of condensation occurring after the drop of the water table.

Conclusions

A hypogene cave in Austria, Märchenhöhle, was used as a test ground for testing laser scanning techniques and subsequent data processing schemes for surveying caves in full 3-D. The data, either point-based or based on a 3-D triangulation, allows for analysis of the cave's general shape and identification of cm-scale features.
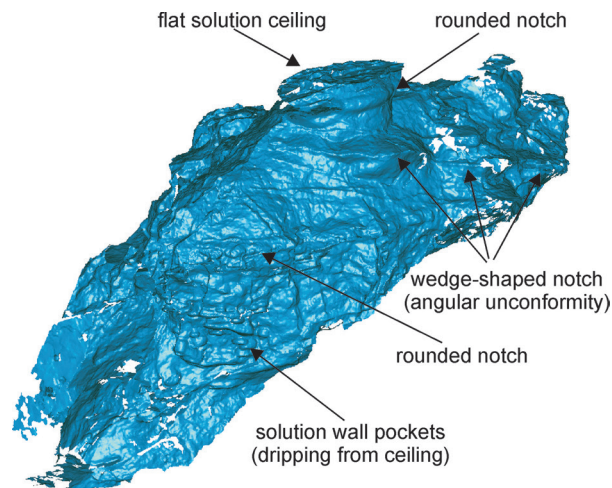

Figure 6.
Visualization of the triangulated 3-D model of one of the chambers in Märchenhöhle. Note rich morphologic information retained by the model. The length of the chamber is approximately 10 m.

Acknowledgements

References

Besl P, McKay N. 1992. A method for registration of 3-D shapes. IEEE Transactions on Pattern Analysis and Machine Intelligence 14 (2): 239-256. http://dx.doi.org/10.1109/34.121791

Dorninger P, Nothegger C, Pfeifer N, Mólnar G. 2008. On-the-job detection and correction of systematic cyclic distance measurement of terrestrial laser scanners. Journal of Applied Geodesy 2 (4): 191-204. http://dx.doi.org/10.1515/JAG.2008.022

Dublyansky YV. 2013. Karstification by geothermal waters. In: Shroder J, Frumkin A, editors. Treatise on geomorphology: vol. 6, karst geomorphology. San Diego (CA): Academic Press. p. 57-71. http://dx.doi.org/10.1016/b978-0-12-374739-6.00110-x

Gallay M, Kaňuk J, Hochmuth Z, Meneely JD, Hofierka J, Sedlák V. 2015. Large-scale and high-resolution 3-D cave mapping by terrestrial laser scanning: a case study of the Domica Cave, Slovakia. International Journal of Speleology 44 (3): 277-291. http://dx.doi.org/10.5038/1827-806X.44.3.6

Geomagic [Internet]. 2015. [Place of publication unknown]: Homepage of the company Geomagic [accessed on 2015 August 31]. Available from: http://www.geomagic.com

Idrees MO, Pradhan B. 2016. A decade of modern cave surveying with terrestrial laser scanning: a review of sensors, method and application development. International Journal of Speleology 45 (1): 71-88. http://dx.doi.org/10.5038/1827-806X.45.1.1923

Kempe S, Brandt A, Seeger M, Vladi F. 1975. ''Facetten'' and ''Laugdecken'', the typical morphology of caves developing in standing water. Annales de Spéléologie 30 (4): 705-708.

Kraus K. 2007. Photogrammetry–geometry from images and laser scans. 2nd ed. Berlin (DE): de Gruyter.

Lauritzen S-E, Lundberg J. 2000. Solutional and erosional morphology. In: Klimchouk AB, Ford DC, Palmer AN, Dreybrodt W, editors. Speleogenesis: evolution of karst aquifers. Huntsville (AL): National Speleological Society. p. 408-426.

Molnár G, Pfeifer N, Ressl C, Dorninger P, Nothegger C. 2009. Range calibration of terrestrial laser scanners with piecewise linear functions. Photogrammetrie, Fernerkundung, Geoinformation 2009 (1): 563-576. http://dx.doi.org/10.1127/0935-1221/2009/0002

Nothegger C, Dorninger P. 2007. Automated modeling of surface detail from point clouds of historical objects. In: 21st CIPA Symposium, International Archives of the Photogrammetry, Remote Sensing and Spatial Information Sciences 36 (Part 5/C53), Athens, Greece. p. 538–543.

Plan L, Spötl C, Pavuza R, Dublyansky Y. 2009. Hypogene caves in Austria. In: Klimchouk AB, Ford DC, editors. Hypogene speleogenesis and karst hydrogeology of artesian basins. Special Paper 1. Simferopol (UA): Ukrainian Institute of Speleology and Karstology. p. 121-127.

Plan L, Xaver A. 2010. Geomorphologische untersuchung und genetische interpretation der Dachstein-Mammuthöhle (Österreich). Die Höhle 61 (1-4): 18-38.

Shapiro LG, Stockman GC. 2001. Computer vision. Upper Saddle River (NJ): Prentice Hall.

Spötl C, Desch A, Dublyansky Y, Plan L, Mangini A. 2016. Hypogene speleogenesis in dolomite host rock by CO_2-rich fluids, Kozak Cave (southern Austria). Geomorphology 255: 39-48. http://dx.doi.org/10.1016/j.geomorph.2015.12.001

Zoller+Fröhlich [Internet]. 2015. [Place of publication unknown]: Homepage of the company Zoller +Fröhlich GmbH; [accessed on 2015 August 31] Available from: http://www.zf-laser.com.

CAVE INCEPTION IN DEDOLOMITE (A CASE STUDY FROM CENTRAL SLOVENIA)

Bojan Otoničar

Karst Research Institute ZRC SAZU
Titov trg 2
Postojna, 6230 Postojna, Slovenija, otonicar@zrc-sazu.si

Yuri Dublyansky

Innsbruck Quaternary Research Group, Institute of Geology of the Innsbruck University
Innrain 52
Innsbruck, A-6020, Austria, juri.dublyansky@uibk.ac.at

Robert Armstrong Osborne

Faculty of Education and Social Work, The University of Sydney
A35 – Education Building
Sydney, NSW, 206, Australia, armstrong.osborne@sydney.edu.au

Andrzej Tyc

Chair for Geomorphology, Faculty of Earth Sciences, University of Silesia in Katowice
Będzińska 60
Sosnowiec, 41-200, Poland, andrzej.tyc@us.edu.pl

Sven Philipp

WASSER UND BODEN GmbH
Am Heidepark 6
Boppard, 56154, Germany, philipp@wasserundboden.de

Abstract

Below the Vrh Sv. Treh Kraljev Hill ("*The Three Holy Kings Hill*") in the Rovte region of central Slovenia, the hilly landscape along the transition between the Dinaric karst of inner Slovenia and the Prealps, are three caves. These three caves are between 300 m and 1000 m long, and exhibit a ramiform and/or maze-like pattern and other evidence indicating their possible hypogene origin.

The wall rock of Mravljetovo brezno v Gošarjevih rupah Cave is mostly composed of a yellowish to reddish-brown calcareous deposit in an otherwise Middle Triassic gray dolomite formation. It was found that the yellowish to reddish-brown material consists mainly of calcite, while the color is derived from small quantities of iron hydroxides. It is suggested that calcite was formed by dedolomitization of the host rock as a result of interaction among limestone, dolomite, and Ca-sulphate rock in the phreatic zone. "Dedolomite" is the term for calcite forced to precipitate by the dissolution of dolomite and Ca-sulphates. It was revealed from oxygen and carbon isotope composition that dedolomite was precipitated from low-temperature meteoric water derived from areas populated by C3 plants.

Subsequently, the cave was developed in phreatic or/and epiphreatic conditions almost exclusively by dissolution of the original dedolomite body. Later, the cave was reshaped and partly infilled by epiphreatic streams and their sediment load. The cave is currently in the vadose zone, where aggressive water creates localized vadose shafts and downcutting vadose meanders.

In the area, there are three wells a few hundred meters deep that, among others, cut Upper Permian to Lower Triassic evaporite horizon and discharging sulphate water to the surface, in contrast to normal meteoric waters from a few karstic springs. The chemical analyses of water discharging from the wells indicate still-ongoing dedolomitization below the surface.

Introduction

When evaluating potential hypogene caves from the cave maps in the Slovenian cave register, the Vrh Sv. Treh Kraljev ("The Three Holy Kings Hill," abbreviated

VSTK) of the Rovte region, the area in the western part of central Slovenia (Figure 1), attracted our special attention. There, three caves, between 300 m and 1000 m long, exhibit ramiform and/or maze-like pattern and other evidence indicating their possible hypogenic origin. Among them, the most peculiar is the Mravljetovo brezno v Gošarjevih rupah (MBGV), a cave full of a yellowish-brown deposit uncommon for Slovenian caves.

This study demonstrates that the cave is preferentially developed in a dedolomitized part of dolomite sequence in which dedolomitization may still be ongoing in the phreatic zone below the land surface.

Geological Setting

The VSTK is topographically well expressed and surrounded by four valleys developed mainly along fault lines and at the contact of different lithologies. Between the faults, the mountain represents a relatively stable block in which the uniform dip of the strata is disrupted only locally by a few limited meter-scale strike-slips along minor local faults.

The VSTK consists of a sequence of Middle Permian to Middle Triassic carbonate and siliciclastic rocks a few hundred meters thick, with intercalations of evaporites. During the 1960s, drilling for mercury ore at Idrija Mine near Rovte Village discovered an evaporite horizon up to 270 m thick that forms up to 59% of the Upper Permian and over 29% of Lower Triassic dolomite succession at depths 130 to 717 m below the surface (Čadež, 1977). There, up to meter-thick lenses of gypsum and anhydrite alternate with dolomite that contains veins and geodes of gypsum.

The geology of the wider area is rather complicated, with the uppermost nappes of the External Dinarides being dissected by numerous faults and frequent lithological changes. South and northeast from the investigation area and in the underlying nappes, the Upper Triassic dolomite is one of the most abundant formations (Mlakar, 1969; Čar, 2010).

Hydrogeology
A mixture of fluvial, karst, and fluviokarst features can be seen in the Rovte area (Mihevc, 2005) (Figure 1). Surface waters in the northern and eastern parts of the area flow into the valleys of the Idrijca, Sora, and Ljubljanica Rivers, while the central and southern parts have only karstic discharge. There are 9 large and 16 small sinking streams in this area (Mihevc, 2005). From these, water flows to the springs of the Idrijca and Ljubljanica Rivers. There are a few springs (D and V

on Figure 1) in the area that mainly drain local waters through perched underground streams developed at contacts between siliciclastics and carbonates, mainly limestones or marly limestones. There is only one "true" permanent karstic spring (P on Figure 1) at the contact between the flank and the bottom of the main valley.

Among more than ten boreholes drilled up to a few hundred meters deep in the 1960s, only three remain preserved today. All three discharge sulphate water. The wells are arranged in a triangular area approximately 3.7 km x 3 km x 5.6 km (Figure 1) and are between 500 m and 800 m deep. They penetrate the evaporite horizon at different depths, from around 130 m below the surface (or erosional base) to more than 500 m.
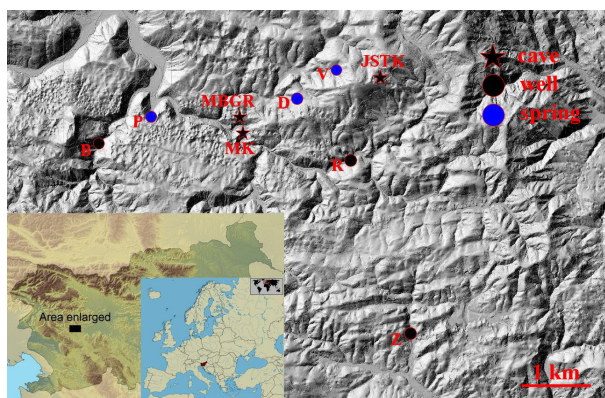

Figure 1.
Geographical position of Slovenia and LiDAR DEM of the investigated area with investigated caves (MBGR: Mravljetovo brezno v Gošarjevih rupah, MK: Matjaževe kamre and JSTK: Jama pri Sv. Treh kraljih), wells (B: Bizjakov mlin, R: Rodolfov mlin and Z: Zavčen), and springs (P: Podklanec, D: Dolina and V: Vrh).

Mravljetovo brezno v. Gošarjevih rupah Cave

The Mravljetovo brezno v. Gošarjevih rupah (MBGR) cave (length = 726 m; depth = 73 m; altitude of the main entrance = 613 m) (Figure 2) is located along the eastern flank of the Sora Valley some 100 m above the river on the lower part of the elongated ridge of VSTK (Figure 1). A newly discovered section, at least 100 m long, has not been measured yet.

In general, the cave is developed in an indistinctly bedded, fine- to medium-grained Middle Triassic (Anisian) dolomite formation. The cave passages exhibit ramiform and maze like patterns (Figure 2) guided by joints. Some conduits and the wall rock morphology shows features characteristic of dissolution by slowly

flowing rising water (i.e., feeders, rising channels, cupolas, lack of fast flow scallops, etc.), while others are related to descending percolating waters (i.e., shafts, downcutting vadose meanders, fluvial sediments of sandy and gravel size particles, etc.). Locally, the wall rock surface is highly irregular and jagged. Fast flow scallops and flowstone deposits are nearly absent. In many places, the cave floor is covered almost entirely with cobbles and blocks of the yellowish to reddish-brown rock. Locally, the host dolomite is affected by condensation corrosion.
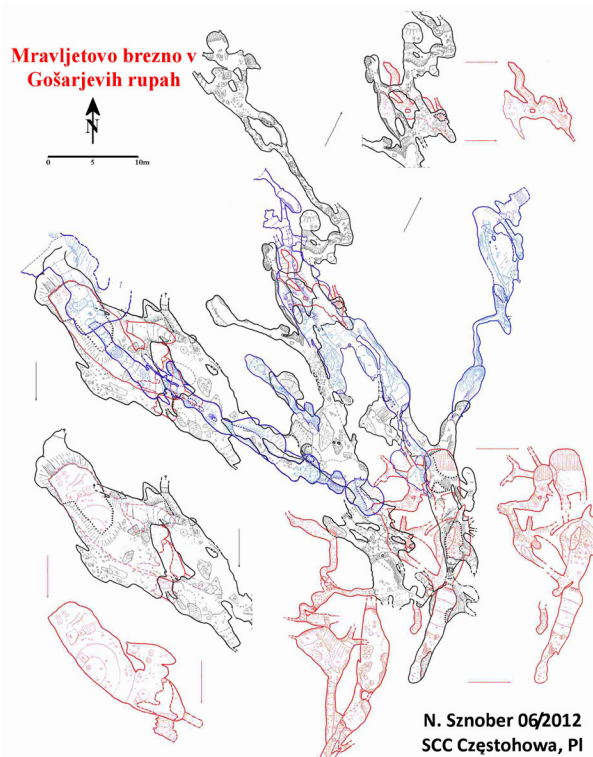
Figure 2.
Ground plan of the Mravljetovo Brezno v Gošarjevih Rupah (MBGR) cave. Blue = upper level; black = middle level; red = lower level.

Petrography of the Wall Rock

One of the most distinctive characteristics of the cave is the peculiar yellowish to reddish brown rock that looks at first like an eroded infilling deposit (Figures 3 and 4). However, the gradual transition between this type of rock and the host rock (Figure 3), its highly calcareous mineralogy, and preserved echinoderm bioclasts similar to those in the host dolomite suggest a different origin. In places between the yellowish-brown deposit and the host rock, there is a crust of coarse-grained calcite crystals up to a few centimeters thick.

As expected from observations of the outcrops and sawed rock slabs, thin sections stained with Alizarin red S also revealed a gradual transition between the host dolomite and the yellowish to reddish-brown calcareous deposit. At the transition, there are dolomite crystals with dissolved crystal faces and patches of more or less unaltered dolomite within calcite (Figure 5).

Petrographically, several major textural groups of calcite crystals can be distinguished: (a) relatively coarse grained xenotopic to locally hypidiotopic mosaic calcite, (b) pseudospherulitic fibrous calcite (Figure 6), (c) cone-like fibrous calcite, (d) fibrous palisade calcite, and (e) brownish micritic calcite with or without a mesh of needle-fiber crystals, etched patches, or individual crystals of coarser grained calcite mosaic. In places, needle-fiber crystals may coalesce in a xenotopic mosaic of fine-grained, almost equant crystals. Coarser-grained calcite crystals commonly include abundant inclusions or remnants of the host dolomite.

Figure 3.
Transition from d=dolostone (dark gray) over partly ddd = dedolomititzed dolostone (pale gray) to dd = dedolomite (yellowish-brown).

XRD analyses reveal that unaltered grayish host rock is composed mainly of dolomite, while the yellowish-brown altered rock is composed of calcite with traces of dolomite in some samples. Between these two end members, pale dolomite with a gradually higher content of calcite occurs. The yellowish to reddish-brown colour of the samples is associated with small amounts of Fe hydroxides (i.e., goethite and ferrihydrite). Among other components in the yellowish-brown deposit are small amounts of kaolinite, illite, sericite, and quartz. Locally, cave walls are coated with a few mm-thick white crusts predominantly composed of hydromagnesite. Some ledges are covered by earthy light rusty-coloured silty material consisting of gypsum with traces of goethite and ferrihydrite and sandy particles of calcite. Both the hydromagnesite and the gypsum are likely to be responsible for the continuing wedging of the yellowish to reddish-brown rock off the cave walls to reveal the underlying dolomite.

Figure 4.
Entrance to a cave passage cut by a vadose shaft in the phreatic maze, partly developed in yellowish-brown dedolomite and partly in gray dolomite. The width of the lens cap is approximately 7 cm.

Geochemistry of the Wall Rock

Chemical analyses (n = 41) of the wall rock (from medium to dark gray dolomite through the pale gray transition zone to the yellowish-brown calcite) reveal the expected decrease in Mg^{2+} content from dolomite to calcite, and also a decrease in Sr^{2+} and an increase in Fe^{2+}/Fe^{3+} content.

Sixty-five samples of dolomite, nine of yellowish-brown calcite, seventeen of intermediate translucent coarse-
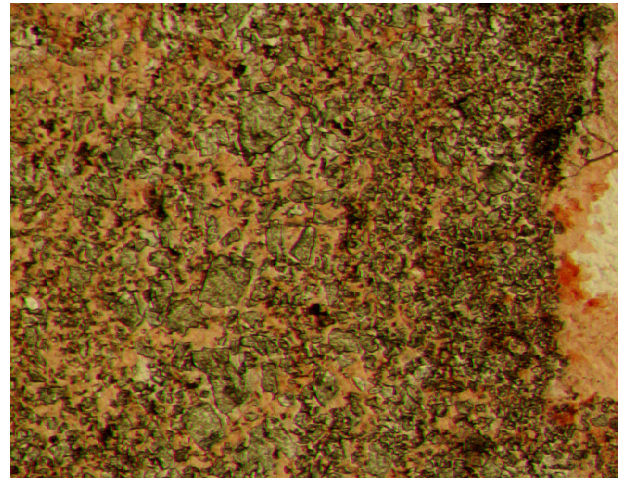

Figure 5.
Transition zone between dolomite (gray) and dedolomite (stained red). Note etched crystals of dolomite. The width of the picture is 2 mm.
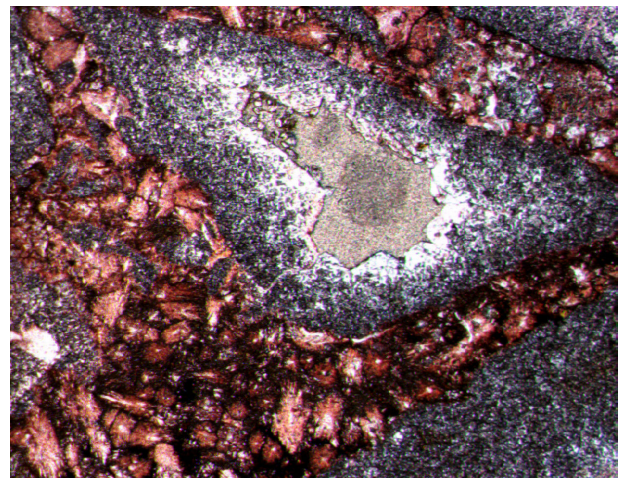

Figure 6.
Xenotopic mosaic of calcite crystals showing pseudospherulitic texture (stained with Alizarin red S) surrounded by dolomite (gray). Note the sharp fissure contact between dolomite with the empty dissolution void and calcite. The width of the picture is 4 mm.

grained mosaic calcite spar, and four of transitional pale dolomite with a gradually higher content of calcite have been analyzed for oxygen and carbon isotope composition. Most of the samples came from two drill holes 10-cm (Figure 7) and 13-cm-long in the wall rock: one of gray host dolomite covered with a yellowish-brown dedolomite crust and intermediate translucent calcite spar (Figure 7), and the other consisting only of gray dolomite. $\delta^{13}C$ and $\delta^{18}O$ values display significant differences between the dolomite host rock and the yellowish-brown calcite (Figure 7). While the isotope values of dolomite are roughly comparable with those of carbonates precipitated from Middle Triassic marine water (see Veizer et al., 1999), the yellowish-brown calcite shows isotopic values characteristic of meteoric diagenesis. Similar to the mineralogical composition, $\delta^{13}C$ and $\delta^{18}O$ values of the transition zone also fall between the values of the dolomite and the yellowish-brown calcite (see Figure 7).

Hydrogeochemistry

Preliminary hydrogeochemical analyses of waters from the wells, three fracture-karst springs and one surface stream reveal significantly different characteristics between waters from deep wells compared with those from the shallower fracture-karst aquifer. Waters from the wells have high SO_4^{2-} concentrations and low Cl^- and NO_3^- concentrations. By contrast, spring and surface waters have low SO_4^{2-} concentrations and high Cl^- and NO_3^- concentrations. Three general trends in water chemistry can be detected among springs, surface streams and different wells (Figure 8): (1) from lower to higher SO_4^{2-} concentration, (2) from higher to lower total alkalinity, and (3) from molar Mg^{2+}/Ca^{2+} ratios lower than 1 to molar Mg^{2+}/Ca^{2+} ratios of almost 1.

Thus, the waters can be categorized: The southern-most well that penetrates the evaporites at the shallowest depth below the surface (Z) discharges a sulfate-rich
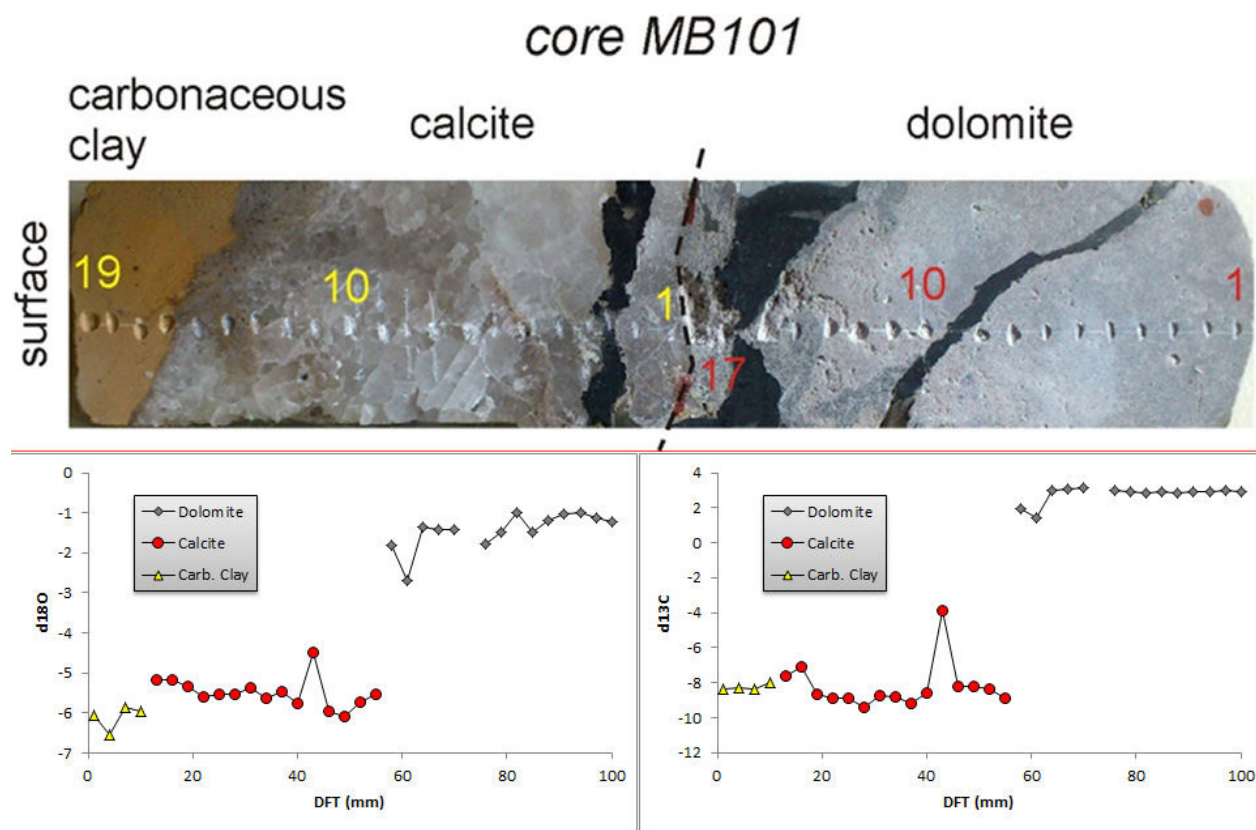

Figure 7.
Top: The core of the cave wall (Mravljetovo brezno v Gošarjevih rupah) showing the sharp transition between dedolomite (coarse-grained translucent calcite spar and yellowish-brown, fine-grained calcite with a mesh-like distribution of needle-fiber calcite crystals) and the host rock dolomite.
Bottom: $\delta^{18}O$ and $\delta^{13}C$ values of the core (note sampling points made by microdrilling).
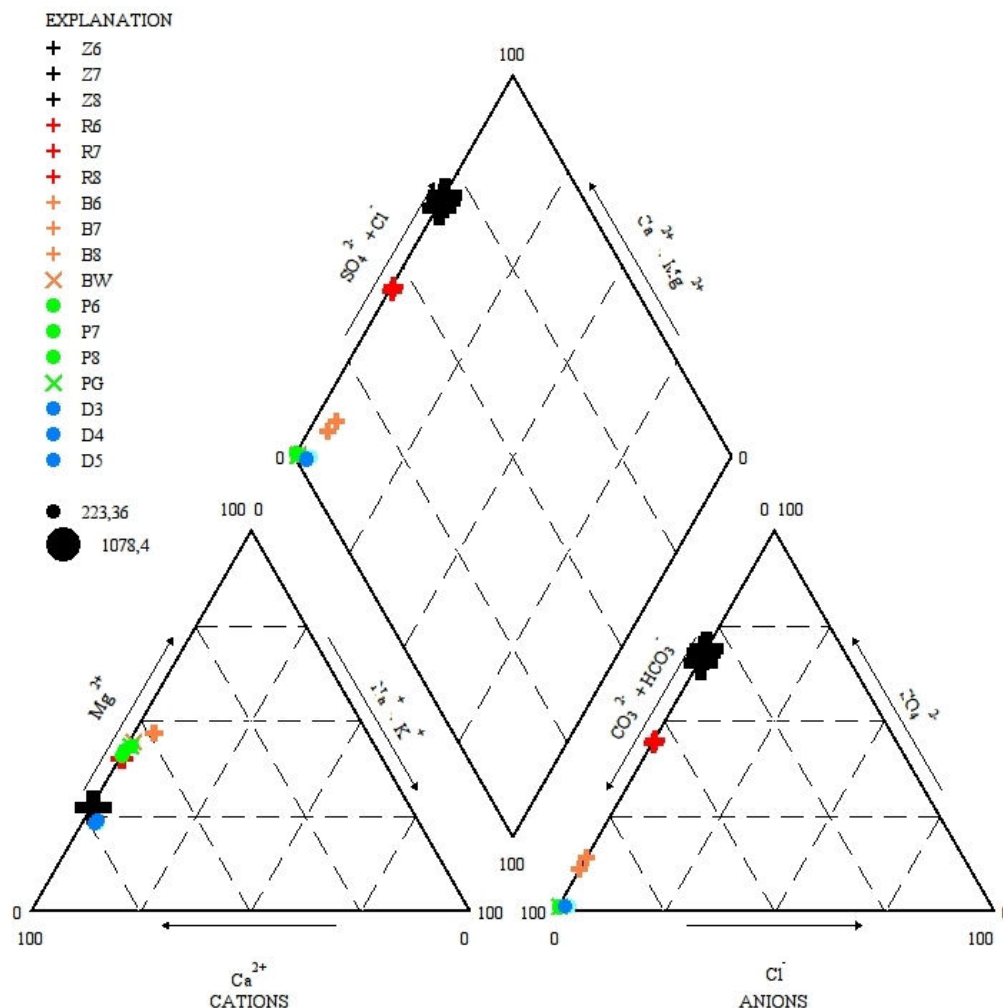
Figure 8.
Hydrochemistry (Piper diagram) of deep wells (Z, R and B) and springs (P, PG and D) in the Rovte area; size of symbols correspond to total dissolved solids.

Ca^{2+}-type water with high electrical conductivity. The well in the valley just below the VSTK (R) and closest to the cave of interest discharges a Ca^{2+}-Mg^{2+}-type water relatively rich in sulfate. The westernmost well that penetrates evaporites deepest below the surface (B) discharges Ca^{2+}-Mg^{2+}-bicarbonate-rich water with slightly elevated sulfate. BW (not in Figure 1; surface stream near B), P, PG (not in Figure 1; pipe near P) and D are bicarbonate-rich Ca^{2+}-Mg^{2+}-type waters with low electrical conductivity.

Water samples from Z and R show relatively constant δ^2H and $\delta^{18}O$ values (Table 1). One group of samples from B exhibits values similar to Z and other more negative δ^2H and $\delta^{18}O$ values, closest to values of surface water taken for analyses in the nearby stream. In contrast to Z and R, the samples from springs yield more variable δ^2H and $\delta^{18}O$ values. All measured isotopes are above the Global Meteoric Water Line.

All samples have a molar-Mg^{2+}/Ca^{2+}-ratio < 1. Nearly all samples are supersaturated or in equilibrium with respect to calcite and undersaturated or in equilibrium with respect to dolomite (Figure 9). The water from the springs shows more constant saturation indexes with respect to dolomite than water from the wells. All samples are undersaturated with respect to gypsum and anhydrite.

The pH and SO_4^{2-} concentrations in water samples in each well and especially among the wells show high correlation (Table 1).

Table 1.

Mean and standard deviation of δ2H and δ18O values, pH and SO42- concentrations of water from deep wells in the Rovte area.

| mean ± std	Z (n=8)	R (n=8)	B (n=8)
$\delta^{18}O$ [‰]	-9.57±0.11	-9.66±0.18	-9.27±0.32
$\delta^{2}H$ [‰]	-59.85±0.33	-62.23±0.36	-59.53±0.67
pH	7.31±0.13	7.63±0.12	7.59±0.11
SO_4^{2-} [mg/l]	740.6±65.2	273.3±21.3	68.5±28.4

Discussion

On the basis of known general geological data (e.g., an evaporite horizon at the P/T boundary), basic pattern of the cave passages, cave rocky relief, field and mineralogical evidence of host rock alteration, and the hydrogeochemical data, we suggest that the major part of the cave has been primarily developed in phreatic conditions initially by the dissolution of a previously dedolomitized portion of the host dolomite. Later, the cave has been modified and perhaps significantly enlarged in the epiphreatic zone (wall rock features characteristic of ascending and/or oscillating water speleogenesis, perched conduits with clastic sediments) and vadose zone (shafts with active dripping or even flowing water). At present, it is difficult to confirm that the passages were at least partly formed with the involvement of sulphuric acid, but cave wall rock features, traces of secondary gypsum,

and evidence of later invasion by allogenic waters that possibly dissolved the majority of gypsum do not preclude this option. Although we found some clay minerals in the dedolomite samples, so far no clay minerals diagnostic of sulphuric acid alteration (see Polyak & Provencio, 2001) have been found. In one of the wells, despite the common strong characteristic smell, relatively low concentrations of H_2S have been detected, probably produced by bacterial reduction of sulphates (Eleršek & Mulec, 2014). In addition, the reported native sulphur occurrence in dolomites at the P/T boundary (Ramovš, 1954; Čadež, 1977), which most likely denotes the former location of gypsum, suggests incomplete oxidation of hydrogen sulphide.

Dedolomitization may occur in various diagenetic environments (see Nader et al., 2008 and references therein) and the dissolution of dolomite alone can bring the water roughly to saturation with calcite, especially if the water already contains dissolved calcite (Palmer, 2007). However, we suggest from the geological situation of the area (see Mlakar, 1969 and Čadež, 1977) and hydrogeochemistry of the analysed water from the wells that dedolomitisation was the result of interaction among limestone, dolomite, and Ca-sulphate rock in a deep (?) fractured karstic aquifer.

Stable isotope values of oxygen and carbon of dedolomite are roughly similar to those of flowstone
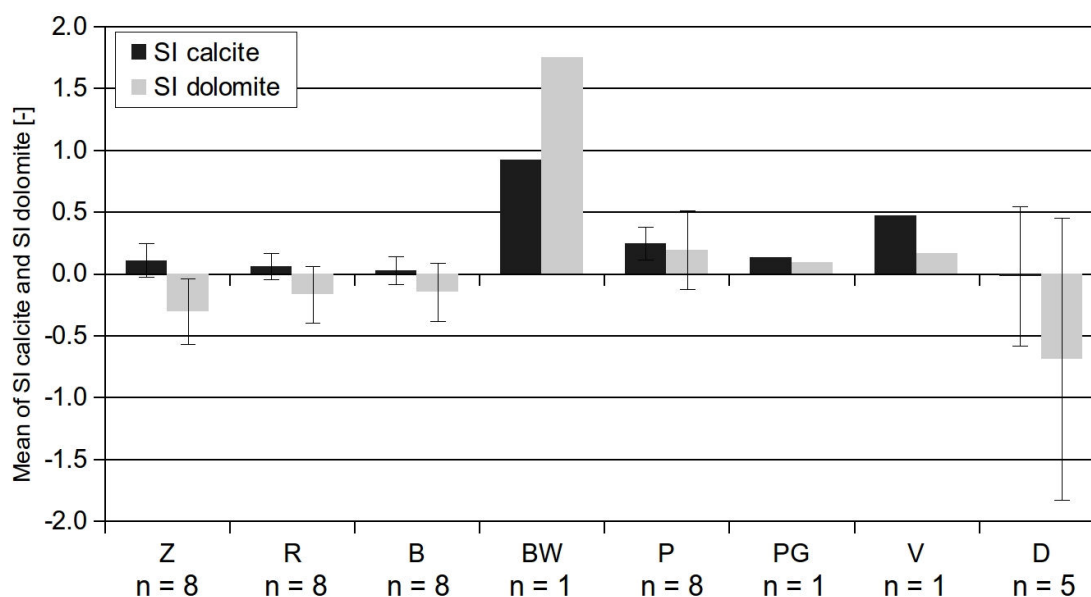
Figure 9.

Mean with standard deviation of the SI calcite and SI dolomite from wells and springs in the Rovte area. Note the high saturation indices of calcite and dolomite from surface stream BW (due to outgassing of CO₂).

from lower-altitude areas in Slovenia populated by C3 plants (Urbanc et al., 1985; 1990), which suggests that dedolomite was precipitated from low-temperature meteoric water. If we assume that the $\delta^{18}O$ values of water from which dedolomite had been precipitated were similar to the $\delta^{18}O$ values of water from the wells, then the calculated temperature (after Anderson & Arthur, 1983) at which dedolomite had been precipitated was even lower than the temperature of the waters discharging from the wells today. It is highly possible though that the relief at the time of dedolomite precipitation was much lower and so the mountain rainout effect upon oxygen isotope values of rain water should be reduced. Thus, $\delta^{18}O$ values of water from which dedolomite was precipitated should be lower than the $\delta^{18}O$ values of water from the wells at present and the water should also be warmer. This is in accordance also with the general geological evolution of the western Slovenia since Middle Miocene (Marton et al. 1995; Bressan et al. 1998; Placer, 2008; Placer et al. 2010), when more or less continuous tectonic uplifting was occasionally interrupted by periods of relative tectonic quiescence. This is reflecting in periods of valley incision with intermittent planation surfaces along river valleys of the area. During the evolution of the landscape surface, conditions in the cave changed from phreatic to oscillating epiphreatic with a sediment load. At present, vadose shafts and perched streams cut older phreatic and epiphreatic features.

The characteristic yellowish-brown colour of dedolomite that arises from a relatively low quantity of goethite and ferrihydrite suggests oxidizing conditions during its precipitation. Iron may have been partly derived from pyrite in the host dolomite. But in view of the significant increase in $Fe^{2+}/Fe^{/3+}$ content in dedolomite as compared to the host dolomite, ferrous ions should be released into the water and later oxidized to form ferric ions, perhaps mediated by iron oxidizing bacteria and precipitated as a solid iron oxide. A similar reaction is clearly seen at the outflow from the well with the highest sulphate content where deposits in a small pond around the well mouth are rusty reddish-stained.

In the field area, two rather different fracture-karst aquifers (or at least clearly separated zones) of this type occur. Relatively uniform hydrological and physicochemical characteristics of waters from the wells, compared to water from the springs, suggest that those two zones are not significantly connected. However, although we have no data about quality, quantity, and depth of water recharge to the wells, we assume from the depth at which the wells penetrate the evaporite horizon that a significant share of shallower and colder water should be discharged from the wells. Namely, on average, the temperature of water from the wells is only about $1°C$ warmer than the water from the closest karstic spring. In spite of all that, according to geological data from the wells, the lower parts of the aquifer may be at least partly artesian, with aquiclude mainly represented by the lower Triassic siliciclastic sequence. However, this is not the case for the well with the shallowest evaporite horizon and highest sulphate content where the evaporite horizon is overlain by a dolomite sequence only.

In much groundwater, dolomite and calcite are close to equilibrium with Mg/Ca = 1 at T=25°C, but if this ratio is less than 1, dolomite will dissolve (Back et al., 1983). Thus, on one hand, dissolution of Ca-sulphates that provides enough Ca-ions to maintain a low Mg/Ca ratio is crucial in the process of dedolomitization, while on the other hand, precipitation of calcite and consequently removal of carbonate ions from solution is a necessary condition to keep the solution undersaturated with respect to dolomite. Ca-ions released from dissolving Ca-sulphates keep the water solution saturated or slightly oversaturated with respect to calcite, which consequently leads to precipitation of calcite because of the common-ion effect. With precipitation of calcite, pH of groundwater will drop. More importantly, carbonate ions will also be consumed and, consequently, more dolomite will be dissolved. Therefore, the amount of SO_4^{2-} and Mg^{2+} in groundwater would increase, which is actually the case for the water that discharges from the wells. Other indicators of dedolomitization observed in the well samples are: (1) decreasing pH with increasing SO_4^{2-} concentration (see Back et al.,1983), (2) correlation between Ca^{2+} and SO_4^{2-} and Mg^{2+} and SO_4^{2-} concentrations (see Cardenal et al., 1994), (3) increase of SI calcite and decrease of SI dolomite with increasing SO_4^{2-} concentration (see Plummer et al., 1990), (4) increase of SO_4^{2-} and decrease of HCO_3^- concentrations (see Plummer et al., 1990), (5) stabilisation or even a slight fall in the alkalinity (see Cardenal et al., 1994) (trend observed in well R and Z), and (6) well waters slightly oversaturated with respect to calcite and undersaturated with respect to dolomite and gypsum (see Plummer et al., 1990).

In addition, the Piper-Diagram (Figure 8) shows differences between springs and different wells that may directly or indirectly suggest dedolomitization in the subsurface: (1) from lower to higher SO_4^{2-} concentration, (2) from higher to lower total alkalinity, and (3) from molar-Mg^{2+}/Ca^{2+}-ratios smaller than 1 to almost 1.

Conclusion

In conclusion, we suggest that the MBGR cave was developed almost exclusively in a dedolomite body that represents an inception zone for subsequent speleogenesis. According to the stratigraphic position of the evaporite horizon, we suggest that "dedolomitizing" groundwater rose through sets of fissures and faults. That the fissures and faults represent an important prerequisite for dedolomitization is evident also from the pattern of the cave passages, which mimic the pattern of mapped fissures and faults in the cave. Although during the process of dedolomitization overall porosity would increase because calcite precipitated this way occupies less than one third of the volume of the dissolved gypsum and dolomite (Palmer, 2007), it is still unclear what the initial porosity of dedolomite was and what type of water dissolved it. Numerous wall rock features in the cave typical for ascending and/or hypogene speleogenesis may just represent the shape of a dissolved dedolomite body. It can readily be observed in the cave that dolomite wall rock is generally much smoother than dedolomite surfaces, probably because dolomite was initially "protected" from dissolving water by dedolomite, which was later removed from the wall by wedging (the bottom of the cave contains many cobbles and blocks of dedolomite). It seems likely that the dolomite walls were preferentially smoothened by condensation corrosion which is documented in a large part of the cave. Locally, the dolomite wall rock is soft and disintegrates into dolomitic silt and sand.

References

Anderson TF, Arthur MA. 1983. Stable isotope of oxygen and carbon and their application to sedimentologic and paleoenvironmental problems. Society of Economic Paleontologists and Mineralogists, Short Course 10: 1-151.

Back W, Hanshaw BB, Plummer LN, Rahn PH, Rightmire CT, Rubin M. 1983. Process and rate of dedolomitization: mass transfer and ^{14}C dating in a regional carbonate aquifer. Geological Society of America Bulletin 94: 1415-1429. http://dx.doi.org/10.1130/0016-7606(1983)94<1415:PARODM>2.0.CO;2

Bressan G, Snidarcig A, Venturini C. 1998. Present state of tectonic stress of the Friuli area (eastern Southern Alps). Tectonophysics 292 (3-4): 211-227. http://dx.doi.org/10.1016/S0040-1951(98)00065-1

Čadež F. 1977. Sadra in anhidrit na Idrijskem. Geologija 20: 289-301.

Čar J. 2010. Geological Structure of the Idrija – Cerkno hills: explanatory book for the Geological map of the Idrija – Cerkljansko hills between Stopnik and Rovte 1:25.000. Ljubljana (SI): Geološki zavod Slovenije.

Cardenal J, Benavente J, Cruz-Sanjulian JJ. 1994. Chemical evolution of groundwater in Triassic gypsum-bearing carbonate aquifers (Las Alpujarras, southern Spain). Journal of Hydrology 161: 3-30. http://dx.doi.org/10.1016/0022-1694(94)90119-8

Eleršek T, Mulec J. 2014. The algal community at an eocline of a cold sulphidic spring (Sovra artesian borehole, Slovenia). Environmental Earth Sciences 71 (12): 5255-5261. http://dx.doi.org/10.1007/s12665-013-2928-4

Marton E, Drobne K, Cimerman F, Ćosović V, Košir A. 1995. Paleomagnetism of latest Maastrichtian through Oligocene rocks in Istria (Croatia), the Karst region, and S of the Sava fault (Slovenia). In: Vlahovic I, Velić I, Šparica M, editors. Proceedings of the First Croatian Geological Congress (2); 1995 Oct. 18-21; Opatija, Croatia. Zagreb (HR): Institut za geološka istraživanja i Hrvatsko geološko društvo. p. 355-360.

Mihevc A. 2005. Excursion to dolomite karst of Logaške Rovte. Guidebook of the 13th International Karstological School „Classical karst": Karst in various rocks; 2005 June 27-30; Postojna, Slovenia. Postojna (SI): Karst Research Institute SRC SASA. p. 1-42.

Mlakar I. 1969. Nappe structure of the Idrija-Žiri region. Geologija 12: 5-72.

Nader FH, Swennen R, Keppens E. 2008. Calcitization/ dedolomitization of Jurassic dolostones (Lebanon): results from petrographic and sequential geochemical analyses. Sedimentology 55: 1467-1485. http://dx.doi.org/10.1111/j.1365-3091.2008.00953.x

Palmer AN. 2007. Cave geology. Dayton (OH): Cave Books.

Placer L. 2008. Principles of the tectonic subdivision of Slovenia. Geologija 51 (2): 205-217. http://dx.doi.org/10.5474/geologija.2008.021

Placer L, Vrabec M, Celarc B. 2010. The bases for understanding of the NW Dinarides and Istria peninsula tectonics. Geologija 5 (1): 55-86. http://dx.doi.org/10.5474/geologija.2010.005

Plummer LN, Busby JF, Lee RW, Hanshaw BB. 1990. Geochemical modeling of the Madison aquifer in parts of Montana, Wyoming and South Dakota. Water Resources Research 26 (9): 1981-2014. http://dx.doi.org/10.1029/WR026i009p01981

Polyak VJ, Provencio P. 2001. By-product materials related to H_2S-H_2SO_4 influenced speleogenesis of Carlsbad, Lechuguilla, and other caves of the Guadalupe Mountains, New Mexico. Journal of Cave and Karst Studies 63 (1): 23-32.

Ramovš A. 1954. *Edmondia permiana bisulcata* n.subsp. iz belerofonskih skladov pri Žažarju. Razprave 4. razr. SAZU 2: 319-328.

Urbanc J, Kogovšek J, Pezdič J. 1990. Isotopic composition of oxygen and carbon in waters from Taborska jama. Acta carsologica 19: 157-163.

Urbanc J, Pezdič J, Dolenec T, Perko S. 1985. Isotopic composition of oxygen and carbon in cave water and speleothems of Slovenia. Acta carsologica 13: 99-112.

Veizer J. et al. 1999. Sr-87/Sr-86, $\delta^{13}C$ and $\delta^{18}O$ evolution of Phanerozoic seawater. Chemical Geology 161 (1-3): 59-88. http://dx.doi.org/10.1016/S0009-2541(99)00081-9

BANQUET LECTURE

IS HYPOGENE KARST A PLAUSIBLE MODEL FOR FORMATION OF EXTENSIVELY DEVELOPED NON-TECTONIC SYNCLINES IN EOCENE LIMESTONE OF THE WESTERN DESERT, EGYPT?

Barbara J. Tewksbury
Department of Geosciences, Hamilton College
198 College Hill Road
Clinton, NY 13323 USA, btewksbu@hamilton.edu

Elhamy A. Tarabees
Department of Geology, Faculty of Science
Damanhour University
Damanhour, Egypt 22516, etarabees@yahoo.com

Charlotte J. Mehrtens
Department of Geology, University of Vermont
180 Colchester Avenue
Burlington, VT 05405 USA, cmehrten@uvm.edu

Abstract

High-resolution satellite imagery of the Western Desert of Egypt reveals an extensively developed but enigmatic network of thousands of open synclinal structures in limestone bedrock of Early Eocene age. Individual synclines are narrow (100-400 m across) (Figure 1a). Field data and satellite image analysis shows that syncline limb dips are low, and hinges plunge shallowly, "porpoising" along trend to create multiple basin closures. Although surficial deposits are common in the synclines, bedrock layers are clearly visible in the cores of many synclines. Where syncline cores are visible in satellite imagery in wadi cliff exposures, bedrock layers appear be continuous beneath the synclines.

Two dominant orientations of synclines are common (NNW-SSE and WNW-ESE) and these orientations are parallel to two prominent joint sets, neither of which is parallel to Red Sea Rift structural trends. Individual synclines typically transition from one orientation to the other along their lengths, as well as merge with synclines of the other dominant trend (Figures 1b and 2). Synclines are typically separated by 1-3 km, and many are isolated "singlets." Dips are shallowly inward in the synclines, forming isolated downwarps in otherwise flat-lying limestone (Figure 1b). Where anticlinal/domal structures occur, they are broad, flat-topped, and "accidental," occurring where synclines are more closely spaced.

The Desert Eyes Project has mapped every syncline in an area of more than 4000 km² using high-resolution
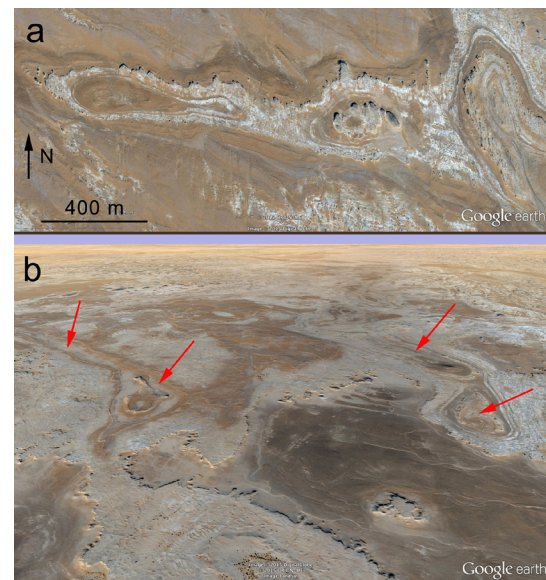

Figure 1.
(a) High-resolution satellite image of synclines in Eocene limestone bedrock. Limb dips are shallow, and synclines typically have multiple basin closures. (b) Oblique view in Google Earth showing synclines with multiple basin closures (arrows) developed in otherwise flat-lying white limestone. Image centers: (a) 26.262504, 30.899906; (b) 26.285514, 30.959436.

satellite imagery (a map of a subset of the area is shown in Figure 2b). We are struck by how similar

all the synclines are—same scale, no parasitic folds, no larger structures. Our reconnaissance mapping using high-resolution satellite imagery also shows that the synclines and syncline networks are not a local phenomenon—they occur, albeit somewhat sporadically developed—over an area of nearly 100,000 km² in limestone of Early Eocene age. Although synclines occur in a variety of orientations in all of the networks, WNW-ESE and NW-SE orientations dominate in virtually all of the regions.
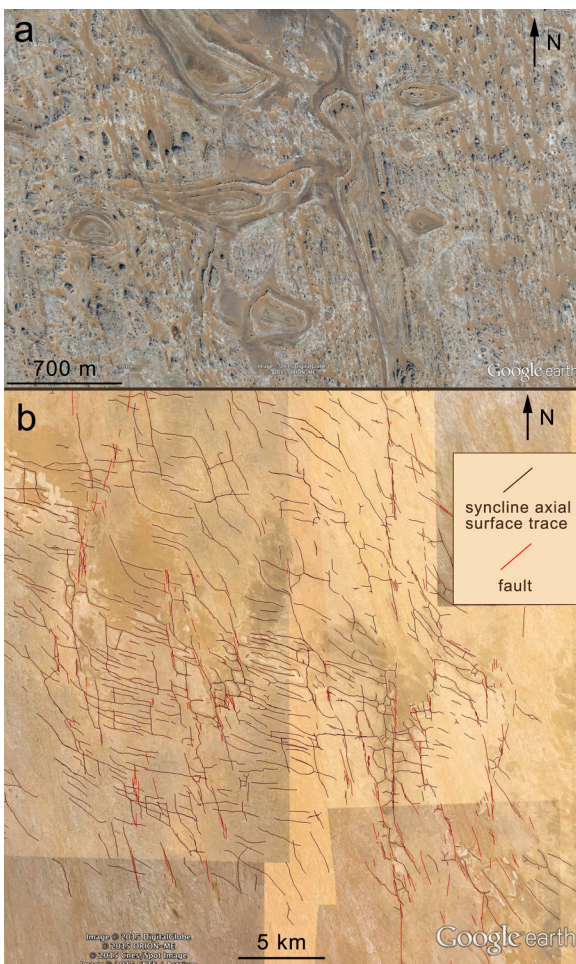

Figure 2.
(a) Elongate structural basins and synclines with multiple basin closures. Illustrates the isolated nature of some of the elongate basins. (b) Axial surface traces of all synclines in a portion (~1,200 km²) of the mapped area referred to in the text. Shows the two dominant orientations of synclines (NNW-SSE and WNW-ESE) and the merging/branching of synclines with these two orientations. Image centers: (a) 26.219674, 30.921328; (b) 26.079148, 31.008571.

Fold geometries and scales are very different from those in typical regional tectonic fold systems, and our synclines are too extensively developed over large areas to be explained by fault propagation folding associated with strike slip faults, as suggested by Youssef et al. (1998) for a small area in the Eastern Desert. They are better described as sag structures, with no accompanying active anticline/dome-forming process. Whatever process caused the sag, the network developed in a narrow time window between Early Eocene deposition of the limestones and formation of cross-cutting faults associated with Red Sea rifting (Figure 3).
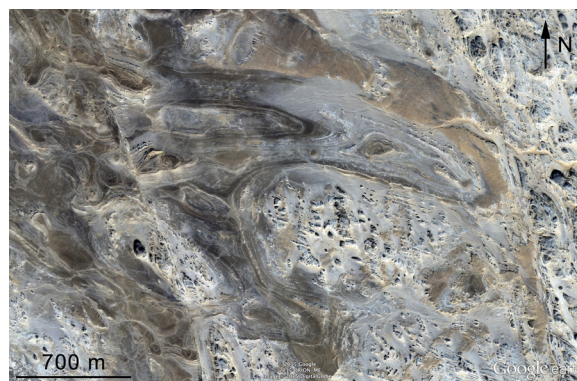

Figure 3.
Normal faults associated with rifting of the Red Sea cut and offset the synclines, indicating that the synclines predate Red Sea rift-related extension in the Western Desert. Image center: 26.762238, 31.091612.

Sag of sedimentary layers can be caused by a variety of subsurface volume reduction mechanisms (dissolution, diagenesis, mining) or may accompany mobilization of underlying shale sequences. The likely suspect mechanisms, however, all have problems when applied to the Western Desert synclines. Deep dissolution of evaporites (suggested for similar structures in Qatar by Prost, 2014) cannot play a role in formation of our syncline network, because there are no evaporites reported in the stratigraphic section underlying our Eocene carbonates (e.g., Issawi, 1999). Shallow dissolution of limestone has been reported in Egypt, but the scale of epigenic caves and sinkholes is small (e.g., Abdeltawab, 2013). Furthermore, our synclines have features that are much more like sags formed by deep mine collapse. We have seen nothing in the high-resolution imagery to suggest widespread shallow collapse and formation of sinkholes, let alone features on the scale of our synclines.

Collapsed paleokarst sounded promising to us, because the scale, features, and geometries of our syncline network are strikingly similar to those of collapsed paleokarst. Unfortunately, the stratigraphic record indicates that extensive and long-term subaerial exposure occurred at the top of shale units (the Kharga Shale and within the Esna Shale) rather than in limestone (e.g., the Tarawan or lower Thebes) (El-Azabi and Farouk, 2011; Keheila and Kassab, 2001; Aubry, 2014, personal communication).

We have previously proposed (Tewksbury et al., 2014) that mobilization in underlying sediments (as suggested by Loseth et al., 2011 for an area in the North Sea) might have created sag structures in the overlying Eocene carbonates, which are underlain by several Late Cretaceous and Paleogene shale units that have the potential for instability. This seemed like a viable model to us for our syncline network until we recently completed our country-wide survey and realized not only the extent of development of the features but the remarkable consistency in dominant orientations of the sag structures, both of which make downslope mobilization a less likely model.

So, to paraphrase Sherlock Holmes, when you have eliminated the impossible, whatever remains, however improbable, might be the truth. So, what about hypogene karst? Although our synclines are developed over a truly enormous area, what we currently know about the network is better explained by hypogene speleogenesis than by any other model we have considered to date. Hypogene speleogenesis could produce deep-seated collapse and sag of surface layers without requiring either subsurface evaporites or the presence of buried paleokarst. Joints and faults are controlling factors for upward fluid migration in hypogene speleogenesis, and orientations in our syncline network are strongly correlated with joint and fault orientations that predate Red Sea Rift-related extension. In addition, virtually the entire outcrop area of Eocene carbonates overlies a sequence that is dominantly shale. Contrasting lithologies and aggressive fluid chemistries play an important role in hypogene speleogenesis. Post early-Eocene igneous activity, which was widespread in Egypt (e.g., Meneisy, 1990 and Bosworth et al., 2015), could also have played a critical role. Or, is there another possibility that we have yet to consider?

References

Abdeltawab S. 2013. Karst limestone geohazards in Egypt and Saudi Arabia. International Journal of Geoengineering Case Histories 2 (4): 258-269.

Bosworth W, Stockli DF, Helgeson DE. 2015. Integrated outcrop, 3D seismic, and geochronologic interpretation of Red Sea dike-related deformation in the Western Desert of Egypt – the role of the 23 Ma Cairo "mini-plume". Journal of African Earth Sciences 109: 107-119. http://dx.doi.org/10.1016/j.jafrearsci.2015.05.005

El-Azabi MH, Farouk S. 2011. High-resolution sequence stratigraphy of the Maastrichtian-Ypresian succession along the eastern scarp face of Kharga Oasis, southern Western Desert, Egypt. Sedimentology 58: 579-617. http://dx.doi.org/10.1111/j.1365-3091.2010.01175.x

Issawi B, El Hinnawi M, Fransic M, Mazhar A. 1999. The Phanerozoic geology of Egypt, a geodynamic approach. Cairo, Egypt: Egyptian Geological Survey.

Keheila EA, Kassab AS. 2001. Stratigraphy and sedimentation-tectonics of the Campanian-Thanetian succession in North Wadi Qena and southern Galala, Eastern Desert, Egypt: evidence for major and regional erosive unconformities. Bulletin of the Faculty of Science, Assiut University 30 (1-F): 73-109.

Loseth H, Wensaas L, Gading M. 2011. Deformation structures in organic-rich shales. AAPG Bulletin 95 (9): 729-747. http://dx.doi.org/10.1306/09271010052

Meneisy MY. 1990. Vulcanicity In: Said R, editor. The geology of Egypt. Rotterdam: A.A. Balkema, p. 157-172.

Prost, G. 2014. Remote sensing for geoscientists: image analysis and integration. 3rd ed. New York: CRC Press.

Tewksbury BJ, Tarabees EA, Mehrtens CJ, Wolpert JA, DeGennaro JA, Dennison-Leonard GS, McLean TJ. 2014. Extensive syncline network in Eocene limestone of the Western Desert, Egypt: regional folding? collapsed paleokarst? mobilization of underlying shale?. Geological Society of America Annual National meeting, Vancouver, BC. 46 (6): 154.

Youssef MM, Ibrahim HA, Bakheit AA, Senosy MM. 1998. Tectonic patterns developed within the Sohag region, middle Egypt. Journal of African Earth Sciences 26 (2): 327-339. http://dx.doi.org/10.1016/S0899-5362(98)00015-3